E-ISSN: 2148-6247

Turkish Journal of PHARMACEUTICAL SCIENCES

An Official Journal of the Turkish Pharmacists' Association, Academy of Pharmacy

Volume: 21 Issue: 1 February 2024

www.turkjps.org

PubMed Central PubMed Scopus TRDİZİN

galenos

Turkish Journal of
PHARMACEUTICAL SCIENCES

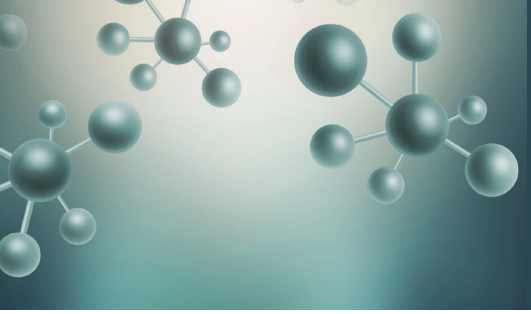

Turkish Journal of
PHARMACEUTICAL SCIENCES

Turkish Journal of
PHARMACEUTICAL SCIENCES

Please refer to the journal's webpage (https://www.turkjps.org/) for "Editorial Policy" and "Instructions to Authors".

The editorial and publication process of the **Turkish Journal of Pharmaceutical Sciences** are shaped in accordance with the guidelines of ICMJE, WAME, CSE, COPE, EASE, and NISO. The Turkish Journal of Pharmaceutical Sciences is indexed in **PubMed, PubMed Central, Thomson Reuters / Emerging Sources Citation Index, Scopus, ULAKBİM, Türkiye Atıf Dizini, Embase, EBSCO Host, Türk Medline, Cabi, CNK**I.

The journal is published online.

Owner: Turkish Pharmacists' Association, Academy of Pharmacy

Responsible Manager: İlkay Erdoğan Orhan

galenos yayınevi

Publisher Contact
Address: Molla Gürani Mah. Kaçamak Sk. No: 21/1
34093 İstanbul, Türkiye
Phone: +90 (530) 177 30 97
E-mail: info@galenos.com.tr/yayin@galenos.com.tr
Web: www.galenos.com.tr | **Publisher Certificate Number:** 14521

Publication Date: February 2024
E-ISSN: 2148-6247
International scientific journal published bimonthly.

Turkish Journal of
PHARMACEUTICAL SCIENCES

CONTENTS

Original Articles

Turk J Pharm Sci 2024;21(1):1-6
DOI: 10.4274/tjps.galenos.2023.82353

ORIGINAL ARTICLE

Analysis of Surgical Masks Adverse Effects on Facial Skin in Long Term Usage During COVID-19 Pandemic

Abdullah Levent ALPARSLAN[1]*, Kıvanç YÜKSEL[2], Khaetthareeya SUTTHANUT[3]

[1]İstinye University, Faculty of Pharmacy, Department of Pharmaceutical Technology, İstanbul, Türkiye
[2]Ege University Center for Drug Research and Development and Pharmacokinetic Applications (ARGEFAR), İzmir, Türkiye
[3]Khon Kaen University Faculty of Pharmaceutical Sciences, Department of Pharmaceutical Chemistry, Khon Kaen, Thailand

ABSTRACT

Objectives: During the coronavirus disease-2019 pandemic, masks have become mandatory for protection against the virus transmitted by breathing. This study examined the impact of surgical masks used daily on civilian facial skin.

Materials and Methods: Moisture, elasticity, pore, melanin, acne, wrinkle, and sensitivity parameters of 83 volunteers were measured numerically using an API-100 skin analyzer and camera recordings. Numerical values were compared following the device's algorithm calibrated according to age, gender, and race. Finally, the obtained data were statistically evaluated and compared with the averages.

Results: Pore, melanin, acne, and wrinkle parameters were higher without gender discrimination, whereas moisture and elasticity parameters were low. While a significant increase was observed in women for sensitivity, the increase was not statistically significant in men.

Conclusion: The negative effects of long-term daily wearing of surgical masks on facial skin were statistically significant. Therefore, taking outdoor breaks during mask use, washing the face intermittently, using moisturizing and purifying cosmetic products, and anti-wrinkle effects have been proposed to reduce the possible defects.

Keywords: Surgical mask, COVID-19, acne, moisture, wrinkle

INTRODUCTION

Social protection methods are being investigated with the coronavirus disease-2019 (COVID-19) pandemic. Because the virus is transmitted through respiration, it is scientifically recommended to use masks and protective equipment. Studies analyzing the effect of masks on the general population have concluded that masks are associated with a reduction in transmission and cases.[1-4] Surgical masks can prevent the inhalation of large droplets. They are useful for avoiding infection by noticing distance. Surgical masks have also been shown to intercept other human coronaviruses during coughing to filter submicron-sized airborne particles.[5,6] It has been stated that the rate of virus transmission is significantly lower in countries with mandatory mask requirements. Furthermore, studies conducted in different countries have reported that the use of masks causes significant decreases in mortality rates.[7-9]

People who work, spend time, and travel in closed places wear masks on their faces for a long time. Long-term use of masks can create negative effects in terms of hindering fresh air ventilation in the areas they cover. In addition, the mask used to prevent the virus from being transmitted through the respiratory tract may cause some undesirable effects on the face because it obstructs the outflow of breath from the mouth and nose simultaneously. The types and duration of masks affect intact

*Correspondence: levent.alparslan@istinye.edu.tr, Phone: +90 542 313 45 16, ORCID-ID: orcid.org/0000-0003-0113-6850
Received: 22.11.2022, Accepted: 12.02.2023

skin differently. The increased skin temperature and incident adverse effects such as acne, redness or erythema, drying, itching, allergies, burning, and wounds have been reported when covered by masks for a long time.[10-13]

Although the impact of N95 masks on healthcare professionals during the COVID-19 pandemic has been extensively studied, the effect of the surgical mask on the skin has been limited, although it was widely used by civilian users for a prolonged period. Though labor-intensive healthcare staff wear masks longer than civilians, this study was conducted for this purpose. The data were evaluated statistically according to the measurement values by conducting analysis, not based on surveys and observations.

High moisture at the mask-covered facial skin lesion due to low breathability and deficit air ventilation can lead to dermatological disorders due to accumulated sweat, dirt, and oil on the skin surface. The severity is varied by multiple factors, resulting in acne, hyperpigmentation, and irritation as signs of skin problems that can only be investigated clinically using a specific skin analyzer. Therefore, this study aimed to examine the impact of prolonged use of surgical masks in İstanbul metropolitan city civilians, who live and spend a lot of time indoors. The obtained results are expected to deliver the statement and beneficial information for hygienic and preventive practices and suitable skincare and cosmetic products of choice.

MATERIALS AND METHODS

API-100 skin analyzer was used in the scientific evaluation of moisture, elasticity, pores, melanin, acne, wrinkles, and sensitivity parameters on the skin according to age, gender, and race. According to the device algorithm, the parameters can be measured using numerical values and compared with the average of parameters in the same categories. By measuring from the same point on face, it is ensured that the comparison is realistic and optimized.[14-16]

The technical specifications of the API-100 device are given below:

Image Sensor 1/4 inch Color CMOS UXGA (2 mega pixels)

Pixel effective pixel: 1.624 x 1.212 Pixel

Image Capture size WI-FI video streaming VGA (640 x 480) | 2M (1.600 x 1.200)

Image Frame Rate VGA (640 x 480) - 30 frame max 2M (1.600 x 1.200)

LED Dip LED X8 & UV - Chip LED X8 (NICHIA/Japan) Dip LED X8 (NICHIA/Japan) Dip LED X8 (Nichia/Japan)

In the evaluation of the elasticity parameter, the skin was categorized by low, normal, and high levels. The looseness of the skin structure and the width of the pores was evaluated. In the graph, moisture and elastic parameters were scored depending on the image and compared with the average age. The state of the porosity structure of the skin was defined as good, normal, and porous. The pores in the camera image were shown as dots and compared with a good skin image of the same age, gender, and race. In the evaluation of melanin, an interpretation was made depending on the width and tone of the black spots. In the acne evaluation, sebum density and brightness were determined. Acne areas were scored and shown by color. Wrinkle assessments were scored according to their depth and intensity. Wrinkle-detected areas were shown as dots. In the sensitivity assessment, the thickness of the skin layer and physical resistance were interpreted. Where the coloration is intense, the sensitivity parameter is scored low.

In the study, healthy subjects with ages ranging from 18 to 61 years were included from domestic and foreign students studying and working at İstinye University. The ratio of Turkish volunteers to foreign attendees was 8.2. The distribution of ages, gender, and nationality is demonstrated in Figure 1, where the percentages of male and female subjects were 16.9% and 83.1%, respectively. The obligatory inclusion criteria were no use of colored cosmetics or dermocosmetic products at the application site throughout the study. The subjects were informed about the research in accordance with the Declaration of Helsinki. People with chronic diseases, those who used drugs, those with COVID-19 infection, and those with cosmetic products on their faces were excluded from the study. Skin measurements were taken at the designated points using an API-100 skin analyzer. Points are shown in Figure 2. Then, data comparison was conducted according to the algorithm of the skin analyzer device. This study was approved by the İstinye University Human Research Ethics Committee (protocol number: 21-103, date: 22.12.2021) informed consent was obtained from all participants.

Statistical analysis

Statistical evaluations were performed using the SAS version 9.4 program. The type I error was accepted as 0.05. In the statistical evaluation, each individual's difference scores (Δ) calculated for hydration, elasticity, pores, melanin, acne, wrinkles, and sensitivity measurements were taken into account. For each category, the difference score of the subjects (Δ) was calculated by subtracting the measurement score of each subject from the average score: $\Delta = X\text{-}X_{mean}$.

Descriptive statistics (n, mean, standard deviation, median, 25th and 75th percentiles) were depending on gender grouping, for difference scores (Δ) for moisture, elasticity, pores, melanin, acne, wrinkles, and sensitivity measurements. Statistical evaluation was performed in the following two sections:

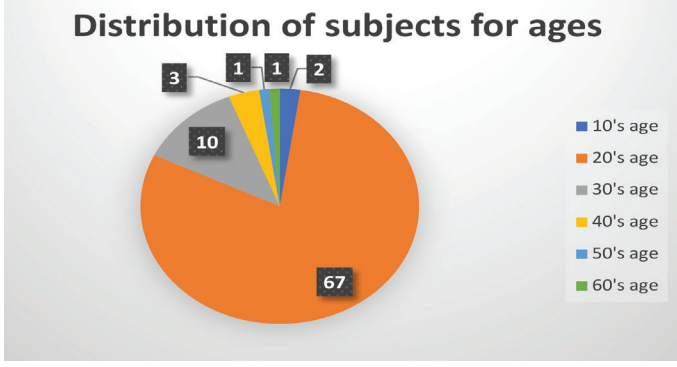

Figure 1. Age distribution of subjects for the skin analysis study

Comparison with the normal value

Depending on the distribution of the data, we investigated whether the mean (arithmetic mean/median) of the difference scores (Δ) of the subjects (n= 83) was different from zero. The evaluation was made with the one-sample *t*-test (arithmetic mean) in the data suitable for normal distribution and with the Wilcoxon signed rank test (median) for non-normally distributed data.

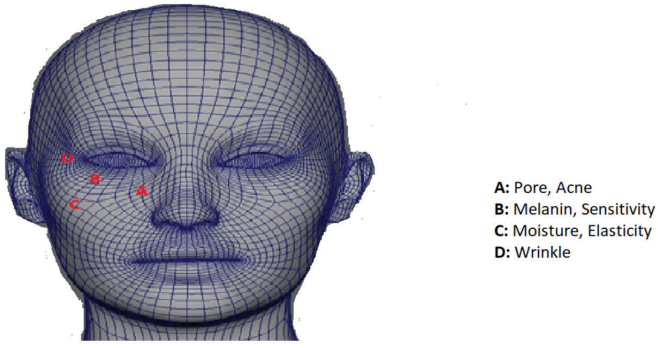

Figure 2. Analyze points for skin parameters

Comparison by gender

Depending on the distribution of the data, a two-sample *t*-test (arithmetic mean) was used for data with normal distributions, and the Wilcoxon rank sum test (median) was used for non-normal distributions. The comparison of the mean (arithmetic mean/median) difference scores of females (n= 64) and males (n= 19).

In case of statistical difference according to gender, separate evaluations were made for the male and female groups when the subtraction scores differed from zero. While comparing the means in these evaluations, the one-sample *t*-test was used for data that were suitable for normal distribution and the Wilcoxon signed rank test was used for non-normal distributions.

RESULTS

Descriptive statistics (n, mean, standard deviation, median, 25th and 75th percentiles) for the difference scores (Δ) of elasticity, pore, melanin, acne, wrinkle, and sensitivity measurements were demonstrated depending on gender grouping (Table 1). The data distribution differed among the studied categories: the pore (Δ) and wrinkle (Δ) scores showed normal distribution ($p > 0.05$), and arithmetic mean values were considered in the

Table 1. Descriptive statistics for difference scores (Δ) for elasticity, pores, melanin, acne, wrinkles, and sensitivity measurements

Parameters		Numbers (n)	Arithmetic mean	SD	Median	75th percentile	75th percentile
Pore (Δ)	Male	19	9.68	11.25	7.0	1.0	19.0
	Female	64	6.12	12.71	7.5	-2.0	15.5
	Total	83	6.93	12.41	7.0	-1.0	16.0
Sensitivity (Δ)	Male	19	19.57	31.48	0.0	-7.0	52.0
	Female	64	-1.42	17.62	-9.0	-9.0	1.5
	Total	83	3.38	23.13	-8.0	-9.0	3.0
Moisture (Δ)	Male	19	-39.53	2.874	-40.0	-40.0	-40.0
	Female	64	-38.02	5.799	-40.0	-40.0	-35.0
	Total	83	-38.36	5.297	-40.0	-40.0	-35.0
Elasticity (Δ)	Male	19	-42.16	5.580	-44.0	-44.0	-44.0
	Female	64	-40.30	8.337	-44.0	-44.0	-35.0
	Total	83	-40.72	7.801	-44.0	-44.0	-38.0
Melanin (Δ)	Male	19	60.15	17.57	65.0	54.0	72.0
	Female	64	59.37	18.15	67.0	50.0	72.0
	Total	83	59.55	17.92	66.0	50.0	72.0
Acne (Δ)	Male	19	52.57	25.46	61.0	43.0	73.0
	Female	64	27.15	34.44	31.5	-4.5	58.0
	Total	83	32.97	34.19	43.0	2.0	61.0
Wrinkle (Δ)	Male	19	33.05	23.69	29.0	23.0	41.0
	Female	64	17.35	18.21	19.0	2.0	35.0
	Total	83	20.95	20.54	23.0	2.0	38.0

SD: Standard deviation

evaluations; in contrast, the other scores were not normally distributed ($p < 0.05$), and the median (median) values were considered in the evaluations.

In the skin analyses performed on 83 volunteers, the images of the two volunteers with the highest and lowest scores of the device were compared. In addition to statistical differences, visual differences were recorded. The highest and lowest humidity comparison profiles determined by the age and gender of the volunteers were demonstrated (Figure 3). The highest and lowest scored elasticity profiles are indicated on the graph (Figure 4). The porous skin with the highest score according to the pore status was compared with the skin that appeared to be better than the average (Figure 5). In the comparison of melanin balance, the skin with the highest score and black pigment, with a large spot area, and healthy skin without significant coloration were observed (Figure 6). Skin with excess sebum turning into acne with porous blackheads *versus* healthy skin with high moisture and sebum balance were compared (Figure 7). Wrinkle assessment is important for the youthful and healthy appearance of the skin. Young and healthy skin should have a low wrinkle score. Low- and high-score wrinkles were compared (Figure 8). In the sensitivity assessment, the thickness of the skin layer was interpreted. A low score indicates high physical resistance. Low- and high-score skin images were compared (Figure 9).

Comparison with normal value

Medical mask use induced significant changes, including an increase in pore size, melanin, and wrinkles, but a reduction in

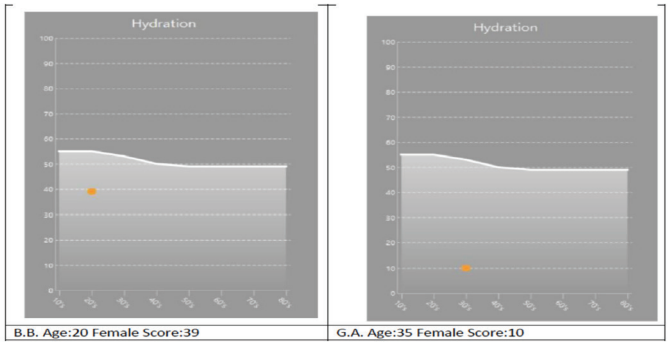

Figure 3. Best and worst scored hydration analysis of volunteers

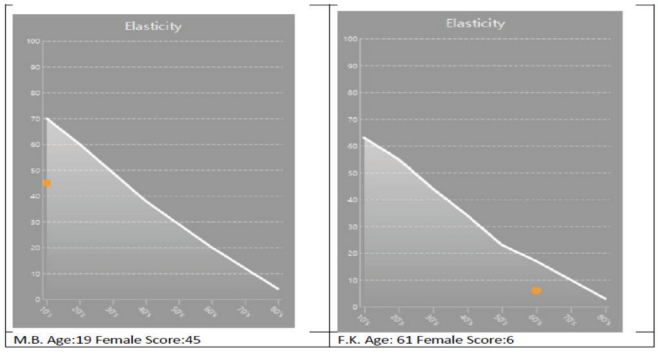

Figure 4. The best and the worst scored elasticiy analysis of volunteer

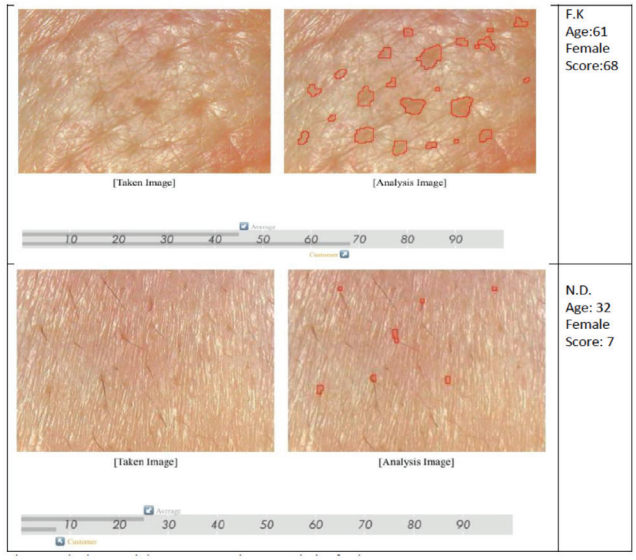

Figure 5. Best and worst scored pore analysis of volunteers

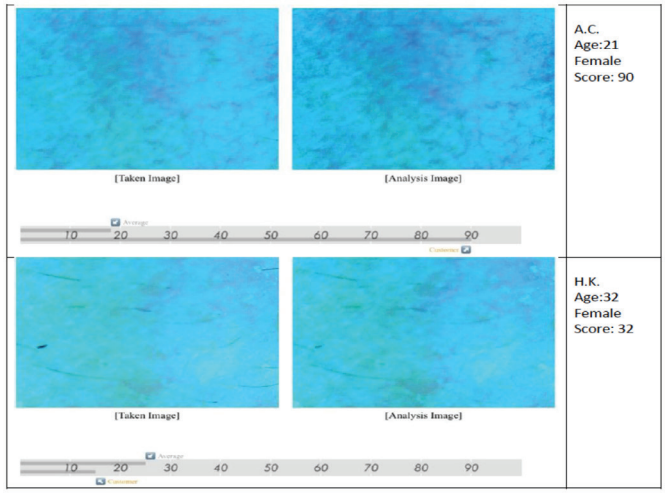

Figure 6. Best and worst scored melanin analysis of volunteers

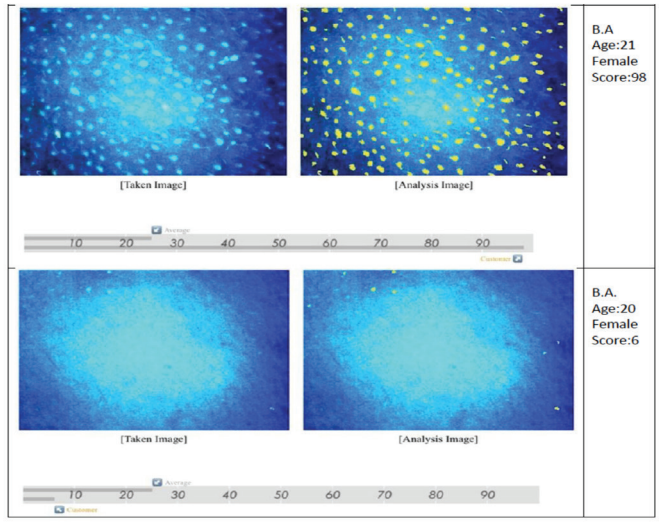

Figure 7. Best and worst scored acne analysis of volunteers

the moisture and elasticity of facial skin. The arithmetic mean values of the pore (Δ), melanin (Δ), acne (Δ), and wrinkle (Δ) scores were 6.93, 66.0, 43.0, and 20.95, respectively, which statistically increased and differed from zero ($p < 0.05$). The median values of moisture (Δ) and elasticity (Δ) scores were -40.0 and -44.0, respectively, which statistically decreased and differed from zero ($p < 0.05$). In contrast, the median sensitivity (Δ) of -8.0 indicated the change with no statistical difference from zero ($p > 0.05$) (Table 1).

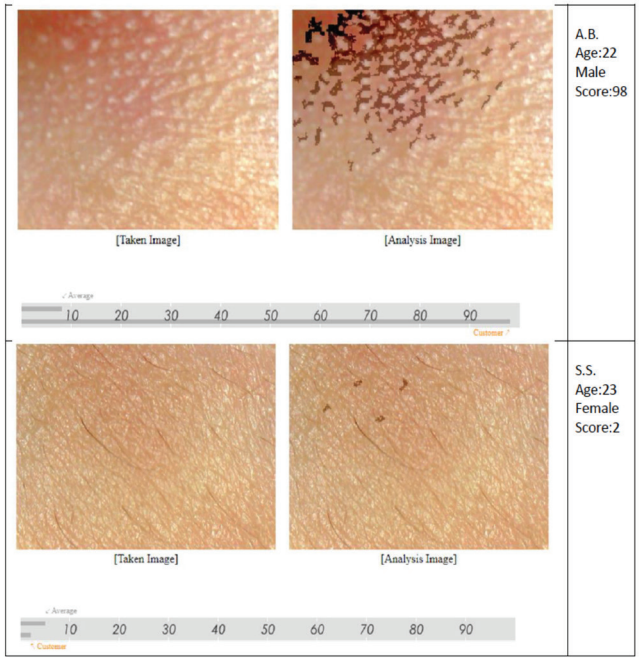

Figure 8. Best and worst scored wrinkle analysis of volunteers

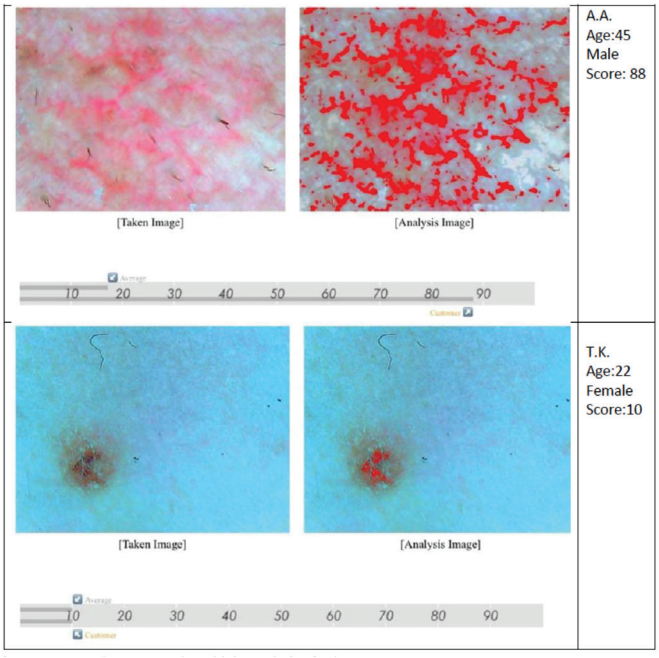

Figure 9. Best and worst scored sensitivity analysis of volunteers

Gender comparison

The impact of surgical mask use between male and female groups was significantly different for sensitivity, acne, and wrinkles. Long-term surgical mask wearing induced acne and wrinkle development in both male [with zero-different (Δ) scores of 61.0 and 33.05, respectively] and female facial skin (with Δ scores of 31.5 and 17.35, respectively); however, in male rather than female groups; while there was no significant change on facial skin sensitivity in both genders.

The arithmetic mean/median of pores (Δ), moisture (Δ), elasticity (Δ), and melanin (Δ) did not significantly differ between the groups of males and females ($p > 0.05$). The arithmetic mean/median of the pore (Δ), moisture (Δ), elasticity (Δ), and melanin (Δ) were 9.68, 6.12, and -40.0 - 40.0 for males and -44.0, -44.0, 65.0, and 67.0 for females, respectively (Table 1).

The statistically significant difference between the arithmetic mean/median of sensitivity (Δ), acne (Δ) and wrinkle (Δ) scores depending on gender ($p < 0.05$) was exhibited with the arithmetic mean/median sensitivity (Δ), acne (Δ) and wrinkle (Δ) of 0.0, 61.0, and 33.05 for the male group and -9.0, 31.5, and 17.35 for the female group, respectively.

Since sensitivity (Δ), acne (Δ) and wrinkle(Δ) scores statistically differed in terms of gender, comparison with normal values was performed separately for males and females. The arithmetic mean/median increase in sensitivity (Δ) and acne (Δ) and wrinkle (Δ) in females were -9.0, 31.5, and 17.35, respectively, compared with the normal value. It was found to be significantly different from zero ($p < 0.05$). In males, the difference for sensitivity (Δ) was found to be 0.00, and it was not significantly different from zero ($p > 0.05$); the median for acne (Δ) and mean for wrinkle (Δ) were 61.0 and 33.05, respectively, and both were significantly different from zero ($p < 0.05$) (Table 1).

DISCUSSION

The influence of surgical masks on long-term use in 83 volunteers during the COVID-19 pandemic was demonstrated. The overall results indicated that prolonged surgical mask usage could cause superficial maceration and damage the skin barrier. The adverse effects were detected as a significant increase in skin pore numbers and acne formation, which was presumed to be anticipated by skin cell damage associated with limited air ventilation during surgical mask wearing, followed by oil and bacteria deposits. Thus, the enlargement of skin pores and the formation of pimples, acne, and blackheads have developed. Furthermore, increased melanin pigment represented skin-darkening induction. In addition, a relationship between parameters of decreation in skin elasticity and higher wrinkles was suggested. Interestingly, a more significant influence on males than on females was found.

CONCLUSION

The obtained results suggest the undesirable effects of prolonged mask usage, which could lead to more severe dermatological and cosmetic problems depending on wearing duration and personal hygiene factors. Furthermore, the

significant increase in skin pore numbers, melanin pigment, and acne formation suggests a disorder of dermal physiology throughout the dermis and epidermis layers. In addition, melanin pigment inscription has indicated the potential for skin blemishes. Therefore, preventive practices are crucial, including periodic unmasking in open environments between prolonged usage, cleansing facial skin, and applying skin barrier creams to prevent skin deterioration. In addition, suitable choices of skincare and cosmetic products are also important: facial skin washing every morning and night with an oil-free, fragrance-free cleanser and treatment with non-comedogenic facial moisturizers or gels one hour before being on masks are recommended. Conversely, skincare and cosmetic products with high contents of oils and pigments should be avoided to avert skin pore formation and obstruction worsening.

Acknowledgement

We would like to thank Nacar Group for its support for the supply of the API-100 skin analyzer.

Ethics

Ethics Committee Approval: This study was approved by the İstinye University Human Research Ethics Committee (approval number: 21-103, date: 22.12.2021).

Informed Consent: Informed consent was obtained from all participants.

Authorship Contributions

Design: A.L.A., K.S., Data Collection or Processing: A.L.A., K.S., Analysis or Interpretation: K.Y., Literature Search: A.L.A., Writing: A.L.A.

Conflict of Interest: The authors have no conflicts of interest to declare.

Financial Disclosure: This study was carried out in the Pharmaceutical Technology Laboratory of the Faculty of Pharmacy at İstinye University.

REFERENCES

1. Chu DK, Akl EA, Duda S, Solo K, Yaacoub S, Schünemann HJ. COVID-19 systematic urgent review group effort (SURGE) study authors. Physical distancing, face masks, and eye protection to prevent person-to-person transmission of SARS-CoV-2 and COVID-19: a systematic review and meta-analysis. Lancet. 2020;395:1973-1987.
2. MacIntyre CR, Chughtai AA. A rapid systematic review of the efficacy of face masks and respirators against coronaviruses and other respiratory transmissible viruses for the community, healthcare workers and sick patients. Int J Nurs Stud. 2020;108:103629.
3. Gupta M, Gupta K, Gupta S. The use of facemasks by the general population to prevent transmission of Covid 19 infection: a systematic review. https://doi.org/10.1101/2020.05.01.20087064
4. Mitze T, Kosfeld R, Rode J, Wälde K. Face masks considerably reduce COVID-19 cases in Germany. Proc Natl Acad Sci U S A. 2020;117:32293.
5. Migliori GB, Nardell E, Yedilbayev A, D'Ambrosio L, Centis R, Tadolini M, van den Boom M, Ehsani S, Sotgiu G, Dara M. Reducing tuberculosis transmission: a consensus document from the World Health Organization Regional Office for Europe. Eur Respir J. 2019;53:1900391.
6. Leung NHL, Chu DKW, Shiu EYC, Chan KH, McDevitt JJ, Hau BJP, Yen HL, Li Y, Ip DKM, Peiris JSM, Seto WH, Leung GM, Milton DK, Cowling BJ. Respiratory virus shedding in exhaled breath and efficacy of face masks. Nat Med. 2020;26:676-680.
7. Lyu W, Wehby GL. Community use of face masks and COVID-19: evidence from a natural experiment of state mandates in the US. Health Aff (Millwood). 2020;39:1419-1425.
8. Wong SH, Teoh JYC, Leung CH, Wu WKK, Yip BHK, Wong MCS, Hui DSC. COVID-19 and public interest in face mask use. Am J Respir Crit Care Med. 2020;202:453-455.
9. Cheng VC, Wong SC, Chuang VW, So SY, Chen JH, Sridhar S, To KK, Chan JF, Hung IF, Ho PL, Yuen KY. The role of community-wide wearing of face mask for control of coronavirus disease 2019 (COVID-19) epidemic due to SARS-CoV-2. J Infect. 2020;81:107-114.
10. Lan J, Song Z, Miao X, Li H, Li Y, Dong L, Yang J, An X, Zhang Y, Yang L, Zhou N, Yang L, Li J, Cao J, Wang J, Tao J. Skin damage among health care workers managing coronavirus disease-2019. J Am Acad Dermatol. 2020;82:1215-1216.
11. Hadjieconomou S, Hughes J, Kamath S. Occupational skin disease during the COVID-19 pandemic, as captured in a Dermatology staff clinic in the United Kingdom. J Eur Acad Dermatol Venereol. 2020;34:670-671.
12. Techasatian L, Lebsing S, Uppala R, Thaowandee W, Chaiyarit J, Supakunpinyo C, Panombualert S, Mairiang D, Saengnipanthkul S, Wichajarn K, Kiatchoosakun P, Kosalaraksa P. The effects of the face mask on the skin underneath: a prospective survey during the COVID-19 pandemic. J Prim Care Community Health. 2020;11:2150132720966167.
13. Thatiparthi A, Liu J, Martin A, Wu JJ. Adverse effects of COVID-19 and face masks: a systematic review. J Clin Aesthet Dermatol. 2021;14(9 Suppl 1):39-45.
14. Jablonska I, Mielicki W. Analysis of the effect of serum estradiol concentration on facial skin moisture, pore width, discoloration and smoothness in 16- to 50-year-old women at the 5th and 25th days of the menstrual cycle. Skin Pharmacol Physiol. 2019;32:125-131.
15. Sikora E, Michorczyk P, Olszańska M, Ogonowski J. Supercritical CO_2 extract from strawberry seeds as a valuable component of mild cleansing compositions. Int J Cosmet Sci. 2015;37:574-578.
16. Cynthia G, Fachrial E, Ehrich Lister IN. The biorevitalization effect of serum containing rose apple leaf extract on the parameters of premature skin aging. BJHR. 2022;9:228-248.
17. Foo CC, Goon AT, Leow YH, Goh CL. Adverse skin reactions to personal protective equipment against severe acute respiratory syndrome-a descriptive study in Singapore. Contact Dermatitis. 2006;55:291-294.
18. Desai SR, Kovarik C, Brod B, James W, Fitzgerald ME, Preston A, Hruza GJ. COVID-19 and personal protective equipment: treatment and prevention of skin conditions related to the occupational use of personal protective equipment. J Am Acad Dermatol. 2020;83:675-677.

Turk J Pharm Sci 2024;21(1):7-24
DOI: 10.4274/tjps.galenos.2023.60543

ORIGINAL ARTICLE

Genistein Enhances TRAIL-Mediated Apoptosis Through the Inhibition of *XIAP* and *DcR1* in Colon Carcinoma Cells Treated with 5-Fluorouracil

Tuğbagül ÇAL DOĞAN[1]*, Sevtap AYDIN DİLSİZ[2], Hande CANPINAR[3], Ülkü ÜNDEĞER BUCURGAT[2]

[1]Turkish Pharmaceuticals and Medical Devices Agency, Ankara, Türkiye
[2]Hacettepe University, Faculty of Pharmacy, Deparment of Pharmaceutical Toxicology, İstanbul, Türkiye
[3]Hacettepe University, Faculty of Medicine, Department of Basic Oncology, İstanbul, Türkiye

ABSTRACT

Objectives: Colorectal cancer is one of the most common cancers worldwide. However, surgical intervention and chemotherapy provide only limited benefits for the recovery and survival of patients. The anticarcinogenic effect of genistein has attracted attention because epidemiological studies have shown that soybean consumption is associated with a decrease in the incidence of cancer. There are limited studies on the effects of genistein in colorectal carcinoma cells. We aimed to investigate the cytotoxic, genotoxic, and apoptotic effects of genistein in SW480 and SW620 colon adenocarcinoma cells treated with 5-fluorouracil, the basis of chemotherapy, and the tumor necrosis factor-related apoptosis-inducing ligand (TRAIL) ligand, the mediator of apoptosis, both alone and in combination.

Materials and Methods: Cytotoxicity and genotoxicity were determined by MTT and comet assays, respectively. The apoptotic effects were evaluated by reverse transcription-polymerase chain reaction assay, with the additional use of Annexin V FITC, mitochondrial membrane potential (MMP), caspase 3, 8, and 9 activity, and reactive oxygen species (ROS) assay kits.

Results: According to our findings, genistein, 5-fluorouracil, and TRAIL had synergistic apoptotic effects because of DR5 upregulation, ROS production, and DNA damage, which were mediated by increased caspase-8, and -9 activity and decreased MMP.

Conclusion: The applied combinations of these compounds may contribute to the resistance problem that may occur in treating colorectal cancer, with a decrease in *DcR1* and *XIAP* genes.

Keywords: Genistein, 5-fluorouracil, TRAIL, apoptosis, colorectal cancer

INTRODUCTION

According to the International Agency for Research on Cancer, 23 million new cancer cases are expected annually by 2030. Colorectal cancer is among the most diagnosed cancers in the world, along with breast and lung cancers.[1] Although the incidence and mortality of colorectal cancer vary by gender, age, and race, colorectal cancer ranks third among cancers diagnosed in men and second in women according to GLOBOCAN (2018) data.[2,3] In Türkiye, colorectal cancer ranks 3rd and 4th in terms of prevalence in women and men, respectively.[4]

Colorectal cancer is characterized by the transformation of intestinal epithelial cells into carcinoma tissue due to inflammatory stress, genetic variation, and environmental factors such as modern consumption habits, smoking, and alcohol consumption.[5] Highly invasive and metastatic colorectal cancer cells, if left untreated, can spread to other organs, most often the liver and lymphoid organs.[6] However, patients are often diagnosed only at an advanced or metastatic stage. The presence of problems such as tumor regeneration and progression due to drug resistance in the applied chemotherapeutic treatment and

*Correspondence: tgcal89@gmail.com, Phone: +90 505 798 43 90, ORCID-ID: orcid.org/0000-0002-1476-0233
Received: 06.11.2022, Accepted: 18.02.2023

the cellular damage caused by mechanisms such as apoptosis or cell cycle arrest with chemotherapeutic drugs is found not only in cancer cells but also in normal cells. It has necessitated the development of different treatment principles for cancers.[5,7] Therefore, it is important to increase the effectiveness of existing chemotherapeutic drugs by combining them with some agents and to find a solution to the drug resistance problem.[7]

Epidemiological data have shown that soy consumption reduces the risk of colon cancer and phytoestrogens may protect against colorectal cancer.[1] Genistein, which was first isolated from *Genista tinctoria* L., a phytoestrogenic isoflavonoid compound that is particularly abundant in Fabaceae (formerly Leguminosae) plants, has drawn attention with its anticarcinogenic effect.[1,8,9] It has been suggested that genistein may be beneficial in the prevention and treatment of many types of cancer, including colorectal cancer, by showing anticancer activity in several ways, including the inhibition of Nf-κB signaling, accumulation of cancer cells in the G2/M phase with the affecting of cyclin-dependent kinases (CDK), induction of apoptosis, attenuation of multiple drug resistance through various signaling pathways [protein kinase B, mitogen-activated protein kinase, epidermal growth factor receptor (EGFR)], and induction of proapoptotic caspase-3, caspase-9, and *Bax* protein expressions in the apoptotic pathway.[10-15]

Tumor necrosis factor (TNF)-related apoptosis inducing ligand (TRAIL) is a type II transmembrane protein consisting of 281 amino acids belonging to the TNF superfamily and is synthesized in tissues such as the colon and thymus. It induces apoptosis through the extrinsic pathway by binding to 5 different membrane-bound receptors, namely *DR4, DR5, DcR1, DcR2,* and osteoprotegerin. *DcR4, DcR5,* and osteoprotegrin inhibit apoptosis by acting as decoy receptors.[16] Although the induction of the extrinsic pathway *via* the TRAIL ligand, which does not have a cytotoxic effect on normal cells, is a potential alternative in cancer treatment,[17,18] the development of resistance to TRAIL-induced apoptosis can also be seen in some cancer cells.[19,20] However, it has been determined that the combination of TRAIL and chemotherapeutics or phytotherapeutics may overcome TRAIL resistance in cancer cells.[21-23]

In this study, we aimed to investigate whether the combination of genistein and 5-fluorouracil, a backbone of colorectal cancer treatment,[24] can enhance TRAIL-mediated apoptosis in SW480 and SW620 human colorectal adenocarcinoma cells.

MATERIALS AND METHODS

Cell culture

The SW480 and SW620 cell lines were derived from a single patient at the primary and secondary stages. Therefore, these cell lines may represent a useful model for colon cancer progression. The SW480 cell line (human colorectal adenocarcinoma) was provided by Serkan İsmail Göktuna (Bilkent University Faculty of Science, Department of Molecular Biology and Genetics, Türkiye), and the SW620 (metastatic human colorectal adenocarcinoma) cell line (ATCC® CCL-227) was purchased from the American Type Culture Collection (ATCC). Cells were cultured in Dulbecco's Modified Eagle Medium (Wisent) containing 1% penicillin-streptomycin (Wisent) and 10% fetal bovine serum (Capricorn). The cells were maintained at 37 °C in an incubator in a humidified atmosphere of 5% CO_2 (Heraeus Instruments).

Cell viability assay

Thiazolyl blue tetrazolium bromide (MTT, Sigma) assay was used to assess cell viability and determine IC_{50} values. IC_{50} value is the concentration of the compounds necessary to kill one-half of the cell population,[25] as previously described by Mosmann[26] and Ferrari et al.[27] Briefly, SW480 and SW620 cells were cultured, and 10,000 cells were seeded in the chambers of a 96 well plate and allowed to attach for 24 hours. After incubation, the cells were exposed to different concentrations of genistein LKS (5-200 µM) dissolved in dimethyl sulfoxide [DMSO (Sigma)]. The final concentration was 0.5% (*v/v*). For 5-fluorouracil (Sigma-Aldrich) (5-800 µM) dissolved in DMSO, the final concentration was 0.5% (*v/v*). TRAIL (Cell Applications) (50-200 ng/mL) dissolved in sterile distilled water containing 0.1% (*v/v*) bovine serum albumin (Capricorn) in the medium for 24, 48, and 72 hours at 37 °C in a humidified atmosphere of 5% CO_2. When the exposure time ended, the cell medium was aspirated and 10 µL of MTT (Sigma) solution [5 mg/mL in phosphate buffer saline (PBS)] was added to each well. After 4 hours of incubation, the cell medium was replaced with 100 µL DMSO and the plates were shaken for 5 min. The absorbance was determined at 570 nm using a microplate reader (SpectraMax M2), and IC_{50} values were calculated using concentration-response curves to express the effects of the test materials on cell viability. The combination index (CI) for drug interaction was calculated using CompuSyn software (ComboSyn, Inc., Paramus, NJ, USA). The values of CI < 1 indicate synergistic interaction, while the values > 1 or not significantly different from 1 specify antagonistic or additive interaction, respectively.[28] After determining the synergistic effects of the test compounds by the MTT assay, the cells were exposed to the double and triple combination of these compounds for 48 hours, and the same procedure was followed as described previously. The results are presented as the mean ± standard deviation from three independent experiments.

Cell recovery assay

The cell recovery assay was performed as described by Li et al.[29] with modifications to determine the proliferative capacity of the cells after the removal of genistein (0.25 µM, 7.5 µM), 5-fluorouracil (1 µM), TRAIL (5 and 10 ng/mL), and their combinations. Briefly, SW480 and SW620 cells were cultured and 2 x 10^4 cells were seeded in the chambers of a 96 well plate and allowed to attach for 24 hours. After incubation, the cells were exposed to several concentrations of genistein, 5-fluorouracil, TRAIL, and their combinations in a medium for 48 hours at 37 °C in a humidified atmosphere of 5% CO_2. Then, the cells for each treatment group were typsinized (Trypsin-EDTA, Sigma) and counted (5 x 10^3) to seed in triplicate in a 96 well plate in test compound-free medium for 48 hours incubation. The MTT assay was used to evaluate cell recovery. The results are presented as the mean ± standard deviation from three independent experiments.

Alkaline comet assay

The basic alkaline comet assay was performed to determine DNA damage as described by Singh et al.[30] with the modifications of Hartmann et al.[31] Briefly, SW480 and SW620 cells were seeded at a density of 15000 cells/200 µL in 96 well plates and allowed to attach for 24 hours. The cells were then exposed to different concentrations of genistein (0.125 µM, 0.25 µM, 0.5 µM), 5-fluorouracil (1 µM), TRAIL (5 and 10 ng/mL), and their combinations for 48 hours. A negative control (0.5% DMSO) and a positive control [15 µM H_2O_2 (Merck)] were used. After incubation, the cells were re-suspended in 0.75% low melting point agarose (Boehringer Mannheim) and this suspension was spread on pre-coated slides coated with 1% normal melting point agarose (Sigma) and allowed to dry. After removing the coverslip, the slides (Marienfeld) were submerged in lysing solution [2.5 M NaCl (Sigma), 100 mM EDTA (Merck), 100 mM Tris (Sigma), 1% sodium sarcosinate (Sigma), 1% Triton-X 100 (Sigma), and 10% DMSO, pH 10] at 4 °C for 24 hours. Afterwards, the slides were left in an electrophoresis solution [300 mM NaOH (Merck) and 1 mM sodium EDTA (Merck), pH 13] at 4 °C for 20 min, and electrophoresis was performed at 4 °C for 20 min by applying an electrical current of 300 mA and 24 V in the electrophoresis equipment (Biometra Analytical). The slides were then washed in a neutralizing solution [0.4 M Tris-HCl (Sigma), pH 7.5] for 15 min and incubated in 50%, 75%, and 98% ethyl alcohol (Sigma-Aldrich) for 5 min successively. The dried slides were stained with EtBr (Sigma-Aldrich, 20 µg/mL in distilled water, 60 µg/slide) and examined using a Leica® fluorescence microscope. A computer-based analysis system (Comet Analysis Software, version 4.0, Kinetic Imaging Ltd., Liverpool, UK) was used to measure DNA damage. To visualize DNA damage, 100 nuclei *per* slide were examined at 400x magnification. DNA damage was expressed as the percentage of DNA in the tail (tail intensity). Values are expressed as the mean ± standard deviation from three independent experiments.

Analysis of cell surface expressions of DR4 and DR5 surface receptor proteins

Cells were cultivated at a density of 6 x 10^6 cells/25 cm^2 cell culture flask (Nest) for 24 hours and treated with genistein (0.5 µM for SW620; 1 µM for SW480 cells), 5-fluorouracil (1 µM) and their combinations for 48 hours. After incubation, the cells were trypsinized and suspended in a serum-free medium (Wisent) at a density of 1 x 10^6 cells/mL. The cells were then washed twice with 2 mL cell-staining buffer (Biolegend) and suspended in cell-staining buffer at a density of 1 x 10^6 cells/500 µL. 5 µL Phycoerythrin-conjugated mouse anti-human DR4, DR5, and IgG2B for isotype control (Biolegend) was added to cells and incubated at 4 °C for 30 min. After staining, the cells were washed twice with 2 mL cell staining buffer and suspended in 0.5 mL cell staining buffer for flow cytometry (Beckman Coulter, Cytoflex USA).

Cell cycle analysis by flow cytometry

The cells were cultivated at a density of 2 x 10^6 cells/4 mL in 25 cm^2 cell culture flasks. After incubation for 24 hours, the cells were treated with genistein (1 µM for SW480; 0.5 µM for SW620), 5-fluorouracil (1 µM), TRAIL (10 ng/mL for SW480; 5 ng/mL for SW620), and their combinations for 48 hours. The cells were trypsinized and suspended in 1 mL PBS (Wisent) at a density of 1.5 x 10^6 cells/mL. The cells were then fixed with 2 mL of ethanol (99%) and incubated for 24 hours. After washing the cells twice with PBS, 70 µL Ribonuclease A from bovine pancreas (RNase A, Sigma Aldrich) and 100 µL propidium iodide (PI, Sigma Aldrich) were added and incubated in the dark for 30 min. Cell cycle analysis was then performed using a flow cytometer (Beckman Coulter, Cytoflex USA). The results are presented as the mean ± standard error from three independent experiments.

Apoptosis detection

Apoptosis was measured with an Annexin V FITC apoptosis detection kit I (BD Pharmingen) according to the manufacturer's instructions. Briefly, the cells were collected after treatment with genistein (1 µM for SW480, 0.5 µM for SW620), 5-fluorouracil (1 µM), TRAIL (10 ng/mL for SW480, 5 ng/mL for SW620) for 48 hours and washed twice with PBS. Then, 1X binding buffer was added (10^6 cells/mL) to cells and 100 µL of the cell suspension was transferred to 5 mL culture tubes. Cells were incubated with 5 µL Annexin V FITC and 5 µL PI for 15 min at room temperature in the dark. Subsequently, apoptosis was analyzed using a flow cytometer after adding 400 µL 1X binding buffer. The results are presented as the mean **±** standard error from three independent experiments.

Measurement of intracellular reactive oxygen species (ROS) levels

The intracellular ROS level was determined using a ROS detection assay kit (Biovision), following the kit instructions. In brief, the cells were washed with 100 µL assay buffer and 100 µL 1X ROS label was added and incubated at 37 °C for 45 min in the dark. Cells were washed with PBS and treated with genistein (1 µM for SW480, 0.5 µM for SW620), 5-fluorouracil (1 µM), and TRAIL (10 ng/mL for SW480, 5 ng/mL for SW620) for 48 h. Fluorescence was measured at the desired time intervals by a microplate reader (SpectraMax M2) at an excitation of 495 nm and emission of 529 nm (Ex/Em= 495/529 nm).

Measurement of the mitochondrial membrane potential (MMP)

The effect of the test compounds on MMP was determined using a JC-1 MMP Assay Kit (Cayman). Briefly, the cells were collected after treatment with genistein (1 µM for SW480, 0.5 µM for SW620), 5-fluorouracil (1 µM), and TRAIL (10 ng/mL for SW480, 5 ng/mL for SW620) for 48 hours. Then, JC-1 staining solution was added to the cells. The cells were then incubated at 37 °C for 15 min in a humidified atmosphere of 5% CO_2 and washed twice with the assay buffer. Measurements were performed using a fluorescent plate reader (SpectraMax M2) for healthy cell detection (E_x/E_m= 535/595 nm) and for apoptotic cells (E_x/E_m= 485/535 nm).

Determination of activities of caspase 3, 8 and 9

Caspase 3, 8, and 9 activities were determined using the caspase 3, 8, and 9 Multiplex Activity Assay Kit (Abcam). In brief, the cells were collected after incubation with genistein

(1 μM for SW480, 0.5 μM for SW620), 5-fluorouracil (1 μM), and TRAIL (10 ng/mL for SW480, 5 ng/mL for SW620) for 48 hours. Next, caspase assay solution (containing caspase 3, 8, and 9 substrates) was added to the cells, followed by incubation at room temperature for 60 min. The fluorescence was measured at an excitation of 535 nm and emission of 620 nm for caspase 3, at an excitation of 490 nm and emission of 525 nm for caspase 8, and at an excitation of 370 nm and emission of 450 nm for caspase 9.

Reverse transcription-polymerase chain reaction analysis of gene expression

Reverse transcription-polymerase chain reaction (RT-PCR) analysis was used to determine the effects of the test compounds on apoptotic and antiapoptotic gene expression. First, total RNA was isolated from cells treated with genistein (1 μM for SW480, 0.5 μM for SW620), 5-fluorouracil (1 μM), and TRAIL (10 ng/mL for SW480, 5 ng/mL for SW620) for 48 hours using an RNeasy Plus Mini Kit (Qiagen) according to the manufacturer's instructions. Then, an RT² HT First Strand Kit (Qiagen) was used to synthesize the first strand cDNA. In brief, reverse transcription was performed using 500 ng of total RNA at 42 °C (15 min) and 95 °C (5 min) in a thermal cycler (Corbett). Afterward, real-time PCR reactions were performed using RT² qPCR SYBR Green MasterMix-2 (Qiagen) and RT² qPCR Primer Assay (Qiagen). Primers *Bcl-XL* (PPH00082C), *Bcl-2* (PPH00079B), *XIAP* (PPH00323A), *DR4* (PPH00842A), *DR5* (PPH00241C), *DcR1* (PPH00837A), *DcR2* (PPH00838B), and glyceraldehyde 3-phosphate dehydrogenase (GAPDH) (PPH00150F) were purchased from Qiagen. Each cycle was performed at the conditions of holding 95 °C for 15 min, cycling at 95 °C for 15 s, and cycling at 60 °C for 30 s for 40 cycles. The relative changes in the number of transcripts in each treatment were calculated by normalizing with *GAPDH* mRNA levels. The values indicate the mean ± standard error.

Statistical analysis

Statistical analysis of data was performed using SPSS 20.0 for Windows. The distribution of the data was checked for normality using the Shapiro-Wilk test. The Levene test verified the homogeneity of variance. The differences among the means of data with normal distribution were evaluated by one-way variance analysis (ANOVA), and *post-hoc* analyses of group differences were performed by Tukey's test for homogeneous variance and Dunnett's T3 test for non-homogeneous variance. Differences among the groups without normal distribution were evaluated by the Kruskal-Wallis test followed by the Mann-Whitney U test. *p* values of 0.05 and 0.001 were considered statistically significant.

Statistics of the Ct values for RT-PCR analysis were performed using the RT² Profiler PCR Data Analysis program of QIAGEN. Significance was determined on the basis of fold change from the control ΔΔCt value and $p < 0.05$ was considered statistically significant.

RESULTS

Genistein, 5-fluorouracil, and TRAIL inhibit colon cancer cell growth in vitro

Genistein, 5-fluorouracil, and TRAIL dose-dependently inhibited the growth of SW480 and SW620 cells for 24, 48, and 72 hours. In addition, 5-fluorouracil had time-dependent inhibitory effects in SW480 and SW620 cells. The IC_{50} values of genistein and 5-fluorouracil could not be determined in the studied concentration range for 24 hours and 72 hours, but IC_{50} of TRAIL was determined to be 93.35, 138.4, and 192.9 ng/mL for 24 hours, 48 hours, and 72 hours, respectively, in SW480 cells. Furthermore, IC_{50} of genistein was 375.8 μM for 48 hours and had a significant inhibitory effect above 200 μM in SW480 cells compared with the negative control (0.5% DMSO). The IC_{50} values of genistein were 351.1 μM and 190.6 μM for 48 and 72 hours, respectively, in SW620 cells. Additionally, the IC_{50} of 5-fluorouracil-treated SW620 cells was 794.4 μM for 48 hours. The IC_{50} values of TRAIL for 24, 48, and 72 hours in SW620 cells were determined to be 20, 19.43, and 50.16 ng/mL, respectively (Figure 1 a-f).

The combined effects of genistein (G), 5-fluorouracil (F), and TRAIL (T) were also evaluated, and more growth inhibition was observed in double and triple combinations than in single treatment with these compounds. In addition, triple combinations had more inhibitory effects than double combinations (Figure 1g and h).

A CI-based analysis was used to determine the synergistic effects of the compounds (Figure 2). 1 μM genistein for SW480 cells and 0.5 μM genistein for SW620 cells were selected according to the analysis. The CI values of G + T, G + F, and G + F + T were 0.02, 0.003, and 0.123 for 1 μM genistein, respectively, in SW480 cells and 0.73, 0.015, and 0.59 for 0.5 μM genistein, in SW620 cells. Furthermore, the reversibility of cell growth inhibition was evaluated using a recovery MTT assay. It was found that TRAIL had the most significant effect on the loss of ability to recover in SW480 and SW620 cells (Figure 3). Triple combinations were more effective than double and single concentrations of the compounds. The results showed that there were irreversible changes such as apoptosis in SW480 cells.

Genistein, 5-fluorouracil, and TRAIL cause DNA damage in SW480 and SW620 cells

According to the data of the comet assay, genistein, 5-fluorouracil, and TRAIL caused increases in DNA damage expressed as tail intensity, when compared with the negative control in SW480 and SW620 cells (Figures 4 and 5). The increases in DNA damage in SW480 cells treated with double and triple compounds were more significant than those in the single treatment and negative control groups (0.5% DMSO). However, the highest increases in DNA damage were observed at the concentrations of "0.125 μM G + 5 ng/μL TRAIL" and "0.25 μM G + 5 ng/μL TRAIL" in SW620 cells compared with the negative control (0.5% DMSO).

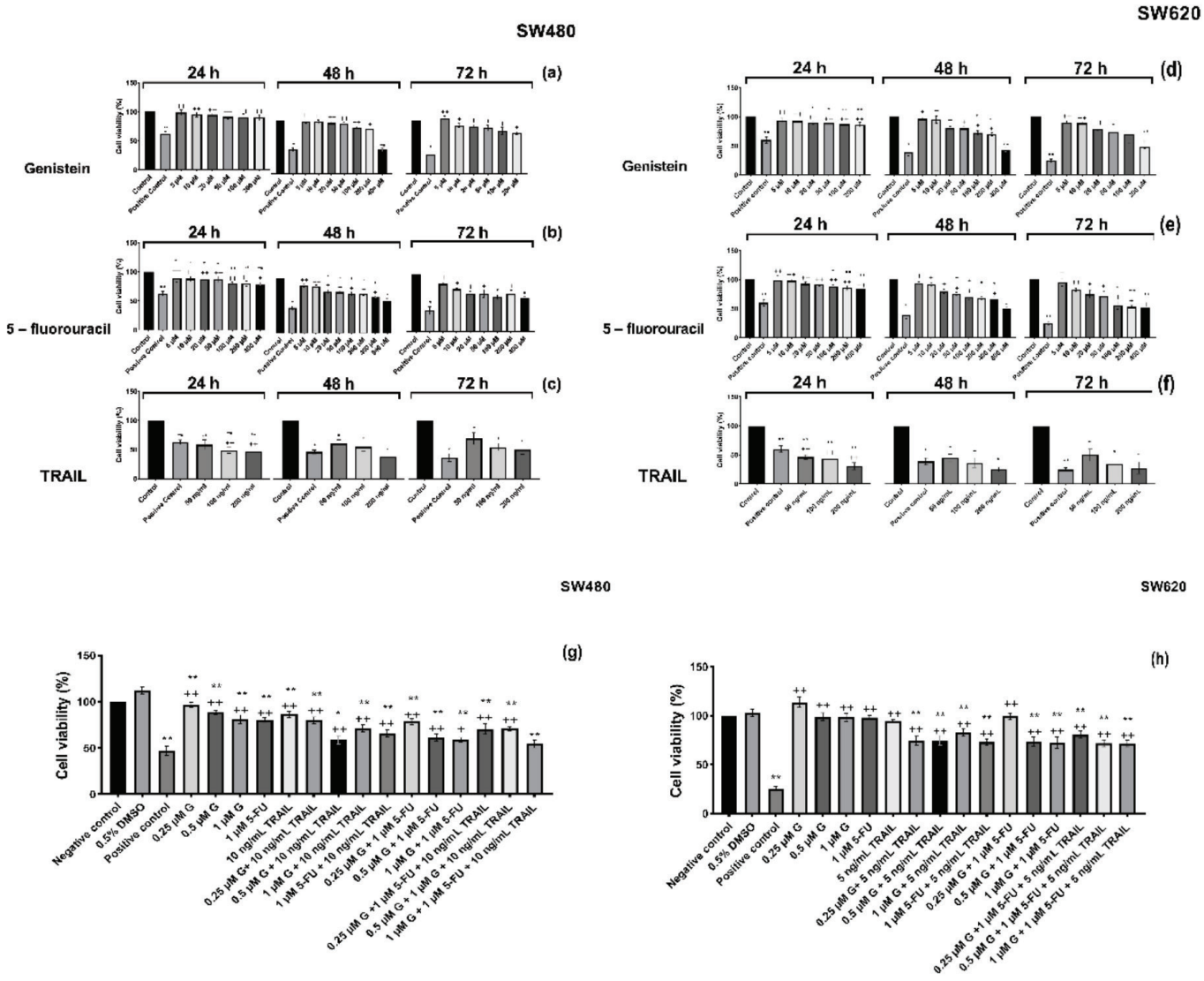

Figure 1. MTT assay results of SW480 and SW620 cells incubated with genistein, 5-fluorouracil (5-FU), and TRAIL. Effects of genistein (a), 5-FU (b), and TRAIL (c) on SW480 and genistein (d), 5-FU (e), and TRAIL (f) on SW620 cell viability for 24, 48, and 72 hours. SW480 (g) and SW620 (h) cell viability after incubation with G, 5-FU, TRAIL, and their combinations for 48 hours

*$p < 0.05$, **$p < 0.001$, indicates significant difference from the negative control. +$p < 0.05$, ++$p < 0.001$, indicates significant difference from the positive control. Results are expressed in the mean ± standard deviation, 5-FU: 5-Fluorouracil, TRAIL: Tumor necrosis factor-related apoptosis-inducing ligand

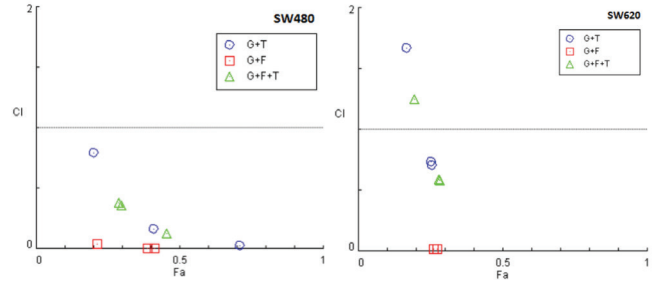

Figure 2. MTT assay results of SW480 and SW620 cells incubated with genistein **(G)**, 5-fluorouracil (5-FU) **(F)**, and TRAIL **(T)** used for calculating the CI by CompuSyn software. CI *versus* Fa graphs of double and triple combinations for interaction of G, F, and T in SW80 and SW620 cells. The values below and above the dashed line indicate synergistic and antagonistic effects, respectively

TRAIL: Tumor necrosis factor-related apoptosis-inducing ligand, CI: Combination index, Fa: Factor affected

Genistein and 5-fluorouracil sensitizes TRAIL mediated apoptosis

The effects of genistein, 5-fluorouracil, and TRAIL on the cell cycle were examined by flow cytometry (Supplementary Material 1). When compared with the negative control, the highest percentages of cells in the G0/G1 phase were the 0.5 and 1 µM genistein treated SW620 cells and SW480 cells, respectively. The highest proportions of cells in the S phase were "1 µM 5-FU + 5 ng/mL" TRAIL-treated SW620 cells and 10 ng/mL TRAIL-treated SW480 cells. Furthermore, 0.5 µM genistein and 1 µM 5-fluorouracil increased accumulation of the G2/M phase in SW480 and SW620 cells, respectively.

To examine the apoptotic mechanism of genistein and 5-fluorouracil, DR4, and DR5 surface expressions were investigated. It was found that genistein and 5-fluorouracil sensitized apoptosis *via* the induction of the expression of the

DR5 surface protein (Figure 6 and Supplementary Materials 2 and 3). The proportion of surface DR5 + s in cells treated with 5-fluorouracil was higher than that in both control and genistein-treated cells. In addition, SW480 cells were more sensitive to the apoptotic effects of genistein and 5-fluorouracil than SW620 cells.

The results of the Annexin V FITC apoptosis assay were consistent with *DR5* expression levels. The percentage of apoptotic cells significantly increased at all concentrations of genistein, 5-fluorouracil, TRAIL, and their combinations in SW480 cells. However, triple combinations of these compounds had the highest percentage of early apoptosis, and 5 ng/mL TRAIL significantly increased apoptosis in SW620 cells compared with the negative control (Figure 7).

In addition, the apoptotic mechanism was evaluated by the changes in apoptotic (*DR4* and *DR5*) and antiapoptotic (*Bcl-XL*, *Bcl-2*, *XIAP*, *DcR1*, and *DcR2*) gene expression. Genistein reduced *DcR2* expression in SW480 cells and increased *Bcl-XL*, *Bcl-2*, and *DR4* expression in SW620 cells. When genistein was applied along with the *TRAIL* ligand in SW480 cells, it was determined that *Bcl-XL*, *XIAP*, and *DR5* gene expressions increased when compared with the application of genistein and TRAIL alone. In SW620 cells, this combination was found to cause a decrease in *Bcl-XL*, *DcR1*, and *DcR2* gene expressions and an increase in *DR4* agonistic surface receptors compared with the groups in which they were administered alone. When 5-fluorouracil was administered alone, it caused a significant reduction in *XIAP* genes in SW480 cells. However, it caused significant increases in *Bcl-XL*, *Bcl-2*, *DR4*, and *DcR2* gene expression in SW620 cells.

Bcl-XL and *Bcl-2* gene expressions increased in SW480 cells treated with double and triple combinations of 5-fluorouracil,

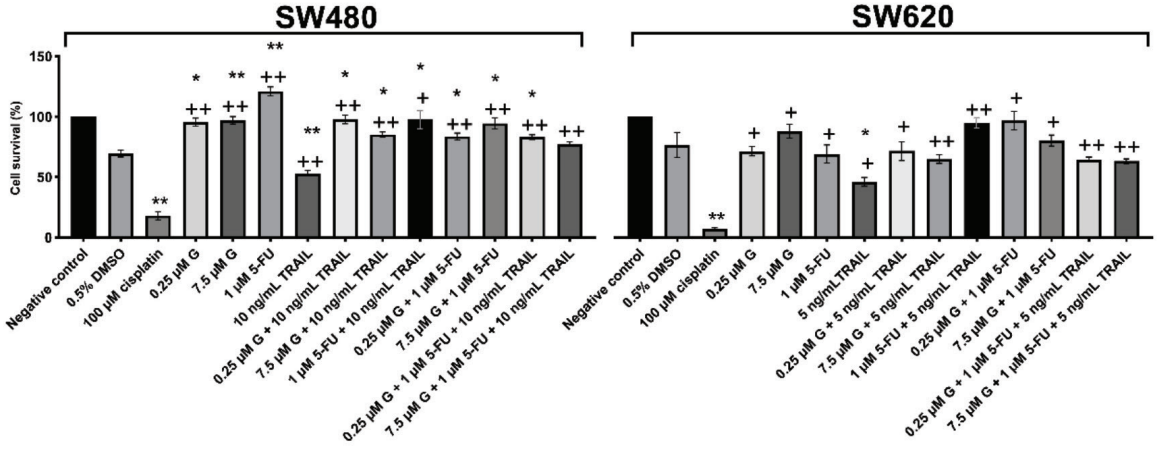

Figure 3. Effects of genistein **(G)**, 5-FU, and TRAIL on proliferation/survival in SW480 and SW620 cells using cell recovery assay

*$p < 0.05$, **$p < 0.001$, indicates a significant difference from the negative control. +$p < 0.05$, ++$p < 0.001$, indicates a significant difference from the positive control. Results are expressed in the mean ± standard deviation.

5-FU: 5-Fluorouracil, TRAIL: Tumor necrosis factor-related apoptosis-inducing ligand

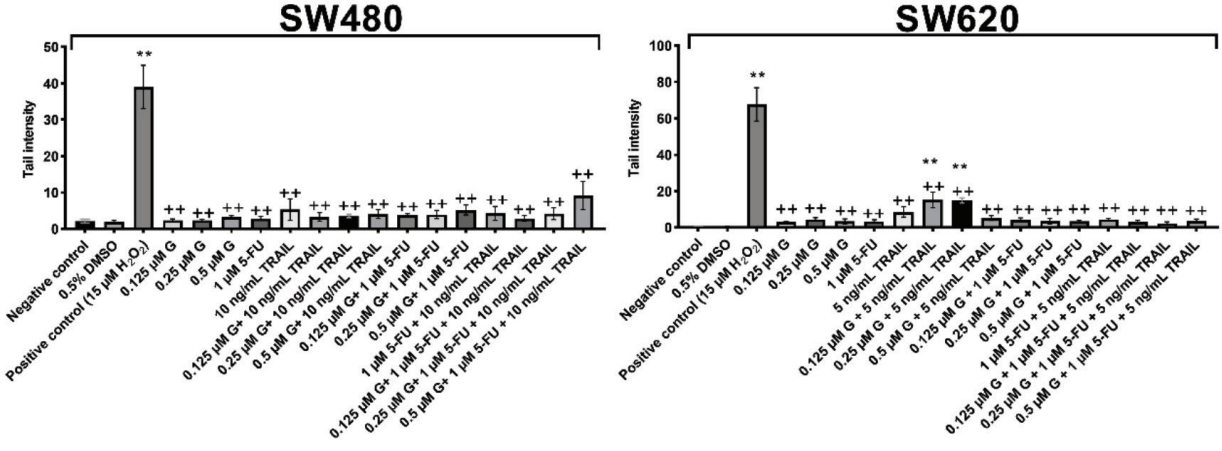

Figure 4. Tail intensity from the comet assay of SW480 and SW620 cells treated with genistein **(G)**, 5-FU, TRAIL, and their combinations for 48 hours

*$p < 0.05$, **$p < 0.001$, indicates significant difference from the negative control. +$p < 0.05$, ++$p < 0.001$, indicates significant difference from the positive control. The values are expressed in the mean ± standard deviation

5-FU: 5-Fluorouracil, TRAIL: Tumor necrosis factor-related apoptosis-inducing ligand

genistein, and TRAIL ligand; however, a significant decrease in *XIAP* gene expression was observed in all combinations when compared with the groups in which they were administered alone. Similarly, in SW620 cells, *Bcl-XL* and *Bcl-2* expressions increased and there was a decrease in *XIAP* gene expression when compared with the group in which the TRAIL ligand was applied alone (Figures 8, 9).

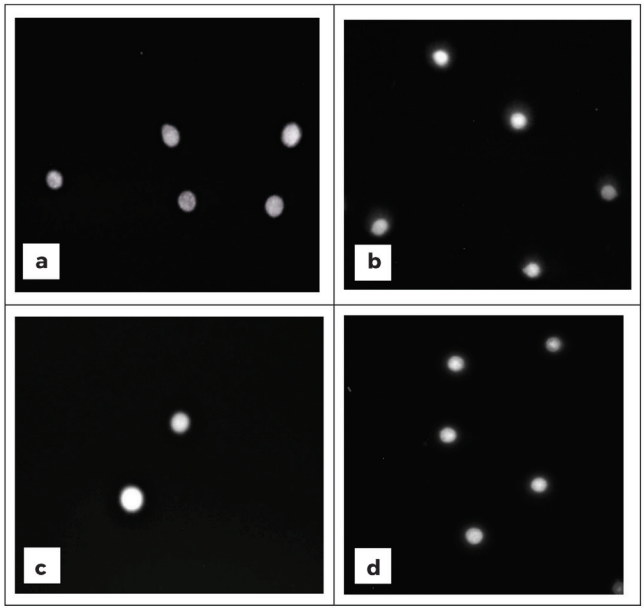

Figure 5. Comet images of SW480 (a, b) and SW620 cells (c, d)

Effects of genistein, 5-fluorouracil, and TRAIL on caspase 3-8-9 activities, MMP, and ROS levels in SW480 and SW620 cells

Caspase activities were investigated to clarify the apoptotic cell death pathway in SW480 and SW620 cells treated with genistein, 5-fluorouracil, and TRAIL. In both cell lines, the triple combination caused the most significant increase in caspase activity compared with the negative control and the groups in which they were administered separately. In addition, the genistein and TRAIL combination was found to be the most effective in increasing caspase 3, 8, and 9 activities (Figure 10).

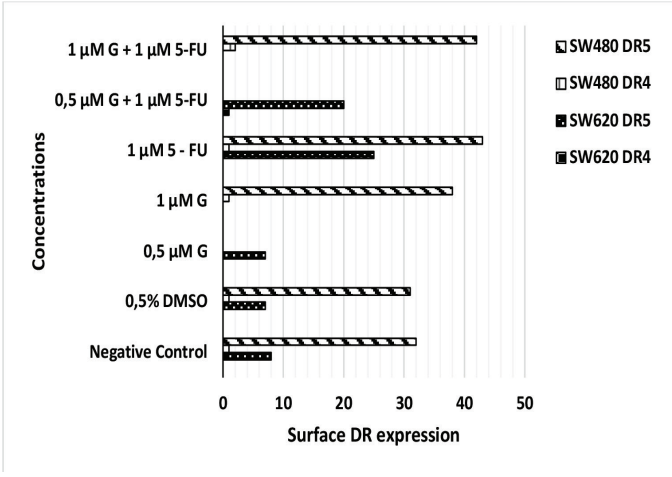

Figure 6. DR4 and DR5 surface expressions of SW480 and SW620 cells incubated with genistein **(G)** and 5-FU by flow cytometry assay

5-FU: 5-Fluorouracil

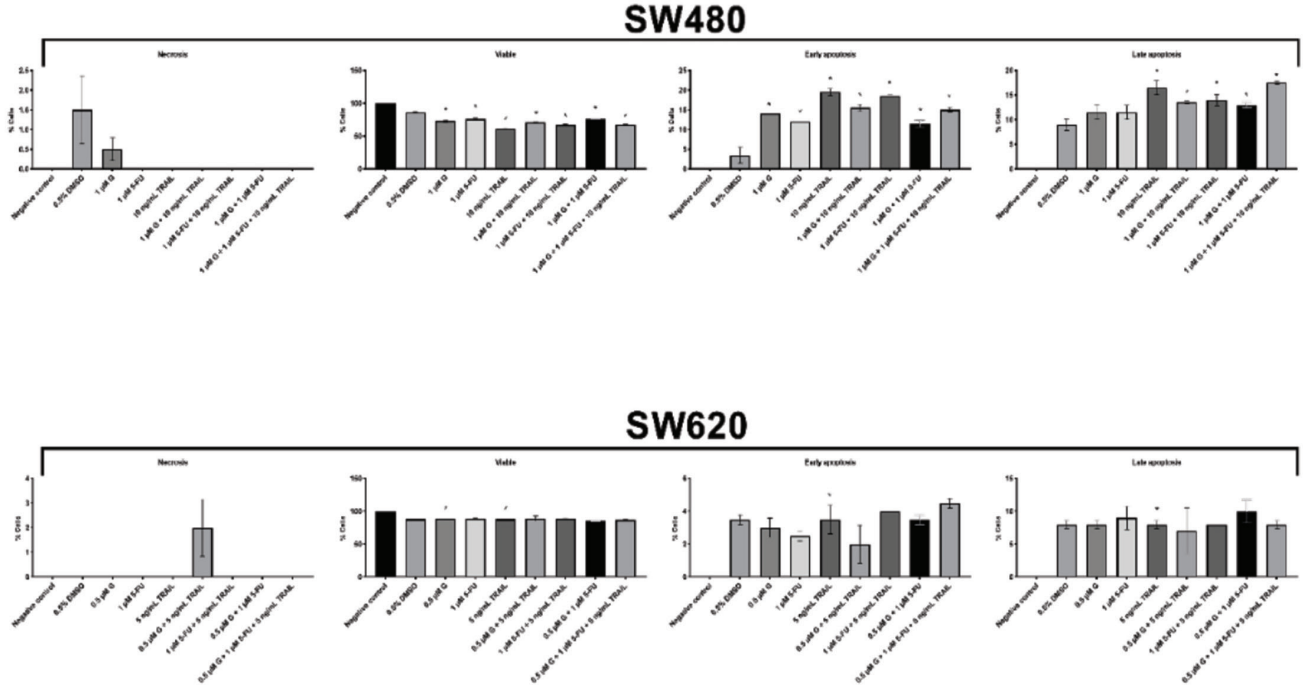

Figure. 7 Results of Annexin V FITC apoptosis assay showing apoptotic effects of genistein, 5-FU, and TRAIL in SW480 and SW620 cells. Results are presented as the mean ± standard error.

*$p < 0.05$, **$p < 0.001$, indicates a significant difference from the negative control, 5-FU: 5-Fluorouracil, TRAIL: Tumor necrosis factor-related apoptosis-inducing ligand

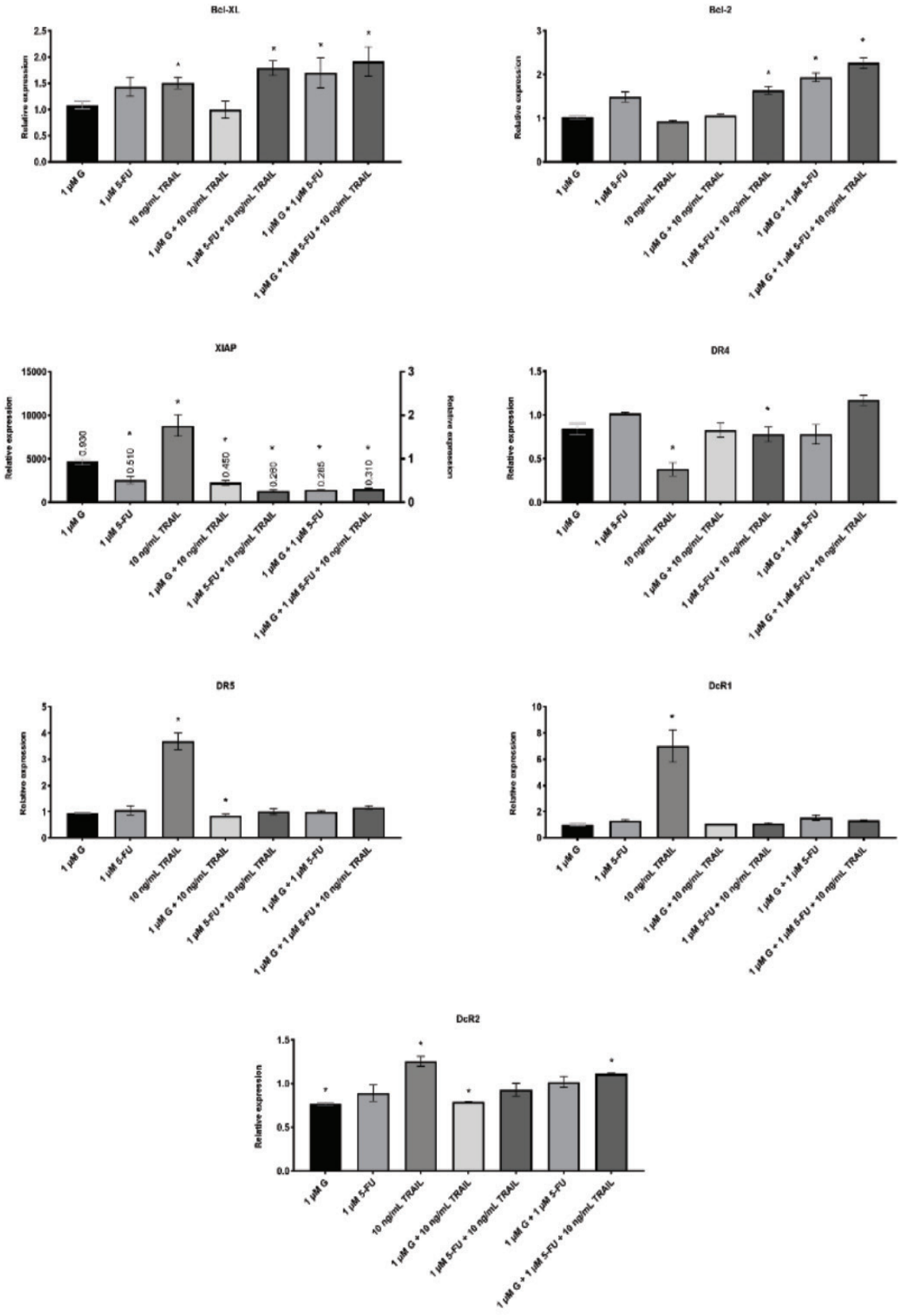

Figure. 8 Relative gene expression of SW480 cells treated with genistein **(G)**, 5-FU, TRAIL, and their combinations by RT-PCR. Results are given as the mean of fold change compared to control (negative and 0.5% DMSO control). The values indicate the mean ± standard error and normalized with *GAPDH*

*$p < 0.05$, indicates a significant difference from the negative control, TRAIL: Tumor necrosis factor-related apoptosis-inducing ligand, RT-PCR: Reverse transcription-polymerase chain reaction, DMSO: Dimethyl sulfoxide, 5-FU: 5-fluorouracil, GAPDH: Glyceraldehyde 3-phosphate dehydrogenase

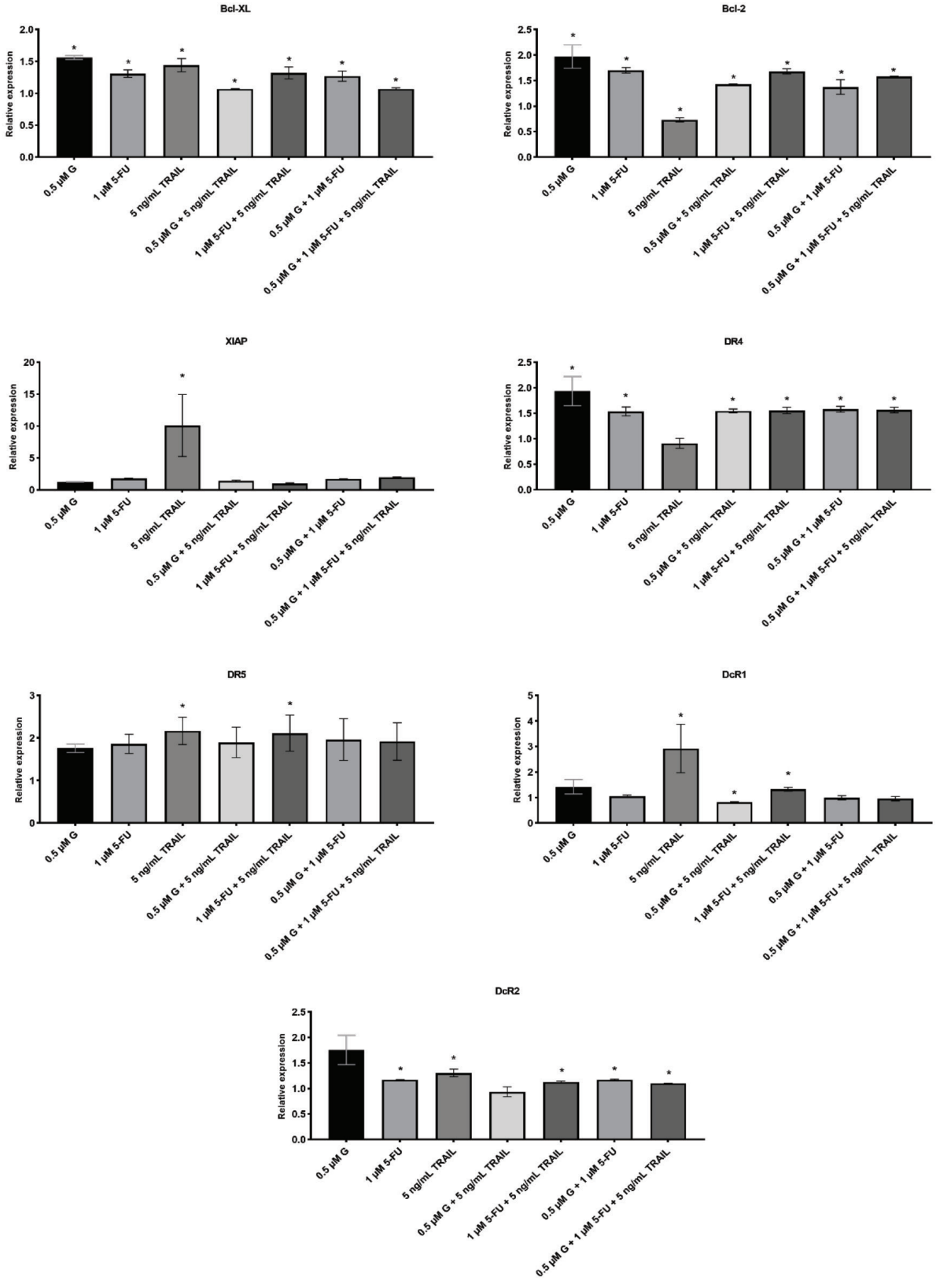

Figure 9. Relative gene expression of SW620 cells treated with genistein **(G)**, 5-FU, TRAIL, and their combinations by RT-PCR. Results are given as the mean of fold change compared with controls (negative and 0.5% DMSO control). The values indicate the mean ± standard error and are normalized with *GAPDH*

*$p < 0.05$, indicates significant difference from the negative control, 5-FU: 5-Fluorouracil, TRAIL: Tumor necrosis factor-related apoptosis-inducing ligand, RT-PCR: Reverse transcription-polymerase chain reaction, DMSO: Dimethyl sulfoxide, GAPDH: Glyceraldehyde 3-phosphate dehydrogenase

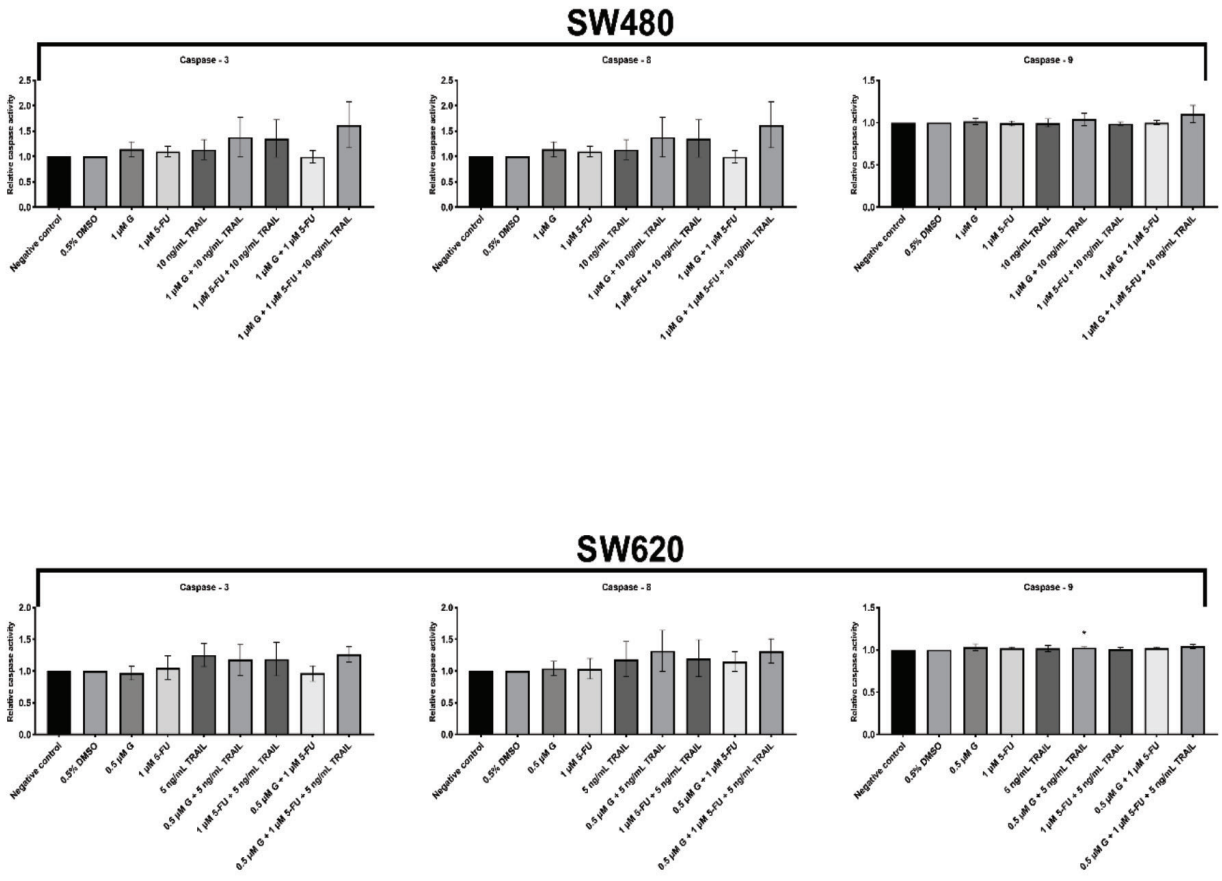

Figure 10. Caspase 3, 8, and 9 activities relative to control in SW480 and SW620 cells by Multiplex Activity Assay Kit (Abcam). Results are presented as the mean ± standard deviation

*$p < 0.05$, **$p < 0.001$, indicates significant difference from the negative control, 5-FU: 5-fluorouracil

MMP was expressed by the JC-1 fluorescence ratio showing the ratio of healthy cells to apoptotic cells. These results were statistically insignificant, but double and triple combinations of genistein and 5-fluorouracil caused the greatest reduction ratio in SW480 cells compared with the negative control and single treatments. However, genistein and TRAIL were the most effective at reducing MMP in SW620 cells (Supplementary Material 4).

ROS levels in cells treated with genistein, 5-fluorouracil, and TRAIL were evaluated to clarify the role of ROS production in the apoptotic mechanism. The percentages of ROS production increased in all studied groups compared with the negative control after 48 hours of incubation. 5-Fluorouracil caused the highest production of ROS in SW480 cells compared with the negative control. The highest ROS production was also observed in SW620 cells treated with double and triple combinations of genistein and 5-fluorouracil (Supplementary Material 5).

DISCUSSION

It is estimated that cancer is the leading cause of death today and that the incidence of cancer will continue to increase in the coming years.[32] Among the cancer types, colorectal cancer ranks second, with an estimated 881,000 deaths worldwide in 2018.[33] While the lifetime risk of colorectal cancer in the general population is approximately 5-6%, patients with familial risk comprise approximately 20% of all patients with colorectal cancer, and colorectal cancer is known to be transmitted in an autosomal dominant manner.[34] Colorectal cancer begins as a benign adenomatous polyp and progresses to invasive cancer due to inherited mechanisms such as genomic instability, DNA repair defects, tumor suppressor gene mutations, and environmental factors such as obesity, physical inactivity, and diets lacking vegetables and fruits.[35-36]

Despite the improvements in systemic treatment, the 5-year survival rate is 12.5%, and the chemotherapeutic combination applied for treating metastatic colorectal cancer fails because of treatment resistance seen in 90% of the patients.[37] Therefore, it is important to determine the treatment resistance mechanisms.[38] Based on the fact that defects in apoptotic processes also cause resistance to anticarcinogens and radiotherapy,[39] the effects of genistein, 5-fluorouracil, and TRAIL were evaluated alone or in double/triple combinations in SW480 and SW620 cell lines to determine, if they had synergistic apoptotic effects.

Genistein, a major phytoestrogen in soybeans, has attracted attention as an anticarcinogen because epidemiological studies have shown that soybean consumption is associated with reduced cancer incidence. In addition, genistein has a place in phase II clinical trials for the treatment of a variety of human cancers. Genistein has a synergistic effect on endogenous hormones such as estradiol through its metabolite formed by intestinal microbiota metabolism. In contrast, it has an antagonistic effect on estrogen receptors such as Erα and Erβ.[40] Genistein has a 30-fold greater affinity for Erβ receptors than for Erα receptors.[41] ERs regulate gene expression as transcription factors that bind to DNA, and their activities vary depending on the cell type and Erα/Erβ ratio.[41,42] Erβ inhibits cell proliferation by suppressing the activity of Erα.[41] While Erα expression is low in normal colon cells and cancer cells, Erβ level varies inversely with the stage of the disease in cancer cells compared with normal cells.[43] Erβ expression in sw480 cells, Erα and Erβ expression both in sw620 cells.[44] In a study by Hartman et al.[31] in SW480 cells, it was determined that the proliferation of Erβ-transduced cells decreased compared with that of control cells.[45] In another study, the effects of 17β estradiol and 5-fluorouracil alone and in combination were investigated in SW480 and SW620 cells. It has been determined that estradiol alone causes cell accumulation in the SubG1 phase more effectively in SW620 cells and increases the induction of apoptosis. However, the anticancer effect of the combination was higher in SW480 cells.[44] These studies show that the Erβ receptor has an important place in treating colon cancer in terms of the anticancer effect of genistein. Previous studies have shown that genistein increases the cell growth inhibition and apoptotic effects of chemotherapeutic drugs such as doxorubicin, paclitaxel, and cisplatin.[9,14,46,47] Genistein acts as a protein tyrosine kinase (EGFR, insulin receptor) inhibitor that regulates protein phosphorylation and is effective in processes such as differentiation, angiogenesis, metastasis, and apoptosis through pathways such as Akt, NFκB, and ERK1/2.[11,48,49] In a study by Qi et al.,[50] genistein inhibited EGF-induced loss of *FOXO3* that led to increased p27kip1 (cell cycle inhibitor) expression activity by targeting the PI3K/Akt pathway.[50] In addition, genistein inhibited cell invasion and migration of colon cancer cells by regulating the expression of migration-associated factors and genes (MMP9, E-cadherin, β-catenin, c-Myc, and cyclin D1).[51] Genistein causes DNA strand breaks and induction of apoptosis through topoisomerase inhibition, which occurs in steps such as DNA replication and recombination.[52] Genistein inhibits adipogenesis by inducing peroxisome proliferator-activated receptor-γ (PPARγ), a transcriptional factor for adipogenesis, through activating Erα or Erβ.[53] The increased PPARγ expression leads to an anti-inflammatory effect by decreasing prostaglandin E_2 and cyclooxygenase-2. In addition, genistein induces the apoptotic pathway *via* PPARγ, including *Bcl-2*, phosphatase and tensin homolog, survivin, and cyclin B1.[54]

A study of NCM460 colon mucosa epithelial cells and HT29, SW620, LoVo, and HCT116 colon cancer cell lines by Zhu et al.[55] found that genistein inhibits cell vitality proportionally to concentration and incubation time, reducing HT29 cell viability by 38% after 72 hours of incubation. In other studies conducted on HT29 cells, it was determined that 72 hours of incubation with 60 μM genistein resulted in 67.3% cell viability, and 47% in 200 μM and 48 hours of incubation. In another study, the IC_{50} value was 50 μM for 48 hours, showing that the effects of genistein depend on the properties of cell lines.[50,56-58] The cytotoxic effects of 5-fluorouracil in colorectal cancer cells are also known.[59,60] In our study, the effects of genistein, 5-fluorouracil, and TRAIL were evaluated in SW480 and SW620 cells. They reduced cell viability in a dose-dependent manner. As reported previously, SW480 cells were found to be less sensitive to 5-FU-induced cell growth inhibition. However, contrary to the literature,[5,61-63] SW480 cells were more resistant to the inhibitory effects of TRAIL than SW620 cells, which may be the result of more *XIAP* expression ($p < 0.05$), as the TRAIL resistance mechanism is known for.[64] Genistein, 5-fluorouracil, and TRAIL in double and triple combinations had synergistic effects on reducing the cell viability and recovery ability of SW480 and SW620 cells showing apoptotic changes.[29] Furthermore, this effect was determined by an Annexin V FITC assay and the highest early apoptotic cell percentage was observed in SW620 cells treated with the triple combination and in SW480 cells treated with the 5-fluorouracil + TRAIL combination. Studies show the synergistic effects of double combinations of these compounds for various types of cancer.[65-68] However, the effects of triple combinations of subtoxic concentrations and double combinations in the concentrations we studied were not evaluated previously in SW620 and SW480 cells. In the current study, genistein and 5-fluorouracil caused the activation of G0/G1 and G2/M cell cycle arrest, which are known to be the checkpoints for DNA damage,[69] and prevented mitosis by the inactivation of CDK.[14,15,57,70] In addition, combinations of genistein, 5-fluorouracil, and TRAIL caused increased S cycle arrest, which is known to cause DNA damage, compared with both cell lines treated with single compounds.[71] In addition, DNA damage that may be caused by ROS production[72] induced by genistein, 5-fluorouracil, and TRAIL supported the results regarding cell cycle and apoptosis.

In our study, we demonstrated that genistein and 5-fluorouracil sensitized SW480 and SW620 cells to TRAIL-induced apoptosis *via* DR5 agonistic surface receptors and DR5 gene expression in accordance with the literature.[73,74] Additionally, it was observed that *DcR1* and *XIAP* antiapoptotic gene expressions in double and triple combinations of the studied compounds decreased significantly compared with the group in which TRAIL was applied alone in both cell lines. When caspase 3, 8, and 9 activities and MMP were investigated to explain the apoptotic mechanism, it was also found that triple combinations of the compounds were the most effective in reducing MMP in SW480 cells and in increasing caspase activities in both cell lines. Previous studies have shown that genistein[73,75] and 5-fluorouracil[67,74] sensitized TRAIL-induced apoptosis by increasing caspase activity and the loss of MMP, decreasing *XIAP* gene expression, which plays a critical role in the suppression of apoptosis.[76] ROS production leads to mitochondria-derived apoptosis induction, which leads

to cytochrome c release interacting with caspase 9 and the binding of TRAIL to death receptors initiates the caspase 8-3 cascade,[19,75,77] in accordance with our results. However, it was observed that the concentrations of the compounds used in our study were insufficient for the expected reduction effect on *Bcl-XL* and *Bcl-2* gene expression.

Study limitations

It has been determined that genistein, 5-fluorouracil and TRAIL have more cytotoxic, genotoxic, and apoptotic effects in combination and show synergistic effects together. These effects may contribute to the resistance problem that may occur in treating colorectal cancer with an increase in ROS, a decrease in MMP, and an increase in caspase 3, 8, and 9. However, the combination concentrations should be chosen from a slightly higher range to see the expected synergistic effect as statistically significant.

CONCLUSION

In conclusion, genistein and 5-fluorouracil sensitized TRAIL-induced apoptosis *via* the DR5 surface receptor protein in SW480 and SW620 cells. The induction of DNA damage and ROS production, increased caspase activities, decreased MMP, and decreased *XIAP* and *DcR1* gene expression may play a role in the apoptotic mechanism of a combination of genistein, 5-fluorouracil, and TRAIL. It is thought that combinations of these compounds at subtoxic dosage levels may contribute to the resistance problem for colorectal cancer treatment.

Acknowledgment

This work was supported by The Scientific and Technological Research Council of Türkiye (TÜBİTAK) under grant number: 219S200 and Hacettepe University Scientific Research Projects Coordination Unit under grant number TDK-2019-18077.

Ethics

Ethics Committee Approval: Not necessary.

Informed Consent: Not necessary.

Authorship Contributions

Concept: T.Ç.D., S.A.D., H.C., Ü.Ü.B., Design: T.Ç.D., S.A.D., H.C., Ü.Ü.B., Data Collection or Processing: T.Ç.D., Analysis or Interpretation: T.Ç.D., S.A.D., Ü.Ü.B., Literature Search: T.Ç.D., Writing: T.Ç.D., Ü.Ü.B.,

Conflict of Interest: No conflict of interest was declared by the authors.

Financial Disclosure: This work was supported by the Scientific and Technological Research Council of Türkiye (TÜBİTAK) under Grant number 219S200 and Hacettepe University Scientific Research Projects Coordination Unit under Grant Number TDK-2019-18077.

REFERENCES

1. Spagnuolo C, Russo GL, Orhan IE, Habtemariam S, Daglia M, Sureda A, Nabavi SF, Devi KP, Loizzo MR, Tundis R, Nabavi SM. Genistein and cancer: current status, challenges, and future directions. Adv Nutr. 2015;6:408-419.
2. Rossi M, Jahanzaib Anwar M, Usman A, Keshavarzian A, Bishehsari F. Colorectal cancer and alcohol consumption-populations to molecules. Cancers (Basel). 2018;10:38.
3. Macrae FA.. Colorectal cancer: Epidemiology, risk factors, and protective factors. https://medilib.ir/uptodate/show/2606
4. Gültekin M, Boztaş G. Türkiye kanser istatistikleri. Sağlık Bakanlığı, Türkiye Halk Sağlığı Kurumu. 2014;43:12-32.
5. Chen X, Gu J, Wu Y, Liang P, Shen M, Xi J, Qin J. Clinical characteristics of colorectal cancer patients and anti-neoplasm activity of genistein. Biomed Pharmacother. 2020;124:109835.
6. Chen X, Wu Y, Gu J, Liang P, Shen M, Xi J, Qin J. Anti-invasive effect and pharmacological mechanism of genistein against colorectal cancer. Biofactors. 2020;46:620-628.
7. Zhang HH, Guo XL. Combinational strategies of metformin and chemotherapy in cancers. Cancer Chemother Pharmacol. 2016;78:13-26.
8. Bontempo P, Rigano D, Doto A, Formisano C, Conte M, Nebbioso A, Carafa V, Caserta G, Sica V, Molinari AM, Altucci L. *Genista sessilifolia* DC. extracts induce apoptosis across a range of cancer cell lines. Cell Prolif. 2013;46:183-192.
9. Dixon RA, Ferreira D. Genistein. Phytochemistry. 2002;60:205-211.
10. Sarkar FH, Li Y. Mechanisms of cancer chemoprevention by soy isoflavone genistein. Cancer Metastasis Rev. 2002;21:265-280.
11. Qin J, Chen JX, Zhu Z, Teng JA. Genistein inhibits human colorectal cancer growth and suppresses miR-95, Akt and SGK1. Cell Physiol Biochem. 2015;35:2069-2077.
12. Pavese JM, Farmer RL, Bergan RC. Inhibition of cancer cell invasion and metastasis by genistein. Cancer Metastasis Rev. 2010;29:465-482.
13. Zhang Z, Jin F, Lian X, Li M, Wang G, Lan B, He H, Liu GD, Wu Y, Sun G, Xu CX, Yang ZZ. Genistein promotes ionizing radiation-induced cell death by reducing cytoplasmic *Bcl-xL* levels in non-small cell lung cancer. Sci Rep. 2018;8:328.
14. Park OJ, Surh YJ. Chemopreventive potential of epigallocatechin gallate and genistein: evidence from epidemiological and laboratory studies. Toxicol Lett. 2004;150:43-56.
15. Mukund V, Mukund D, Sharma V, Mannarapu M, Alam A. Genistein: its role in metabolic diseases and cancer. Crit Rev Oncol Hematol. 2017;119:13-22.
16. Yuan X, Gajan A, Chu Q, Xiong H, Wu K, Wu GS. Developing TRAIL/TRAIL death receptor-based cancer therapies. Cancer Metastasis Rev. 2018;37:733-748.
17. Jung EM, Lim JH, Lee TJ, Park JW, Choi KS, Kwon TK. Curcumin sensitizes tumor necrosis factor-related apoptosis-inducing ligand (TRAIL)-induced apoptosis through reactive oxygen species-mediated upregulation of death receptor 5 (DR5). Carcinogenesis. 2005;26:1905-1913.
18. Wu GS. TRAIL as a target in anti-cancer therapy. Cancer Lett. 2009;285:1-5.
19. Wang S, El-Deiry WS. TRAIL and apoptosis induction by TNF-family death receptors. Oncogene. 2003;22:8628-8633.
20. Ozören N, Fisher MJ, Kim K, Liu CX, Genin A, Shifman Y, Dicker DT, Spinner NB, Lisitsyn NA, El-Deiry WS. Homozygous deletion of the death receptor DR4 gene in a nasopharyngeal cancer cell line is associated with TRAIL resistance. Int J Oncol. 2000;16:917-942.

21. Szliszka E, Zydowicz G, Mizgala E, Krol W. Artepillin C (3,5-diprenyl-4-hydroxycinnamic acid) sensitizes LNCaP prostate cancer cells to TRAIL-induced apoptosis. Int J Oncol. 2012;41:818-828.
22. Tang SY, Zhong MZ, Yuan GJ, Hou SP, Yin LL, Jiang H, Yu ZY. Casticin, a flavonoid, potentiates TRAIL-induced apoptosis through modulation of anti-apoptotic proteins and death receptor 5 in colon cancer cells. Oncol Rep. 2013;29:474-480.
23. Yoshida T, Horinaka M, Sakai T. "Combination-oriented molecular-targeting prevention" of cancer: a model involving the combination of TRAIL and a DR5 inducer. Environ Health Prev Med. 2010;15:203-210.
24. Meyerhardt JA, Mayer RJ. Systemic therapy for colorectal cancer. N Engl J Med. 2005;352:476-487.
25. Kumar P, Nagarajan A, Uchil PD. Analysis of cell viability by the MTT assay. Cold Spring Harb Protoc. 2018:2018.
26. Mosmann T. Rapid colorimetric assay for cellular growth and survival: application to proliferation and cytotoxicity assays. J Immunol Methods. 1983;65:55-63.
27. Ferrari M, Fornasiero MC, Isetta AM. MTT colorimetric assay for testing macrophage cytotoxic activity *in vitro*. J Immunol Methods. 1990;131:165-172.
28. Zhang T, Qu S, Shi Q, He D, Jin X. Evodiamine induces apoptosis and enhances TRAIL-induced apoptosis in human bladder cancer cells through mTOR/S6K1-mediated downregulation of Mcl-1. Int J Mol Sci. 2014;15:3154-3171.
29. Li L, Aggarwal BB, Shishodia S, Abbruzzese J, Kurzrock R. Nuclear factor-kappaB and IkappaB kinase are constitutively active in human pancreatic cells, and their down-regulation by curcumin (diferuloylmethane) is associated with the suppression of proliferation and the induction of apoptosis. Cancer. 2004;101:2351-2362.
30. Singh NP, McCoy MT, Tice RR, Schneider EL. A simple technique for quantitation of low levels of DNA damage in individual cells. Exp Cell Res. 1988;175:184-191.
31. Hartmann A, Kiskinis E, Fjällman A, Suter W. Influence of cytotoxicity and compound precipitation on test results in the alkaline comet assay. Mutat Res. 2001;497:199-212.
32. Ferlay J, Soerjomataram I, Dikshit R, Eser S, Mathers C, Rebelo M, Parkin DM, Forman D, Bray F. Cancer incidence and mortality worldwide: sources, methods and major patterns in GLOBOCAN 2012. Int J Cancer. 2015;136:359-386.
33. Rawla P, Sunkara T, Barsouk A. Epidemiology of colorectal cancer: incidence, mortality, survival, and risk factors. Prz Gastroenterol. 2019;14:89-103.
34. Lynch HT, de la Chapelle A. Hereditary colorectal cancer. N Engl J Med. 2003;348:919-932.
35. Markowitz SD, Bertagnolli MM. Molecular origins of cancer: molecular basis of colorectal cancer. N Engl J Med. 2009;361:2449-2460.
36. Center MM, Jemal A, Smith RA, Ward E. Worldwide variations in colorectal cancer. CA Cancer J Clin. 2009;59:366-378.
37. Hammond WA, Swaika A, Mody K. Pharmacologic resistance in colorectal cancer: a review. Ther Adv Med Oncol. 2016;8:57-84.
38. Temraz S, Mukherji D, Alameddine R, Shamseddine A. Methods of overcoming treatment resistance in colorectal cancer. Crit Rev Oncol Hematol. 2014;89:217-230.
39. Van Geelen CM, de Vries EG, de Jong S. Lessons from TRAIL-resistance mechanisms in colorectal cancer cells: paving the road to patient-tailored therapy. Drug Resist Updat. 2004;7:345-358.
40. Sharifi-Rad J, Quispe C, Imran M, Rauf A, Nadeem M, Gondal TA, Ahmad B, Atif M, Mubarak MS, Sytar O, Zhilina OM, Garsiya ER, Smeriglio A, Trombetta D, Pons DG, Martorell M, Cardoso SM, Razis AFA, Sunusi U, Kamal RM, Rotariu LS, Butnariu M, Docea AO, Calina D. Genistein: an integrative overview of its mode of action, pharmacological properties, and health benefits. Oxid Med Cell Longev. 2021;2021:32668136.
41. Taylor CK, Levy RM, Elliott JC, Burnett BP. The effect of genistein aglycone on cancer and cancer risk: a review of *in vitro*, preclinical, and clinical studies. Nutr Rev. 2009;67:398-415.
42. Edvardsson K, Ström A, Jonsson P, Gustafsson JÅ, Williams C. Estrogen receptor β induces antiinflammatory and antitumorigenic networks in colon cancer cells. Mol Endocrinol. 2011;25:969-979.
43. Barzi A, Lenz AM, Labonte MJ, Lenz HJ. Molecular pathways: estrogen pathway in colorectal cancer. Clin Cancer Res. 2013;19:5842-5848.
44. Mahbub AA. 17β-Estradiol enhances 5-fluorouracil anti-cancer activities in colon cancer cell lines. Med Sci (Basel). 2022;10:62.
45. Hartman J, Edvardsson K, Lindberg K, Zhao C, Williams C, Ström A, Gustafsson JA. Tumor repressive functions of estrogen receptor beta in SW480 colon cancer cells. Cancer Res. 2009;69:6100-6106.
46. Zhang L, Ma X, Dong Y. Effect of genistein on apoptosis of lung adenocarcinoma A549 cells and expression of apoptosis factors. J BUON. 2018;23:641-646.
47. Banerjee S, Li Y, Wang Z, Sarkar FH. Multi-targeted therapy of cancer by genistein. Cancer Lett. 2008;269:226-242.
48. Yan GR, Xiao CL, He GW, Yin XF, Chen NP, Cao Y, He QY. Global phosphoproteomic effects of natural tyrosine kinase inhibitor, genistein, on signaling pathways. Proteomics. 2010;10:976-986.
49. Gruca A, Krawczyk Z, Szeja W, Grynkiewicz G, Rusin A. Synthetic genistein glycosides inhibiting EGFR phosphorylation enhance the effect of radiation in HCT 116 colon cancer cells. Molecules. 2014;19:18558-18573.
50. Qi W, Weber CR, Wasland K, Savkovic SD. Genistein inhibits the proliferation of colon cancer cells by attenuating a negative effect of epidermal growth factor on tumor suppressor *FOXO3* activity. BMC Cancer. 2011;11:219.
51. Rendón JP, Cañas AI, Correa E, Bedoya-Betancur V, Osorio M, Castro C, Naranjo TW. Evaluation of the effects of genistein *in vitro* as a chemopreventive agent for colorectal cancer-strategy to improve its efficiency when administered orally. Molecules. 2022;27:7042.
52. Zhou N, Yan Y, Li W, Wang Y, Zheng L, Han S, Yan Y, Li Y. Genistein inhibition of topoisomerase II alpha expression participated by *Sp1* and *Sp3* in HeLa cell. Int J Mol Sci. 2009;10:3255-3268.
53. Zhang LY, Xue HG, Chen JY, Chai W, Ni M. Genistein induces adipogenic differentiation in human bone marrow mesenchymal stem cells and suppresses their osteogenic potential by upregulating PPARγ. Exp Ther Med. 2016;11:1853-1858.
54. Tuli HS, Tuorkey MJ, Thakral F, Sak K, Kumar M, Sharma AK, Sharma U, Jain A, Aggarwal V, Bishayee A. Molecular mechanisms of action of genistein in cancer: recent advances. Front Pharmacol. 2019;10:1336.
55. Zhu J, Ren J, Tang L. Genistein inhibits invasion and migration of colon cancer cells by recovering *WIF1* expression. Mol Med Rep. 2018;17:7265-7273.

56. Liang YS, Qi WT, Guo W, Wang CL, Hu ZB, Li AK. Genistein and daidzein induce apoptosis of colon cancer cells by inhibiting the accumulation of lipid droplets. Food Nutr Res. 2018:62.
57. Yu Z, Li W, Liu F. Inhibition of proliferation and induction of apoptosis by genistein in colon cancer HT-29 cells. Cancer Lett. 2004;215:159-166.
58. Shafiee G, Saidijam M, Tavilani H, Ghasemkhani N, Khodadadi I. Genistein induces apoptosis and inhibits proliferation of HT29 colon cancer cells. Int J Mol Cell Med. 2016;5:178-191.
59. Sasaki K, Tsuno NH, Sunami E, Tsurita G, Kawai K, Okaji Y, Nishikawa T, Shuno Y, Hongo K, Hiyoshi M, Kaneko M, Kitayama J, Takahashi K, Nagawa H. Chloroquine potentiates the anti-cancer effect of 5-fluorouracil on colon cancer cells. BMC Cancer. 2010;10:370.
60. Toden S, Okugawa Y, Jascur T, Wodarz D, Komarova NL, Buhrmann C, Shakibaei M, Boland CR, Goel A. Curcumin mediates chemosensitization to 5-fluorouracil through miRNA-induced suppression of epithelial-to-mesenchymal transition in chemoresistant colorectal cancer. Carcinogenesis. 2015;36:355-367.
61. Du Q, Wang Y, Liu C, Wang H, Fan H, Li Y, Wang J, Zhang X, Lu J, Ji H, Hu R. Chemopreventive activity of GEN-27, a genistein derivative, in colitis-associated cancer is mediated by p65-CDX2-β-catenin axis. Oncotarget. 2016;7:17870-17884.
62. Mhaidat NM, Bouklihacene M, Thorne RF. 5-Fluorouracil-induced apoptosis in colorectal cancer cells is caspase-9-dependent and mediated by activation of protein kinase C-δ. Oncol Lett. 2014;8:699-704.
63. Kong CK, Lam WS, Chiu LC, Ooi VE, Sun SS, Wong YS. A rice bran polyphenol, cycloartenyl ferulate, elicits apoptosis in human colorectal adenocarcinoma SW480 and sensitizes metastatic SW620 cells to TRAIL-induced apoptosis. Biochem Pharmacol. 2009;77:1487-1496.
64. Trivedi R, Mishra DP. Trailing TRAIL resistance: novel targets for TRAIL sensitization in cancer cells. Front Oncol. 2015;5:69.
65. Suzuki R, Kang Y, Li X, Roife D, Zhang R, Fleming JB. Genistein potentiates the antitumor effect of 5-fluorouracil by inducing apoptosis and autophagy in human pancreatic cancer cells. Anticancer Res. 2014;34:4685-4692.
66. Hwang JT, Ha J, Park OJ. Combination of 5-fluorouracil and genistein induces apoptosis synergistically in chemo-resistant cancer cells through the modulation of AMPK and COX-2 signaling pathways. Biochem Biophys Res Commun. 2005;332:433-440.
67. Nazim UM, Rasheduzzaman M, Lee YJ, Seol DW, Park SY. Enhancement of TRAIL-induced apoptosis by 5-fluorouracil requires activating *Bax* and *p53* pathways in TRAIL-resistant lung cancers. Oncotarget. 2017;8:18095-18105.
68. Nazim UM, Park SY. Genistein enhances TRAIL-induced cancer cell death *via* inactivation of autophagic flux. Oncol Rep. 2015;34:2692-2698.
69. Li MH, Ito D, Sanada M, Odani T, Hatori M, Iwase M, Nagumo M. Effect of 5-fluorouracil on G1 phase cell cycle regulation in oral cancer cell lines. Oral Oncol. 2004;40:63-70.
70. Yoshikawa R, Kusunoki M, Yanagi H, Noda M, Furuyama JI, Yamamura T, Hashimoto-Tamaoki T. Dual antitumor effects of 5-fluorouracil on the cell cycle in colorectal carcinoma cells: a novel target mechanism concept for pharmacokinetic modulating chemotherapy. Cancer Res. 2001;61:1029-1037.
71. De Angelis PM, Svendsrud DH, Kravik KL, Stokke T. Cellular response to 5-fluorouracil (5-FU) in 5-FU-resistant colon cancer cell lines during treatment and recovery. Mol Cancer. 2006;5:20.
72. Srinivas US, Tan BWQ, Vellayappan BA, Jeyasekharan AD. ROS and the DNA damage response in cancer. Redox Biol. 2019;25:101084.
73. Jin CY, Park C, Kim GY, Lee SJ, Kim WJ, Choi YH. Genistein enhances TRAIL-induced apoptosis through inhibition of *p38* MAPK signaling in human hepatocellular carcinoma Hep3B cells. Chem Biol Interact. 2009;180:143-150.
74. Yang L, Wang Y, Zheng H, Zhang D, Wu X, Sun G, Yang T. Low-dose 5-fluorouracil sensitizes HepG2 cells to TRAIL through TRAIL receptor DR5 and survivin-dependent mechanisms. J Chemother. 2017;29:179-188.
75. Jin CY, Park C, Cheong J, Choi BT, Lee TH, Lee JD, Lee WH, Kim GY, Ryu CH, Choi YH. Genistein sensitizes TRAIL-resistant human gastric adenocarcinoma AGS cells through activation of caspase-3. Cancer Lett. 2007;257:56-64.
76. Deveraux QL, Leo E, Stennicke HR, Welsh K, Salvesen GS, Reed JC. Cleavage of human inhibitor of apoptosis protein *XIAP* results in fragments with distinct specificities for caspases. EMBO J. 1999;18:5242-5251.
77. Simon HU, Haj-Yehia A, Levi-Schaffer F. Role of reactive oxygen species (ROS) in apoptosis induction. Apoptosis. 2000;5:415-418.

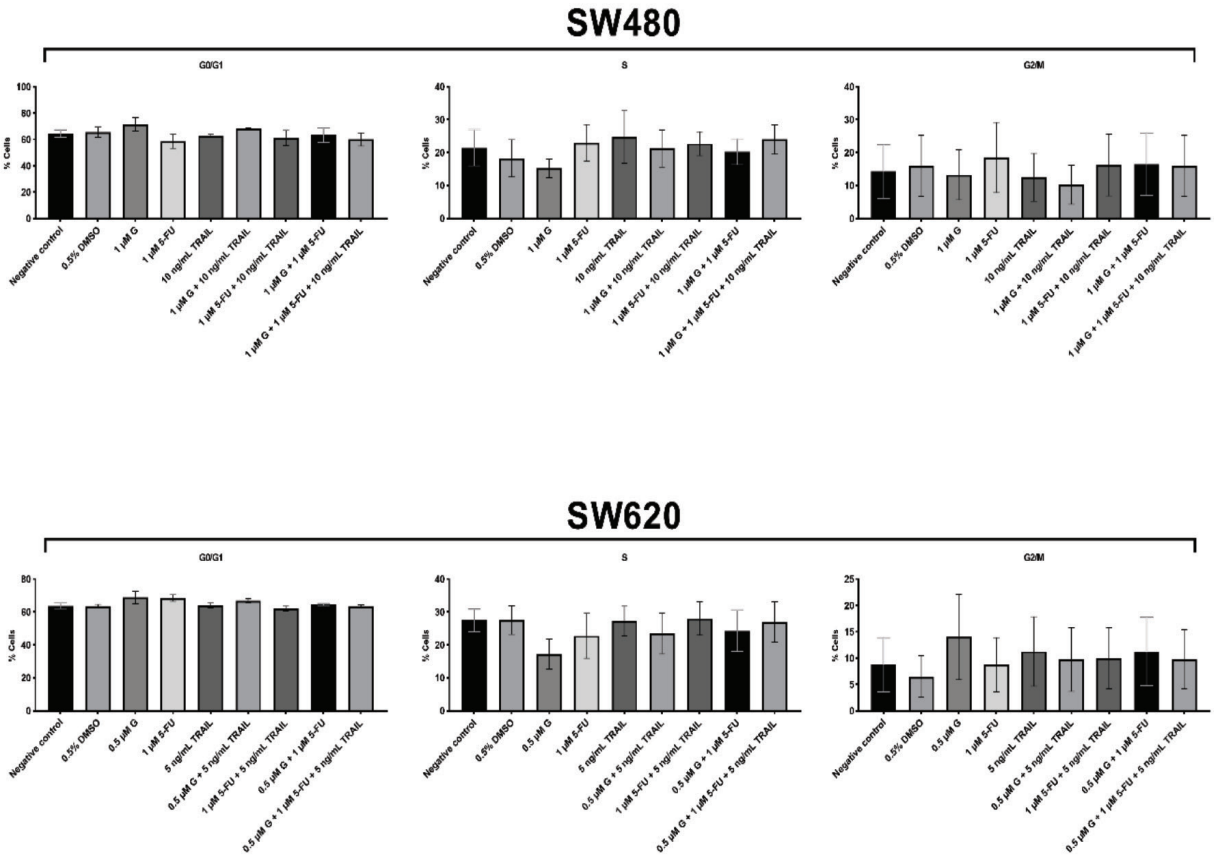

Supplementary Material 1. Effects of genistein, 5-FU, and TRAIL on the cell cycle in SW480 and SW620 cells examined by flow cytometry
5-FU: 5-Fluorouracil, TRAIL: Tumor necrosis factor-related apoptosis-inducing ligand

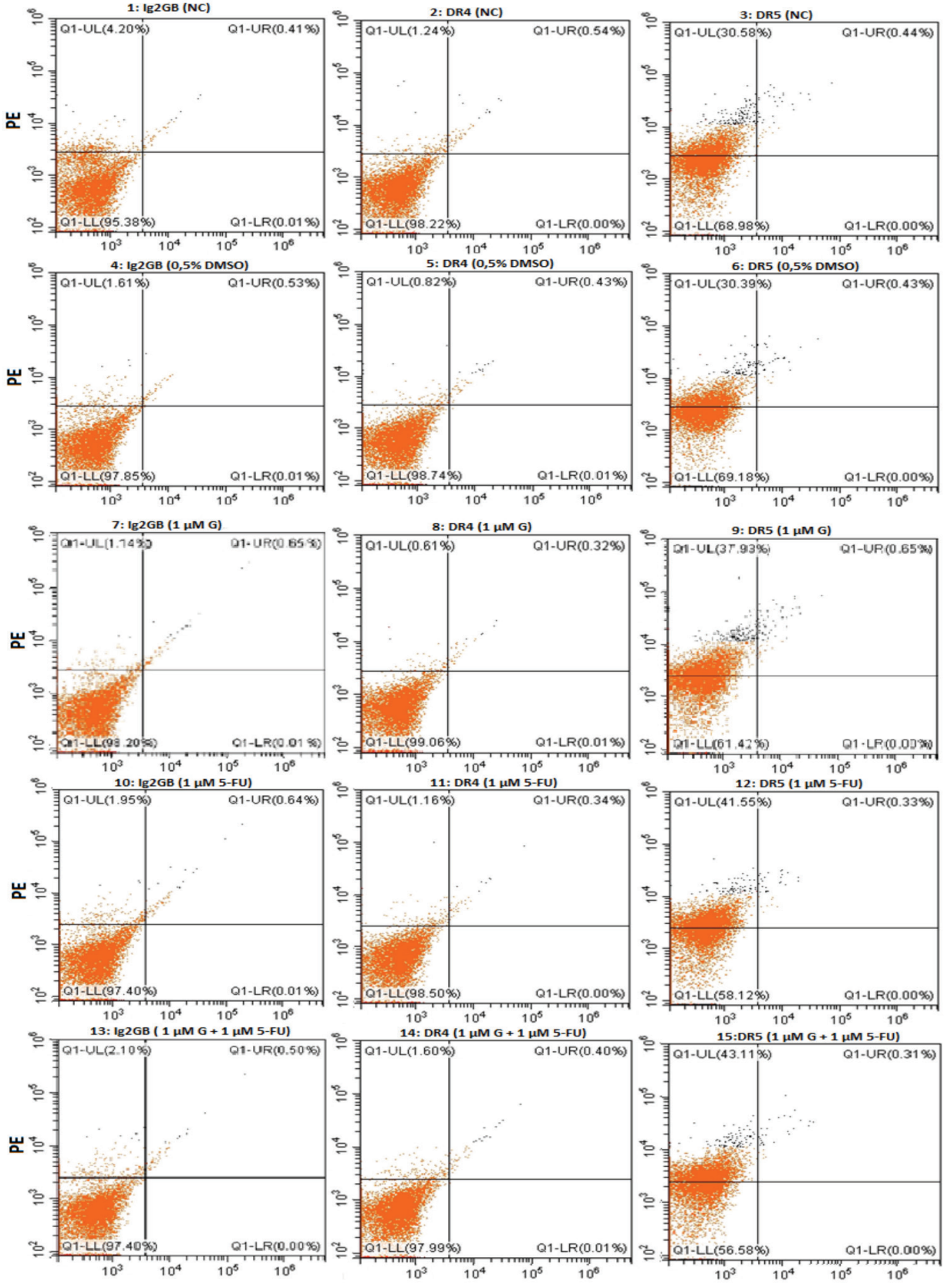

Supplementary Material 2. Effects of genistein **(G)** and 5-FU on the surface expression levels of DR4 and DR5 in SW480 cells by flow cytometry
5-FU: 5-Fluorouracil

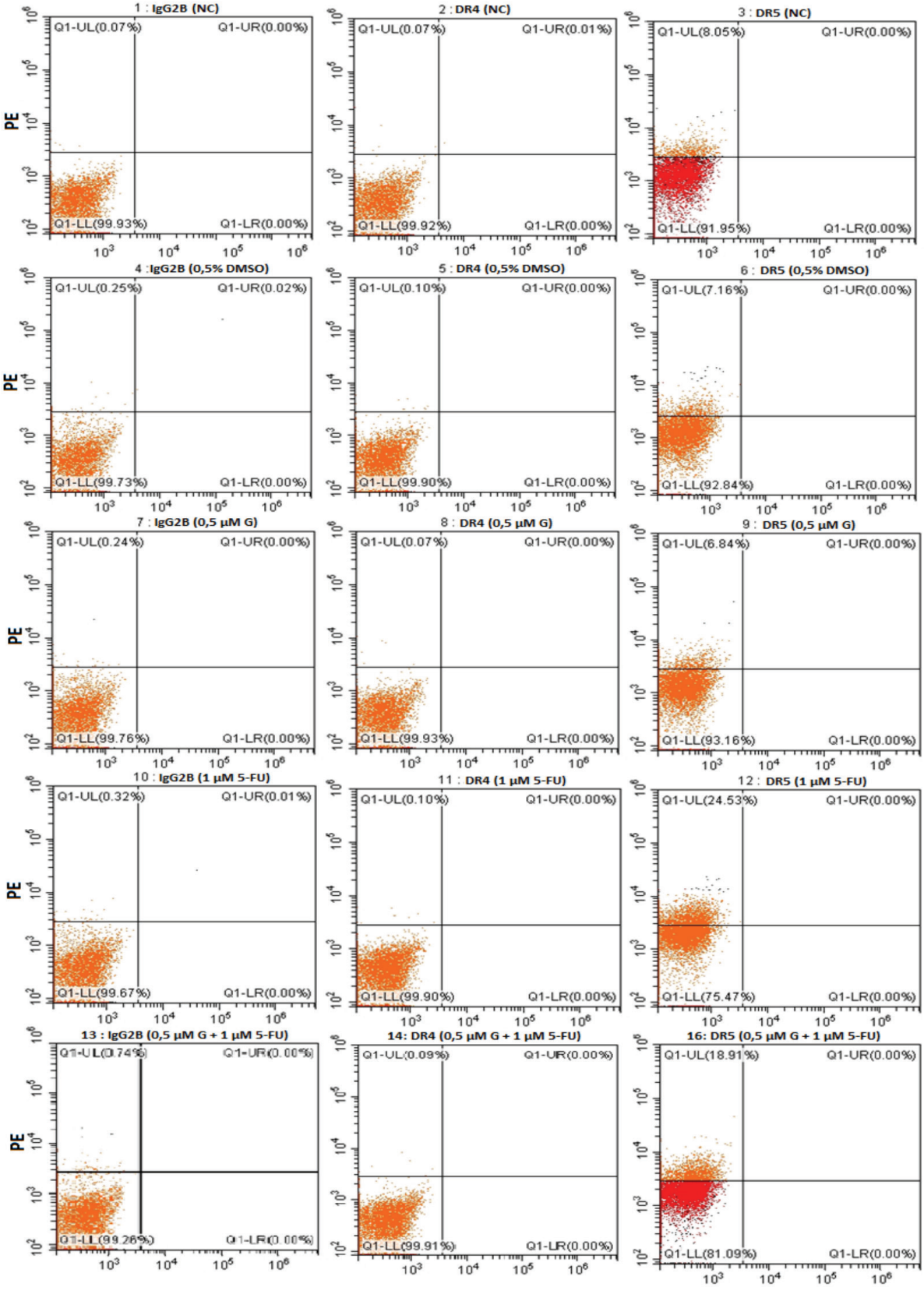

Supplementary Material 3. Effects of genistein **(G)** and 5-FU on the surface expression levels of DR4 and DR5 in SW620 cells by flow cytometry
5-FU: 5-Fluorouracil, DMSO: Dimethyl sulfoxide

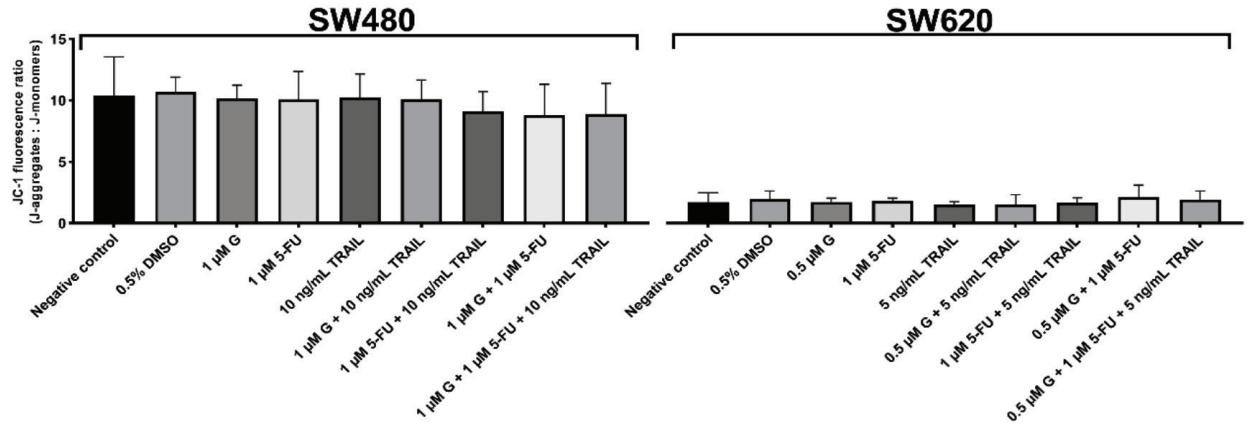

Supplementary Material 4. The changes in MMP of SW480 and SW620 cells are presented as the mean ± standard deviation of the ratio between aggregates and monomeric forms of JC-1 using the JC-1 MMP Assay Kit (Cayman)

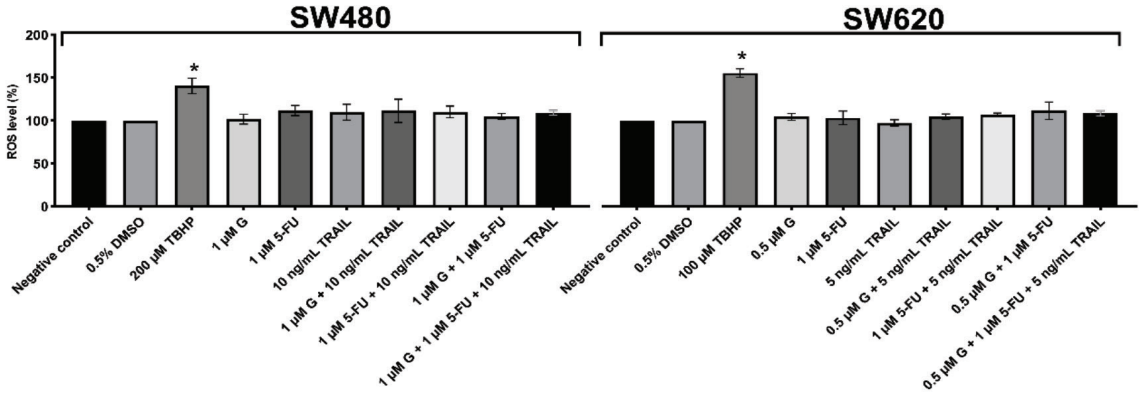

Supplementary Material 5. Effects of genistein, 5-FU, TRAIL, and their combinations on ROS levels in SW480 and SW620 cells for 48 hours using a ROS detection assay kit (Biovision). Results are given as mean ± standard deviation of ROS level percentage compared with negative and DMSO controls

*$p < 0.05$, **$p < 0.001$, indicates a significant difference from the negative control, 5-FU: 5-Fluorouracil, TRAIL: Tumor necrosis factor-related apoptosis-inducing ligand, ROS: Reactive oxygen species, DMSO: Dimethyl sulfoxide

Turk J Pharm Sci 2024;21(1):25-35
DOI: 10.4274/tjps.galenos.2023.18124

ORIGINAL ARTICLE

Development of a Stability Indicating UPLC Method for the Determination of Tirbanibulin in Bulk and Its Pharmaceutical Dosage Form

Pridhvi Krishna GADDEY, Raja SUNDARARAJAN*

GITAM (Deemed to be University), School of Pharmacy, Visakhapatnam, India

ABSTRACT

Objectives: The primary goal of this study was to create and validate a simple, precise, sensitive, and accurate ultra-performance liquid chromatography (UPLC) method for estimating tirbanibulin in pure and dosage form.

Materials and Methods: A UPLC technique was developed using a Waters Acquity UPLC Phenyl (100 x 2.1 mm, 1.7 µm) column. The developed technique was validated in accordance with the International Conference on Harmonization (ICH) guidelines.

Results: Tirbanibulin was separated chromatographically with high resolution using the mobile phase acetonitrile: buffer (30:70 *v/v*) at 0.5 mL/min, 5 µL injection volume, and 220 nm wavelength. The validated technique was found to be linear in the 1-15 µg/mL range. The detection and quantification limits for tirbanibulin were 0.03 and 0.1 µg/mL, respectively. The percentage relative standard deviation was less than 2%, demonstrating the precision of the developed technique. Furthermore, the recovery rate was nearly 100%, confirming the accuracy of the method. Minor modifications to the chromatographic conditions demonstrated the robustness of the method.

Conclusion: The developed analytical method was precise, simple, reproducible, and sensitive. Consequently, it can be used to determine tirbanibulin.

Keywords: UPLC, tirbanibulin, apoptosis, actinic keratosis, forced degradation studies

INTRODUCTION

Actinic keratosis (AK) is a precancerous skin condition affecting the face, balding scalp, and extremities. It is caused by the proliferation of atypical keratinocytes in response to prolonged intermittent ultraviolet-visible (UV) light exposure. AK starts with DNA damage and mutation and then progresses to neoplastic transformation and growth[1]. These lesions may develop into squamous cell carcinoma (SCC) once abnormal cell invasion affects the dermis structures and can metastasize.[2] Long-term UV exposure causes various epigenetic and genetic alterations, disrupting the activity of crucial genes in keratinocytes that promote the progression of AK to SCC.[3]

The chemical name of tirbanibulin is *N*-benzyl-2-[5-(4-(2-morpholinoethoxy) phenyl) pyridine-2-yal] acetamide. Tirbanibulin is a microtubule inhibitor. Tirbanibulin is a non-adenosine triphosphate (ATP)-competitive inhibitor that disrupts the proto-oncogenic Src tyrosine kinase signaling pathway.[4] Tirbanibulin also promotes the G2/M arrest of proliferating cell populations, upregulated *p53*, and triggers apoptosis by activating caspase-3 and cleaving poly [adenosine diphosphate (ADP) ribose] polymerase. Only the topical use of tirbanibulin is currently approved, which should not be applied in close proximity to the mouth, lips, or eyes. Patients must take extra care to avoid tirbanibulin in their eyes or periocular region because it can cause unfavorable ophthalmic reactions. At present, only AKs on the face and scalp can be treated with tirbanibulin.[5]

*Correspondence: sraja61@gmail.com, Phone: +09 160508261, ORCID-ID: orcid.org/0000-0003-2229-6423
Received: 26.11.2022, Accepted: 19.02.2023

A thorough review of the literature revealed that there is no reported ultra-performance liquid chromatography method for estimating tirbanibulin that could indicate stability. Due to the high cost and fragility of analytical studies conducted using gas chromatography-mass spectrometry (GC-MS) or liquid chromatography-mass spectrometry (LC-MS) in comparison to ultra-performance liquid chromatography (UPLC), the main focus was on developing an analytical method that was quick, precise, repeatable, and affordable. The UPLC method was chosen for the development of a stability-indicating method for determining tirbanibulin. According to the Q2 (R1) guidelines of the International Conference on Harmonization (ICH) procedure, the developed method was validated.[6] In this experiment, a UPLC method for determining the concentration of tirbanibulin in bulk form was established. The method was further successfully applied to the determination of tirbanibulin in the pharmaceutical dosage form.

MATERIALS AND METHODS

Chemicals and reagents

Tirbanibulin (Figure 1), a pure bulk drug, a marketed dosage form of tirbanibulin (Klysiri), orthophosphoric acid, acetonitrile (HPLC grade), and HPLC-grade water (Milli Q or equivalent) were the chemical materials and reagents used. All HPLC-grade solvents were produced by Merck (Mumbai, India). The tirbanibulin drug sample was obtained as a gift sample from Shree Icon Labs, Vijayawada, Andhra Pradesh, India.

Instrument and chromatographic conditions

Chromatographic analysis was accomplished using a Waters Acquity ultra-performance liquid chromatographic system equipped with a PDA detector. A phenyl chromatographic column (100 x 2.1 mm, 1.7 µm) was employed with a flow rate of 0.5 mL/min. The following additional parameters were also set: an injection volume of 5.0 µL, and ambient column temperature. Acetonitrile and buffer were used in the mobile phase at a 30:70 ratio. There was a 2.0-min runtime.

Preparation of the buffer

Orthophosphoric acid (1 mL) was taken and dissolved in 1 L of HPLC-grade water.

Preparation of the mobile phase

Acetonitrile and buffer were mixed in a ratio of 30:70 and filtered through 0.45 µm membrane filter paper.

Preparation of the standard stock solution

Five mg of tirbanibulin were weighed and transferred to a 50 mL volumetric flask. It was then diluted to a volume with acetonitrile (diluent) to prepare a standard solution.

Preparation of the standard working solution

Five mL of the standard stock solution were pipetted into a 50 mL volumetric flask. It was then reconstituted using a diluent (acetonitrile).

Preparation of the sample stock solution

A tirbanibulin sample of 100 mg was accurately weighed and transferred into a 10 mL volumetric flask by adding a diluent (acetonitrile). Then, it was sonicated to dissolve for 15 min and diluted to volume with the diluent.

Preparation of the sample working solution

From the sample standard solution, 1 mL was pipetted out and transferred into a volumetric flask (10 mL). Then, it was made up with a diluent (acetonitrile).

Method validation

The analytical method validation for the estimation of the assay of tirbanibulin in bulk and pharmaceutical dosage forms was conducted. According to the International Council for Harmonisation of Technical Requirements of Pharmaceuticals for Human Use (ICH) guidelines, the effectiveness of analytical method validation parameters such as system suitability, linearity, limit of detection (LOD), limit of quantitation (LOQ), specificity (interference and forced degradation), precision (method precision and intermediate precision), robustness, and accuracy was evaluated to show the method's suitability for the estimation of tirbanibulin assay.

System suitability

By injecting 5 µL of the sensitivity standard solution in 6 replicates, the suitability of the system was demonstrated. Standard chromatograms were used to assess system suitability parameters such as plate count, relative standard deviations (RSDs), retention time, resolution, and variation.

Selectivity

A comparison-based approach was employed to ensure the absence of interference and confirm method selectivity. Chromatograms of blank and placebo samples were used for this purpose.

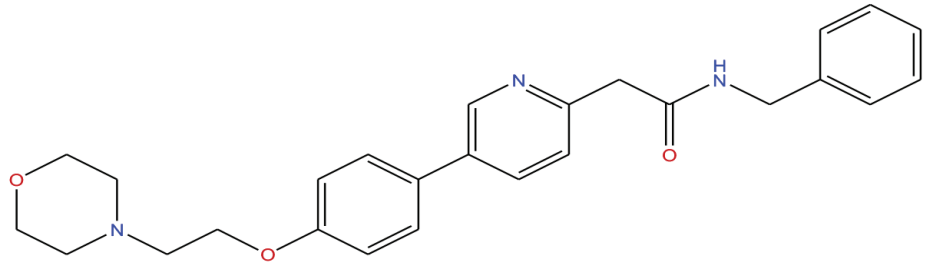

Figure 1. Structure of the tirbanibulin

Linearity

Tirbanibulin concentration and peak area were plotted to assess the linearity of the analytical method and demonstrate that the absorbance is directly proportional to the analyte concentration in the sample. The tirbanibulin stock solution (100 µg/mL) was serially diluted to concentrations ranging from 1.0 to 15 µg/mL and then tested in accordance with the test procedure. A regression line was used to calculate the correlation coefficient (CC), regression coefficient (R^2), intercept, and slope.

Precision

To obtain method and intermediate precision, samples at 10 µg/mL concentration level were analyzed, and on each validation day, individual calibrations were performed. Six different test preparations with a strength of 10 µg/mL each were assayed to evaluate the precision of the test method. For intermediate precision, evaluation was completed by performing the required assay for six different test preparations with a strength of 10 µg/mL. The RSD (%) was used to express precision.

Accuracy

For tirbanibulin, a recovery study was conducted at concentrations between 50% and 150% of the initial assay value. Individual-level sample solutions were prepared in triplicate, and test-specific method analyses were conducted. Percentages of recovery, mean recovery, and RSD were computed.

Sensitivity

The lower LOQ and the LOD were derived using the subsequent equations based on the slope of the calibration curve and the SD of responses.

LOD = 3.3 × standard deviation (SD)/slope

LOQ = 10 × SD/slope

Assay of tirbanibulin

The sample (100 mg) was accurately weighed and transferred into a 10 mL volumetric flask by adding some diluents. Then, it was sonicated to dissolve for 15 min and diluted to volume with the diluent. From the sample standard solution, 1 mL was pipetted out and transferred into a volumetric flask (10 mL). Then, it was made up with a diluent.

Robustness

By purposefully altering the chromatographic parameters, the robustness of the analytical technique was examined under a range of circumstances. The impact of the acetonitrile and buffer composition in organic phase plus (33:67) and organic phase minus (27:73), as well as the impact of flow rate plus (0.55 mL/min) and flow rate minus (0.45 mL/min), were assessed during the robustness study. In all robustness conditions, the theoretical plates, RSD (%), and tailing factor were evaluated as system suitability criteria. Each robustness condition received an injection of a spiked sample, and the resolution between impurities was assessed.

Forced degradation studies

A study was conducted to show the effective separation of degradants from the tirbanibulin peak in the assay method.

Acid degradation

Accurately weighed 1 mL the sample stock solution was transferred to a dry and clean 10 mL volumetric flask. To this solution, 1 mL of 1 N hydrochloric acid was added and left undisturbed for 15 min. Then, 1 mL of 1 N NaOH was added to neutralize and made up to the mark with a diluent (acetonitrile). Samples were taken out and processed through a UPLC at certain intervals of time (0, 6, 12, 18, and 24 hours).

Base degradation

The possible degradation peaks and rate of degradation of tirbanibulin were assessed by weighing a sample stock solution of 1 mL and transferring it into a 10 mL volumetric flask. Then, it was subjected to forced degradation by adding 1 mL of 1 N NaOH and left for 15 min. After 15 min, 1 mL of 1 N HCl was added and left. Then, it is diluted with diluent (acetonitrile) to volume. Samples were withdrawn at specific time (0, 6, 12, 18, and 24 hours) intervals and subjected to UPLC.

Hydrolytic degradation

Tirbanibulin was tested for the rate of degradation and potential degradation peaks. The sample stock solution (1 mL) was transferred to a volumetric flask with a volume of 10 mL. Then, it was forcedly degraded by adding 3 mL of HPLC-grade water and kept aside for 15 min. The sample was diluted with diluent to volume. Further, 1 mL was pipetted out into a 10 mL volumetric flask and made up with diluent (acetonitrile) up to the mark. Samples were taken out and processed through UPLC at certain time points (0, 6, 12, 18, and 24 hours).

Peroxide degradation

Peroxide degradation was performed by assessing the probable peaks and the rate of degradation of tirbanibulin by weighing a sample stock solution of 1 mL. Then, the solution was transferred into a volumetric flask of 10 mL. Further, it was subjected to forced degradation by adding 1 mL of 10% H_2O_2. It was left for fifteen minutes. Then, the sample was diluted to volume with diluent (acetonitrile) and mixed. Further, 1 mL was pipetted out and diluted to 10 mL with the diluent. Samples were withdrawn at a specific time (0, 6, 12, 18, and 24 hours) intervals and subjected to UPLC.

Reduction degradation

Tirbanibulin was tested for the rate of degradation and potential degradation peaks. A volume of 1 mL of the sample stock solution was transferred into a 10 mL volumetric flask. Then, it was forcedly degraded by adding 1 mL of 10% sodium bi-sulfate. It was undisturbed for 15 minutes. Then, the sample was diluted with diluent (acetonitrile) to volume. Samples were taken out and processed through a UPLC at certain intervals of time (0, 6, 12, 18, and 24 hours).

Thermal degradation

A sample of 500 mg was weighed and exposed at 105 °C for 6 hours. The exposed sample was used for the analysis. The sample (100 mg) was transferred into a volumetric flask (10 mL). This sample

was diluted with the diluent and sonicated for 15 min to solubilize the contents. Further, 1 mL was pipetted into a 10 mL volumetric flask and diluted with acetonitrile. Samples at a specific time (0, 6, 12, 18, and 24 hours) points were withdrawn and subjected to UPLC runs to identify probable degradation chromatograms.

Photostability degradation

The degradation rate and possible peaks of degradation for tirbanibulin were assessed by weighing 500 mg of the sample. The sample was exposed to sunlight for 6 hours. 100 mg of the above sample was weighed. Transfer to a volumetric flask (10 mL). Diluents were added and sonicated for 15 min to dissolve the contents. Further, from the above solution, 1 mL was pipetted out into a volumetric flask of volume 10 mL and made up to volume with diluent (acetonitrile). Samples at specific times (0, 6, 12, 18, and 24 hours) points were withdrawn and put through UPLC runs.

RESULTS

Optimized process

After a series of trials, the mobile phase composition of acetonitrile: buffer in the proportion of 30:70 (*v/v*) showed both peaks with good resolution, tailing factor, and theoretical plate count. Hence, this method was optimized and validated. The Waters Acquity LC autosampler enabled the elution, method development, and validation of tirbanibulin. The method was proven to be simple to use, with high recovery, high sensitivity, and high specificity through thorough methodological validation. The optimized chromatogram is shown in Figure 2.

System suitability parameters

Many analytical processes include testing for system compatibility. The system suitability characteristics were investigated and used to determine the best settings. The theoretical plate number (N), retention time, and tailing factor (T) were all studied for this purpose. Six replicate injections of the tirbanibulin standard working solution were used to perform the procedure. It was observed that tirbanibulin was retained for 0.814 (average) min, with a tailing factor of not more than 1.31 in all peaks, indicating good peak symmetry. Theoretical plates were discovered to be greater than 3981 in all peaks. The results are tabulated in Table 1.

Linearity

The linearity of the analytical method was its capacity to produce test results within a specified range that was directly proportional to the concentration of the analyte in the test sample. Seven concentrations in the range of 1 and 15 µg/mL were used to test the linearity of the analytical method. The regression coefficient, y-intercept, and slope of the regression line were calculated. The observed correlation coefficient value was 0.9996. The results are shown in Tables 2, 3 and Figure 3.

Accuracy

A method's accuracy reflects how closely the outcomes it produces match the actual value. According to the accuracy results, the RSD (%) was 0.11%, and the percentage recovery at all three levels ranged from 99.7% to 100.9%. The results are tabulated in Table 4.

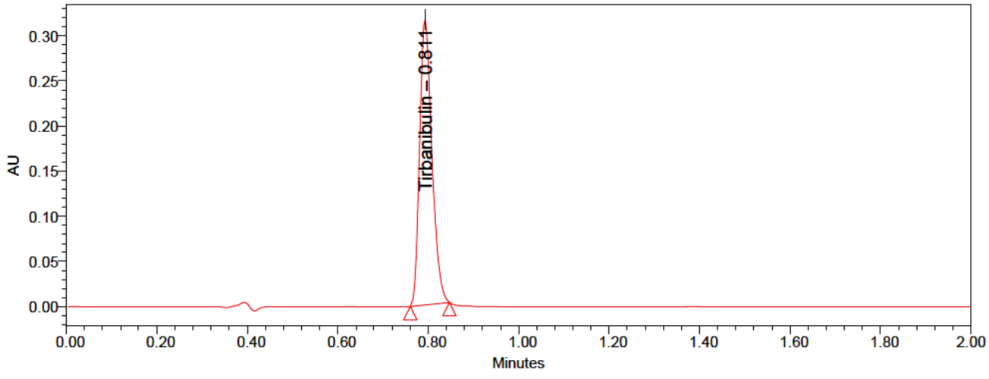

Figure 2. Optimized chromatogram of tirbanibulin
AU: Absorbance units

Table 1. System suitability parameters for tirbanibulin

Sample number	RT (min)	USP plate count	Tailing
1	0.811	4004	1.31
2	0.814	3981	1.31
3	0.810	4008	1.31
4	0.818	4067	1.27
5	0.818	4016	1.30
6	0.817	4022	1.30

RT: Retention time, USP: United States Pharmacopoeia

Table 2. Linearity studies of tirbanibulin

Sample number	Concentration (µg/mL)	Peak area
1	1	352095
2	2.5	824524
3	5	1578906
4	7.5	2411569
5	10	3039528
6	12.5	3919186
7	15	4691400

Precision

When multiple samples of the same homogeneous sample were taken under specified conditions, the precision of the method was defined as the degree of agreement between the measurements obtained. The RSD was typically used to express precision. The percent RSD value for the method precision results of tirbanibulin was found to be 0.47%. The percent RSD value for the intermediate precision results of tirbanibulin was found to be 0.33%. The results are shown in Tables 5 and 6.

Sensitivity

The LOQ was defined as the lowest amount of analyte in a sample that could be quantitatively determined with appropriate precision, as opposed to the LOD, which was the lowest amount of analyte in a sample that could be detected but not necessarily

Table 3. Optical characteristics of tirbanibulin

Parameters	Tirbanibulin
Linearity (µg/mL)	1-15 µg/mL
Regression equation	y= 309884.02x + 29801.60
Slope	309884.02
Intercept	29801.60
Correlation coefficient (R^2)	0.9996

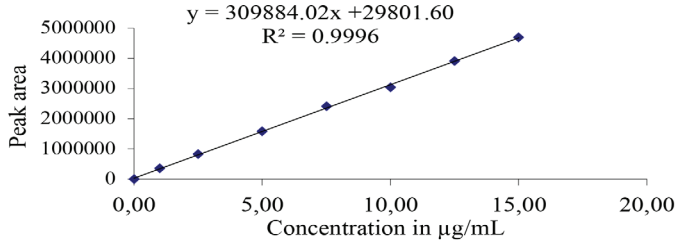

Figure 3. Linearity plot of tirbanibulin

Table 4. Recovery studies of tirbanibulin

Recovery level	Amount spiked (µg/mL)	Amount recovered (µg/mL)	Recovery (%)	Mean	SD	RSD (%)
50%	0.50	0.497	99.4	100	0.60	0.6
	0.50	0.5	100			
	0.50	0.503	100.6			
100%	1.0	1.001	100.1	100.2	0.50	0.5
	1.0	0.997	99.7			
	1.0	1.007	100.7			
150%	1.5	1.495	99.7	100.2	0.61	0.6
	1.5	1.502	100.1			
	1.5	1.513	100.9			
Mean				100.1		
SD				0.115		
RSD (%)				0.11		

SD: Standard deviation, RSD: Relative standard deviation

Table 5. Method precision studies of tirbanibulin

Sample number	Area of tirbanibulin	Label claim (%)
1.	3024698	100
2.	3046952	100.7
3.	3036756	100.4
4.	3065289	101.3
5.	3026985	100.1
6.	3034356	100.3
Mean		100.5
SD		0.476
RSD (%)		0.47

SD: Standard deviation, RSD: Relative standard deviation

Table 6. Intermediate precision studies of tirbanibulin

Sample number	Area of tirbanibulin	Label claim (%)
1.	3026985	100.1
2.	3032534	100.3
3.	3042589	100.7
4.	3045824	100.8
5.	3049269	100.8
6.	3050687	100.9
Mean		100.6
SD		0.337
RSD (%)		0.33

SD: Standard deviation, RSD: Relative standard deviation

quantitated. The LOD and LOQ for tirbanibulin were 0.03 and 0.1 µg/mL, respectively. The results are tabulated in Table 7.

Assay

According to the label claim, the drug content obtained from the values of the sample solutions was found to be in the permissible range of 90-110%. The percentage assay of tirbanibulin was found to be 100.5% (*w/w*). The results are displayed in Table 8.

Robustness

The influence of slight alterations in the chromatographic settings was used to determine the robustness of the analytical process. The percent RSD of tirbanibulin was less than 2.0 in all deliberately changed chromatographic settings. The results are shown in Table 9.

Selectivity

In the retention time ranges, the UPLC chromatograms for the drug matrix (combination of the medicine and placebos) revealed nearly no interference peaks. As a result, the proposed UPLC approach in this study was selective. The method's specificity and selectivity were tested by looking for interference peaks in the chromatograms of blank and placebo samples. Because of the excipients, there were no interfering peaks. Consequently, the procedure was specific and selective. Figures 4 and 5 show the chromatograms of the blank and working placebo solutions, respectively.

Table 7. LOD and LOQ of tirbanibulin

Drug	LOD (µg/mL)	LOQ (µg/mL)
Tirbanibulin	0.03	0.1

LOD: Limit of detection, LOQ: Limit of quantification

Table 8. Results of the marketed formulation analysis

Compound name	Brand name	Label claim (mg)	Assay (%) [*w/w* (%)]
Tirbanibulin	Klysiri	2.5	100.5

Table 9. Robustness studies of tirbanibulin

Condition	Peak area	Label claim (%)	Mean	SD	RSD (%)
Flow rate (+) 0.55 mL/min	2785496	100.4	99.6	0.764	0.77
	2758463	99.4			
	2745818	98.9			
Flow rate (-) 0.45 mL/min	3365289	100.2	100.1	0.173	0.17
	3352144	99.9			
	3362569	100.2			
Mobile phase (+) 33 O:67 B	2652542	99.4	99.7	0.252	0.25
	2665324	99.9			
	2659868	99.7			
Mobile phase (-) 27 O:73 B	3345781	99.7	99.9	0.153	0.15
	3354787	99.9			
	3356253	100			

SD: Standard deviation, RSD: Relative standard deviation

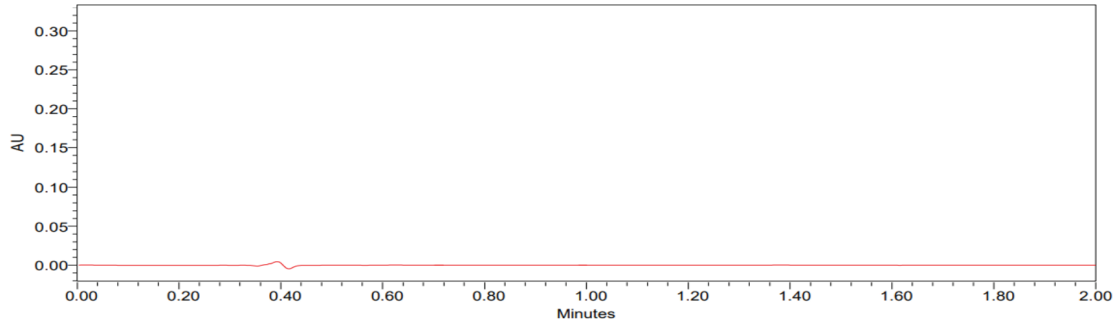

Figure 4. Chromatogram of the blank
AU: Absorbance units

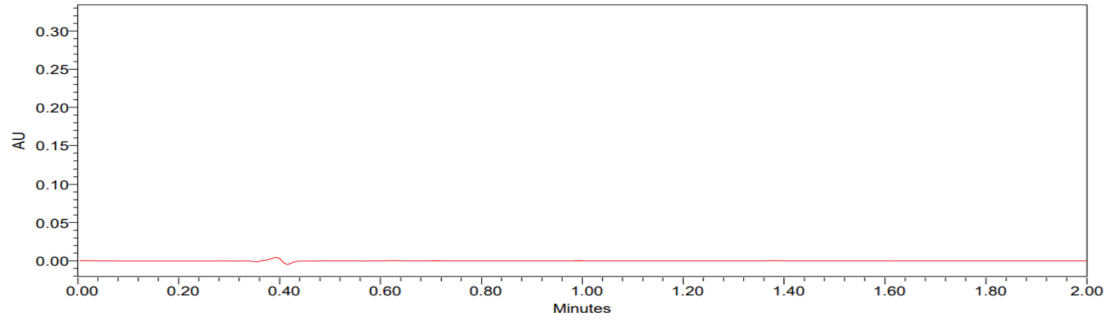

Figure 5. Chromatogram of the placebo
AU: Absorbance units

Forced degradation studies

Tirbanibulin was subjected to various stress conditions, including hydrolysis, base, oxidative, acid, photostability, and thermal degradation, as *per* the ICH guidelines. The proposed UPLC approach was used to monitor the degradation behavior regularly. The PDA detector results from the forced deterioration results revealed that the tirbanibulin peaks were pure and homogenous in all of the stressful conditions studied. This demonstrates that the proposed approach is both particular and stable. All the results of the stability studies are displayed in Tables 10-16. The degradation chromatograms are displayed in Figures 6-17.

Table 10. Acid degradation of tirbanibulin

Time	Peak area	Label claim (%)	Degraded (%)	Purity angle	Purity threshold
Initial	2896528	95.8	4.2	0.157	1.052
6 hours	2701953	89.4	10.4	0.148	1.058
12 hours	2542200	84.1	15.7	0.136	1.049
18 hours	2416121	79.9	19.9	0.124	1.052
24 hours	2318506	76.7	23.1	0.125	1.063

Table 11. Base degradation of tirbanibulin

Time	Peak area	Label claim (%)	Degraded (%)	Purity angle	Purity threshold
Initial	2926358	96.8	3.2	0.163	1.047
6 hours	2765472	91.5	8.5	0.166	1.047
12 hours	2556387	84.6	15.4	0.139	1.037
18 hours	2446953	81	19	0.149	1.071
24 hours	2384105	78.9	21.1	0.129	1.034

Table 12. Peroxide degradation of tirbanibulin

Time	Peak area	Label claim (%)	Degraded (%)	Purity angle	Purity threshold
Initial	2905874	96.1	3.9	0.144	1.057
6 hours	2763592	91.4	8.6	0.142	1.053
12 hours	2575219	85.2	14.8	0.159	1.066
18 hours	2429856	80.4	19.6	0.162	1.062
24 hours	2306598	76.3	23.7	0.168	1.069

Table 13. Reduction degradation of tirbanibulin

Time	Peak area	Label claim (%)	Degraded (%)	Purity angle	Purity threshold
Initial	2910368	96.3	3.7	0.169	1.032
6 hours	2758292	91.3	8.7	0.171	1.063
12 hours	2552875	84.5	15.5	0.129	1.042
18 hours	2455937	81.3	18.7	0.154	1.069
24 hours	2340156	77.4	22.6	0.125	1.044

DISCUSSION

Tirbanibulin is a microtubule inhibitor. Tirbanibulin is a non-ATP-competitive inhibitor that disrupts the proto-oncogenic Src tyrosine kinase signaling pathway.[4] Therefore, a technique for tirbanibulin determination is required. According to the ICH, a system suitability test is frequently used to assess a chromatographic system's resolution, column efficiency, and repeatability to ensure that it is suitable for a certain analysis.[6] The new approach was tuned to produce symmetrical peaks and high theoretical plates (N). The total number of theoretical plates was above 2000, which was deemed sufficient for the system suitability test. According to the standards, the tailing factor was within the specified limits. These findings demonstrate that the proposed strategy can produce data of acceptable quality. The suggested method's application to the analysis of formulations is a key feature. Hence, the market sample of tirbanibulin was collected and analyzed by employing the proposed method. The study confirmed that the created UPLC method was accurate and easy enough to be used daily. The suggested assay method's high content results indicate that this technique can be employed for quantitative regular quality control studies of pharmaceutical dosage forms.

Table 14. Thermal degradation of tirbanibulin

Time	Peak area	Label claim (%)	Degraded (%)	Purity angle	Purity threshold
Initial	2896237	95.8	4.2	0.135	1.064
6 hours	2845421	94.1	5.9	0.129	1.072
12 hours	2790124	92.3	7.7	0.145	1.076
18 hours	2729638	90.3	9.7	0.138	1.068
24 hours	2609856	86.3	13.7	0.147	1.064

Table 15. Photolysis degradation of tirbanibulin

Time	Peak area	Label claim (%)	Degraded (%)	Purity angle	Purity threshold
Initial	2997541	99.2	0.8	0.178	1.074
6 hours	2976412	98.5	1.5	0.149	1.069
12 hours	2954638	97.8	2.2	0.143	1.052
18 hours	2938721	97.2	2.8	0.146	1.054
24 hours	2906352	96.2	3.8	0.158	1.069

Table 16. Hydrolytic degradation of tirbanibulin

Time	Peak area	Label claim (%)	Degraded (%)	Purity angle	Purity threshold
Initial	2980574	98.6	1.4	0.149	1.067
6 hours	2967521	98.2	1.8	0.143	1.064
12 hours	2932547	97	3	0.148	1.062
18 hours	2916359	96.5	3.5	0.146	1.062
24 hours	2902593	96	4	0.164	1.065

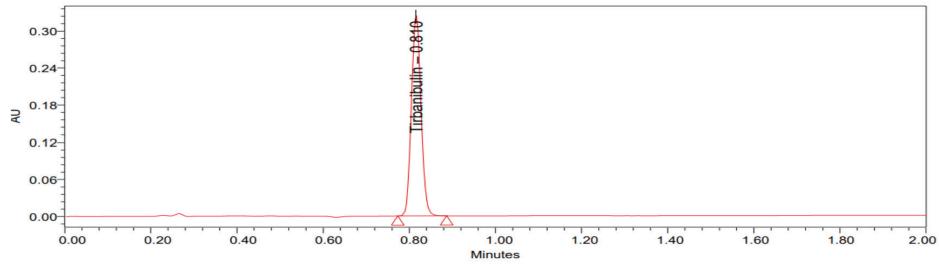

Figure 6. Acid degradation chromatogram of tirbanibulin: initial
AU: Absorbance units

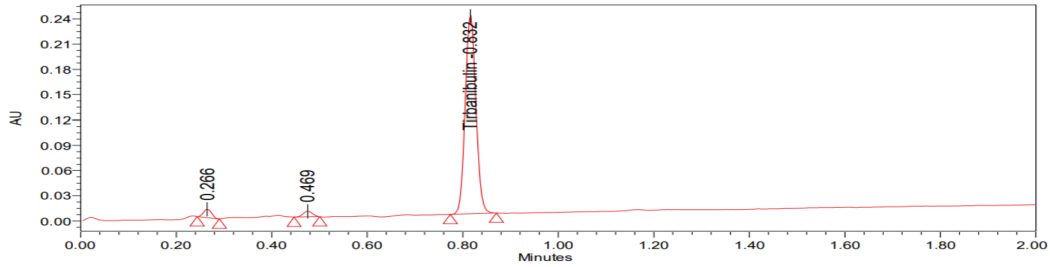

Figure 7. Acid degradation chromatogram of tirbanibulin at 24 hours
AU: Absorbance units

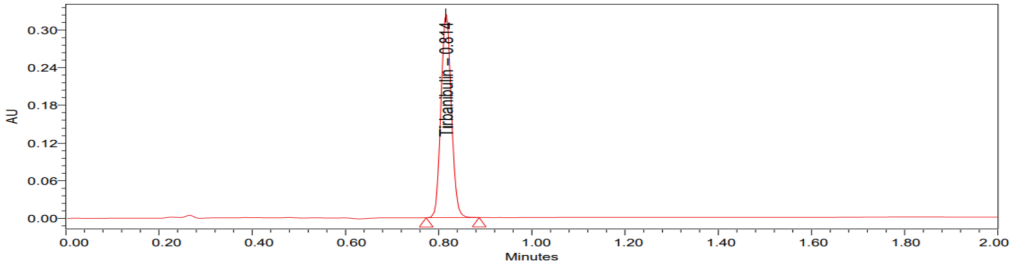

Figure 8. Base degradation chromatogram of tirbanibulin: initial
AU: Absorbance units

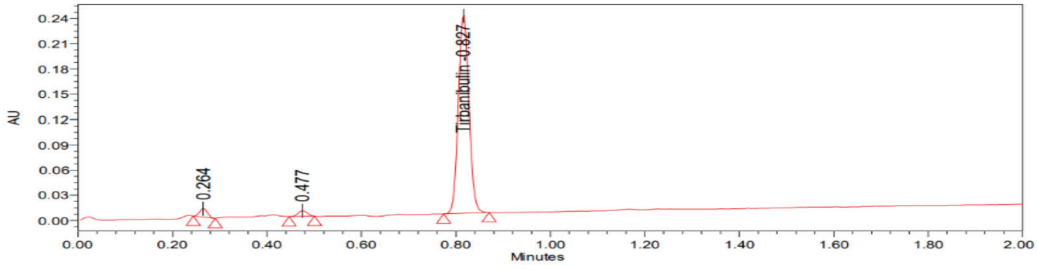

Figure 9. Base degradation chromatogram of tirbanibulin at 24 hours
AU: Absorbance units

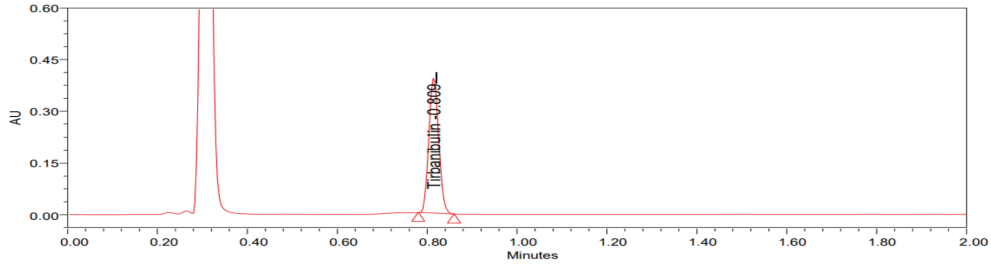

Figure 10. Peroxide degradation chromatogram of tirbanibul in: the initial
AU: Absorbance units

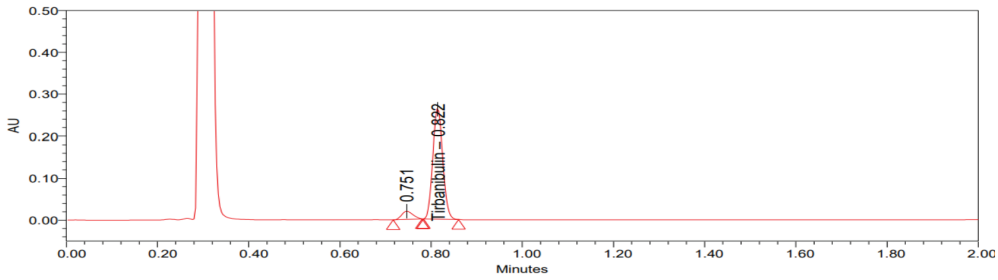

Figure 11. Peroxide degradation chromatogram of tirbanibul in: at 24 hours
AU: Absorbance units

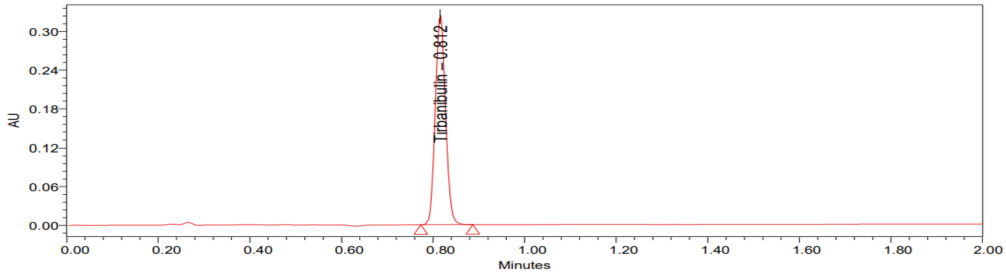

Figure 12. Reduction degradation chromatogram of tirbanibulin: initial
AU: Absorbance units

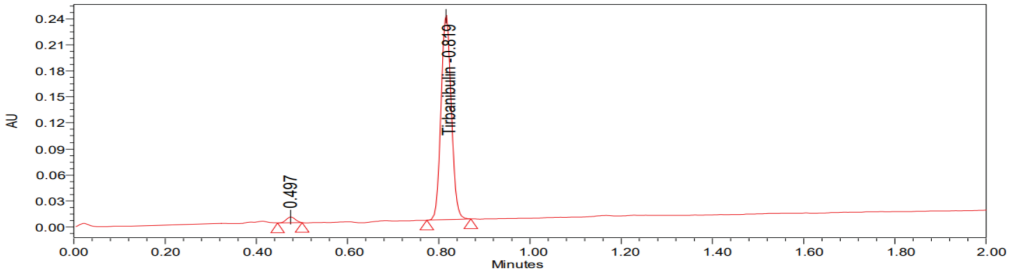

Figure 13. Reduction degradation chromatogram of tirbanibulin at 24 hours
AU: Absorbance units

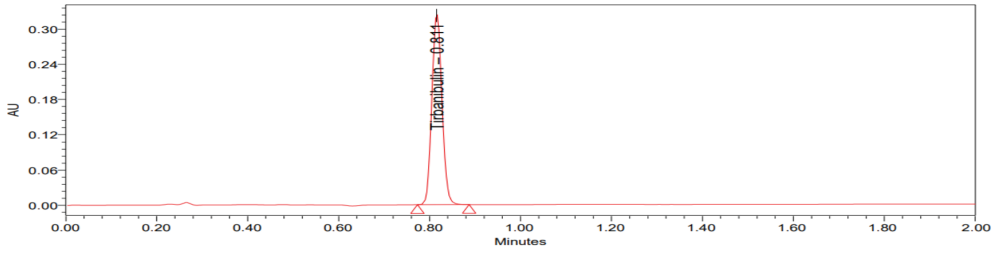

Figure 14. Thermal degradation chromatogram of tirbanibulin: initial
AU: Absorbance units

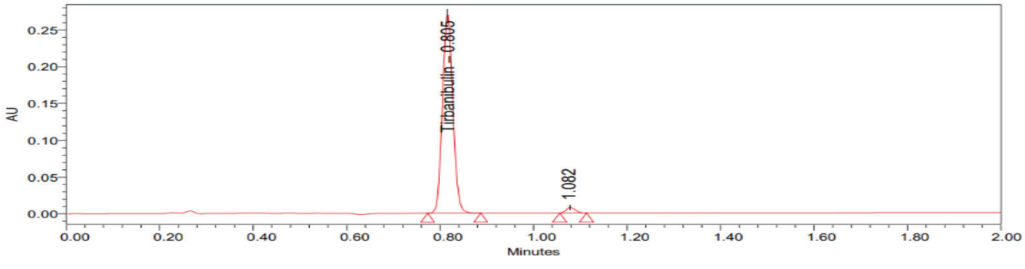

Figure 15. Thermal degradation chromatogram of tirbanibulin after 24 hours
AU: Absorbance units

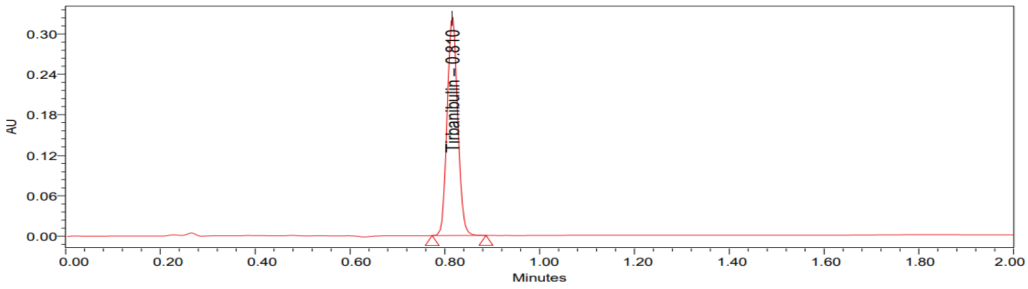

Figure 16. Hydrolysis degradation chromatogram of tirbanibul in: the initial
AU: Absorbance units

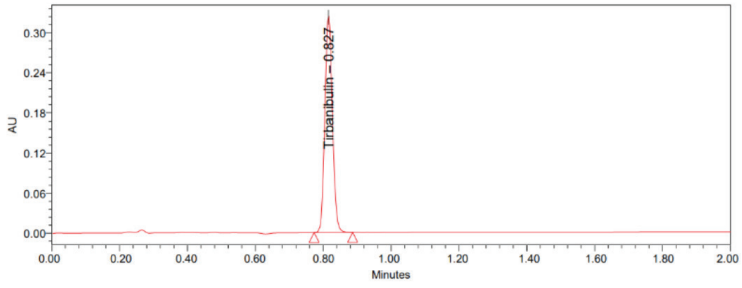

Figure 17. Hydrolysis degradation chromatogram of tirbanibulin after 24 hours
AU: Absorbance units

The linearity of the analytical method was it is capacity to produce test findings within a specified range that directly relates to the analyte concentration in the test sample.[6] The regression line of analysis expresses the relationship between the concentration and peak area of tirbanibulin. The findings revealed that the peak area and analyte concentration showed a strong correlation. The R^2 high value indicated good linearity. An analytical technique's accuracy shows the closeness of the outcomes produced by that technique to the true value.[6] The percentage recovery and percent RSD results fell within the acceptable ranges of 98.0-102.0% and not more than 2.0%, respectively, demonstrating the suitability of the method for routine drug analysis. The degree of agreement between a set of measurements made using repeated samples of the same homogeneous material under specified conditions was considered the precision of the method, and it was typically stated as the RSD.[6] The results were well under the usually accepted 2% limit. As a result, the new method's precision has been confirmed. The LOQ was defined as the smallest amount of analyte in a sample that could be identified quantitatively with adequate accuracy. The lowest amount of analyte in a sample that could be detected but not necessarily quantitate was defined as the LOD.[6] The LOD and LOQ for tirbanibulin were 0.03 and 0.1 µg/mL, respectively. The system suitability parameters did not significantly change, while varying the conditions. Hence, the method was robust. In the retention time ranges, the UPLC chromatograms for the drug matrix (combination of the medicine and placebos) revealed nearly no interference peaks. As a result, the proposed UPLC approach in this study was selective. The drug tirbanibulin was found to undergo extreme degradation under peroxide degradation conditions. The tirbanibulin peaks were homogenous and showed results within acceptance limits in all forced degradation studies. This demonstrates that the proposed approach is both particular and stable. The developed method effectively passed all the validation parameters and was applied efficaciously for the determination of tirbanibulin.

CONCLUSION

To estimate tirbanibulin in dosage form, a simple, accurate, and specific approach was established. Tirbanibulin had a retention time of 0.811 min. The percent RSD of method precision and intermediate precision was found to be 0.47 and 0.33%, respectively. For tirbanbulin, the percent recovery was 100.1%. The LOD and LOQ values for tirbanibulin calculated from regression equations were 0.03 µg/mL and 0.1 µg/mL, respectively. The regression equation of tirbanibulin was y = 309884.02x + 29801.60. There were some degradation peaks in acid, base, thermal, reduction, and peroxide stressed conditions according to the results of the forced degradation test. Because retention times and run times were reduced, the method created was simple and economical, and it might be used in frequent quality control tests in industries.

Ethics

Ethics Committee Approval: Not necessary.

Informed Consent: The present research work was based on sample analysis using the UPLC technique.

Authorship Contributions

Concept: P.K.G., R.S., Design: P.K.G., R.S., Data Collection or Processing: P.K.G., Analysis or Interpretation: P.K.G., Literature Search: P.K.G., Writing: P.K.G.

Conflict of Interest: No conflict of interest was declared by the authors.

Financial Disclosure: The authors are thankful to the management of GITAM (deemed to be University), Visakhapatnam, Andhra Pradesh, India, for providing the necessary facilities and M.V.V.S Murthi fellowship grants to carry out the research work.

REFERENCES

1. Fania L, Didona D, Di Pietro FR, Verkhovskaia S, Morese R, Paolino G, Donati M, Ricci F, Coco V, Ricci F, Candi E, Abeni D, Dellambra E. Cutaneous squamous cell carcinoma: from pathophysiology to novel therapeutic approaches. Biomedicines. 2021;9:171.
2. Cockerell CJ. Pathology and pathobiology of the actinic (solar) keratosis. Br J Dermatol. 2003;149(Suppl 66):34-36.
3. Shen Y, Ha W, Zeng W, Queen D, Liu L. Exome sequencing identifies novel mutation signatures of UV radiation and trichostatin a in primary human keratinocytes. Sci Rep. 2020;10:4943.
4. Niu L, Yang J, Yan W, Yu Y, Zheng Y, Ye H, Chen Q, Chen L. Reversible binding of the anticancer drug KXO1 (tirbanibulin) to the colchicine-binding site of β-tubulin explains KXO1's low clinical toxicity. J Biol Chem. 2019;294:18099-18108.
5. Dao DD, Sahni VN, Sahni DR, Balogh EA, Grada A, Feldman SR. 1% Tirbanibulin ointment for the treatment of actinic keratoses. Ann Pharmacother. 2022;56:494-500.
6. ICH Guideline. "Validation of analytical procedures: text and methodology," in Proceedings of International Conference on Harmonization, Topic Q2 (R1), Geneva, Switzerland: 2005.

Turk J Pharm Sci 2024;21(1):36-41
DOI: 10.4274/tjps.galenos.2023.36974

ORIGINAL ARTICLE

Assessment of Knowledge and Attitudes of Physicians and Pharmacists on Probiotics: A Cross-Sectional Survey

Hülya BAŞAR GÜNEŞ[1], Aygin BAYRAKTAR EKİNCİOĞLU[2]*, Tarkan KARAKAN[3], Kutay DEMİRKAN[2]

[1]Yeni Oyak Pharmacy, Ankara, Türkiye
[2]Hacettepe University, Faculty of Pharmacy, Department of Clinical Pharmacy, Ankara, Türkiye
[3]Gazi University, Faculty of Medicine, Department of Gastroenterology, Ankara, Türkiye

ABSTRACT

Objectives: Probiotics have been gaining increased attention from the public recently, which originates concerns about their rationale use among healthcare professionals. Although there is evidence on the efficacy and safety of probiotics in certain gastrointestinal disorders, it is important to identify healthcare professionals' opinions on probiotics. This study aimed to identify the opinions of pharmacists and physicians on the use of probiotics.

Materials and Methods: This cross-sectional study was conducted between November, 2017 and August, 2018 among pharmacists and physicians practicing in Ankara, Türkiye. An electronic survey was designed and sent to the participants *via* e-mail.

Results: A total of 361 pharmacists (74.5% female) and 356 physicians (42.4% female) participated in the study. Approximately two-thirds of pharmacists and physicians were familiar with the mechanism of action and indications of probiotics. Most pharmacists and physicians recommended probiotics to be used in gastrointestinal system disorders (99.7% and 97.7%). Other areas that probiotics are commonly recommended was genitourinary system (29.3%) by pharmacists and dermatological symptoms (15.1%) by phycisians, respectively. Considering patient advice regarding the probiotics, pharmacists (63.3%) seemed to receive more requests compared to physicians (30.9%); and with regard to the probiotic recommendation, 70.7% and 38.2% of pharmacists and physicians, respectively, indicated that they have no concerns, but 61% of physicians have concerns on reimbursement policy when prescribing.

Conclusion: Pharmacists and physicians are healthcare providers commonly asked about probiotics by patients. Therefore, it is important to address healthcare professionals' concerns and increase their knowledge of the use of probiotics for different health conditions. Given that probiotic products can be purchased without a prescription, healthcare professionals in primary care settings should be more vigilant about the rational use of probiotics.

Keywords: Probiotics, pharmacist, physician, community

INTRODUCTION

A balance between the amount and types of microorganisms in the human gastrointestinal tract provides a healthy immune system. Any deficiency or dysfunction in the immune system can lead to infections, necessitating the use of antibiotics. Gut flora is responsible for 80% of the immune system and has to be reinforced through healthy nutrition to maintain balance within the gastrointestinal system; however, inappropriate use of antibiotics damages the flora.[1] According to the research, bacterial diversity has been found to be high in people who have not been exposed to antibiotics before, and it has also been shown that malnutrition causes microorganism loss in urban life. Therefore, it is recommended that the human body be physically strengthened with supplementary food, nutritional support, or probiotics to prevent unintentional loss of microorganisms.

*Correspondence: aygin@hacettepe.edu.tr, Phone: +90 312 305 20 43, ORCID-ID: orcid.org/0000-0002-3481-0074
Received: 10.01.2023, Accepted: 04.03.2023

The intestinal microbiota is a unique structure and is associated with various diseases ranging from allergies to inflammatory bowel disease. While a causal relationship has not been fully defined and has been investigated for safety issues in certain populations (such as immunocompromised patients), the use of probiotics is considered a dietary supplement for treating disease. The use of probiotics is recommended for treating many diseases, such as inflammatory bowel disease, short bowel syndrome, antibiotic-associated and acute diarrhea, *Clostridium difficile* and *Helicobacter pylori* infections, urogenital infections, food sensitivity, and allergies.[2] In the pediatric population, they are also used for treating diarrhea, atopic dermatitis, and colitis.[3] Probiotics were defined by the World Health Organization in 2002[4] as "live microorganisms which, when administered in adequate amounts, confer a health benefit on the host". The most commonly used microorganisms are *Lactobacillus (rhamnosus, casei, casei shirota, acidophilus, johnsonii, plantarum, bulgaricus,* and *reuteri), Bifidobacterium* (*breve, bifidum, infantis,* and *animalis*) genera and the fungus *Saccharomyces boulardii*.[5,6] Probiotic products that can be easily purchased from supermarkets or community pharmacies are described as yogurt, capsules, powders, or tablets.[7] The use of commercially available products is increasing in the general population, both in the community and in other healthcare settings. Therefore, clinicians should evaluate the evidence of efficacy and safety of probiotics in specific indications that meet the needs of the individual patient.

Primary healthcare professionals are often the first contact person in the community for healthcare advice, especially in the context of self-care. Therefore, before making any recommendations for probiotics, it is important for healthcare professionals for a particular patient to know the probiotic's dosage form, content (especially the genera, not the strain), total dose, and duration of use.[8] Furthermore, any potential interactions with concurrently used antibiotics and antifungals may result in a loss of efficacy in probiotic treatment. The use of probiotics in immunosuppressive patients, patients with central venous catheters, individuals with hypersensitivity to milk/lactose, or certain patient groups, such as those with severe pancreatitis, may also be problematic.[7]

There are few studies that have investigated the attitudes and practices of healthcare professionals toward probiotic use and have addressed the demands of patients and the public regarding probiotic consumption in health issues.[2,8-10] The aim of this study was to determine the knowledge and attitudes of physicians and pharmacists regarding the use of probiotics in general practice.

MATERIALS AND METHODS

This cross-sectional study was conducted between November, 2017 and August, 2018 through an electronic survey of pharmacists and physicians in Ankara (Türkiye). The structured questions specific to the research were developed by the researchers through a comprehensive literature review, and the final version of the questionnaires for both pharmacists and physicians was developed separately using a survey platform (Google Docs). Each survey consisted of two sections; the first part questioned the demographics of participants (8 questions for pharmacists and 11 questions for physicians) and the second part focused on the knowledge and attitudes of participants (12 multiple choice questions for pharmacists and 10 questions for physicians) on probiotic use. The study protocol conformed to the ethical guidelines of the Helsinki Declaration and was approved by the Ethics Committee (Zekai Tahir Burak Maternity Hospital Ethics Board, no: 23/2018).

The survey was delivered to a convenient sample of physicians and pharmacists working in Ankara, who were invited to participate in the survey *via* professional e-mail groups. The participants responded to the online survey, if they volunteered to participate in the study, and informed consent was obtained *via* the survey link.

Statistical analysis

The data were analyzed as descriptive statistics (mean and percentages) using IBM SPSS version 22 (IBM SPSS Inc., Chicago, USA) after a normalization test was performed. Comparison of the responses between pharmacists and physicians was analyzed using Student's *t*-test. Statistical significance was expressed as $p < 0.05$.

RESULTS

A total of 361 pharmacists and 356 physicians participated in the study. Among them, 88.1% of pharmacists and 84.8% of physicians were practicing in community settings. The majority of physicians was over 40 years old and had more than 10 years of experience in the profession (Table 1). The participating physicians were slightly older and had a longer duration of experience in the profession compared with the pharmacists ($p < 0.05$). The specialties of the physicians were internal medicine in 227 (63.8%), basic medical science in 114 (32%), and surgical medicine in 15 (4.2%) participants, and no difference was found in terms of their attitudes toward probiotic usage ($p > 0.05$).

Unfortunately, 60.4% of physicians and 72.2% of pharmacists have indicated not to follow any national or international literature with regard to general information sources on drugs and/or diseases; however, almost half of the participants (50.6% and 54.3% of physicians and pharmacists, respectively) were influenced by information given by medical representatives of the pharmaceutical industry. In particular to probiotics, a majority of physicians (89.6%) and pharmacists (85.3%) stated that they were first informed about probiotics more than 2 years ago through congress/symposium/workshop/meeting (75.7% and 54.2%, respectively), medical representatives (46.3% and 31.2%, respectively), and literature (33.7% and 26.4%, respectively). Interestingly, 9.3% of physicians and 32.4% of pharmacists were introduced to probiotics by a pharmacist.

Healthcare professionals were also evaluated for their personal use and suggestions for using probiotics to their families and friends, when necessary; 79.2% of physicians and 88.3% of pharmacists stated that they used probiotics, 90.7% of physicians and 97.2% of pharmacists stated that they

Table 1. Demographics of the participants

Participants	n (%)		
	Pharmacists (n= 361)	Physicians (n= 356)	*p* value*
Female	269 (74.5)	151 (42.4)	
Male	92 (25.5)	205 (57.6)	
Age, years			
20-29	126 (34.9)	37 (10.4)	
30-39	86 (23.8)	77 (21.6)	< 0.00001
≥ 40	149 (41.3)	242 (68)	
Years in the profession			
< 5	120 (33.2)	40 (11.2)	
5-10	44 (12.2)	47 (13.2)	< 0.00001
> 10	197 (54.6)	269 (75.6)	

*Chi-square test

recommended probiotics to their family members. Although 62.5% of pharmacists and 59% of physicians stated that they have sufficient knowledge (or are more familiar with) about the mechanism of action and indications of probiotics, their attitudes toward probiotic use differed (Table 2).

Opinions of healthcare professionals on the attitudes of their colleagues revealed that 62.2% of pharmacists and 55.6% of physicians believed that their colleagues do not have sufficient knowledge of probiotics, and 9.5% of pharmacists and 14.3% of physicians believed that their colleagues have prejudices.

DISCUSSION

Probiotics have been recognized as useful options for treating a variety of gastrointestinal disorders, but note that their efficacy depends on the species, dose, disease, and duration of treatment.[7,11,12]

A study conducted in China showed that 65% of physicians prescribe antibiotics, whereas 57% prescribe probiotics for treating acute diarrhea during hospitalization.[13] In contrast, 53% of surgeons and 81% of gastroenterologists in the UK recommended or prescribed probiotics for the treatment of irritable bowel syndrome (IBS) (71%) and functional diarrhea (48%) for >12 months.[14] The practice of gastroenterologists in the USA is similar to that of their UK counterparts; 98% of them believed probiotics had a role in the treatment of gastrointestinal symptoms, while 93% of them reported that patients they examined took probiotics for IBS and *Clostridioides*-associated diarrhea.[15] Similar to the findings of these studies, pharmacists (99.7%) and physicians (97.7%) suggested the use of probiotics mainly for gastrointestinal diseases in this study.

Probiotics are perceived as natural and safe products by the public and can easily be purchased from supermarkets or pharmacies without a prescription or any prior medical consultation. According to a study conducted in Australia, 72% of the population had used complementary medicine (CM) in the last year and 17% had used probiotics; moreover, pharmacy customers indicated that they want to have information from a pharmacist on the safety, interactions, and effectiveness of CMs.[16] The most commonly used CM products by pediatric patients (or caregivers) with gastrointestinal disorders in gastroenterology outpatient clinics in Canada were multivitamins (65%), calcium (35%), probiotics (14%), and fish oil-omega-3 fatty acids (13%); 76% of respondents reported that they would like to discuss issues with a physician on the use of CM concurrently with prescribed medicines and 52% indicated that they would seek advice from a pharmacist.[17] In this study, 30.9% of physicians and 63.6% of pharmacists stated that their patients requested information about probiotics. These percentages may reflect the fact that the purchase of those products does not require a prescription; therefore, people can easily obtain them at pharmacies. In addition, 62.9% of physicians and 70.3% of pharmacists stated that they had received positive feedback from patients on probiotic usage, and 43.5% of physicians recommended probiotics to patients who were also prescribed antibiotics. These findings have highlighted the role of primary care health professionals in the community's perception of the use of probiotics.

A study on the knowledge and attitudes of physicians on infantile colic revealed that only 2.2% reported that parents have used probiotics and 4.5% of pediatricians considered using probiotics in cases of infantile colic. Although pediatricians acknowledge the relationship between colic symptoms and adjunctive remedies, they were less likely to counsel parents on probiotic use, and therefore probiotics were used in only 4.5% of cases.[18] Similar issues emerged in this study in which physicians and pharmacists had different perspectives on probiotic advice (p < 0.00001); 59.6% and 97.7% of the physicians stated that they recommended probiotics for 0-18 age group and gastrointestinal diseases, respectively. However, pharmacists reported to recommend probiotics for people aged 0-18 years (54.6%) and 18-40 years (54%).

Table 2. Attitudes of healthcare professionals toward the use of probiotics

Participants	n = number of respondents (%)		
	Pharmacists	Physicians	*p* value*
Age group frequently suggested to be used	**326 (100)**	**356 (100)**	
0-18 years	178 (54.6)	212 (59.6)	
18-40 years	176 (54)	67 (18.8)	< 0.00001
40-64 years	111 (34)	45 (12.6)	
≥ 65 years	64 (19.6)	32 (9)	
Diseases frequently suggested to be used	**338 (100)**	**344 (100)**	
Gastrointestinal system	337 (99.7)	336 (97.7)	
Genitourinary system	99 (29.3)	28 (8.1)	
Endocrine system	32 (9.5)	38 (11)	
Cardiovascular system	10 (3)	16 (4.7)	
Neurological system	31 (9.2)	31 (9)	
Dermatological	89 (26.3)	52 (15.1)	
Requests for advice from patients regarding probiotics	**338 (100)**	**349 (100)**	
Yes, received	215 (63.6)	108 (30.9)	
Receive feedback from patients regarding probiotic usage	**337 (100)**	**356 (100)**	
None	99 (29.4)	127 (35.7)	0.05
Positive	237 (70.3)	224 (62.9)	
Negative	1 (0.3)	5 (1.4)	
Concerns on suggesting probiotics;	**328 (100)**	**356 (100)**	
No concerns	232 (70.7)	136 (38.2)	
Recently developed drug	19 (5.8)	23 (6.5)	
The same effect can be achieved in a non-medical way	25 (7.6)	48 (13.5)	< 0.00001
Not have sufficient knowledge of the mechanism	48 (14.6)	50 (14)	
No reimbursement when prescribed	N/A	217 (61)	
Others	16 (4.9)	5 (1.4)	
Allocated space for probiotics at the pharmacy;	**331 (100)**	N/A	
Yes, it is allocated	215 (63.6)		
Suggested to a patient who is also prescribed an antibiotic by myself	N/A	**356 (100)** 155 (43.5)	

*Chi-square test, N/A: Not applicable

While probiotics are commonly recommended and purchased at primary care, 80% of pharmacists working in intensive care units (ICU) indicated that they would never consider recommending probiotics for the prevention of ventilator-associated pneumonia because of not being sure of the safety (43%) and efficacy (47%) of probiotics. Nevertheless, they were more likely to recommend probiotics for preventing *Clostridioides* diarrhea in the ICU. They further indicated that they obtain information on probiotics by communicating with their colleagues (78%), scientific journals (67%), media (15%), and medical representatives (7%).[19] Regarding the sources of information, healthcare professionals in Europe indicated that they acquired knowledge on probiotics from books (53.3%), websites (34.9%), at work (28%), pharmacies (25%), and radio/television (9.7%).[2]

The study by Marupuru et al.[9] has shown that probiotics were used by 53% of pharmacists (mainly for general health and wellness but also treating stomach and intestinal illness), and 89% of pharmacists would recommend probiotics to patients, friends, and relatives. In the study where the participants were all healthcare professionals from Europe stated that 92% of pharmacists and allied health professionals and more than 84% of physicians and dentists had already used probiotics, and in general 87.5% of health professionals advised people (such as

patients, friends, and relatives),[2] whereas it was found in this study that 88.3% of pharmacists had used probiotics and 97.2% recommended it for relatives and friends.

Research conducted in community care settings in Canada revealed that most community pharmacists (66%) recommend natural products, including probiotics, to patients, most frequently concurrently with other drugs (69%).[20] In a study conducted in South Africa, 78% of pharmacists reported being slightly too familiar with probiotics.[8] Another study that included all healthcare professionals from different parts of Europe reported that pharmacists' self-evaluated (on a 5 point Likert scale) knowledge on probiotics (rated as "good") was significantly higher than that of physicians (rated as "medium").[2] Just over one-third of pharmacists in this study indicated to have sufficient knowledge on probiotics, whereas 23.2% believed that physicians in general have sufficient knowledge and recommend probiotics to patients. With regard to having concerns before giving advice on probiotics, 70.7% of pharmacists reported having no concerns, whereas 60.9% of physicians stated that they have concerns about prescribing because of probiotics having no reimbursement. A study conducted among pharmacists reported that 15% of pharmacists had negative attitudes that CM products (including probiotics) interfered with standard medical care.[8] The findings from Pakistan revealed that only 15.1% of healthcare professionals (including pharmacists and physicians) had a good knowledge regarding the use of probiotics, and lack of knowledge about the clinical use of probiotics (57%) and the high cost of probiotics (35.4%) were the most common reasons for not recommending.[10] These concerns can be overcome by globally accepted expert recommendations. Guidance for probiotic use was issued,[21,22] which indicated that knowing the correct definition of probiotics, making the correct choice among mono-strain or multi-strain products, being sure about the safety and clinical efficacy of the strains, avoiding antibiotic resistance genes, and choosing probiotic strains resistant to the gastrointestinal environment will help to maintain rational use of probiotics.

Study limitations

According to the health statistics report by the Turkish Ministry of Health,[23] approximately 28,000 pharmacists and 145,000 physicians practice in different settings in Türkiye. In particular, in Ankara province, 2,278 general practitioners and 2,297 pharmacists were registered in 2016. Therefore, reaching approximately 15% of the targeted population is one of the main limitations of this study. In addition, pharmacists and physicians unfamiliar with probiotics may not have responded to the survey, which may have caused sampling bias. The participants of this study were mainly from metropolitan cities, and the findings may not reflect the practice norms nationwide; however, it will help to provide comparative views for further studies to be conducted in developed and/or developing countries.

CONCLUSION

A discrepancy in knowledge, attitudes, and practices among healthcare professionals still exists in local settings, which may affect public perception and health behavior regarding probiotic use. The aggregated data from local exploratory studies would indicate practice patterns for probiotic use and identify further needs of patients and healthcare professionals in different health settings. Due to the increasing number of licensed probiotic products, insufficient knowledge of practitioners, and influence of medical representatives on practitioners, it is important to have scientific and updated information sources available for healthcare practitioners.

Acknowledgements

The authors would like to thank Mr. Erdal Kart (B. Pharm.) for technical & IT support in this study.

Ethics

Ethics Committee Approval: Zekai Tahir Burak Maternity Hospital Ethics Board, Ankara (no: 23/2018).

Informed Consent: Informed consent was obtained by the participants once they agreed to participate in the online survey.

Authorship Contributions

Concept: H.B.G., K.D., T.K., Design: H.B.G., K.D., T.K., Data Collection or Processing: H.B.G., Analysis or Interpretation: K.D., A.B.E., Literature Search: H.B.G., Writing: A.B.E., H.B.G., K.D.

Conflict of Interest: The authors have no relevant financial or non-financial interests to disclose.

Financial Disclosure: The authors declared that this study received no financial support.

REFERENCES

1. Markowiak P, Śliżewska K. Effects of probiotics, prebiotics, and synbiotics on human health. Nutrients. 2017;9:1021.
2. Fijan S, Frauwallner A, Varga L, Langerholc T, Rogelj I, Lorber M, Lewis P, Povalej Bržan P. Health professionals' knowledge of probiotics: an international survey. Int J Environ Res Public Health. 2019;16:3128.
3. Ottman N, Smidt H, de Vos WM, Belzer C. The function of our microbiota: who is out there and what do they do? Front Cell Infect Microbiol. 2012;2:104.
4. Food and Agricultural Organization of the United Nations, World Health Organization. Joint FAO/WHO Working Group Report on Drafting Guidelines for the Evaluation of Probiotics in Food. 2002.
5. Floch MH, Walker WA, Sanders ME, Nieuwdorp M, Kim AS, Brenner DA, Qamar AA, Miloh TA, Guarino A, Guslandi M, Dieleman LA, Ringel Y, Quigley EM, Brandt LJ. Recommendations for probiotic use-2015 update: proceedings and consensus opinion. J Clin Gastroenterol. 2015;49(Suppl 1):69-73.
6. Sanders ME. Probiotics in 2015: their scope and use. J Clin Gastroenterol. 2015;49(Suppl 1):2-6.
7. Wilkins T, Sequoia J. Probiotics for gastrointestinal conditions: a summary of the evidence. Am Fam Physician. 2017;96:170-178.

8. Thin SM, Thet D, Li JY, Nakpun T, Nitadpakorn S, Phanudulkitti C, Sorofman BA, Watcharadamrongkun S, Kittisopee T. A systematic review of community pharmacist practices in complementary medicine. Pharm Pract (Granada). 2022;20:2697.

9. Marupuru S, Axon DR, Slack MK. How do pharmacists use and recommend vitamins, minerals, herbals and other dietary supplements? BMC Complement Altern Med. 2019;19:229.

10. Arshad MS, Saqlain M, Majeed A, Imran I, Saeed H, Saleem MU, Abrar MA, Islam M, Hashmi F, Akbar M, Chaudhry MO, Ramzan B, Rasool MF. Cross-sectional study to assess the healthcare professionals' knowledge, attitude and practices about probiotics use in Pakistan. BMJ Open. 2021;11:e047494.

11. Boyle RJ, Robins-Browne RM, Tang ML. Probiotic use in clinical practice: what are the risks? Am J Clin Nutr. 2006;83:1446-1447.

12. Verna EC, Lucak S. Use of probiotics in gastrointestinal disorders: what to recommend? Therap Adv Gastroenterol. 2010;3:307-319.

13. Ke B, Ran L, Wu S, Deng X, Ke C, Feng Z, Ma L, Varma JK. Survey of physician diagnostic and treatment practices for patients with acute diarrhea in Guangdong province, China. Foodborne Pathog Dis. 2012;9:47-53.

14. Cordina C, Shaikh I, Shrestha S, Camilleri-Brennan J. Probiotics in the management of gastrointestinal disease: analysis of the attitudes and prescribing practices of gastroenterologists and surgeons. J Dig Dis. 2011;12:489-496.

15. Williams MD, Ha CY, Ciorba MA. Probiotics as therapy in gastroenterology: a study of physician opinions and recommendations. J Clin Gastroenterol. 2010;44:631-636.

16. Braun LA, Tiralongo E, Wilkinson JM, Spitzer O, Bailey M, Poole S, Dooley M. Perceptions, use and attitudes of pharmacy customers on complementary medicines and pharmacy practice. BMC Complement Altern Med. 2010;10:38.

17. Adams D, Schiffgen M, Kundu A, Dagenais S, Clifford T, Baydala L, King WJ, Vohra S. Patterns of utilization of complementary and alternative medicine in 2 pediatric gastroenterology clinics. J Pediatr Gastroenterol Nutr. 2014;59:334-339.

18. Indrio F, Miqdady M, Al Aql F, Haddad J, Karima B, Khatami K, Mouane N, Rahmani A, Alsaad S, Salah M, Samy G, Tafuri S. Knowledge, attitudes, and practices of pediatricians on infantile colic in the Middle East and North Africa region. BMC Pediatr. 2017;17:187.

19. Wheeler KE, Cook DJ, Mehta S, Calce A, Guenette M, Perreault MM, Thiboutot Z, Duffett M, Burry L. Use of probiotics to prevent ventilator-associated pneumonia: a survey of pharmacists' attitudes. J Crit Care. 2016;31:221-226.

20. Ogbogu U, Necyk C. Community pharmacists' views and practices regarding natural health products sold in community pharmacies. PLoS One. 2016;11:e0163450.

21. Hill C, Guarner F, Reid G, Gibson GR, Merenstein DJ, Pot B, Morelli L, Canani RB, Flint HJ, Salminen S, Calder PC, Sanders ME. Expert consensus document. The International Scientific Association for Probiotics and Prebiotics consensus statement on the scope and appropriate use of the term probiotic. Nat Rev Gastroenterol Hepatol. 2014;11:506-514.

22. Toscano M, De Grandi R, Pastorelli L, Vecchi M, Drago L. A consumer's guide for probiotics: 10 golden rules for a correct use. Dig Liver Dis. 2017;49:1177-1184.

23. Bora Başara B, Soytutan Çağlar İ, Aygün A, Özdemir TA, Kulali B, Uzun SB, Birge Kayış B, Yentür GK, Pekeriçli A, Kara S. Republic of Turkey Ministry of Health General Directorate of Health Research. Health Statistics Yearbook 2016. Republic of Turkey Ministry of Health; 2017. https://sbsgm.saglik.gov.tr/Eklenti/30148/0/ingilizcesiydijiv1pdf.pdf

Turk J Pharm Sci 2024;21(1):42-51
DOI: 10.4274/tjps.galenos.2023.11823

ORIGINAL ARTICLE

Alpha Amyrin Nano-Emulsion Formulation from Stem Bark of *Ficus Benghalensis* and its Characterization for Neuro-Behavioral Studies

Ratna BABURAJ[1], Rajendra Sandur VEERABHADRAPPA[2], Kuntal DAS[2]

[1]Krupanidhi College of Pharmacy, Department of Pharmacology, Bangalore, India
[2]Mallige College of Pharmacy, Department of Pharmacology and Department of Pharmacognosy and Natural Product Chemistry, Bangalore, India

ABSTRACT

Objectives: Alpha-amyrin (AA) is a pentacyclic triterpene that exhibits erratic gastrointestinal absorption and poor blood-brain barrier permeability. The study aims to isolate AA from the stem bark of *Ficus benghalensis* L. (Fb) (Moraceae), purify it, and formulate a nanoemulsion (NE) that may improve its bioavailability, characterization, and intranasal (IN) administration to Swiss albino mice to check its neurobehavioral effects in aluminum-induced neurotoxicity.

Materials and Methods: AA was isolated from the stem bark of Fb by Soxhlet extraction, purified by analytical methods, prepared chitosan-decorated NE of the same, and characterized. It was then administered through IN route to aluminum-treated Swiss albino mice for 28 days to check its effect on neurobehavioral parameters.

Results: IN delivery of chitosan-decorated AA, NE resulted in significant improvement in neurobehavioral parameters. It reduced the fall-off period in the rotarod test and the escape latency in the Morris water maze test, and animals showed improved learning and spatial memory in the elevated plus maze. The transfer latency of animals improved with treatment compared with the aluminum-induced groups, indicative of the neuroprotective role of the drug.

Conclusion: IN administration of AA, NE isolated from the stem bark of Fb improved neurobehavioral parameters in aluminum-induced neurotoxicity in Swiss albino mice.

Keywords: Aluminium, alpha amyrin, nanoemulsion, intranasal, neurobehavioral

INTRODUCTION

Alpha-amyrin (AA) is a pentacyclic triterpene of the urbane group with an attractive pharmacological profile. The drug possesses bioavailability issues due to poor water solubility, whimsical gastrointestinal (GI) absorption, and poor blood-brain barrier (BBB) permeability, which restrains its usage as a drug. Plant-derived secondary metabolites are formidable moieties that are abundant in plant species from tropical rainforests.

Ficus benghalensis L. (Fb) (Moraceae) or the Great Indian banyan, a good source of phytocompounds, can be used to isolate triterpenes such as AA. It is found all over Indian rainforests. The root contains phytosterols, the leaves contain triterpenes, fridelin, and beta-sitosterol, and the bark is rich in bengalinoside, flavonoid glycoside, leucocyanidin, leucopelargonidin, AA, phenols, alkaloids, and tannins. Heartwood consists of alpha-taraxasterol and tiglic acid. Milky latex is used for wound healing, swelling, skin diseases, to treat vaginal diseases, and diabetes, as a uterine tonic, in diarrhea, nausea, vomiting, ulcers, irritable bowel syndrome (IBS), bleeding disorders, *etc*. Studies related to the antimicrobial, anti-arthritic, and wound-healing effects of Fb confirm the potential of the Banyan tree.[1-3]

Studies reveal that amyrins possess GI-protective action,[4] anti-inflammatory activity, hepatoprotective,[5] help to regulate blood

*Correspondence: ratnababuraj2@gmail.com, Phone: +919741201876, ORCID-ID: orcid.org/0000-0002-3826-3661
Received: 10.11.2022, Accepted: 13.03.2023

glucose levels, and are useful against various cancer cell lines, including liver and breast colorectal cancers, as they induce cell death by apoptosis.[6,7] The drug AA has also been reported to possess antihyperglycemic and hypolipidemic action,[8] and it plays a role in modulating enzymatic, hormonal, and inflammatory responses.[9] Although it has a potential, factors such as poor water solubility, extensive half-life, deplorable clearance, and wavering GI absorption evinced by AA impede its usage as a drug.[10] The route through, which a drug is administered, plays a vital role in determining the bioavailability of a drug, especially when the candidate exhibits poor absorption through the GI route. To overcome this predicament, various approaches may be adopted, such as complexation of the drug moiety or conversion into salt form, preparing nanoformulations, *etc*.[11] When a drug is supposed to target complex systems such as the central nervous system (CNS), the blood brain barrier (BBB) acts as a major barrier as it restricts and hinders the entry of xenobiotics. Various parameters related to the drug, such as acid dissociation constant, log P, lipophilicity, bioavailability, and first-pass metabolism, are important to ensure proper drug action on the system involved. The problems associated with drug solubility, poor oral bioavailability, poor GI absorption, *etc*., may be solved through the formulation of nanoparticles or any nanopreparation. The same, when administered through an alternate route such as an intranasal (IN) or intravenous route, would help to surpass the issues associated with GI absorption and first-pass metabolism.[12] Such alternate routes improve the bioavailability of the drug and ensure full-fledged use of the drug moiety's pharmacological potential.

Nanotechnology is a promising Promethean science that helps to meet the hurdles associated with absorption, distribution, metabolism, and excretion, and thereby attenuates bioavailability issues. Incorporation of a mucoadhesive polymer such as chitosan would help overcome mucociliary clearance[13] and help to carry the IN administered drug moiety across the tight junctions of the BBB.[14,15] The approach opted for here is through the formulation of a NE of the drug AA[16] to be administered IN which would be carried to the brain[17] through the olfactory and trigeminal nerve supply which links the nasal mucosa directly to the brain.[18] This work aims at isolating AA from the stem bark of *Fb* and developing an AA-loaded chitosan NE suitable for IN delivery, targeting the brain, and studying its effect in altering neurobehavioral parameters in aluminum chloride-induced neurotoxicity.

MATERIALS AND METHODS

Chemicals and reagents

Extraction and isolation

AA standard (Sigma Aldrich, 98% pure), methanol, chloroform, petroleum ether, toluene, ethyl acetate, and formic acid (SDFCL Mumbai).

Thin layer chromatography (TLC): *n-hexane*, ethyl acetate (analytical grade), and iodine crystals (SDFCL Mumbai) instead of *n-hexane*, ethyl acetate (analytical grade), and iodine crystals.

Apparatus

Soxhlet apparatus, column chromatography: performed on silica gel (60-120 mesh, Thermofisher Scientific) and TLC plates, iodine chamber, glass chamber (Twin-trough).

Isolation of AA from Fb stem bark

Plant raw material collection, handling, and extraction

Fb stem bark gathered during January, 2022 from it is habitat in Bengaluru (India), authenticated by a taxonomist, and preserved as a herbarium (KCP-PCOG/FB/330/2021-22). The stem barks were segregated, followed by air drying and drying in an oven at 45 °C, and coarsely powdered. A total of 850 g of the powdered stem bark was subjected to exhaustive Soxhlet extraction with methanol-water (1:4) at 70 °C for about 2 hours and 3 washes. The final liquid extract was reduced using a rotary evaporator and was conserved in a glass container for further studies.[19] The Institutional Animal Ethics Committee of Kruanidhi College of Pharmacy approved the protocol under the reference number: KCP/IAEC/PCOL/61/2020.

Isolation of AA

TLC was performed using the methanolic extract of Fb. A measure of the extract was mixed with little methanol and stowed and adsorbed on silica gel (grade 60-120 mm, 245 g). The extract was loaded into a silica gel column. The column was packed with petroleum ether, and the phytoconstituents were eluted first with petroleum ether (60-80 °C), followed by petroleum ether-chloroform (9:1, 1:1, 1:3, *v/v*), and finally with chloroform, chloroform-methanol (99:1, 98:2, 95:5, 9:1, 3:1, 1:1, 1:3, *v/v*), and methanol. Eluting the column with petroleum ether: chloroform (1:1) yielded colorless AA acetate crystals. AA was obtained by recrystallizing the same from acetone.[19-21]

TLC: The crystallized form of AA was then subjected to TLC [mobile phase: *n*-hexane: ethyl acetate (9:1)], infrared (IR) spectroscopy (ATR-IR), high performance liquid chromatography (HPLC) (mobile phase A- ammonium acetate 10 mm unadjusted, mobile phase B: acetonitrile: methanol (1:1), isocratic method: flow-1.2 mL/min; A-25% and B-75%, column temp: 35 °C, sample temperature: 15 °C) (HPLC waters 2695) and LC-MS/MS (LC-MS/MS condition: LC condition: solution A: 0.1% formic acid in water, solution B: acetonitrile MS grade, flow rate: 1.2 mL/min, column: Waters XBridge 50 x 4.6 mm 3.5 µ, C18, mode of elution: gradient, diluent: methanol, detector: ultraviolet-visible (UV-vis). LC-MS/MS -(MS quadrupole: capillary-3.45, cone-3.3, extractor-3, source temperature-110, desolvation temperature-500, gas flow-desolvation L/h-800 cone (L/h)-50, scan time-0.2 s). The spectroscopic analysis confirmed the presence of AA (purity: 98.37%) in Fb stem bark.

Preparation of AA-loaded chitosan-decorated NEs

Pre-formulation studies

The melting point of AA was determined using the Thiele tube method. Drug solubility in different solvents was assessed by the saturation shake flask method by dissolving the

drug in solvents such as water, phosphate buffer, dimethyl sulfoxide (DMSO), and methanol. The λ_{max} of AA was determined by preparing solutions of different concentrations and was then scanned from 200 to 400 nm using a UV-vis spectrophotometer.

Calibration curve of AA in methanol

A standard calibration curve of AA was made by drawing and making serial dilutions with AA stock solution, and the absorbance of the same was measured at 205 nm by the UV method with methanol as the blank.

Compatibility studies

Physicochemical characterization of AA NE formulation: [drug excipient compatibility study (ATR-IR analysis)]

The physicochemical interactions of AA with chitosan were studied using attenuated total reflectance-fourier transform infrared (FTIR) (Bruker ATR Alpha). Drugs and other ingredients (1:1) were stored in hermetically sealed glass vials at 40 °C and 75% relative humidity for one week. IR spectra of AA and the physical mixture were recorded using an ATR-IR (Bruker ATR alpha) instrument at wavelengths of 4400 cm^{-1} and 400 cm^{-1}. This was done to check for the compatibility between the drug and other components to check for any interaction.

Formulation of the chitosan decorated NE

Chemicals and reagents

AA, low-molecular-weight chitosan [ICAR Central Institute of Fishery Technology (85% deacetylated)], sesame oil, Tween 80, poly ethylene glycol (PEG) 400 (Sigma-Aldrich), glacial acetic acid, deionized water.

Apparatus

Polytron high-speed homogenizer [Kinematica PolytronTM (PT-2100)], magnetic beads, stirrers, 0.2 μ syringe filters, Horiba scientific particle size and zeta potential analyzer (Horiba SZ-100, Z-type, version 2.0), digital pH meter (Digisun electronics system), Brookfield viscometer (Brookfield Ametek), UV/Visible spectrophotometer (Shimadzu-1800).

Procedure

A spontaneous emulsification technique was utilized to prepare a chitosan-decorated NE of AA.[22] The procedure was carried out at 25 °C. NEs were prepared by adding the organic phase (AA, sesame oil, and polyethylene glycol stirred continuously) to the aqueous phase (chitosan solution and Tween 80)[23] followed by continuous stirring. Chitosan solution (2% *w/v*; low molecular weight, ~50 kDa) was prepared by dissolving chitosan in 100 mL of 1% glacial acetic acid and homogenizing at 2000 rpm for 24 hours. To 25 mL of chitosan solution, 2.5 mL of Tween 80 was added, blended well for 20 min, and homogenized at 2000 rpm. The oil phase consisting of AA mixed with 10 mL sesame oil and 5% polyethylene glycol was stirred for 1 h at high speed and added dropwise to the mixture of chitosan and Tween. The mixture was agitated for 60 min at room temperature with continuous stirring at 2000 rpm (Kinematica Polytron™ PT2100).[24,25] The mixture was homogenized for approximately 2 min at 4000 rpm to produce NE with homogeneity and passed through a 0.2-micron syringe filter to reduce and homogenize the size of droplets. NE formed was collected and centrifuged, and the supernatant was collected to determine the percentage of drug content.

Evaluation of AA chitosan NE

The optimized AA-NE was investigated for 28 days under vigorous conditions as *per* International Council for Harmonisation (ICH) of Technical Requirements for Pharmaceuticals for Human Use guidelines to analyze it is thermodynamic constancy, followed by cycles of heating and cooling to observe the physical appearance, evidence of creaming or turbidity, *etc*., and was centrifuged for about 10 min at 4000 rpm for 10 min to check for any signs of instability.

The pH of the prepared chitosan NE was determined using a digital pH meter at room temperature. The globule size, size distribution, and zeta potential of AA-NE were determined using a Horiba scientific instrument.

The morphology and structural attributes of the prepared formulation were examined using a simple light microscope. The viscosity of the formulation was checked using a Brookfield viscometer at room temperature. All investigations were performed in triplicate.

The percentage of drug content was assessed using UV spectroscopy. A measured volume of the NE was centrifuged for 40 min at a speed of 15,000 rpm at 25 °C to separate the drug, which is separated in the supernatant, from the drug in the NE after dilution. The percentage drug content was calculated using the formula;

$$\text{Drug content (\%)} = \frac{\text{Absorbance}}{\text{Slope}} \times \text{Dilution factor} \quad (1)$$

Surface morphology

Transmission electron microscopy (TEM) analysis was used to determine the morphological attributes of the AA-NE formulation and NE images were taken at various resolutions.[25]

Neurobehavioral studies

Apparatus used

Rolex digital rotarod apparatus, elevated plus maze, and Morris water maze were used. Swiss albino mice were procured from the animal house at Krupanidhi College of Pharmacy (in-house) after ethical clearance (KCP/IAEC/PCOL/61/2021). Animals were grouped into 4 groups with 6 animals in each group. Normal, positive control ($AlCl_3$ 100 mg/kg *p.o.*), treatment group 1 [10 mg/mL IN of AA-NE + $AlCl_3$ (100 mg/kg *p.o*)], and treatment group 2 [20 mg/mL IN of AA-NE + $AlCl_3$ (100 mg/kg *p.o.*)] for 28 days. Neurobehavioral tests such as the rotarod test, Morris water-maze test, and elevated plus-maze tests were performed on days 14 and 28 of the study.

Statistical analysis

Statistical significance of all the results was tested by comparing AA treatment groups with respective control. It was performed by one-way ANOVA ordinary measures followed by Dunnett's comparison test where data are expressed as mean ± standard deviation (SD) (n= 6).

RESULTS

Isolation of AA from Fb stem bark

The Fb stem bark extract yielded a brownish mass (74 g, 11%) from which 0.457 g of the pure compound was isolated (0.609% yield).

Confirmation of AA using the analytical method

TLC shows AA in the sample compared with the standard (Figure 1). FT-IR of isolated AA compared with the standard confirms the purity of the isolated compound (Figure 2). LC-MS/MS results (Figures 3 and 4) confirmed the presence of AA with evident peaks at 426.61 and 218.72. Ions with mass-to-charge ratios of 218 and 426.6 were identified as AA. Isolated AA displays an *m/z* value of 426.61, similar to the standard AA of 426.7.[26]

HPLC of AA

HPLC demonstrated that isolated AA, as well as standard, has retention at 5, confirming the purity of AA (Figure 5).

Preparation of AA chitosan NE

Pre-formulation studies

The melting point of AA was 186 °C. Solubility studies of AA in various solvents showed it is solubility (Table 1) in methanol and DMSO.

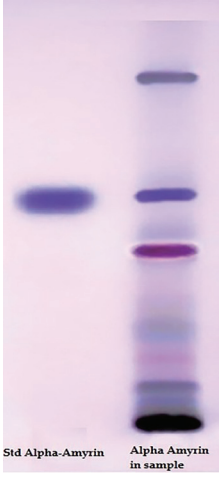

Figure 1. TLC of alpha-amyrin
TLC: Thin layer chromatography

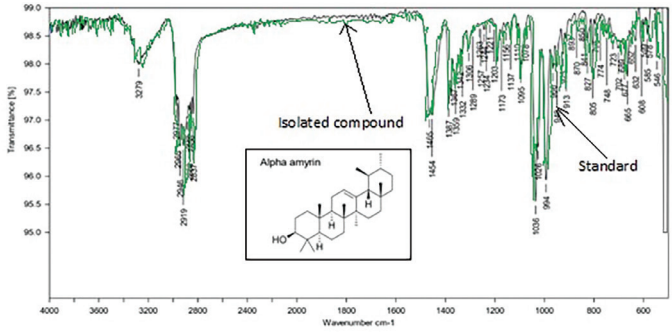

Figure 2. FT-IR of isolated AA compared to the standard
FT-IR: Fourier transform infrared, AA: Alpha-amyrin

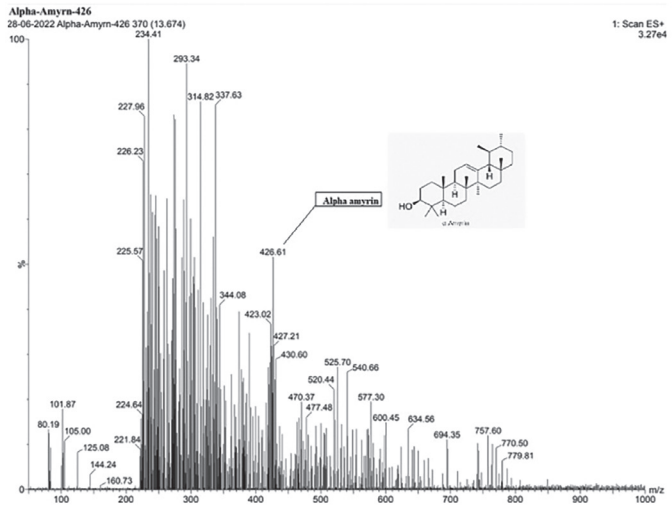

Figure 3. LC-MS/MS analysis of AA
AA: Alpha-amyrin

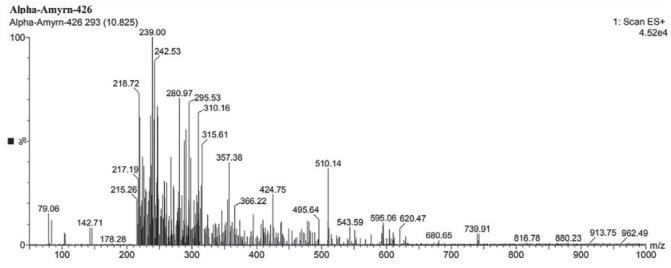

Figure 4. LC-MS/MS of isolated AA
AA: Alpha-amyrin

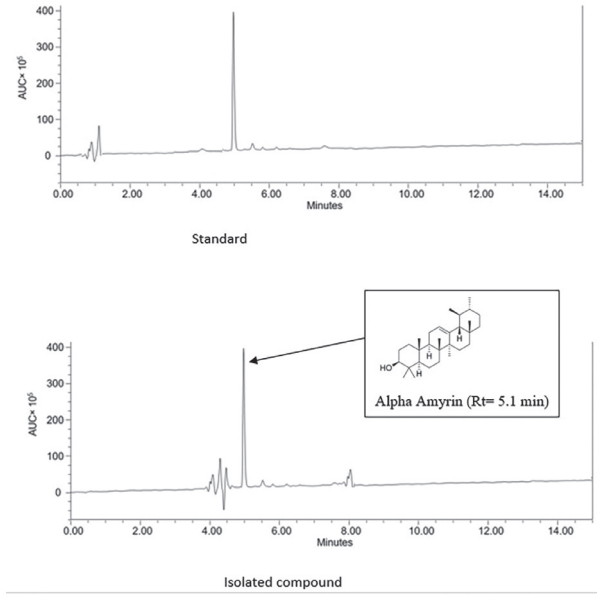

Figure 5. HPLC of isolated AA *vs.* standard
AA: Alpha-amyrin, HPLC: High performance liquid chromatography

Table 1. Solubility of alpha amyrin in different solvents

Solvent	Type
Phosphate buffer pH 6.4	Insoluble
Methanol	Very soluble
Water	Insoluble
DMSO	Soluble

DMSO: Dimethyl sulfoxide

Calibration curve of AA

AA showed λ_{max} at 205 nm, and this wavelength was chosen for analysis. Serial dilutions from a solution from a stock solution (10 mg of AA dissolved in 50 mL of methanol and sonicated) were prepared and analyzed using a UV spectrophotometer, which gave the calibration curve (Figure 6).

Compatibility studies

FT-IR analysis

FT-IR studies of the drug and mixture of drug, polymer, and other components were performed to investigate the interaction at a wavelength between 4400 and 400 cm^{-1} (Figures 7 and 8). O-H stretching between 3550 and 3200 cm^{-1}, C-H bending at 3550 and 3200 cm^{-1}. C-H Bending at 1465. C=C bending at 995-985 cm^{-1}. The mixture of AA with chitosan, tween, PEG, and sesame oil has all the characteristic peaks of AA, which confirms that the components are compatible (Figures 7 and 8).

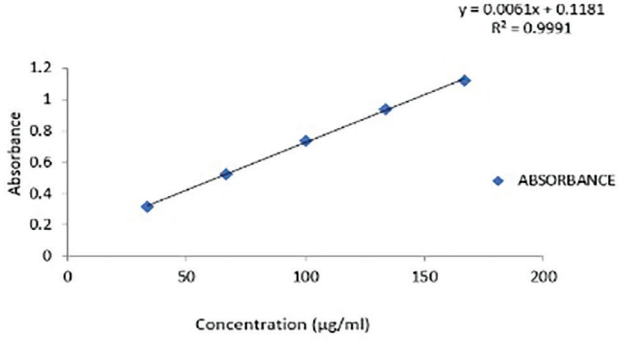

Figure 6. Calibration curve of AA

AA: Alpha-amyrin

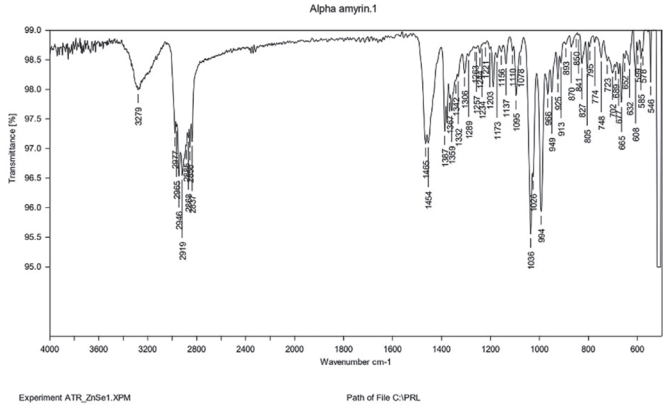

Figure 7. FT-IR of AA

FT-IR: Fourier transform infrared, AA: Alpha-amyrin

Evaluation of the AA Chitosan NE

The NE was found to be thermodynamically stable. The physical appearance remained unaffected, and the preparation did not show a creaming effect or turbidity, when subjected to heating and cooling cycles upon centrifugation. It did not show phase separation and was stable.

Particle size (globule size), zeta potential, and polydispersity index (PDI) determination

The compositions of formulations F1 and F2 are given in Table 2, using the same components in both formulations at different ratios. The average size distribution of prepared NEs F2(a) and F2(b) was 57.9 nm and 63 nm, respectively, with PDI values of 0.4 and 0.9, which suggests the formation of nanosized formulations (Table 3). F1 exhibited a greater particle size, higher polydispersity index, and unstable zeta potential; hence, F1 was not studied further and F2 was selected for the rest of the analysis (Figures 9-12).

The pH and viscosity of NE are depicted in Table 4. NE was found to have a percentage drug content of 98%.

Surface morphology by TEM analysis

TEM images indicated that the average particle size of the NE F2 was between 50 and 100 nm. The particle size of the chitosan NE abides by the literature (Figure 13).

Neurobehavioral studies

Rotarod test

The fall-off time of animals using the rotarod apparatus was measured on days 14 and 28.

Statistical significance of the results of the rotarod test was established by collating treatment groups with the respective positive control group by applying one-way ANOVA ordinary measures followed by Dunnett's test. The data are expressed as mean ± SD (n= 6), and $^{a}p < 0.001$ when in contrast with the normal group. $^{b, c}p < 0.01$ & when in contrast with the positive control group (Figure 14).

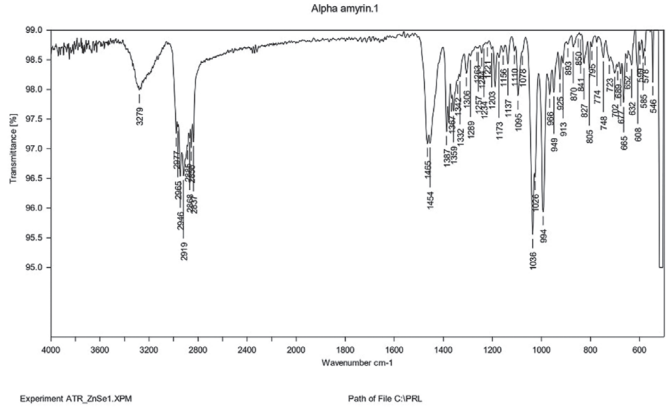

Figure 8. FT-IR of physical mixture

FT-IR: Fourier transform infrared, AA: Alpha-amyrin

Table 2. Formulation of alpha amyrin chitosan NE: Composition of formulation

Code	Acetic acid (v/v%)	Chitosan (w/v%) (25 mL)	PEG-400 (w/v%)	Sesame oil (mL)	Tween 80	Drug incorporated
F1(a)	1	0.5	5	10 mL	1.25 mL	400 mg
F1(b)	1	0.5	5	10 mL	1.25 mL	800 mg
F2(a)	1	2	5	10 mL	2.5 mL	400 mg
F2(b)	1	2	5	10 mL	2.5 mL	800 mg

NE: Nanoemulsion, PEG: Poly ethylene glycol

Table 3. Particle size (globule size), zeta potential, and PDI determination

Sample number	Globule size	Zeta potential	PDI
F1(a)	116.2 nm	14.7 mV	1.64
F1(b)	114.4 nm	-10.8	2.04
F2(a)	57.9 nm	22.1 mV	0.4
F2(b)	63 nm	25.6 mV	0.9

PDI: Polydispersity index

Table 4. pH and viscosity of chitosan NE F2

Sample number	Ph	Viscosity (cP) (20 rpm)
1.	4.9 ± 0.1	Spindle 1-48 cP Spindle 2-61 cP

NE: Nanoemulsion

The positive control group ($AlCl_3$) animals exhibited a significant reduction in fall-off period, motor coordination, and balance, when compared with the normal group on days 14 and 28. The experimental animals under $AlCl_3$ (100 mg/kg *p.o.*) induced oxidative stress exhibited significant improvement in the fall period, when treated with AA at a dose of 10 mg/mL *IN* and at a dose of 20 mg/mL *IN* compared with the positive control group. The results suggested that AA treatment improved aluminum chloride-induced impairment in balance and coordination in animals at doses of 10 and 20 mg/mL *IN*, respectively.

Morris water maze test

Escape latency, spatial memory and learning in animals were tested using the Morris water maze. The statistical significance of the results of the Morris water maze test was determined by collating treatment groups with the respective positive control group by applying one-way ANOVA ordinary measures followed

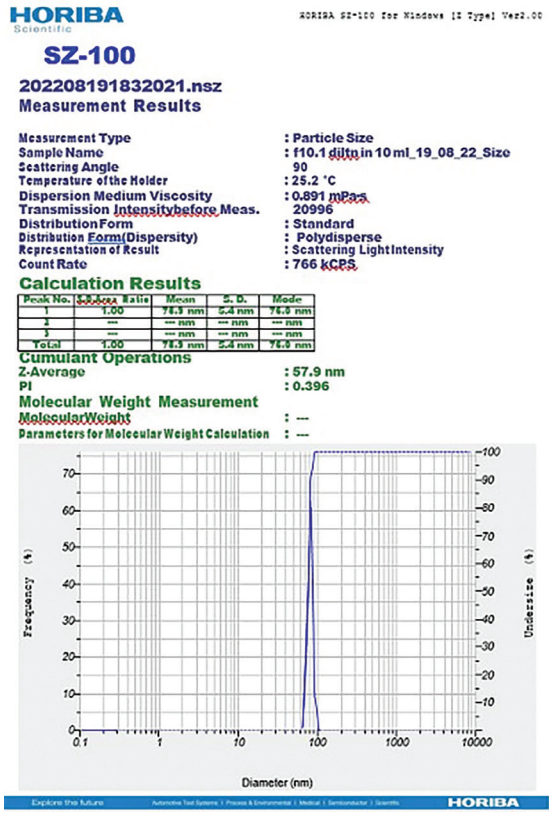

Figure 9. Globule size of the NE F2 (a)

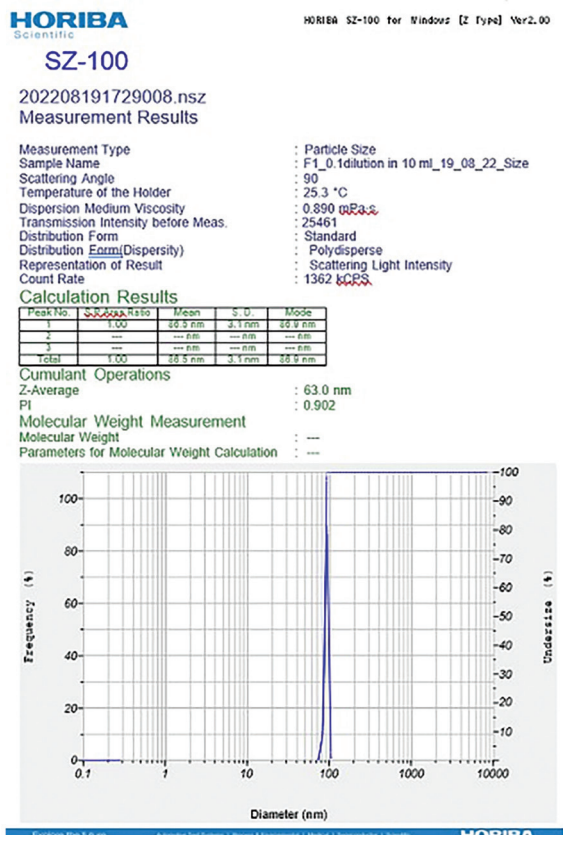

Figure 10. Globule size of the NE F2 (b)

Table 5. Transfer latency of animals (initial, first, and second transfer latency) in the elevated plus maze

Sample number	Group	Initial transfer latency	First transfer latency	Second transfer latency
1	Normal	11.67 + 1.87	10.66 ± 1.63	5.83 ± 1.47
2	$AlCl_3$ group (positive control)	23.5 + 1.87	27 ± 1.78	29.16 ± 2.04[a]
3	Alpha amyrin 10 mg/mL	18 ± 1.89 [b]	15.16 ± 1.60[c]	11.33 ± 1.75[b]
4	Alpha amyrin 20 mg/mL	19.5 ± 1.87 [c]	14.66 ± 1.75[d]	9.5 ± 1.87[c]

One-way ANOVA ordinary measures followed by Dunnett's comparison test where data are expressed as mean ± SD (n = 6), [a]$p < 0.001$ and significant compared to the normal group, [b, c]$p < 0.01$ were significant compared to the positive control ($AlCl_3$) group
SD: Standard deviation

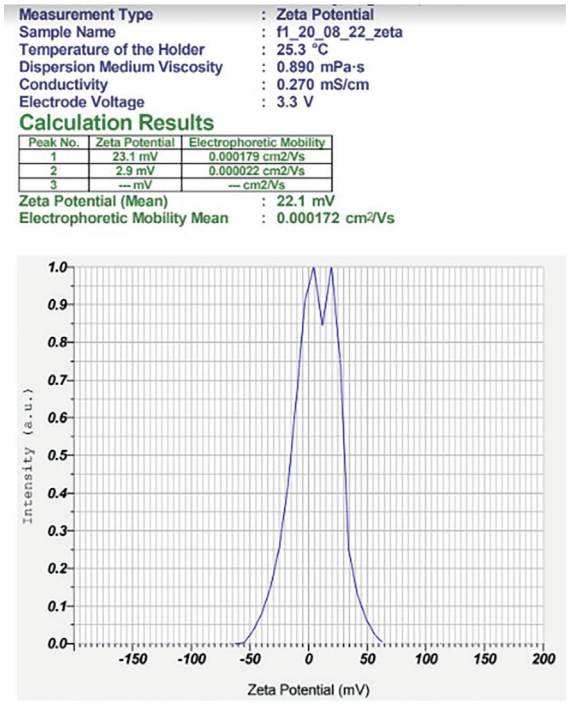

Figure 11. Zeta potential of the NE F2 (a)

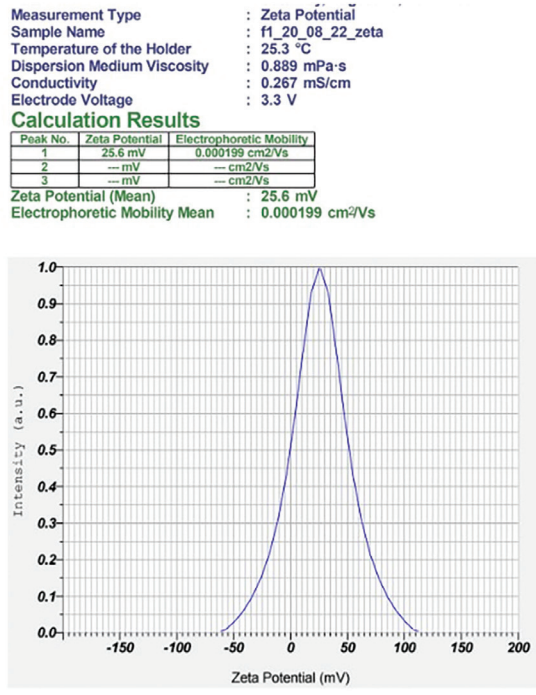

Figure 12. Zeta potential of the NE F2 (b)

by Dunnett's test. The data are expressed as mean ± SD (n= 6), and [a,b]$p < 0.001$ and significant in contrast to the positive control ($AlCl_3$) group. Treatment with AA at doses of 10 mg/mL and 20 mg/mL *IN* significantly reduced escape latency, indicating that AA at both doses helps to improve learning and spatial memory in animals despite $AlCl_3$ treatment (Figure 15).

Elevated plus maze test

Statistical significance of the initial, first, and second transfer latency of animals in the elevated plus maze test was established by collating treatment groups with the respective positive control group by applying one-way ANOVA ordinary measures followed by Dunnett's test. Here the initial transfer latency data are revealed as mean ± SD (n= 6), [a]$p < 0.001$ and significant concerning the normal group, [b, c]$p < 0.01$ were significant concerning the positive control ($AlCl_3$) group (Table 5). The first transfer latency data are expressed as mean ± SD (n= 6), $p < 0.01$ and significant compared to the positive control ($AlCl_3$) group, and data related to the second transfer latency are expressed as mean ± SD (n= 6), and [a]$p < 0.001$ when compared to the normal group and [b, c]$p < 0.01$ compared to positive control ($AlCl_3$) group (Table 5).

DISCUSSION

The investigation involved the isolation of AA from Fb, devising a chitosan-decorated NE of AA, characterization and evaluation of its effect on neurobehavioral parameters after IN administration to aluminum chloride administered Swiss albino mice. AA was isolated from the methanolic extract of Fb stem bark in colorless crystals by silica gel column chromatography. The obtained was subjected to TLC, FT-IR, HPLC, and LC-MS/MS. The spectroscopic analysis confirmed the presence of AA (purity: 98.37%) in the Fb bark.

Chitosan-decorated NE of AA for *IN* administration was prepared and characterized, and it showed the desired size range, zeta potential, PDI, percentage drug content, *etc*. Upon treatment, animals showed significant improvement in neurobehavioral

parameters in the AA treatment groups compared with the groups with aluminum chloride-induced neurotoxicity. The amount of chitosan plays a role in the size and proper coating of the globule. An optimum amount of chitosan resulted in F2 in particles with an appropriate globule size below 100 nm with zeta potential and PDI. The viscosity of the nasal preparation is essential as it should have optimum viscosity and should remain in the nasal cavity, resisting mucociliary clearance and increasing the residence time. This attribute was also confirmed by the incorporation of chitosan in the preparation. The optimum pH for the IN formulation is 4.5-6.5, and formulation F2 abides the same.[26]

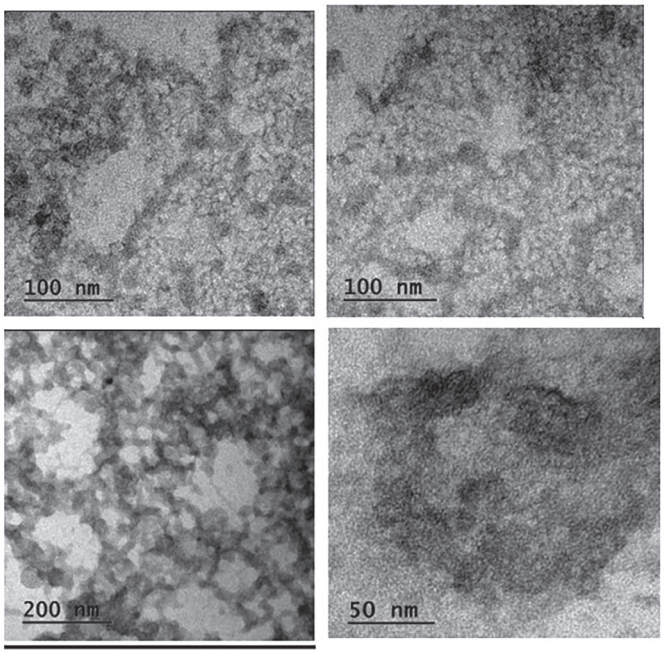

Figure 13. TEM images of AA, NEs F2(a) and F2 (b)
TEM: Transmission electron microscopy, AA: Alpha-amyrin

$AlCl_3$ induced impairment in motor coordination and balance compared with the normal group, which reduced the fall-off time on both days 14 and 28. The experimental animals under $AlCl_3$ (100 mg/kg *p.o*) induced oxidative stress exhibited improvement in the fall period when treated with AA administered *IN* at doses of 10 mg/mL and 20 mg/mL, respectively, with a better effect on day 28. The results suggest that AA treatment improved aluminum chloride-induced impairment in balance and coordination in animals at doses of 10 and 20 mg/mL *IN*, respectively. The results are contrary to the results of a study where amyrin (30 mg/kg), given *i.p.* 30 min prior, could not alter the motor response of the animals. The probable reason is thought to be due to the effect of the NE form of AA administered through an *IN* route that allowed direct action of the drug on centers for coordination and balance in the brain.

In the Morris water maze, normal animals showed shorter escape latency on days 14 and 28 in a dose-dependent manner, and the results were quite good as they expressed good learning and spatial memory as they identified the cues quickly and showed shorter escape latency in the positive control group. AA at doses of 10 mg/mL and 20 mg/mL *IN* significantly reduced escape latency, and the animals could find the hidden platform very quickly, no matter from which quadrant they started. A supportive study involving the administration of

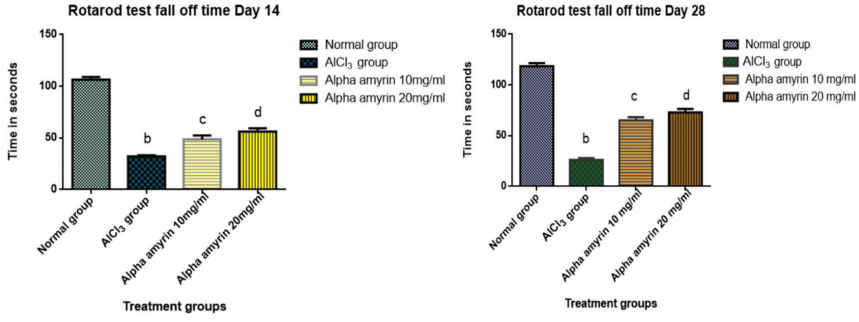

Figure 14. Estimation of fall-off period using the rotarod test

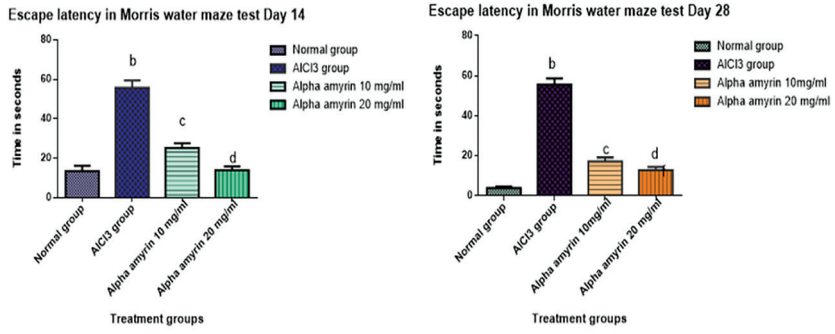

Figure 15. Estimation of escape latency using the Morris water maze test

amyrin-rich bombax ceiba extract showed a good effect in animals as it increased the escape latency in animals.[27] In the case of the elevated plus maze test, the total entries made by the animals to the open arm increased in AA-treated groups (results not given here), indicative of its anti-anxiety and antidepressant potential[28] and its a role in the improvement of retention memory in treated animals compared with the induced group. This indicates that AA at both doses helps improve learning and spatial memory in AA-treated animals despite $AlCl_3$ treatment.

The results convey that AA brought about significant improvement in learning, spatial memory, retention memory, motor coordination, balance, *etc*., in aluminum chloride-induced oxidative stress.

Acknowledgment

We would like to thank ICAR-Central Institute of Fisheries Technology for providing a sample of low-molecular-weight chitosan and Poornayu Research Lab, Bengaluru for the analytical part of the study.

Ethics

Ethics Committee Approval: The Institutional Animal Ethics Committee of Kruanidhi College of Pharmacy approved the protocol under the reference number: (KCP/IAEC/PCOL/61/2020).

Informed Consent: Not required.

Authorship Contributions

Surgical and Medical Practices: R.B., Concept: R.S.V., K.D., Design: R.S.V., K.D., Data Collection or Processing: R.B., Analysis or Interpretation: R.B., Literature Search: R.B., Writing: R.B.

Conflict of Interest: No conflict of interest was declared by the authors.

Financial Disclosure: The authors declare that they have no financial interests that could have influenced the research or its interpretation. This study was completely a self-funded work.

REFERENCES

1. Banyan Tree: *Ficus benghalensis*: uses, research, remedies, side effects. https://www.easyayurveda.com/2017/05/22/banyan-tree:ficus-benghalensis
2. Murugesu S, Selamat J, Perumal V. Phytochemistry, pharmacological properties, and recent applications of *Ficus benghalensis* and *Ficus religiosa*. Plants (Basel). 2021;10:2749.
3. Etratkhah Z, Ebrahimi SES, Dehaghi NK, Seifalizadeh Y. Antioxidant activity and phytochemical screening of *Ficus benghalensis* aerial roots fractions. J Rep Pharm Sci. 2019;8:24-27.
4. Vyas TK, Babbar AK, Sharma RK, Singh S, Misra A. Preliminary brain-targeting studies on intranasal mucoadhesive microemulsions of sumatriptan. AAPS PharmSciTech. 2006;7:49-57.
5. Oliveira FA, Chaves MH, Almeida FR, Lima RC Jr, Silva RM, Maia JL, Brito GA, Santos FA, Rao VS. Protective effect of alpha- and beta-amyrin, a triterpene mixture from *Protium heptaphyllum* (Aubl.) March. trunk wood resin, against acetaminophen-induced liver injury in mice. J Ethnopharmacol. 2005;98:103-108.
6. Barros FW, Bandeira PN, Lima DJ, Meira AS, de Farias SS, Albuquerque MR, dos Santos HS, Lemos TL, de Morais MO, Costa-Lotufo LV, Pessoa Cdo Ó. Amyrin esters induce cell death by apoptosis in HL-60 leukemia cells. Bioorg Med Chem. 2011;19:1268-1276.
7. Mishra T, Arya RK, Meena S, Joshi P, Pal M, Meena B, Upreti DK, Rana TS, Datta D. Isolation, characterization and anticancer potential of cytotoxic triterpenes from *Betula utilis* bark. PLoS One. 2016;11:e0159430.
8. Santos FA, Frota JT, Arruda BR, de Melo TS, da Silva AA, Brito GA, Chaves MH, Rao VS. Antihyperglycemic and hypolipidemic effects of α, β-amyrin, a triterpenoid mixture from *Protium heptaphyllum* in mice. Lipids Health Dis. 2012;11:98.
9. Carvalho KM, de Melo TS, de Melo KM, Quinderé AL, de Oliveira FT, Viana AF, Nunes PI, Quetz JD, Viana DA, da Silva AA, Havt A, Fonseca SG, Chaves MH, Rao VS, Santos FA. Amyrins from *Protium heptaphyllum* reduce high-fat diet-induced obesity in mice *via* modulation of enzymatic, hormonal and inflammatory responses. Planta Med. 2017;83:285-291.
10. Ching J, Lin HS, Tan CH, Koh HL. Quantification of α- and β-amyrin in rat plasma by gas chromatography-mass spectrometry: application to preclinical pharmacokinetic study. J Mass Spectrom. 2011;46:457-464.
11. Ferreira RG, Silva Júnior WF, Veiga Junior VF, Lima ÁA, Lima ES. Physicochemical characterization and biological activities of the triterpenic mixture α, β-amyrenone. Molecules. 2017;22:298.
12. Thakker A, Shanbag P. A randomized controlled trial of intranasal-midazolam *versus* intravenous-diazepam for acute childhood seizures. J Neurol. 2013;260:470-474.
13. Cui F, Qian F, Yin C. Preparation and characterization of mucoadhesive polymer-coated nano-particles. Int J Pharm. 2006;316:154-161.
14. Fessi H, Puisieux F, Devissaguet JP, Ammoury N, Benita S. Nano-capsule formation by interfacial polymer deposition following solvent displacement. Int J Pharm. 1989;55:1-4.
15. Md S, Khan RA, Mustafa G, Chuttani K, Baboota S, Sahni JK, Ali J. Bromocriptine loaded chitosan nano-particles intended for direct nose to brain delivery: pharmacodynamic, pharmacokinetic and scintigraphy study in mice model. Eur J Pharm Sci. 2013;48:393-405.
16. Rodrigues IV, Seibert JB, Carneiro SP, de Souza GH, dos Santos OD, Lopes NP. Preparation and *in vitro* evaluation of α and β-amyrins loaded nano-emulsions. Curr Pharm Biotechnol. 2013;14:1235-1241.
17. Al-Ghananeem AM, Saeed H, Florence R, Yokel RA, Malkawi AH. Intranasal drug delivery of didanosine-loaded chitosan nano-particles for brain targeting; an attractive route against infections caused by AIDS viruses. J Drug Target. 2010;18:381-388.
18. Fazil M, Md S, Haque S, Kumar M, Baboota S, Sahni JK, Ali J. Development and evaluation of rivastigmine loaded chitosan nano-particles for brain targeting. Eur J Pharm Sci. 2012;47:6-15.
19. Naquvi KJ, Ali M, Ahamad J. Two new phytosterols from the stem bark of *Ficus bengalensis* L. J Saudi Chem Soc. 2015;19:650-654.
20. Ali M, Ravinder E, Ramachandran R. New ursane-type triterpenic esters from the stem bark of *Thevatia peruviana*. Pharmazie. 2000;55:385-389.
21. Aragão GF, Carneiro LM, Junior AP, Vieira LC, Bandeira PN, Lemos TL, Viana GS. A possible mechanism for anxiolytic and antidepressant effects of alpha- and beta-amyrin from *Protium heptaphyllum* (Aubl.) March. Pharmacol Biochem Behav. 2006;85:827-834.
22. Kandav G, Singh SK. Review of nano-emulsion formulation and characterization techniques. Indian J Pharm Sci. 2018;80:781-789.

23. Kumar K, Singh L, Mishra S, Singh VK. Preparation and optimization of nano-emulsion formulations of antihypertensive drug carvedilol. EJMCM. 2018;5:282-290.

24. Khan RU, Shah SU, Rashid SA, Naseem F, Shah KU, Farid A, Hakeem KR, Kamli MR, Althubaiti EH, Alamoudi SA. Lornoxicam-loaded chitosan-decorated nano-emulsion: preparation and *in vitro* evaluation for enhanced transdermal delivery. Polymers (Basel). 2022;14:1922.

25. Akrawi SH, Gorain B, Nair AB, Choudhury H, Pandey M, Shah JN, Venugopala KN. Development and optimization of naringenin-loaded chitosan-coated nano-emulsion for topical therapy in wound healing. Pharmaceutics. 2020;12:893.

26. Pharma | Lovis 2000 M/ME and pH ME: viscosity and pH of nasal sprays or eye drops. Anton Paar. https://www.anton-paar.com

27. Mostafa MN. β-amyrin rich *Bombax ceiba* leaf extract with potential neuroprotective activity against scopolamine-induced memory impairment in rats. Rec Nat Prod. 2018;12:480-492.

28. Kun X, Zuhua G. Amyrin exerts potent anxiolytic and antidepressant effects *via* mechanisms involving monoamine oxidase and γ-aminobutyric acid in mouse hippocampus. Trop J Pharm Res. 2019;18:1673-1681.

Turk J Pharm Sci 2024;21(1):52-61
DOI: 10.4274/tjps.galenos.2023.05752

ORIGINAL ARTICLE

Olanzapine Liquisolid Tablets Using Kolliphor EL with Improved Flowability and Bioavailability: *In vitro* and *In vivo* Characterization

Rama Devi KORNI[1]*, Chandra Sekhara Rao GONUGUNTA[2]

[1]Raghu College of Pharmacy, Department of Pharmaceutical Technology, Visakhapatnam, India
[2]Vignan Institute of Pharmaceutical Technology, Department of Pharmaceutics, Visakhapatnam, India

ABSTRACT

Objectives: Liquisolid tablets are an innovative approach to enhance the dissolution rate and, thereby, the bioavailability of therapeutic agents with poor aqueous solubility.

Materials and Methods: The objective of the current research was to compare the bioavailability of the optimized formulation of the olanzapine (OLZ) liquisolid tablet with that of the marketed tablet (MT) by conducting pharmacokinetic and behavioral assessment studies. Ten formulations were designed using Kolliphor EL as a non-volatile solvent, and the respective tablets were prepared by the direct compression method.

Results: Pre-compression studies of powders of all the formulations showed good/excellent flow properties and compressibility. The drug release profiles of liquisolid tablets were determined and compared with those of MT. Based on the *in vitro* results, K250 was considered as an optimized formulation and selected for further *in vivo* studies. $AUC_{0-\infty}$ value of K250 formulation was found to be 357.2 ± 35.5 ng.h.mL^{-1}, which was higher than that of the MT (258.4 ± 29.9 ng.h.mL^{-1}). The reduction in locomotor activity was enhanced remarkably in K250 compared with MTs at $p < 0.05$. The time periods taken to fall in the rotarod test were approximately equal in the experimental groups, which indicated the absence of extrapyramidal side effects. There was a remarkable decrease in the number of boxes covered in the open field test.

Conclusion: Kolliphor EL was found to be a potential non-volatile solvent that can be used to produce liquisolid tablets of OLZ with improved flow, compressibility, dissolution, and bioavailability.

Keywords: Liquisolid tablets, olanzapine, Kolliphor EL, pharmacokinetic study, behavioral assessments

INTRODUCTION

The oral route continues to be the major route of drug administration, as it is advantages outweigh it is a major limitation of low and varied bioavailability. Bioavailability depends on several factors, the most important being the drug's solubility and permeability. Drugs are categorized into four classes based on their solubility in aqueous media and permeability through biological membranes.[1] The low bioavailability of drugs of classes II and IV of the biopharmaceutical classification system (BCS) can be improved by solubility enhancement techniques. Chemical synthetic techniques and high-throughput analysis were used for drug targeting and reducing side effects, but this approach resulted in the generation of drug molecules with high lipophilicity.[2] Approximately 40% of currently marketed drugs and 70% of new drug molecules are poorly water-soluble.[3] Poor water solubility is a crucial challenge for a formulation scientist. A number of pharmaceutical methods have been advanced to enhance the drug's aqueous solubility, including micronization,[4] solid dispersion,[5] cyclodextrin complexation,[6] and liquisolid system.[7] Liquisolid method is a new method developed for improving the rate of dissolution and bioavailability of drugs having poor aqueous solubility.[8] It is the transformation of a liquid drug or a solid drug solubilized in a liquid vehicle into a dry powder that is non-tacky, free-flowing, and highly compressible.[9]

*Correspondence: ramakalyank@gmail.com, Phone: +91 800 896 66 83, ORCID-ID: orcid.org/0000-0002-4613-8211
Received: 19.12.2022, Accepted: 13.03.2023

Olanzapine (OLZ) is a second-generation antipsychotic medication used in the treatment of bipolar disorder and schizophrenia. It is a member of class II of the BCS, which comprises drugs having low aqueous solubility and high permeability. It is a yellow crystalline powder that is practically not soluble in aqueous media.[10] The oral bioavailability of OLZ is 60%. It can be administered orally as a conventional tablet and an orally disintegrating tablet available in 2.5, 5, 7.5, 10, 15, and 20 mg dosages. OLZ can also be administered parenterally available in 5 $mg.mL^{-1}$ dosage. Plasma protein binding of OLZ is high (93%) and it undergoes extensive pre-systemic metabolism. The drug's poor water solubility and presystemic metabolism are responsible for its low oral bioavailability. The dissolution rate of OLZ is enhanced by solid dispersions,[11] inclusion complexes,[12] nanosuspensions,[13] liquisolid tablets,[14,15] and self-nanoemulsifying drug delivery systems.[16] Natarajan et al.[13] conducted pharmacokinetic (PK) studies of OLZ nanosuspensions using albino Wistar rats.

Shah and Patel[14] formulated liquisolid compacts of OLZ using PEG 400 as a non-volatile solvent, neusilin as a carrier material, and Aerosil 200 as a coating material. The effect of formulation parameters such as drug: non-volatile solvent ratio and carrier: coating ratio on the angle of repose and percentage drug release was studied by 3^2 full factorial designs. The prepared tablets were evaluated by *in vitro* quality control tests. Ramadevi et al.[15] increased the dissolution rate of OLZ using the liquisolid technique employing tween 80 and propylene glycol as non-volatile solvents. Although the dissolution rate of the drug was increased, the flow properties of the developed pre-compression powder remained poor. Kolliphor EL is a non-ionic solubilizer used for solubility enhancement. The present work aimed at the formulation of liquisolid tablets employing Kolliphor EL as a non-volatile solvent with a view to improving bioavailability by conducting *in vivo* studies. The bioavailability of the optimized formulation was compared with that of the marketed tablet (MT) using PK and behavioral assessment methods. To date, no work has been reported on the PK and behavioral assessment studies of OLZ liquisolid tablets.

MATERIALS AND METHODS

Materials

The drug OLZ and non-volatile solvent Kolliphor EL were obtained from Dr. Reddy's Laboratories, Hyderabad, India, and Baden Aniline and Soda Factory (BASF), Mumbai, India, respectively, as gift samples. Starch and Avicel PH 102 were purchased from Yarrow Chem Products, Mumbai; Aerosil 200 was procured from Oxford Laboratory, Mumbai; hydrochloric acid from Emplura, Mumbai; high-performance liquid chromatography (HPLC) grade methanol and acetonitrile from Rankem, Haryana; and ketamine from a local hospital. All other chemicals used were of analytical grade. The MT Oleanz 10 was obtained from a local pharmacy (Sun Pharma, Gujarat, India).

Determination of the solubility of OLZ in Kolliphor EL and distilled water

The drug's solubility was estimated in Kolliphor EL and distilled water. An excessive quantity of drug (30 mg) was put into each conical flask containing 10 mL of solvent. The flasks were shaken for 24 hours at 25 ± 2 °C on a rotary shaker (Sisco).[17] The drug suspensions were centrifuged, and the clear supernatant liquids were collected. The liquids were appropriately diluted using 0.1 N HCl, and the OLZ content in the supernatants was determined using an ultraviolet-visible (UV-vis) spectrophotometer (Elico, SL159) at 259 nm.[18]

Preparation of liquisolid tablets and directly compressible DCTs

The direct compression technique was used for preparing liquisolid tablets. Kolliphor EL was used as the liquid vehicle, and the composition of ten formulations is shown in Table 1. The required amounts of Avicel PH 102, used as a carrier material, and Aerosil 200, used as a coating material, were

Table 1. Formulation of OLZ liquisolid tablets

Formulations	Wt. of OLZ (mg)	Wt. of Kolliphor EL (mg)	Wt. of avicel PH 102 (mg)	Wt. of aerosil 200 (mg)	Wt. of starch (mg)	Total wt. (mg)	Carrier: coating ratio (R)	Liquid load factor (L_f)
K110	10	10	55.56	5.56	4.06	85.18	10	0.360
K120	10	10	63.49	3.17	4.33	90.99	20	0.315
K130	10	10	66.67	2.22	4.44	93.33	30	0.300
K140	10	10	68.26	1.71	4.50	94.47	40	0.293
K150	10	10	69.44	1.39	4.54	95.37	50	0.288
K210	10	20	83.33	8.33	6.08	127.74	10	0.360
K220	10	20	95.24	4.76	6.50	136.50	20	0.315
K230	10	20	100.00	3.33	6.67	140.00	30	0.300
K240	10	20	102.39	2.56	6.75	141.70	40	0.293
K250	10	20	104.17	2.08	6.81	143.06	50	0.288

Wt.: Weight, OLZ: Olanzapine

obtained from their flowable liquid retention potential (denoted as ϕ) values. Avicel PH 102 and Aerosil 200 have ϕ values of 0.27 and 0.9, respectively, for Kolliphor EL.[19] The drug was mixed thoroughly using a glass rod in a preheated non-volatile solvent (Kolliphor EL) in a beaker until a uniform solution was obtained. The carrier and coating materials were added to the drug solution and transferred to a mortar. The mixing of liquid-powder contents was carried out according to the three-stage standard mixing process described by Spireas.[20] In the first stage, the mixture was blended using a spatula for 1 min to disperse the liquid containing the drug in the carrier and coat the mixture evenly. As the second step, the drug in the liquid/carrier and coating mixture was layered in the mortar for 5 m to permit drug permeation into powder particles. The last step involves scraping off the powder from the mortar and mixing it with starch (5% *w/w*) for 30 s. A rotary tablet machine (Shakti, India) was used to compress tablets from the uniform powder mixture. The number of tablets prepared in each batch was 50.

Micromeritics of the precompression powders

The micromeritic properties of the precompression powder mixtures were evaluated by estimating the Hausner ratio, Carr's index, and angle of repose.[21] Bulk density and tapped density values were measured using a bulk density apparatus (Excel Enterprises), and the Hausner ratio and Carr's index were determined using these values. The experiments were conducted in triplicate, and the mean and standard deviation were calculated.

Characterization of the liquisolid tablets

Hardness, friability, drug content, and disintegration time were determined for the prepared liquisolid tablets. The drug release of liquisolid tablets was evaluated in distilled water (900 mL) using a USP type II apparatus at 37 ± 0.5 °C and operated at 50 rpm. The amount of OLZ released was estimated using a UV-vis spectrophotometer at 259 nm. The dissolution profiles of liquisolid tablets were compared with that of the MT Oleanz 10 (Sun Pharma, Gujarat, India), containing 10 mg of the drug. Fourier transform infrared (FTIR) spectroscopy (Bruker, Alpha-T) was used to determine drug-excipient compatibility. The solid state characterization of OLZ and optimized liquisolid tablets was carried out by differential scanning calorimetry (DSC) (Hitachi, STA-7300), X-ray diffractometer (PANalytical, X'Pert PRO), and scanning electron microscope (SEM) (Jeol Asia PTE Ltd, JSM-6610LV). The hardness, drug content, disintegration time, and dissolution studies were determined in triplicate, and the mean and standard deviation were calculated.

In vivo bioavailability studies

These studies were conducted to quantify optimized liquisolid tablets after oral administration and to compare their bioavailability with that of MT. The studies were conducted according to the Committee for the Purpose of Control and Supervision of Experiments on Animals recommendations and after acquiring owing approval from the Institutional Animal Ethics Committee of Raghu College of Pharmacy, with number RCP/1549/PO/Re/5/11/21/06 dated 11/10/21.

Pharmacokinetic study

Male rabbits weighing 1.5-2.2 kg were randomly assigned to the two treatments (n= 6). The rabbits were abstained from food for 12 hours before starting the experiment and fed 4 hours after dosing. Rabbits were given water as much as desired throughout the study.

Marketed and liquisolid tablets were powdered and dispersed in water. Two milliliters of suspension containing OLZ equivalent to the rabbit dose (1.0 mg) were administered orally. The rabbit equivalent dose was calculated based on the average weight of rabbits (2 kg).[22,23] One milliliter of blood was taken through the marginal vein of the rabbit ear at specific hour intervals of 0, 1, 2, 3, 4, 6, 8, 12, and 24 and was transferred into Eppendorf tubes containing ethylene diamine tetraacetic acid to avoid clotting of the blood sample. The blood samples were subjected to centrifugation using a cooling centrifuge (CM-12 plus, Remi) at 4000 rpm for 10 min to obtain plasma. The samples containing plasma were kept at -20 °C in a deep freezer (Subzero, ULT80) until further evaluation. The proteins in plasma were separated from the drug by a protein precipitation technique using acetonitrile as a protein precipitating agent. To 100 µL of plasma, 1 mL of acetonitrile was added and centrifuged for 15 min at 4000 rpm. OLZ present in the clear supernatant was analyzed by an HPLC (Shimadzu, Prominence) method with a UV detector, which was developed and validated earlier. The HPLC conditions were as follows: column, Hypersil-BDS C18; mobile phase, a mixture of 50 mM phosphate buffer (pH 5.5), acetonitrile, and methanol (50:30:20 *v/v/v*); flow rate-1.2 $mL.min^{-1}$, run time, 10 min; wavelength, 214 nm.

The PK parameters were calculated using PK Solver 2 software. The peak height concentration, which is denoted by the symbol Cmax, and the time of peak height concentration, which is denoted by the symbol tmax, was verified through the drug plasma level-time profile. K_E, the elimination rate constant was obtained by multiplying the slope of the linear elimination phase with 2.303. $t_{1/2}$, the biological half-life was obtained using $0.693/K_E$. The trapezoidal method was used to calculate the area beneath the plasma level-time profile from zero to the last time point, which is denoted as the area under the curve (AUC_{0-24}). The AUC from the last time point to infinity ($AUC_{24-\infty}$) was obtained by dividing the last measured concentration by K_E. The sum of both areas gives the total area beneath the plasma level-time profile from zero to infinity ($AUC_{0-\infty}$). The PK parameters of the two groups were compared for any significant differences using the *t*-test with a probability value < 0.05.

Behavioral assessments

Schizophrenia is a complex psychiatric disorder. Symptoms associated with the disorder are classified into positive symptoms, negative symptoms, and disorganized symptoms.[24] The potency of the drugs to exhibit pharmacological activity can be evaluated using animal models. Various animal models include studies on rats, mice, and monkeys. Behavioral abnormalities are symptoms of psychosis and can be studied using different animal models.[25] In this study, spontaneous

motor activity, rotarod test, and open field test were used to evaluate the pharmacological response of the drug. Male Swiss albino mice were used for spontaneous motor activity and the rotarod test, [25] and male Wistar rats were used for the open-field test.[24] The open field test was performed on rats because it is easy to observe their movements. It is difficult to conduct the test on mice because of their fast movements and small size.

Spontaneous motor activity

Male Swiss albino mice, with an average weight of 25 g, were selected and separated into three groups based on randomization, with six animals in each group. Mice were given access to water and food as much as desired. Locomotor activity was determined by using a digital phototachometer (Indosati, CAT2002E). Normal mice exhibit typical locomotor activity when placed in a phototachometer. The neurotransmitter dopamine regulates a wide array of physiological functions, including locomotor activity, in the central nervous system. The pharmacological blockade of dopamine transmission inhibits locomotor activity.[26] Marketed and liquisolid tablets were powdered and dispersed in water. A volume of suspension (0.1 mL) containing OLZ equivalent to the mice dose (0.05 mg) was administered orally. The mice equivalent dose was calculated based on the average weight of mice (25 g). The third group of mice received distilled water and were considered as controls. The animal to be tested was individually placed in the phototachometer for 10 min, and the score on the digital phototachometer was recorded. The procedure was repeated every hour for 4 hours. The percentage decrease in locomotor activity after the administration of different formulations was calculated based on the locomotion exhibited by the animals in terms of the score given by the digital phototachometer.

Rotarod test

Male Swiss albino mice were placed into three groups, with 6 mice in each group. The rotarod test was conducted according to the method outlined by Dunhan and Miya[27] in 1957. The rotarod apparatus (Indosati, two compartments) is electronic equipment that contains a rotating rod, speed knobs, and a lever. The lever functions to stop the timer, when the mouse drops down from the rod. The mice to be tested were kept on a rotating rod[28] and their latency or time taken to fall was recorded. Drugs that alter neuromuscular coordination decrease the time taken by the animals to stay on the rod.[29]

Open field test

Male Wistar rats with weights between 200 and 250 g were selected for the study. The rats were marked and assigned to four different groups by randomization with six rats in each group. The rats were given water and food as much as required. When ketamine is injected at subanesthetic doses, it induces stereotypic behavior in animals.[24,30] The intensity of behavioral patterns increases, and this occurs because of disturbances in the brain. These disturbances are similar to those experienced by patients suffering from schizophrenia. The effect of the formulations on reversing the stereotypic behavior induced by ketamine was determined. The effect can be used to interpret the efficiency of formulations in controlling the symptoms of schizophrenia. An open-field apparatus (Indosati) was used to observe behavioral changes in the animals. The open field area was equally divided into squares. Marketed and liquisolid tablets were powdered and suspended in water. A suspension of 0.5 mL containing OLZ equivalent to the rat dose (0.25 mg) was administered orally. The rat equivalent dose was calculated based on the average weight of rats (250 g). Ketamine at a dosage of 30 $mg.kg^{-1}$ was injected 30 min after administration of the formulations. The third group received only ketamine and the fourth group received normal saline. The rats were positioned in the open field apparatus and the number of squares crossed was measured.

Statistical analysis

The *t*-test was used to compare the PK parameters. One-way ANOVA was used to observe the remarkable differences between groups in behavioral assessment studies at $p < 0.05$. Dunnett's test was performed to compare the optimized formulation with the control group in the spontaneous motor activity test and with the ketamine group in the open field test at $p < 0.05$. Statistical analysis was performed using Prism 5.0 software.

RESULTS AND DISCUSSION

Solubility analysis of OLZ in Kolliphor EL and distilled water

The determination of the solubility of OLZ in liquid vehicles is the first step in the design of liquisolid systems. A higher quantity of solubilized drug in a liquid vehicle indicates a higher solubility of the drug, thereby improving its dissolution rate. OLZ is a BCS class II drug that is not freely soluble in water. The solubility of OLZ in distilled water was 0.044 $mg.mL^{-1}$ which agrees with the value given in literature.[31] The drug presented higher solubility in Kolliphor EL (3.63 $mg.mL^{-1}$).

Micromeritics of the precompression powders

Uniform and reproducible powder flow from the hopper to the die cavity is highly essential to obtain tablets of constant weight and drug content. The nature of powder flow can be determined using the Hausner ratio, Carr's index, and angle of repose. Good (K210-K250) to excellent (K110-K150) flow properties were observed when liquisolid powders were prepared using Kolliphor EL as the liquid vehicle (Table 2). Liquisolid formulations containing higher drug concentrations (K110-K150) exhibited good flow and compactibility compared with liquisolid formulations containing lower drug concentrations (K210-K250). The results were analogous to those reported by earlier workers.[32] The quantity of Avicel PH 102 increased with an increase in the R value, and thereby the flow properties of liquisolid powders improved with an increase in the R value. These findings can be attributed to the good flow properties of Avicel PH 102.[33]

Characterization of the liquisolid tablets

The values of the post compression parameters of the liquisolid tablets are presented in Table 3 and were found to be within the limits. The findings of the dissolution study of the developed tablets and MT are presented in Figures 1 and 2. The percentage released in 60 min was found to be 44.87 for MTs

Table 2. Flow parameters of precompression blends (mean ± SD, n= 3)

Formulations	Carr's index (%)	Hausner ratio	Angle of repose (degrees)
K110	18.81 ± 0.36	1.23 ± 0.04	21.98 ± 0.44
K120	16.67 ± 0.21	1.20 ± 0.02	21.47 ± 0.63
K130	15.27 ± 0.78	1.18 ± 0.03	19.65 ± 0.21
K140	14.32 ± 0.55	1.16 ± 0.03	18.97 ± 0.28
K150	11.78 ± 0.47	1.13 ± 0.01	17.69 ± 0.57
K210	28.57 ± 0.19	1.40 ± 0.02	24.74 ± 0.17
K220	23.08 ± 0.34	1.30 ± 0.01	23.47 ± 0.26
K230	22.25 ± 0.26	1.29 ± 0.05	23.04 ± 0.31
K240	21.24 ± 0.22	1.27 ± 0.04	22.73 ± 0.38
K250	16.72 ± 0.57	1.20 ± 0.02	22.04 ± 0.54

SD: Standard deviation, n= Number of trials

Table 3. Post compression parameters of liquisolid tablets (mean ± SD, n= 3)

Formulations	Hardness (kg.cm^{-2})	Friability (%)	Drug content (%)	Disintegration time (seconds)
K110	2.98 ± 0.37	0.980	97.26 ± 1.62	125.62 ± 2.40
K120	3.21 ± 0.45	0.914	97.31 ± 2.08	123.75 ± 3.28
K130	3.54 ± 0.28	0.790	99.26 ± 2.74	120.39 ± 2.60
K140	3.78 ± 0.67	0.826	99.86 ± 3.54	119.41 ± 3.34
K150	3.89 ± 0.31	0.880	101.65 ± 3.62	118.47 ± 2.35
K210	3.33 ± 0.34	0.538	98.75 ± 2.46	114.26 ± 1.59
K220	3.81 ± 0.26	0.612	99.29 ± 1.98	113.64 ± 1.56
K230	3.92 ± 0.69	0.674	101.28 ± 2.59	112.4 8 ± 3.42
K240	4.12 ± 0.62	0.706	101.67 ± 3.62	112.23 ± 3.45
K250	4.33 ± 0.56	0.791	102.54 ± 2.76	109.68 ± 5.12

SD: Standard deviation, n= Number of trials

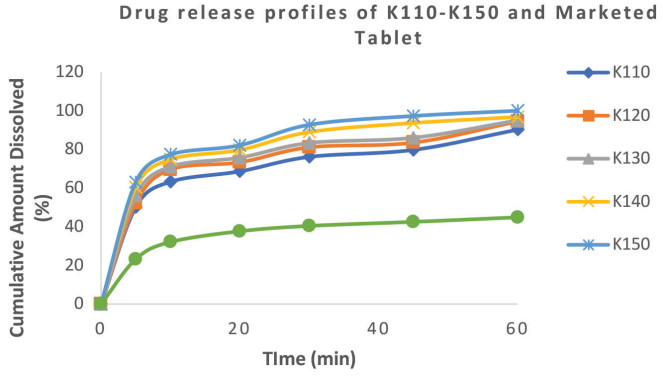

Figure 1. Drug release profiles of K110-K150 and marketed tablets

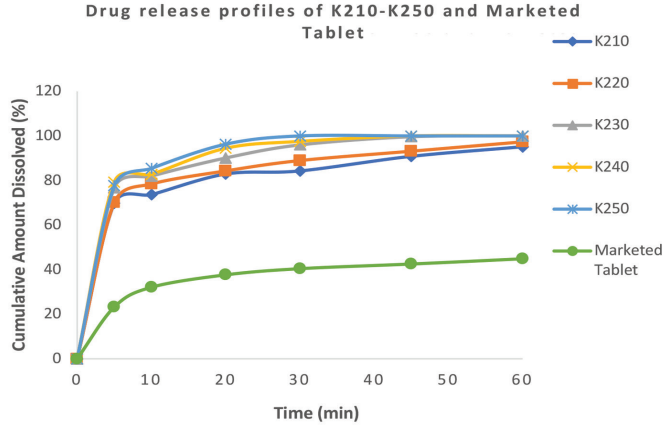

Figure 2. Drug release profiles of K210-K250 and marketed tablets

and 90.21-100 for liquisolid tablets. The results clearly indicate that the dissolution rate of liquisolid tablets is higher than that of MTs. This is best described by the Noyes-Whitney equation given in Equation 1.

$$D_R = \frac{D}{h} S(C_s - C) \quad (1)$$

Equation 1 where, D_R = rate of dissolution of the dissolved drug substances, D= diffusion coefficient of the dissolved drug substances, S= surface area of drug substances opening to the dissolution vehicle, h= diffusion layer thickness, C_S = maximum drug solubility in diffusion layer and C= drug's concentration in the dissolution medium.

The dissolution medium is the same in all studies; hence, there will be no change in the values of D and h. S and (C_s - C) were the variables that influenced the dissolution rate. In the tablet prepared without any liquid vehicle, the surface area of the drug open to the dissolution vehicle is delimited because of the drug's low aqueous solubility. In contrast, the drug substances in the liquisolid tablets were dispersed in a non-volatile solvent, which enormously enhanced the surface area of the drug molecules. The drug's saturation solubility (C_s) is increased as the drug molecules are available in a state of molecular dispersion in liquisolid tablets. The quantity of non-volatile solvent used in the formulation of liquisolid tablets is negligible, and it may not be sufficient to enhance the total saturation solubility of drug molecules in the dissolution vehicle. However, at the junction between liquisolid particles and dissolution vehicles, the quantity of non-volatile solvent that diffuses with the drug substances is sufficient to augment the solubility of drug molecules. The non-volatile solvent acts as a cosolvent in the diffusion layer. In addition, an increase in R value from 10:1 to 50:1 increased the dissolution of liquisolid tablets. The presence of a high amount of Avicel PH 102 in liquisolid tablets with higher R values is responsible for improved imbibing, disintegration, and disaggregation.[34] Liquisolid tablets, K210-K250 comprising 67.77% of Kolliphor EL, exhibited larger drug release in contrast to formulations containing lower Kolliphor EL concentration (50% in K110-150). The calculated difference factors (f1) and similarity factors (f2) show a large difference in the dissolution profiles of K250 and MT. f1 and f2 for K250 and MT were 153.38 and 12.40, respectively. Formulation K250, described with Kolliphor EL as a liquid vehicle containing 67.77% of non-volatile solvent with a carrier: coating ratio of 50, was the best formula selected considering the outcomes obtained from all the studies.

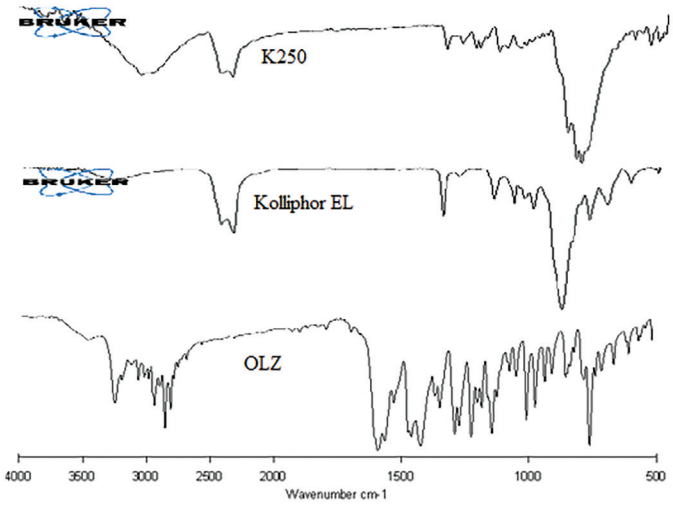

Figure 3. FTIR spectra of OLZ, Kolliphor EL, and K250
FTIR: Fourier transform infrared, OLZ: Olanzapine

The FTIR spectra of OLZ, Kolliphor EL, and the optimized liquisolid formulation with Kolliphor EL are shown in Figure 3 and the values are shown in Table 4. The distinct peaks of OLZ are observed at 2933 cm^{-1} (CH stretching), 1600-1500 cm^{-1} (double bonds attached partially to CH and NH bending deformation), 1500-1300 cm^{-1} (deformation of methyl, methylene and CH groups), 1300-1100 cm^{-1} (CC and CN stretching), 1009 cm^{-1} (deformation of piperazinyl group attached to methyl group) and 745 cm^{-1} (out of plane deformation of CH bonds belonging to the same group).[35] Any drug degradation or drug interaction with additives results in changes in ischemical structure, which is reflected by the changes in the FTIR spectra. The FT-IR spectra of liquisolid tablets exhibited the same distinct drug absorption peaks, indicating the absence of drug-liquid vehicle interaction.[36]

The DSC thermograms of OLZ and K250 are displayed in Figure 4, and their values are given in Table 5. A sharp endothermic peak at 194.25 °C was observed in the OLZ thermogram, which is related to the melting point of the drug.[37] The thermogram of the liquisolid system showed a shift of the endothermic peak to a lower temperature, indicating partial amorphization of the drug.[38]

Table 4. FT-IR peak values of OLZ and K250

Wavenumber (cm^{-1})						
	CH stretching	NH bending	CH_3, CH_2, CH deformation	CC and CN deformation	Piperazinyl deformation	CH out of plane deformation
Literature values	2933	1600-1500	1500-1300	1300-1100	1009	745
OLZ	2926.62	1587.79	1468.23	1268.89	1004.83	746.91
K250	2925.15	1580.63	1463.66	1276.48	1007.35	743.28

FT-IR: Fourier transform infrared, OLZ: Olanzapine

Polymorphism of a drug is an important factor that affects its rate of dissolution, and, eventually, its bioavailability. Hence, it is essential to observe any changes in the drug's polymorphism after formulation as liquisolid tablets. Sharp and distinct peaks at 20.47˚, 21.64˚, and 24.56˚ were observed in the X-ray diffraction (XRD) pattern of the pure drug (Figure 5, Table 5), indicating its high crystalline character.[39] The XRD pattern of the optimized liquisolid formulation (Figure 5) showed the disappearance or a decrease in the intensity of the drug's characteristic peaks, which indicates that the crystallinity of the drug is reduced. This effect was also observed in the reports of earlier workers.[40,41]

Drug crystals of irregular shape were observed in the SEM photomicrograph of OLZ (Figure 6)[12]. The inability to differentiate crystals of OLZ in the photomicrographs of K250 (Figure 6) indicates a solid-state transition in the drug.[42,43] The results of DSC, XRD, and SEM indicate a reduction in the crystallinity of the drug, which is another mechanism that explains the enhancement of dissolution in liquisolid tablets.

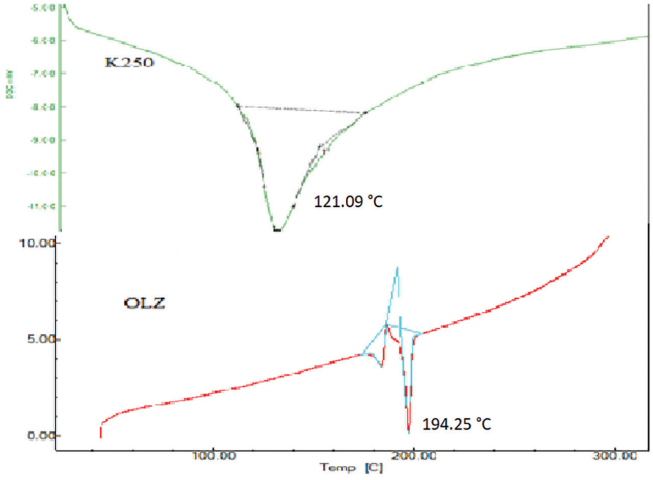

Figure 4. DSC of OLZ and K250
OLZ: Olanzapine, DSC: Differential scanning calorimetry

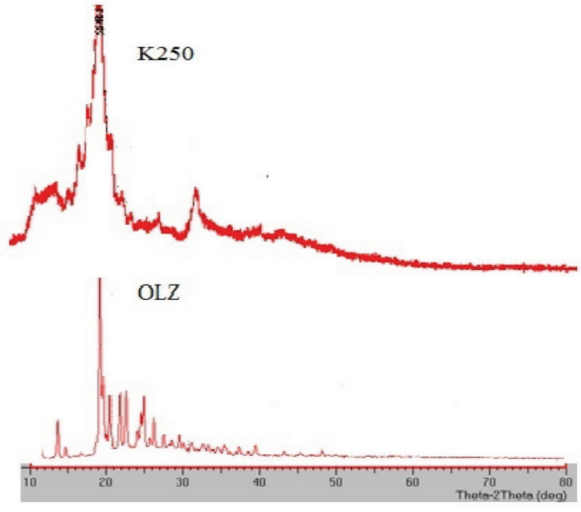

Figure 5. XRD of OLZ and K250
OLZ: Olanzapine, XRD: X-ray diffraction

In vivo studies

Pharmacokinetic study

The plasma drug concentration *versus* time graphs of the marketed formulation and optimized liquisolid formulation are presented in Figure 7, and the PK parameters obtained are given in Table 6. The peak plasma concentration obtained was higher for the optimized liquisolid tablets than for the MTs. However, the time taken to attain C_{max} was 3 hours and it was similar in both treatments. The $AUC_{0-\infty}$ which denotes the quantity of drug absorbed completely from zero to infinite time, was higher for liquisolid tablets (357.2 ± 35.5 ng.h.mL^{-1}) compared to MTs (258.4 ± 29.9 ng.h.mL^{-1}) and a significant difference was observed at $p < 0.05$ among the two groups. The higher

Table 5. DSC and XRD peak values of OLZ and K250

	DSC peak values (˚C)	XRD peak values (˚2θ)		
OLZ	194.25	20.47	21.64	24.56
K250	121.09	19.31	Absent	23.98

OLZ: Olanzapine, XRD: X-ray diffraction, DSC: Differential scanning calorimetry

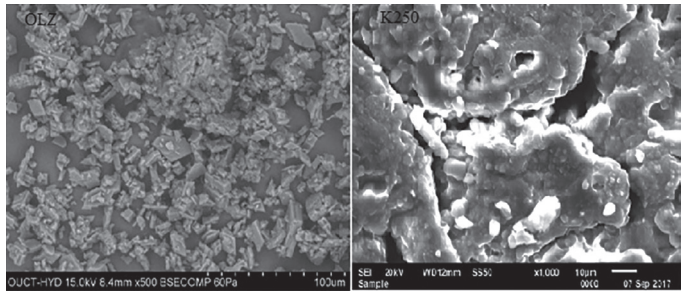

Figure 6. SEM images of OLZ and K250
OLZ: Olanzapine, SEM: Scanning electron microscope

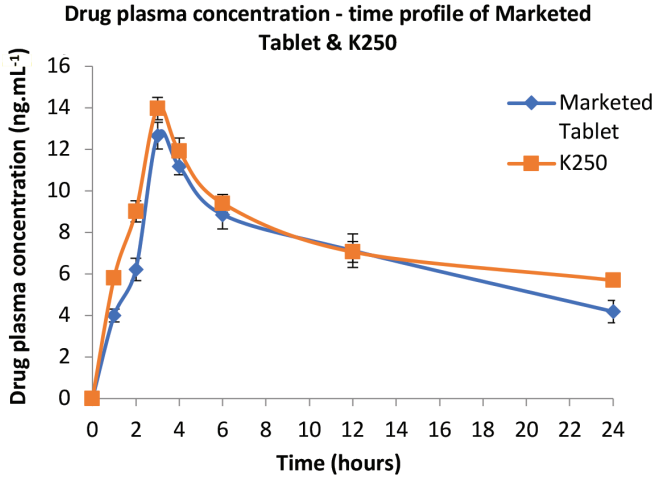

Figure 7. Drug plasma concentration-time profile of marketed tablets and K250, n= 6

Table 6. Pharmacokinetic parameters of marketed tablet and K250 (mean ± SD, n= 6)

Formulations	Pharmacokinetic parameters					
	C_{max}	t_{max}	$t_{1/2}$	AUC_{0-t}	$AUC_{0-\infty}$	K_E
	($ng.mL^{-1}$)	(h)	(h)	($ng.h.mL^{-1}$)	($ng.h.mL^{-1}$)	(h^{-1})
Marketed tablet	12.663 ± 0.643	3.000 ± 0.000	15.238 ± 2.598	165.032 ± 7.218	258.482 ± 29.926	0.046 ± 0.007
K250	13.966 ± 0.538	3.000 ± 0.000	21.276 ± 4.141	182.705 ± 5.979	357.276 ± 35.598	0.034 ± 0.006

SD: Standard deviation, AUC: Area under the curve, n= Number of trials

$AUC_{0-\infty}$ and C_{max} values obtained for the liquisolid tablet relative to the MT could be attributed to the improved dissolution rate of OLZ from the liquisolid tablets, leading to higher absorption. The non-volatile solvent Kolliphor EL used in the formulation of liquisolid tablets inhibits P-glycoprotein.[44] P-glycoprotein is present in the cell membrane and is responsible for the efflux transportation of drugs and toxins. P-glycoprotein reduces the absorption of many drugs through the intestine, thereby decreasing the drug plasma concentration. Thus, the inhibitory effect of Kolliphor EL on P-glycoprotein is an added benefit for enhancing the bioavailability of the drug in the formulation.

Behavioral assessments

The results of locomotor activity are presented in Table 7. The liquisolid tablet formulation showed a higher reduction in locomotor activity compared with the MT. A remarkable difference at $p < 0.05$ was observed in the phototachometer scores using One-Way ANOVA among the three groups. Dunnett's test was performed to determine where the significant difference lay, *i.e.*, whichever two among the three groups were significantly different. It was found that the effect of the liquisolid tablet was significantly different from that of the control.

The results of the rotarod test are given in Figure 8 and Table 8. The test was conducted to check for extrapyramidal side effects of the optimized formulation because of increased bioavailability. The latency to fall after 3 hours after administration of distilled water for control was 236.83 s; for the MT it was 223 s; and for K250 it was 220.35 s. There was no remarkable statistical difference among the three groups for the time taken to fall by the mice. The results indicate the absence of side effects in the optimized formulation.

The reversal of ketamine-induced stereotypic behavior was determined by the number of boxes covered by rats in the open field test apparatus (Figure 9, Table 9). The number of boxes covered was 44 in the control group, 82.5 in the ketamine-administered group, 66.75 in the MT group, and 61.17 in the K250 group. The liquisolid tablet showed a remarkable decrease in the number of boxes covered. A remarkable statistical difference was noticed in the number of boxes covered among the four groups at $p < 0.05$ using One-Way ANOVA. Dunnett's test showed that the effect produced by the liquisolid tablet formulation was significantly different from the group that received only ketamine.

Table 7. Results of spontaneous motor activity of different groups (mean ± SD, n= 6)

Time (hours)	Photoactometer score		
	Control	Marketed tablet	K250
1	591.83 ± 15.82	240.50 ± 6.70	224.17 ± 8.07
2	538.00 ± 14.51	183.00 ± 2.47	159.67 ± 4.86
3	551.83 ± 15.69	159.67 ± 4.86	100.17 ± 5.81
4	540.33 ± 10.43	121.00 ± 3.76	193.50 ± 3.35

SD: Standard deviation, n= Number of trials

CONCLUSION

The dissolution rate and bioavailability of the optimized formulation were assessed by conducting relevant *in vitro* and *in vivo* experiments. The incorporation of Kolliphor EL in the formulation of the liquisolid tablets has resulted in a remarkable improvement in the dissolution rate of OLZ. Precompression powders with improved flow properties were obtained. Formulation K250 prepared with an OLZ:Kolliphor EL ratio of 1:2 and an Avicel PH 102: Aersosil 200 ratio of 50:1 showed the

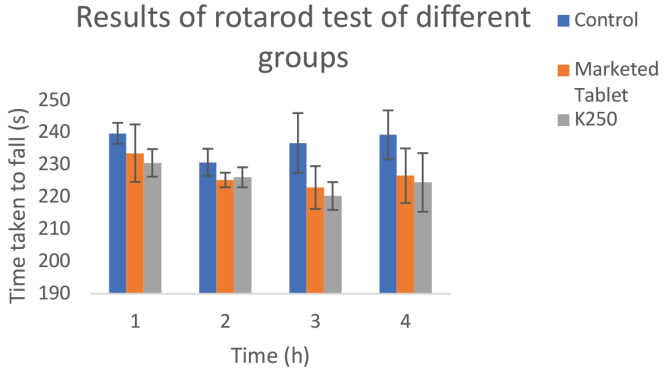

Figure 8. Results of the rotarod test of different groups, n= 6

Table 8. Results of rota rod test of different groups (mean ± SD, n= 6)

Time (hours)	Time taken to fall (seconds)		
	Control	Marketed tablet	K250
1	239.83 ± 3.26	233.67 ± 8.93	230.65 ± 4.28
2	230.83 ± 4.20	225.33 ± 2.28	226.19 ± 3.10
3	236.83 ± 9.28	223.00 ± 6.65	220.35 ± 4.33
4	239.33 ± 7.62	226.67 ± 8.48	224.58 ± 9.10

SD: Standard deviation, n= Number of trials

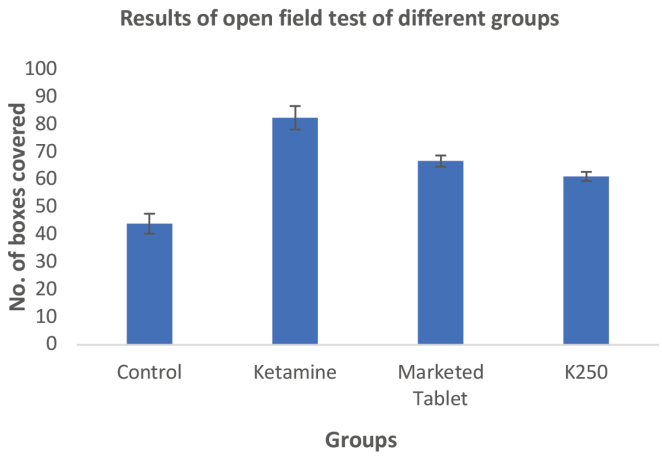

Figure 9. Results of the open field test of different groups, n= 6

Table 9. Results of open field test of different groups (mean ± SD, n= 6)

Groups	No. of boxes covered
Control	44.00 ± 3.63
Ketamine	82.50 ± 4.26
Marketed tablet	66.75 ± 2.05
K250	61.17 ± 1.67

SD: Standard deviation, n= Number of trials

highest dissolution rate and is thus the optimized formulation. A reduction in drug crystallinity is another reason for the additional improvement in the dissolution rate, and it is distinctly observed in the results of solid-state characterization. The PK and behavioral assessment study results clearly indicated the enhancement in bioavailability of the optimized formulation. Kolliphor EL is a potential solubility enhancer for OLZ liquisolid tablets.

Acknowledgments

OLZ was a gift sample from Dr. Reddy's Laboratories, Hyderabad. BASF, Mumbai provided Kolliphor EL as a gift sample. The authors are grateful to both organizations for providing gift samples for this study.

Ethics

Ethics Committee Approval: The studies were conducted according to the Committee for the Purpose of Control and Supervision of Experiments on Animals recommendations and after acquiring due approval from the Institutional Animal Ethics Committee of Raghu College of Pharmacy with number RCP/1549/PO/Re/5/11/21/06 dated 11/10/21.

Informed Consent: Not required.

Authorship Contributions

Surgical and Medical Practices: R.D.K., Concept: R.D.K., C.S.R.G., Design: R.D. K., Data Collection or Processing: R.D.K., Analysis or Interpretation: R.D.K., Literature Search: R.D.K., Writing: R.D.K., C.S.R.G.

Conflict of Interest: No conflict of interest was declared by the authors.

Financial Disclosure: The authors declared that this study received no financial support.

REFERENCES

1. Amidon GL, Lennernäs H, Shah VP, Crison JR. A theoretical basis for a biopharmaceutic drug classification: the correlation of *in vitro* drug product dissolution and *in vivo* bioavailability. Pharm Res. 1995;12:413-420.
2. Lipinski CA. Drug-like properties and the causes of poor solubility and poor permeability. J Pharmacol Toxicol Methods. 2000;44:235-249.
3. Kawabata Y, Wada K, Nakatani M, Yamada S, Onoue S. Formulation design for poorly water-soluble drugs based on biopharmaceutics classification system: basic approaches and practical applications. Int J Pharm. 2011;420:1-10.
4. Vandana KR, Prasanna Raju Y, Harini Chowdary V, Sushma M, Vijay Kumar N. An overview on *in situ* micronization technique-an emerging novel concept in advanced drug delivery. Saudi Pharm J. 2014;22:283-289.
5. Huang Y, Dai W. Fundamental aspects of solid dispersion technology for poorly soluble drugs. Acta Pharm Sin B. 2014;4:18-25.
6. Kurkov SV, Loftsson T. Cyclodextrins. Int J Pharm. 2013;453:167-180.
7. Nokhodchi A, Hentzschel CM, Leopold CS. Drug release from liquisolid systems: speed it up, slow it down. Expert Opin Drug Deliv. 2011;8:191-205.
8. Patil A, Kauthankar B, Kavatagimath S, Masareddy R, Dandagi P. Central composite design for the development and evaluation of liquisolid compacts of glyburide. Indian J Pharm Educ Res. 2022;56:236-244.
9. Spireas S, Bolton SM. Liquisolid systems and methods of preparing same. 1999;US005968550A.
10. Callaghan JT, Bergstrom RF, Ptak LR, Beasley CM. Olanzapine. Pharmacokinetic and pharmacodynamic profile. Clin Pharmacokinet. 1999;37:177-193.
11. Cavallari C, Fini A, Ceschel G. Design of olanzapine/lutrol solid dispersions of improved stability and performances. Pharmaceutics. 2013;5:570-590.
12. de Freitas MR, Rolim LA, Soares MF, Rolim-Neto PJ, de Albuquerque MM, Soares-Sobrinho JL. Inclusion complex of methyl-β-cyclodextrin and olanzapine as potential drug delivery system for schizophrenia. Carbohydr Polym. 2012;89:1095-1100.
13. Jawahar N, Meyyanatha SN, Senthil V, Gowthamarajan K, Elango K. Studies on physico-chemical and pharmacokinetic properties of olanzapine through nanosuspension. J Pharm Sci Res. 2013;5:196-202.
14. Shah DH, Patel MM. Formulation and evaluation of liquisolid compacts of olanzapine. J Drug Deliv Ther. 2019;9:189-202.
15. Ramadevi K, Voodikala S, Gonugunta CSR, Jayanti V. Liquisolid technique: an approach to enhance the dissolution rate of olanzapine. Indian J Pharm Sci. 2018;80:1003-1010.
16. Ambedkar T, Raja Jaya Rao Y. Formulation and evaluation of self-nanoemulsifying drug delivery system of olanzapine. Int J Univers Pharm Bio Sci. 2013;2:571-583.
17. Elkordy AA, Essa EA, Dhuppad S, Jammigumpula P. Liquisolid technique to enhance and to sustain griseofulvin dissolution: effect of choice of non-volatile liquid vehicles. Int J Pharm. 2012;434:122-132.

18. Joseph E, Balwani G, Nagpal V, Reddi S, Saha RN. Validated UV spectrophotometric methods for the estimation of olanzapine in bulk, pharmaceutical formulations and preformulation studies. Br J Pharm Res. 2015;6:181-190.
19. Tiong N, Elkordy AA. Effects of liquisolid formulations on dissolution of naproxen. Eur J Pharm Biopharm. 2009;7:373-384.
20. Spireas S. Liquisolid systems and methods of preparing same. 2002;US6423339B1.
21. Aulton ME. Pharmaceutics: the design and manufacture of medicines. Edinburgh; Churchill Livingstone Elsevier; 2007:355-356.
22. Nair AB, Jacob S. A simple practice guide for dose conversion between animals and human. J Basic Clin Pharm 2016;7:27-31.
23. Shin JW, Seol IC, Son CG. Interpretation of animal dose and human equivalent dose for drug development. Korean J Orient Med. 2010;31:1-7.
24. Becker A, Peters B, Schroeder H, Mann T, Huether G, Grecksch G. Ketamine-induced changes in rat behaviour: a possible animal model of schizophrenia. Prog Neuropsychopharmacol Biol Psychiatry. 2003;27:687-700.
25. Gobira PH, Ropke J, Aguiar DC, Crippa JA, Moreira FA. Animal models for predicting the efficacy and side effects of antipsychotic drugs. Braz J Psychiatry. 2013;35(Suppl 2):132-139.
26. Le Moal M, Simon H. Mesocorticolimbic dopaminergic network: functional and regulatory roles. Physiol Rev. 1991;71:155-234.
27. Dunhan NW, Miya TS. A note on the simple apparatus for detecting neurological deficits in rats and mice. J Am Pharm Assoc. 1957;46:208-209.
28. Mann A, Chasselet MF. Techniques for motor assessment in rodents. Movement Disorders. Academic Press; 2015:139-157.
29. Michael W, Roger DP. CNS safety pharmacology, In: Enna SJ, David BB, eds. xPharm: The Comprehensive Pharmacology Reference. Amsterdam; Elsevier: 2007:1-13.
30. Montgomery KC. The relation between fear induced by novel stimulation an exploratory behavior. J Comp Physiol Psychol. 1955;48:254-260.
31. National Center for Biotechnology Information. PubChem Compound Summary for CID 135398745, Olanzapine. https://pubchem.ncbi.nlm.nih.gov/compound/Olanzapine (accessed 10 April 2022).
32. Yehia SA, El-Ridi MS, Tadros MI, El-Sherif NG. Enhancement of the oral bioavailability of fexofenadine hydrochloride *via* Cremophor® El-Based Liquisolid Tablets. Adv Pharm Bull. 2015;5:569-581.
33. Thakkar HP, Vasava D, Patel AA, Dhande RD. Formulation and evaluation of liquisolid compacts of itraconazole to enhance its oral bioavailability. Ther Deliv. 2020;11:83-96.
34. Burra S, Yamsani M, Vobalaboina V. The liquisolid technique: an overview. Braz J Pharm Sci. 2011;47:475-482.
35. Bright A, Renuga Devi TS, Gunasekharan S. Qualitative and quantitative analysis of antipsychotic drugs- a spectroscopic study. Asian J Chem. 2010;22:5871-5882.
36. Ali B, Khan A, Alyami HS, Ullah M, Wahab A, Badshah M, Naz A. Evaluation of the effect of carrier material on modification of release characteristics of poor water-soluble drug from liquisolid compacts. PLoS One. 2021;16:e0249075.
37. Dixit M, Gopalkrishna A, Keshavarao Kulkarni P. Enhancing the aqueous solubility and dissolution of olanapine using freeze drying. Braz J Pharm Sci. 2011;47:743-749.
38. Kapure VJ, Pande VV, Deshmukh PK. Dissolution enhancement of rosuvastatin calcium by liquisolid compact technique. J Pharm (Cairo). 2013;2013:315902.
39. Tiwari M, Chawla G, Bansal AK. Quantification of olanzapine polymorphs using powder X-ray diffraction technique. J Pharm Biomed Anal. 2007;43:865-872.
40. Madhavi KM, Neelesh M. Formulation and evaluation of liquisolid compacts of BCS class II drug ketoprofen. J Pharm Res Int. 2021;33:322-334.
41. Karmakar AB, Gonjari ID, Hosmani AH, Dhabale PN, Bhise SB. Dissolution rate enhancement of fenofibrate using liquisolid tablet technique. Lat Am J Pharm. 2009;28:219-225.
42. Naureen F, Shah Y, Shah SI, Abbas M, Rehman IU, Muhammad S, Hamdullah H, Goh KW, Khuda F, Khan A, Chan SY, Mushtaq M, Ming LC. Formulation development of mirtazapine liquisolid compacts: optimization using central composite design. Molecules. 2022;27:4005.
43. Sayyad FJ, Tulsankar SL, Kolap UB. Design and development of liquisolid compact of candesartan cilexetil to enhance dissolution. J Pharm Res. 2013;7:381-388.
44. Elkordy AA, Bhangale U, Murle N, Zarara MF. Combination of lactose (as a carrier) with Cremophor EL (as a liquid vehicle) to enhance dissolution of griseofulvin. Powder Technol. 2013;246:182-186.

Turk J Pharm Sci 2024;21(1):62-70
DOI: 10.4274/tjps.galenos.2023.76128

ORIGINAL ARTICLE

Fusariotoxin-Induced Toxicity in Mesenchymal Stem Cells and Fibroblasts: A Comparison Between Differentiated and Undifferentiated Cells

Inji SHIKHALIYEVA[1], Cenk KIĞ[2], Ömer Yavuz GÖMEÇ[3], Gülruh ALBAYRAK[2]*

[1]İstanbul University, Institute of Graduate Studies in Sciences, Programme of Molecular Biology and Genetics, İstanbul, Türkiye
[2]İstanbul University, Faculty of Sciences, Department of Molecular Biology and Genetics, İstanbul, Türkiye
[3]Yeni Yüzyıl University, Faculty of Dentistry, Department of Restorative Dentistry, İstanbul, Türkiye

ABSTRACT

Objectives: Humans are unknowingly exposed to mycotoxins through the consumption of plant-derived foods and processed products contaminated with these toxic compounds. In addition to agricultural losses, *Fusarium* toxins pose a threat to human health. However, the effects of fusariotoxins on the viability and proliferation of stem cells have not been fully explored. We investigated the cytotoxic effects of deoxynivalenol (DON) and B-trichothecene mix (MIX) on mesenchymal stem cells (MSCs) and the L929 fibroblast cell line.

Materials and Methods: MSCs were isolated from the dental pulp tissue. The doubling time and viability of dental pulp stem cells (DPSCs) and L929 cells were determined using the MTT assay. The following doses of B-trichothecenes (0.25-16 µg/mL; 24 hours and 48 hours) were used to evaluate cytotoxicity. In addition, changes in the confluency-dependent response of DPSCs to DON toxicity were determined. Moreover, we investigated the effect of DON on cell death *via* acridine orange/ethidium bromide (AO/EB) double staining.

Results: A DON and MIX showed a dose- and time-dependent inhibitory effect on the proliferation of both cells. DPSCs exposed to DON for 48 hours (IC_{50} = 0.5 µg/mL) were found to be 16-fold more sensitive than L929 cells (IC_{50} = 8 µg/mL). Compared with a culture with 80% confluency, DPSCs from a 50% confluent culture were more sensitive to varying doses of DON (0.25-4 µg/mL, 24-48 hours). Moreover, AO/EB staining showed that treatment of DPSCs with DON led to a significant increase in cell death (17% for 2.4 µg/mL; 50% for 4.8 µg/mL).

Conclusion: This study reveals that undifferentiated MSCs are significantly more sensitive to DON than differentiated somatic cells (L929). Given that humans are frequently exposed to these mycotoxins, our findings imply that prolonged exposure to them may also have harmful effects on cellular differentiation and embryonic development.

Keywords: Mesenchymal stem cells, mycotoxins, deoxynivalenol, fibroblasts, dental pulp stem cells

INTRODUCTION

Mycotoxins are secondary metabolites that support defensive functions for fungi in their ecological niche; however, they can contaminate a wide variety of food sources and animal feed. Therefore, mycotoxins are toxicants for both animals and humans. The Food and Agriculture Organization proposed that one-fourth of the global food crop is contaminated by mycotoxins.[1] Moreover, the International Agency for Research on Cancer and the World Health Organization called for measures to be taken against widespread mycotoxin contamination.[2] Type B-trichothecenes, produced mainly by *Fusarium*, are prevalent contaminants, and the most important of them are deoxynivalenol (DON) and its derivatives. Essentially, over 80% of agricultural goods from Europe and Asia contain at least one type of mycotoxin and among them, DON is reported to be the most widespread.[3] DON, 3-acetyl-DON (3ADON), 15-acetyl-DON (15ADON), and nivalenol (NIV) can maintain their stability even during storage/milling and processing/cooking of food.[4] Exposure assessments in European countries concluded that

*Correspondence: gulruh@istanbul.edu.tr, Phone: +90 541 661 76 25, ORCID-ID: orcid.org/0000-0001-5190-5561
Received: 19.01.2023, Accepted: 30.03.2023

consumers and even young children are exposed to DON at levels close to or precisely higher than the tolerable daily intake.[5] Therefore, high doses or prolonged exposure to DON can also pose a threat to human health.

The genes found in the *tri5* gene cluster and their regulatory mechanisms have been described for the production of B-trichothecene in *Fusarium* species. Insertion deletions (in-dels), changes in tandem repeats, and single nucleotide polymorphisms in the gene cluster determine the final product as DON and its acetylated derivatives or NIV.[6,7] However, we demonstrated in a research project (unpublished data) that both DON and NIV biosynthesis were carried out at the same time in *Fusarium graminearum* and *Fusarium culmorum*. Thus, regardless of the fact that DON is the most prevalent mycotoxin, the cytotoxic effects of NIV also should not be ignored. Several screening studies of *Fusarium*-contaminated food stuff and products showed that two or more mycotoxins frequently co-existed, and co-contamination of DON and NIV was predominant.[2,3,8] All of these studies demonstrate that DON and NIV contaminations are widespread worldwide and therefore can also be regarded as an important risk factor for public health. *In vitro* analyses showed that these mycotoxins could both suppress and stimulate immune functions.[9] In addition, they inhibited RNA, DNA, and protein synthesis by binding to the 60S subunit of eukaryotic ribosomes and disrupting the activity of peptidyl transferase. DON led to changes in mRNA alternative splicing in human cells (HepG2, HEK293 and Caco-2 exposed to relatively low dosages (2 µg/mL).[10] DON suppressed the activity of the Wnt/β-catenin signaling pathway, which affects stem cell fate during development and in adult tissues.[11,12] In addition, DON has a strong embryotoxic effect by inhibiting cell growth in embryonic stem cell lines.[13] Moreover, DON induced apoptosis and inflammation in intestinal cells by increasing ROS accumulation and activating the NF-κB and apoptotic signaling pathways.[14] In human gastric epithelial and intestinal cells, 3ADON had fewer adverse effects than DON, whereas 15ADON appeared to be slightly more effective than DON. It was also revealed that 15ADON was a more potent MAPK inducer than DON and 3ADON.[15-17] Outcomes of various studies on somatic and cancer cell lines revealed that the co-existence of B-trichothecenes might cause a synergistic effect.[16,18-21] Thus, the co-occurrence of B-trichothecenes in foods and diets can cause more health problems than predicted.

Stable cell lines undergo morphological and genetic changes during transformation and/or multiple passage cycles. It can be argued that because of these genetic and phenotypic instabilities, they are not ideal model systems for toxicology studies. Mesenchymal stem cells (MSCs) have attracted attention as an alternative and more sensitive screening platform for assessing chemical toxicity.[22,23] Nevertheless, the effects of fusariotoxins on stem cells have received little consideration. Because dental pulp stem cells (DPSC) can easily be obtained from dental waste, they provide a suitable source for MSCs. A growing body of evidence suggests that differentiated cells are more resistant to DON treatment than undifferentiated stem cells.[19,24-26] However, a comparative analysis of DON-induced effects on MSCs and stable cell lines has not been reported to date. These findings suggest that human MSCs and fibroblasts share many physiological and molecular properties, such as cell surface markers and gene expression patterns.[27,28] Because L929 fibroblasts can serve as an ideal stable cell line model for comparative analysis, the L929 cell line was selected for comparative analysis of the cytotoxic effects of B-trichothecenes on MSCs.

In this study, the effects of DON and MIX, which contains DON, 3ADON, 15ADON, and NIV, on DPSCs were investigated as a model for undifferentiated MSCs and differentiated L929 fibroblast cells.

MATERIALS AND METHODS

Isolation of the stem cells

Human DPSCs were harvested from the extracted human third molars of adult patients. Teeth were collected under guidelines approved by the İstanbul University Medical Faculty Clinical Research Ethics Committee (no: 2019/455, date: 29.03.2019), and informed consent was obtained from the patients. The extracted teeth were transported to the laboratory in Dulbecco's phosphate-buffered saline (DPBS; Wisent) solution containing 200 U/mL penicillin and 200 µg/mL streptomycin (Thermo). After the teeth were cleaned, the dental pulp tissue was separated from the pulp chamber and root canal. The dental pulp tissue was then chopped into pieces and digested in a 2 mL solution of 1 mg/mL collagenase type I (Biochrom) for 1 hour at 37 °C in 5% CO_2 to generate a single-cell suspension, followed by centrifugation at 1000 rpm for 5 min. The cells were seeded on 10 cm^2 plates.

Cell culture conditions

The DPSCs were cultured in the following growth medium: alpha-modified Eagle's medium (α-MEM; Wisent) supplemented with 10% fetal bovine serum (FBS; Gibco), 2.5 mM L-glutamine (Gibco), 50 U/mL penicillin, 50 µg/mL streptomycin (Gibco) and 1.25 µg/mL amphotericin B (Capricorn). Mouse fibroblast L929 cells were a kind gift from the İstanbul Yeni Yüzyıl University Cell Culture Collections. They were maintained in Dulbecco's Modified Eagle Medium (DMEM; Biological Industries, USA). Cells were incubated in a humidified incubator at 37 °C (5% CO_2). The incubation medium was refreshed every 2-3 days.

Calculation of the doubling time (td)

To determine the cell expansion efficiency and calculate the number of cells, DPSCs (passage 5) and L929 were seeded on a 24-well cell culture plate at a density of 5 x 10^3 cells/cm^2. DPSC and L929 cells were incubated for 7 and 4 days, respectively. Cell viability was measured using the 3-(4,5-dimethylthiazol-2-yl)-2,5-diphenyl tetrazolium bromide) assay on the 1st, 2nd, 3rd, 4th, and 7th days of culture. The growth curves were created by plotting the MTT assay absorbance values. The td for DPSCs and L929 were calculated by using the equations obtained from the growth curves. The region that best represents a straight line within the log phase was delineated and transformed into a logarithmic scale. The specific growth rate was calculated

by applying the following equation: $y = Ae^{Bx}$, [y - absorbance (OD), B - specific growth rate, and x time]. td was determined according to the equation td = ln(2)/B.[28]

Treatments with DON and MIX

Acetonitrile was used as the solvent for the preparation of mycotoxins. First, to eliminate the solvent effect, we exposed the cells to acetonitrile for 48 hours. The final concentration of acetonitrile (0.8 µg/mL), which existed in the solution for the highest DON concentration (8 µg/mL), was added to the cell media. Stock solutions of DON (100 µg/mL) and MIX (100 µg/mL from each mycotoxin) were added to the media at specified concentrations. The final concentration of the acetonitrile solvent in a cell culture containing mycotoxin did not exceed 1%. Two different sets of experiments were designed: (1) When the DPSCs and L929 cultures reached 50-55% confluence, the medium was refreshed and DON or MIX at various concentrations (0.25, 0.5, 1, 2, 4, 8, 16 µg/mL) were added; (2) When the DPSCs cultures reached 50% and 80% density, the medium was replaced with a fresh medium containing DON at 0.25, 0.5, 1, 2, 4 µg/mL concentrations. A regular growth medium was used as the control. After incubation for 24 and 48 hours, cell viability was measured (570 nm) *via* the MTT assay.

The mean half-maximal inhibitory concentration (IC_{50}), representing the concentration of DON or MIX that inhibits the proliferation of treated cells by 50% compared to untreated controls, was calculated using the mean absorbance values obtained from the MTT assay. All experiments were performed in three biological and technical replicates.

Cell viability testing

The cytotoxic effects of DON or MIX on undifferentiated DPSCs or differentiated L929 cells were evaluated by MTT assay. 50 µL of MTT solution (2.5 mg/mL in PBS) was added to 500 µL of culture media. The cells were incubated in a 5% CO_2 incubator at 37 °C for 3 hours in the dark. After discarding the media, 400 µL DMSO was added to each well and the formazan crystals were dissolved. The optical density (OD) was measured at 570 nm using a spectrophotometer (BioTek Eon™) and the percentage of cell viability was calculated using the following formula: Cell viability (%) = (OD sample/OD control) x 100. The percentage of cell inhibition was calculated using the formula: 100 - % cell viability.

Fluorescence imaging of cell viability

Acridine orange (AO) penetrates both viable and non-viable cells and emits green fluorescence. Ethidium bromide (EB) is taken up only by non-viable cells and emits red fluorescence. After double staining with AO/EB, four types of cells can be detected according to fluorescence emission and the morphological aspect of chromatin condensation in the stained nuclei: (1) viable, (2) early apoptotic, (3) late apoptotic, and (4) necrotic.[29,30] Dye mixture (300 µg/mL AO and 300 µg/mL EB) was added to the media of cells treated with DON (0.6-4.8 µg/mL) was incubated for 2-3 min in the dark, and was then immediately (fast uptake) examined by fluorescence microscopy (Carl-Zeiss, Axio Observer 3); 604 nm/Texas Red filter for EB and 520 nm/Green fluorescent protein filter for AO.

Statistical analysis

Cytotoxicity was expressed as the mean percentage change relative to the untreated control. The control values were set as 100% of viable cells. All experiments included three biological and three technical repetitions (n= 3). Statistical analysis was performed using the Graph Pad Prism 8 program. Two-way ANOVA, followed by *post-hoc* Dunnett's multiple comparison tests with a single pooled variance, was used to test for differences between the control and treated cell groups. An unpaired *t*-test tested the statistical significance of the time-dependent variations. The results are presented as mean ± SEM (standard error of the mean) and *p* values show statistical significance: statistically significant ($p < 0.05$), very statistically significant ($p < 0.01$), and highly statistically significant ($p < 0.001$).

RESULTS

Morphology and growth characteristics of DPSCs and L929 cells

Within the first five days of the primary culture obtained from the dental pulp tissue, various cell types with different morphological features were observed. By day 5, the majority of cells exhibited an elongated, fibroblast-like (spindle-shaped) morphology under normal culture conditions (Figure 1A). Although there were some variations among the cells from different tissue samples, all established cells exhibited similar growth characteristics and morphologies. The primary cultures reached confluency in approximately 10 days. Subcultures from all cells inclined to exhibit accelerated growth; thus, the cultures reached confluency at a faster rate than primary cultures (in about 5-7 days). The cells maintained their spindle-shaped morphology along passages and during the entire culture period (Figure 1B). L929 stable cell lines exhibited a healthy

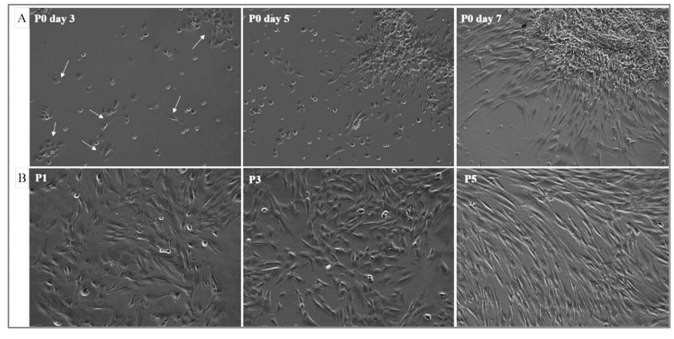

Figure 1. Morphological features of DPSCs. (A) Morphology of DPSCs at primary culture (P_0) investigated under an inverted optic microscope (Nikon Eclipse Ti-E). P_0: days 3, 5, and 7 of primary culture obtained from the dental pulp tissue. Small fibroblast-shaped cells (white arrows) and round-shaped cells appeared on day 3 of primary culture (P_0 day 3). (B) Morphology of DPSCs at different passages (P_1-P_5). Spindle-shaped cells became predominant in the culture after three passages. Original magnifications: x10

DPSC: Dental pulp stem cell

proliferation profile with a typical fibroblastic morphology (Figure 2).

The growth curves of DPSCs and L929 cells were constructed using absorbance values obtained from MTT assays (Figure 3). The td of DPSCs was calculated as 32 hours, and the specific growth rate was determined as 0.0215 h^{-1}. The td and specific growth rate for L929 were calculated as 19 hours and 0.0354 h^{-1}, respectively. Calculations were verified using online computation software (https://www.omnicalculator.com).

Effects of DON and MIX on the viability of DPSCs and the L929 cell line

The dose-response curves indicated that treatment with DON or MIX induced a concentration-dependent reduction in the viability of both cells (Figure 4A). Acetonitrile exposure showed no significant effect compared with the untreated control (Figure 4B). Treatment with DON (8 µg/mL for 24 hours) reduced cell viability by almost 50% in both DPSC and L929 cell lines compared with the untreated controls. However, at lower concentrations, DON treatment for 48 hours showed a more pronounced toxicity in DPSCs (49.7% inhibition at 0.5 µg/mL) at lower concentrations compared with L929 (36.7% inhibition at 0.5 µg/mL). Likewise, after 24 hours of treatment with MIX at a concentration of 7 µg/mL, the survival rate of DPSCs decreased to 50%, and 48 hours of exposure reduced cell viability to 50% at a concentration of 0.25 µg/mL. Next, we calculated IC_{50} values (the concentration that reduces cell viability by 50%) for DPSCs and L929 cells (Table 1). Both DON and MIX showed similar inhibitory effects on cell viability after treatment for 24 hours. However, at longer exposures (48 hours), DON was found to be more toxic to DPSCs. As shown in Table 1, the IC_{50} value for DPSCs was 16-fold lower than that of L929 cells (0.5 µg/mL for DPSCs; 8 µg/mL for L929).

Four different concentrations (0.25, 0.5, 1, and 2 µg/mL) of DON were tested for toxicity, and we also tested the toxicity of DON when combined with the B-trichothecene mix (MIX) (containing 0.25, 0.5, 1, and 2 µg/mL of DON). We found that both DON and MIX dramatically reduced the viability of DPSCs and L929 cells (Figure 5). However, at higher concentrations (1 µg/mL and 2 µg/mL), significant changes were not observed between DON and MIX treatments in DPSCs (Figure 5A), suggesting that DON caused the highest toxicity in MIX. Incubation with DON and MIX for 24 hours did not cause significant changes in cellular morphology (Figure 6). However, the morphology of DPSCs remarkably changed after 48 hours of exposure to DON and MIX. It was observed that cells rounded up and detached from the culture dishes, and the number of viable cells was relatively reduced at higher fusariotoxins concentrations (› 2 µg/mL). DPSCs lost their spindle-shaped morphology and developed a flattened spread-out morphology in contrast to the morphology of untreated control cells. Fusariotoxins induced similar changes in the morphology of L929 cells at concentrations of 4 µg/mL and above.

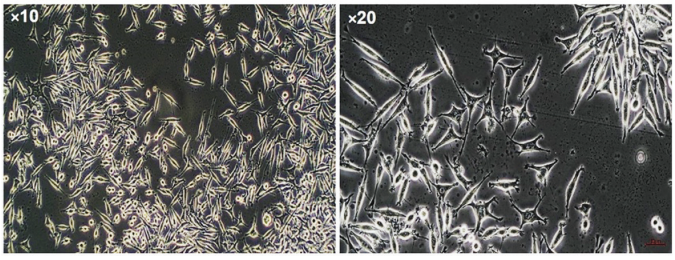

Figure 2. Morphological features of L929 cells. Morphology of L929 under an inverted phase contrast microscope. Representative images of L929 on the 5th day of culture. Cells exhibit spindle-shaped morphology. Original magnifications: x10 and x20

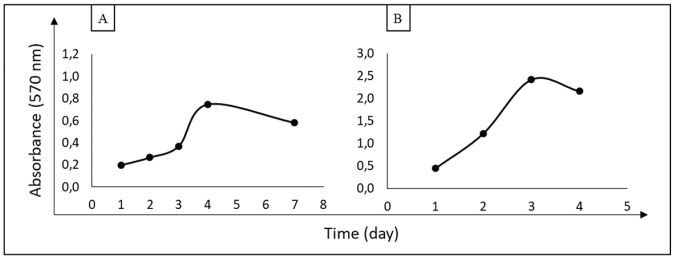

Figure 3. Growth curves of DPSCs (A) and L929 (B) cells

DPSC: Dental pulp stem cell

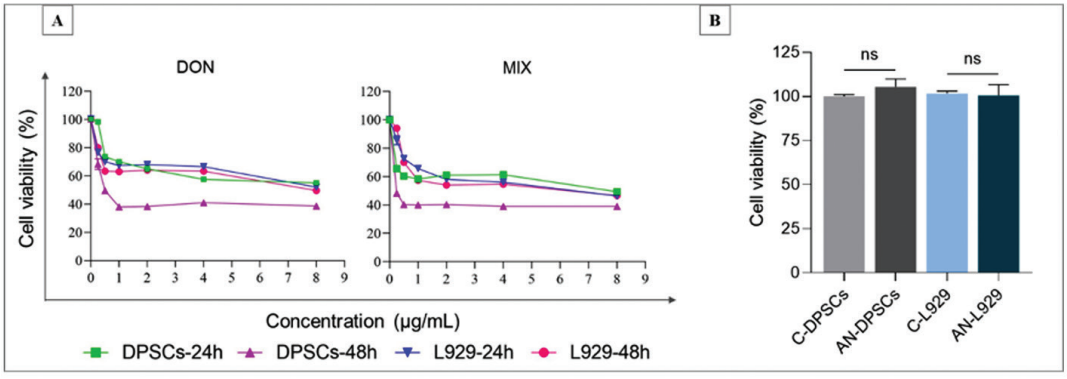

Figure 4. Cytotoxic effects of DON and MIX. (A) The curves demonstrate the dose-dependent toxic effect of DON and MIX (0.25-8 µg/mL) on DPSCs and L929 cells for 24 and 48 hours. (B) Effects of the DON solvent acetonitrile. To eliminate the solvent effect, both cells exposed to a concentration of acetonitrile (0.8 µg/mL) existed in solution for the highest DON (8 µg/mL)

Data are presented as the mean ± standard error of the mean, ns: Not significant, C: Control, AN: Acetonitrile, DON: Deoxynivalenol, DPSC: Dental pulp stem cell, L929: Mouse fibroblast cell line, MIX: B-trichothecene mix (DON, 3ADON, 15ADON, NIV)

Relevance of confluency and DON toxicity in DPSC culture

As shown in the previous sections, our findings suggest that DON is the most potent mycotoxin in the mixture (Figure 5) and that DPSCs are more sensitive to DON toxicity (Figures 5 and 6). Therefore, further analyses were conducted using only DON and DSPCs. We investigated the relationship between DON toxicity and cell density. DPSCs at 50% confluency were found to be more sensitive to DON (Figure 7B). A 24-hours DON exposure (4 µg/mL) caused 40% inhibition in a 50% confluent cell culture. The same dose of DON exhibited only 20% inhibition in an 80% confluent culture (Table 2). However, prolonged DON treatment (48 hours) had a different inhibitory effect on DPSCs. In a 50% confluent culture, 4 µg/mL of DON inhibited the proliferation of cells by 60%. In contrast, in an 80% confluent culture, the inhibitory effect of DON was 35% (Table 2).

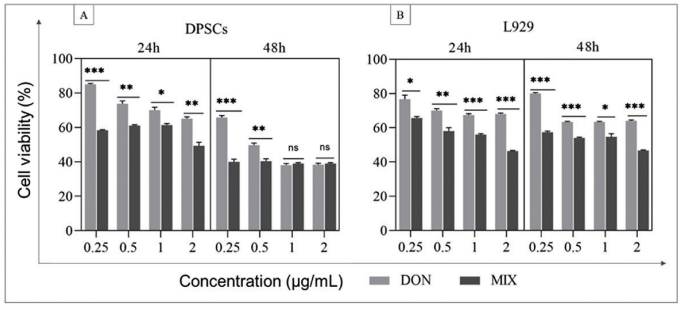

Figure 5. Comparison of the inhibitory effects of DON and MIX on (A) DPSCs and (B) L929. Stock concentrations for DON 100 µg/mL and for MIX 400 µg/mL that contain 100 µg/mL of each of the four mycotoxins (*i.e.,* 1 µg/mL of MIX contains 1 µg/mL of each of four mycotoxins)

Data are presented as the mean ± standard error of the mean, *$p < 0.05$, **$p < 0.01$, ***$p < 0.001$, ns: Not significant, DPSCs: Dental pulp stem cells, L929: Mouse fibroblast cell line, DON: Deoxynivalenol, MIX: B-trichothecene mix (DON, 3ADON, 15ADON, NIV)

Table 1. Mean half-maximal inhibitory concentrations (IC_{50}) of DON and MIX on DPSCs and L929

	DON IC_{50} (µg/mL)		MIX IC_{50} (µg/mL)	
	24 hours	48 hours	24 hours	48 hours
DPSCs	7	0.5	7	0.25
L929	8	8	7	6

IC50: Inhibitory concentration, DON: Deoxynivalenol, MIX: B-trichothecene mix, DPSCs: Dental pulp stem cells, L929: Mouse fibroblast cell line

DON-induced cell death in the DSPC culture

Fluorescence microscopy images of AO/EB stained samples revealed that treatment with 0.6 µg/mL DON did not cause a change in the number of apoptotic or necrotic cells compared with the control (control 1.7 ± 0.3% and 0.6 µg/mL DON treated group resulted in 2.0 ± 0.3%). 1.2 µg/mL of DON (48 hours) increased the rate of apoptotic and necrotic cells by 3.7 ± 0.3% (Figure 8). Higher DON doses (2.4 µg/mL and 4.8 µg/mL) dramatically increased the rate of apoptotic and necrotic cells (up to 50%) (Table 3).

Table 2. Cell viability percentages (%) of 50% and 80% confluent DPSCs treated with DON for 24 and 48 hours (mean ± SEM, n = 3)

Concentrations of DON (µg/mL)	24 hours		48 hours	
	Confluency			
	50%	80%	50%	80%
0	100 ± 0	100 ± 0	100 ± 0	100 ± 0
0.25	90 ± 1.7	85 ± 2.6	65 ± 0.5	68 ± 0.5
0.5	74 ± 1.7	83 ± 1.2	50 ± 1.2	68 ± 1.7
1	70 ± 1.7	85 ± 1.5	38 ± 1	69 ± 1.2
2	67 ± 2	87 ± 0.3	39 ± 1.5	65 ± 2
4	59 ± 2	83 ± 0	41 ± 0.5	64 ± 2.2

MTT: 3-(4,5-Dimethylthiazol-2-yl)-2,5-diphenyltetrazolium bromide, SEM: Standard error of the mean, DPSCs: Dental pulp stem cells, DON: Deoxynivalenol

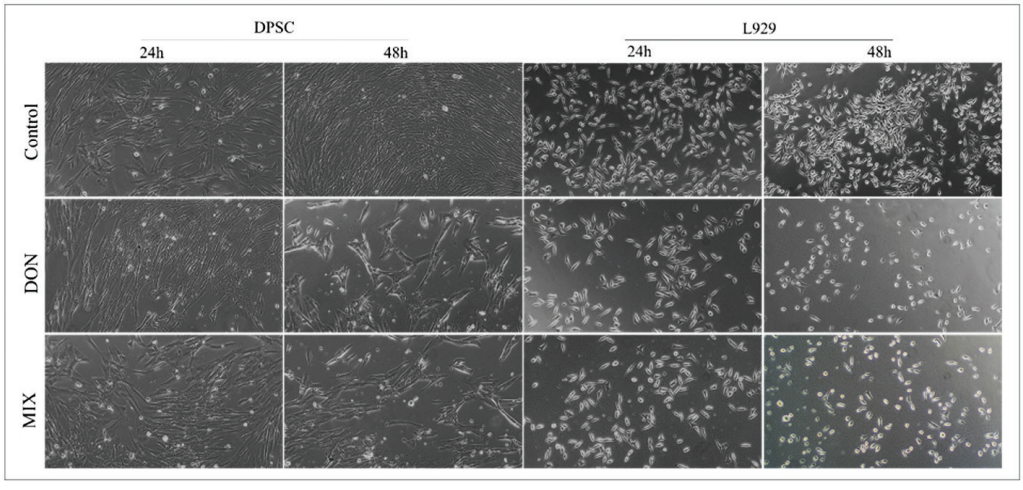

Figure 6. Mycotoxin-induced changes in cell morphology. Representative images showing phenotypic changes in DPSCs and L929 cells after treatment with DON or MIX at a concentration of 8 µg/mL for 24 and 48 hours

DPSCs: Dental pulp stem cells, L929: Mouse fibroblast cell line, DON: Deoxynivalenol, MIX: B-trichothecene mix

DISCUSSION

Analysis of recent data revealed that the most prevalent mycotoxins in contaminated food samples are DON, its acetylated forms (3ADON, 15ADON), and NIV. Plants infected by *Fusarium* spp. can produce conjugated forms of these mycotoxins called masked forms, which are less toxic than the main forms (DON-3-glucoside, NIV-glucoside). DON conjugations can also occur during food processing.[31] Although conjugated forms of mycotoxins are considered to be less toxic, their hydrolysis in the digestive tract may cause their conversion to the main form, thereby increasing their toxicity.[32] Climate change and the increasing world population may impact the augmentation of mycotoxin contamination and distribution on a large scale in the upcoming years.[33]

Although many researchers have investigated the toxic effects of *Fusarium* mycotoxins on various cells using transformed stable cell lines, more information is needed on the effects of these mycotoxins on stem cells.[11,34,35] Currently, stem cells, particularly MSCs, have taken a tremendous interest as an alternative high-efficiency screening platform for appraising the toxicity of several chemicals such as drugs and nanoparticles.[22]

Table 3. Acridine orange/ethidium bromide results of DPSCs treated with DON (mean ± SEM, n= 3)

Concentrations of DON (µg/mL)	Viable cells (%)	Apoptotic/necrotic cells (%)
0	98±0.3	1.7±0.3
0.6	98±0.0	2.0±0.3
1.2	96±0.3	3.7±0.3
2.4	83±1.8	16.7±1.8
4.8	50±2.0	50.3±2.0

DPSCs: Dental pulp stem cells, DON: Deoxynivalenol, SEM: Standard error of the mean

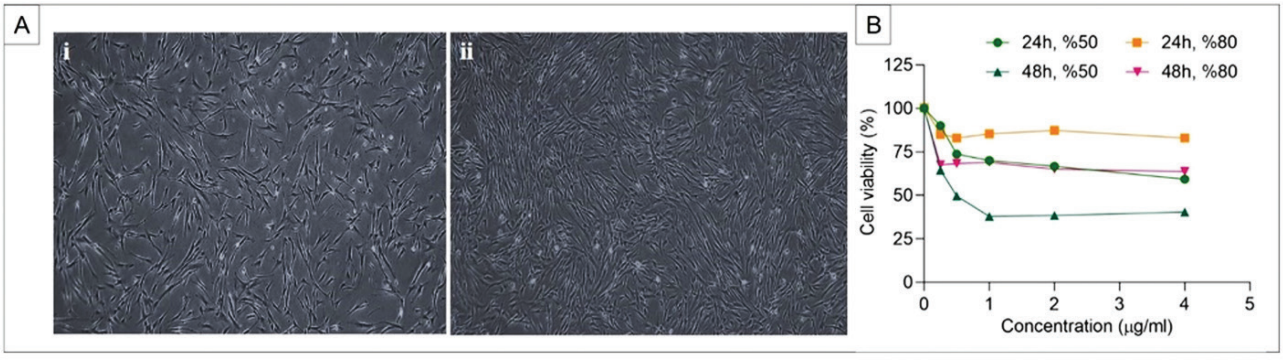

Figure 7. Effect of cell density on toxicity. (A) Confluence of DPSCs. Representative images from cultures with i) 50% and ii) 80% density of cells. Images taken by an inverted optical microscope were analyzed for confluence using ImageJ software. Original magnifications: x4 (B) Cell viability curves showing the effect of DON on DPSCs at two different confluences (50% and 80%)

DPSCs: Dental pulp stem cells, DON: Deoxynivalenol

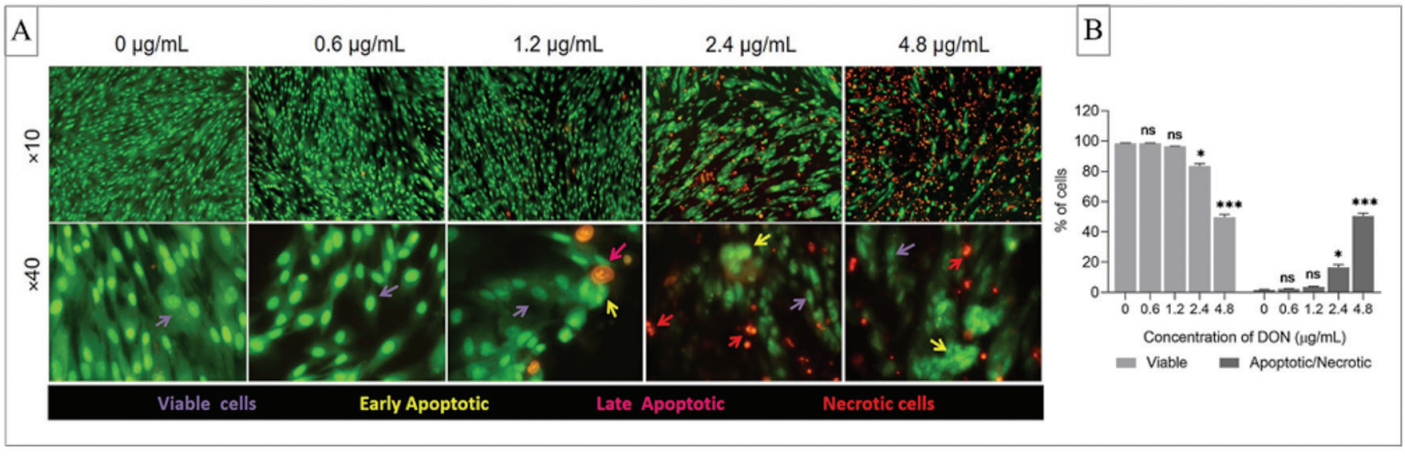

Figure 8. Acridine orange/ethidium bromide double staining of DPSCs 48 hours after treatment with different concentrations of DON. (A) Representative images of viable, apoptotic, and necrotic cells are shown with the arrows in the corresponding colors. Viable cells have uniform bright green nuclei with an organized structure. Early apoptotic cells with irregularly structured green nuclei and chromatin condensations are visible as bright green patches, fragments, or apoptotic bodies. Late apoptotic cells have orange to red nuclei with condensed or fragmented chromatin. Necrotic cells have uniformly orange to red nuclei with an organized structure. Original magnifications: x10 and x40; (B) Percentage of viable and apoptotic/necrotic cells, statistical assessment according to control (0 µg/mL)

*$p < 0.05$, ***$p < 0.001$, ns: Not significant, DPSCs: Dental pulp stem cells, DON: Deoxynivalenol

In contrast to traditional *in vitro* systems based on stable cell lines, MSCs provide a sensitive platform for toxicological studies. One of the readily available sources for MSCs is dental pulp, which can be obtained from dental waste.

Various studies have demonstrated that MSCs and fibroblasts in humans share many characteristics. Both cell types can be isolated from almost all human tissues, and in addition to their morphological features, they share similar gene expression patterns and cell surface markers.[27,28] Therefore, the L929 fibroblast cell line was chosen as the differentiated stable cell line model for comparison with undifferentiated MSCs.

Stem cells from dental pulp tissue showed a high proliferation rate, and there were no obvious alterations in cell morphology and growth patterns in subsequent passages. In addition, the td of cells were in accordance with the data reported by Rajendran et al.[36] for DPSCs, and for L929 by Kubat et al.[37] The inhibitory effect of *Fusarium* toxins on the proliferation of both cells (24 hours and 48 hours) was evaluated *via* MTT assay. The results showed that fusariotoxins affected both cell types in a dose-dependent and time-dependent manner (Figure 4A). Similar to our findings, Lee et al.[22] demonstrated that exposure to chemicals was more toxic to stem cells than to terminally differentiated fibroblasts. Identically, several groups reported that differentiated cells were less sensitive to mycotoxins (DON, 3ADON, 15ADON, and DON3G) than their proliferative counterparts.[19,24] We determined the concentrations of DON and MIX that led to the inhibition of cell viability by 50% (Table 1). It was suggested that DON inhibited the proliferation of DPSCs and L929 cells in a time-dependent manner. We observed that DON-induced toxicity at 24 hours (7 µg/mL) was much lower than that at 48 hours (0.5 µg/mL) (Table 1). However, it can be argued that the significant reduction in proliferation rate can also be attributed to the long td (32 hours) of DPSCs compared with that of fibroblasts (td: 19 hours).

Compared with DON alone, MIX significantly reduced the viability of DPSCs and L929 cells at both 24 and 48 hours of exposure (0.25-2 µg/mL) (Figure 5). Intriguingly, at higher concentrations (1 µg/mL and 2 µg/mL), significant changes were not observed between DON and MIX treatments in DPSCs (Figure 5A), suggesting that DON caused the highest toxicity in MIX. These observations may be attributed to the synergistic effects of mycotoxins in MIX on stem cells. We also observed dramatic changes in the cellular morphologies and viability rates of DPSCs and L929 at concentrations of 2 µg/mL and above, especially after 48 hours of exposure (Figure 6).

Cell confluency enormously affected the response of cells to the tested toxins. Several groups have reported that subconfluent cultures responded vigorously to the toxic effects of a similar number of chemicals or drugs compared with confluent cell cultures.[38,39] Data in the literature suggest that the main differences between cell confluences originate from proliferative capacity, motility, and intercellular cell-cell adhesion contacts. In addition, confluent cells excrete extracellular matrix components that inhibit cell proliferation, make cells quiescent, and induce growth arrest.[40] In this context, we evaluated the relationship between the confluence of DPSCs and DON toxicity. DON treatment (4 µg/mL) inhibited the proliferation of DPSCs by 20% at 80% confluency, whereas 4 µg/mL DON inhibited the proliferation of DPSCs by 40% at 50% confluency. Thus far, this is the only finding that has been reported for DON toxicity in the literature.

AO/EB double staining is an inexpensive and reliable method for evaluating changes in the number of necrotic and apoptotic cells. Changes in the nuclear morphology of cells can be detected *via* fluorescence emission and chromatin condensation in the stained nuclei. Therefore, many researchers have recommended AO/EB as a reliable and correct method for distinguishing viable, apoptotic, and necrotic cells in culture.[29,30,41] In the current study, DON treatment resulted in the degeneration and fragmentation of nuclei in DPSCs in a dose-dependent manner (Figure 8).

CONCLUSION

We investigated the cytotoxic effects of DON, acetylated derivatives of DON (3ADON, 15ADON), and NIV on MSCs and the L929 fibroblast cell line. Here, we report the *in vitro* cytotoxic effect of DON on MSCs by providing a comparative evaluation between the L929 stable cell line and undifferentiated DPSCs. DPSCs demonstrated markedly severe sensitivity to fusariotoxins in contrast to L929. We found that cell confluency is an important factor that should be considered in toxicity studies. Moreover, DON induced apoptotic and necrotic cell death in DSPCs. Based on the findings of this study, the comparable exposure to mycotoxins can be ranked as follows: cytotoxicity DON < MIX; treatment time 24 hours <48 hours; affecting of cells L929 < DPSCs; confluency 50%<80%. In this study, we could not provide mechanistic and molecular insights into the underlying mechanisms that lead to DON-induced toxicity. Further molecular experiments, such as gene expression and oxidative stress determination, are required in this context. These findings could pave the way for future comparative toxicological studies of stem cells and stable cell lines.

Ethics

Ethics Committee Approval: Teeth were collected under guidelines approved by the İstanbul University Faculty of Medicine Clinical Research Ethics Committee (approval no: 2019/455, date: 29.03.2019).

Informed Consent: Informed consent was obtained from the patients.

Authorship Contributions

Surgical and Medical Practices: Ö.Y.G., I.S., Concept: G.A., I.S., Design: G.A., Data Collection or Processing: I.S., G.A., C.K., Analysis or Interpretation: I.S., G.A., C.K., Literature Search: I.S., G.A., C.K., Writing: I.S., G.A., C.K.

Conflict of Interest: No conflict of interest was declared by the authors.

Financial Disclosure: This study was supported by the Scientific Research Project Center (BAP) of İstanbul University (project number: 34442).

REFERENCES

1. Joint FAO/WHO Expert Committee on Food Additives (JECFA). Safety evaluation of certain food additives and contaminants. WHO/FAO Food Additives Series 48. International Programme on Chemical Safety (IPCS). WHO, Geneva. 2001.
2. WHO. A new IARC report urges action against widespread mycotoxin contamination in developing countries. IARC WHO Press Release. 2016.
3. Kovalsky P, Kos G, Nährer K, Schwab C, Jenkins T, Schatzmayr G, Sulyok M, Krska R. Co-occurrence of regulated, masked and emerging mycotoxins and secondary metabolites in finished feed and maize-an extensive survey. Toxins (Basel). 2016;8:363.
4. Khaneghah AM, Mostashari P, Oliveira CAF, Vanin FM, Amiri S, Sant'Ana AS. Assessment of the concentrations of ochratoxin A, zearalenone, and deoxynivalenol during cracker production. J Food Compos Anal. 2023;115:104950.
5. EFSA Panel on Contaminants in the Food Chain (CONTAM). Statement on the risks for public health related to a possible increase of the maximum level of deoxynivalenol for certain semi-processed cereal products. EFSA J. 2013;11:3490.
6. Lee T, Han YK, Kim KH, Yun SH, Lee YW. Tri13 and Ti7 determine deoxynivalenol- and nivalenol-producing chemotypes of *Gibberella zeae*. Appl Environ Microbiol. 2002;68:2148-2154.
7. Kimura M, Tokai T, O'Donnell K, Ward TJ, Fujimura M, Hamamoto H, Shibata T, Yamaguchi I. The trichothecene biosynthesis gene cluster of *Fusarium graminearum* F15 contains a limited number of essential pathway genes and expressed non-essential genes. FEBS Lett. 2003;539:105-110.
8. Del Ponte EM, Garda-Buffon J, Badiale-Furlong E. Deoxynivalenol and nivalenol in commercial wheat grain related to *Fusarium* head blight epidemics in southern Brazil. Food Chem. 2012;132:1087-1091.
9. Bondy GS, Pestka JJ. Immunomodulation by fungal toxins. J Toxicol Environ Health B Crit Rev. 2000;3:109-143.
10. Hu Z, Sun Y, Chen J, Zhao Y, Qiao H, Chen R, Wen X, Deng Y, Wen J. Deoxynivalenol globally affects the selection of 3' splice sites in human cells by suppressing the splicing factors, U2AF1 and SF1. RNA Biol. 2020;17:584-595.
11. Zhou JY, Lin HL, Wang Z, Zhang SW, Huang DG, Gao CQ, Yan HC, Wang XQ. Zinc L-aspartate enhances intestinal stem cell activity to protect the integrity of the intestinal mucosa against deoxynivalenol through activation of the Wnt/β-catenin signaling pathway. Environ Pollut. 2020;262:114290.
12. Li XG, Zhu M, Chen MX, Fan HB, Fu HL, Zhou JY, Zhai ZY, Gao CQ, Yan HC, Wang XQ. Acute exposure to deoxynivalenol inhibits porcine enteroid activity *via* suppression of the Wnt/β-catenin pathway. Toxicol Lett. 2019;305:19-31.
13. Fang H, Zhi Y, Yu Z, Lynch RA, Jia X. The embryonic toxicity evaluation of deoxynivalenol (DON) by murine embryonic stem cell test and human embryonic stem cell test models. Food Control. 2018;86:234-240.
14. Kang R, Li R, Dai P, Li Z, Li Y, Li C. Deoxynivalenol induced apoptosis and inflammation of IPEC-J2 cells by promoting ROS production. Environ Pollut. 2019;251:689-698.
15. Pinton P, Oswald IP. Effect of deoxynivalenol and other type B trichothecenes on the intestine: a review. Toxins (Basel). 2014;6:1615-1643.
16. Yang Y, Yu S, Tan Y, Liu N, Wu A. Individual and combined cytotoxic effects of co-occurring deoxynivalenol family mycotoxins on human gastric epithelial cells. Toxins (Basel). 2017;9:96.
17. Pestka JJ. Deoxynivalenol-induced proinflammatory gene expression: mechanisms and pathological sequelae. Toxins (Basel). 2010;2:1300-1317.
18. Graziani F, Pinton P, Olleik H, Pujol A, Nicoletti C, Sicre M, Quinson N, Ajandouz EH, Perrier J, Pasquale ED, Oswald IP, Maresca M. Deoxynivalenol inhibits the expression of trefoil factors (TFF) by intestinal human and porcine goblet cells. Arch Toxicol. 2019;93:1039-1049.
19. Kadota T, Furusawa H, Hirano S, Tajima O, Kamata Y, Sugita-Konishi Y. Comparative study of deoxynivalenol, 3-acetyldeoxynivalenol, and 15-acetyldeoxynivalenol on intestinal transport and IL-8 secretion in the human cell line Caco-2. Toxicol *In Vitro*. 2013;27:1888-1895.
20. Broekaert N, Devreese M, Demeyere K, Berthiller F, Michlmayr H, Varga E, Adam G, Meyer E, Croubels S. Comparative *in vitro* cytotoxicity of modified deoxynivalenol on porcine intestinal epithelial cells. Food Chem Toxicol. 2016;95:103-109.
21. Smith MC, Hymery N, Troadec S, Pawtowski A, Coton E, Madec S. Hepatotoxicity of fusariotoxins, alone and in combination, towards the HepaRG human hepatocyte cell line. Food Chem Toxicol. 2017;109:439-451.
22. Lee NH, Cho A, Park SR, Lee JW, Sung Taek P, Park CH, Choi YH, Lim S, Baek MK, Kim DY, Jin M, Lee HY, Hong IS. SERPINB2 is a novel indicator of stem cell toxicity. Cell Death Dis. 2018;9:724.
23. Scanu M, Mancuso L, Cao G. Evaluation of the use of human mesenchymal stem cells for acute toxicity tests. Toxicol *In Vitro*. 2011;25:1989-1995.
24. Pierron A, Mimoun S, Murate LS, Loiseau N, Lippi Y, Bracarense AP, Liaubet L, Schatzmayr G, Berthiller F, Moll WD, Oswald IP. Intestinal toxicity of the masked mycotoxin deoxynivalenol-3-β-D-glucoside. Arch Toxicol. 2016;90:2037-2046.
25. Bony S, Carcelen M, Olivier L, Devaux A. Genotoxicity assessment of deoxynivalenol in the Caco-2 cell line model using the Comet assay. Toxicol Lett. 2006;166:67-76.
26. Vandenbroucke V, Croubels S, Martel A, Verbrugghe E, Goossens J, Van Deun K, Boyen F, Thompson A, Shearer N, De Backer P, Haesebrouck F, Pasmans F. The mycotoxin deoxynivalenol potentiates intestinal inflammation by *Salmonella typhimurium* in porcine ileal loops. PLoS One. 2011;6:e23871.
27. Ichim TE, O'Heeron P, Kesari S. Fibroblasts as a practical alternative to mesenchymal stem cells. J Transl Med. 2018;16:212.
28. Ugurlu B, Karaoz E. Comparison of similar cells: mesenchymal stromal cells and fibroblasts. Acta Histochem. 2020;122:151634.
29. Baskić D, Popović S, Ristić P, Arsenijević NN. Analysis of cycloheximide-induced apoptosis in human leukocytes: fluorescence microscopy using annexin V/propidium iodide versus acridin orange/ethidium bromide. Cell Biol Int. 2006;30:924-932.
30. Ciniglia C, Pinto G, Sansone C, Pollio A. Acridine orange/ethidium bromide double staining test: a simple *in-vitro* assay to detect apoptosis induced by phenolic compounds in plant cells. Allelopathy J. 2010;26:301-308.
31. Shikhaliyeva I, Teker T, Albayrak G. Masked mycotoxins of deoxynivalenol and zearalenone-unpredicted toxicity. Biomed J Sci Tech Res. 2020;29:22288-22293.

32. Dall'Erta A, Cirlini M, Dall'Asta M, Del Rio D, Galaverna G, Dall'Asta C. Masked mycotoxins are efficiently hydrolyzed by human colonic microbiota releasing their aglycones. Chem Res Toxicol. 2013;26:305-312.

33. Paterson RRM, Lima N. How will climate change affect mycotoxins in food? Food Res Int. 2010;43:1902-1914.

34. Hanyu H, Yokoi Y, Nakamura K, Ayabe T, Tanaka K, Uno K, Miyajima K, Saito Y, Iwatsuki K, Shimizu M, Tadaishi M, Kobayashi-Hattori K. Mycotoxin deoxynivalenol has different impacts on intestinal barrier and stem cells by its route of exposure. Toxins (Basel). 2020;12:610.

35. Cao H, Zhi Y, Xu H, Fang H, Jia X. Zearalenone causes embryotoxicity and induces oxidative stress and apoptosis in differentiated human embryonic stem cells. Toxicol *In Vitro*. 2019;54:243-250.

36. Rajendran R, Gopal S, Masood H, Vivek P, Deb K. Regenerative potential of dental pulp mesenchymal stem cells harvested from high caries patient's teeth. J Stem Cells. 2013;8:25-41.

37. Kubat E, Gürpınar A, Ertuğrul G, Hakan I, Karasoy D, Onur MA. Is enoxaparin sodium exactly safe for subcutaneous fibroblast: a cell culture study. Acta Med Alanya. 2021;5:18-23.

38. Katayama K, Seyer JM, Raghow R, Kang AH. Regulation of extracellular matrix production by chemically synthesized subfragments of type I collagen carboxy propeptide. Biochemistry. 1991;30:7097-7104.

39. Wada M, Gelfman CM, Matsunaga H, Alizadeh M, Morse L, Handa JT, Hjelmeland LM. Density-dependent expression of FGF-2 in response to oxidative stress in RPE cells *in vitro*. Curr Eye Res. 2001;23:226-231.

40. Patella F, Neilson LJ, Athineos D, Erami Z, Anderson KI, Blyth K, Ryan KM, Zanivan S. In-depth proteomics identifies a role for autophagy in controlling reactive oxygen species mediated endothelial permeability. J Proteome Res. 2016;15:2187-2197.

41. Ribble D, Goldstein NB, Norris DA, Shellman YG. A simple technique for quantifying apoptosis in 96-well plates. BMC Biotechnol. 2005;5:12.

Turk J Pharm Sci 2024;21(1):71-80
DOI: 10.4274/tjps.galenos.2023.64369

ORIGINAL ARTICLE

Pharmacological Potential Effects of Algerian Propolis Against Oxidative Stress, Multidrug-Resistant Pathogens Biofilm and Quorum-Sensing

Widad HADJAB[1], Amar ZELLAGUI[1]*, Meryem MOKRANI[1], Mehmet ÖZTÜRK[2], Özgür CEYLAN[2], Noureddine GHERRAF[3], Chawki BENSOUICI[4]

[1]Larbi Ben M'hidi University, Faculty of Exact Science and Life Science and Nature, Department of Laboratory of Biomolecules and Plant Breeding, Oum el-Bouaghi, Algeria
[2]Muğla Sıtkı Koçman University, Ula Ali Koçman Vocational School, Department of Food Quality and Analysis Program, Muğla, Türkiye
[3]Larbi Ben M'hidi University, Department of Laboratory of Natural Resources and Management of Sensitive Environments, Oum el-Bouaghi, Algeria
[4]Abdelhamid Mehri Constantine 2 University, Biotechnology Research Centre, Constantine, Algeria

ABSTRACT

Objectives: This study sought to examine the chemical profile, antioxidant, antimicrobial, antibiofilm, and anti-quorum sensing potential of two propolis ethanolic extracts (PEEs) collected from northeast Algeria.

Materials and Methods: To achieve the main objectives of this study, multiple *in vitro* tests were employed. The phenolic and flavonoid contents were analyzed, and the chemical composition of both PEE was determined by high-performance liquid chromatography. The antioxidant properties of the propolis extracts were investigated using six complementary tests. The inhibitory effects of propolis extracts were evaluated against multidrug-resistant (MDR) clinical isolates using agar well diffusion and microdilution methods, whereas their antibiofilm and quorum-sensing disruption effects were determined by spectrophotometric microplate methods.

Results: The results demonstrated that phenolic and flavonoid contents were higher in propolis from the Guelma (PEEG) region (PEEG; 188.50 ± 0.33 µg GAE/mg E, 144.23 ± 1.03 µg QE/mg E), respectively. Interestingly, different components were identified, and cynarin was the major compound detected. The PEEG sample exhibited potential antioxidant effects in scavenging $ABTS^{\bullet+}$ radicals with minimal inhibitory concentration values equal to 10.46 ± 1.40 µg/mL. Furthermore, the highest antibacterial activity was recorded by PEEG against Gram-positive *Staphylococcus aureus* MDR1. Similarly, PEEG effectively inhibited the biofilm formation of *S. aureus* MDR1 and the degradation of biofilm was up to 60%. In addition, quorum sensing disruption revealed that both extracts have a moderate capacity for violacein inhibition by the *Chromobacterium violaceum* ATCC 12472 strain in a concentration-dependent manner.

Conclusion: These findings indicate that propolis can be regarded as a natural therapeutic agent for health problems associated with MDR bacteria and oxidative stress.

Key words: Antibacterial, antioxidant, multidrug-resistant, propolis, quorum sensing

INTRODUCTION

Plant-derived natural products are considered an extraordinary source of bioactive compounds that have already proven their feasibility in the therapeutic realm.[1] As one of the major beekeeping products, propolis already has well-known pharmaceutical properties. Propolis is a sticky phytocompound derived from plant exudates, it is rich in polyphenols, especially flavonoids and phenolic acids, which are known as the most active components responsible for its health benefits, including antibacterial, antioxidant, and anticancer.[2] However, the chemical composition of propolis is unstable. Botanical sources and geographical areas highly influence it.[3] Because of the common frequency of diseases related to drug-resistant bacteria and oxidative stress, many world scientists are

*Correspondence: zellaguia@yahoo.com, Phone: +213 559 46 01 48, ORCID-ID: orcid.org/0000-0002-6515-8103
Received: 17.08.2022, Accepted: 08.04.2023

searching for solutions to mitigate these issues. The sharp increase and the widespread of multidrug-resistant (MDR) bacteria compounded by the ability of bacteria to form biofilms is considered an emergent global health problem[4], as bacteria in biofilms are extremely resistant and difficult to treat.[5] Among the reasons that contributed to the worsening of this health problem is the overuse of antibiotics, which has increased in the last decades, especially in the current viral pandemic (coronavirus disease-2019). Furthermore, the scarcity of new antibiotics is one of the devastating purposes that contributed to the incapacity to control the spread of MDR bacteria.[6] On the other hand, oxidative stress and inflammation are no less dangerous than the former issue, and many studies have proved their role in the pathogenesis of many chronic illnesses, including cardiovascular diseases, Alzheimer's disease, and cancer.[7] Dysfunction of the body's antioxidant defense system leads to excess production of reactive oxygen species which causes inflammation *via* the induction of pro-inflammatory signaling pathways and the release of multiple inflammatory mediators, such as cytokines.[8] The World Health Organization describes the current clinical drug pipeline as bleak and warns about the shortage of new therapeutic agents. Thus, it is important to identify new therapeutic strategies that solve these global health problems.

This study was conducted to seek more efficient natural bioactive compounds from propolis. Therefore, the total phenolics and flavonoid contents along with antioxidant activity of the Algerian propolis samples were determined.

Furthermore, *in vitro* studies were conducted to evaluate the antibacterial and antibiofilm activity against several MDR bacteria and the anti-quorum sensing activity of Algerian propolis.

MATERIALS AND METHODS

Propolis sampling and extraction

Propolis samples were collected in the early summer of 2019 from two different regions: Guelma and Ain-Fakroun in Northeast Algeria. 20 g propolis was extracted with 100 mL ethanol (80%). The mixture was kept for 24 hours in dark conditions before it was filtered through the Whatman no. 4 filter paper. The extract was evaporated using rotavapor and stored under dry conditions at 4 °C until use.

Total phenolic content (TPC)

TPC was calculated using the Folin-Ciocalteu (FC) reagent and gallic acid as a standard. A volume of 200 µL of propolis ethanolic extract (PEE) (0.5 mg/mL) was added to 1 mL of FC reagent (10%).

After 10 min of incubation in the dark, 800 µL of 7.5% Na_2CO_3 was added again, after incubation in the dark for 90 min. The absorbance was measured at 760 nm. The results are expressed as micrograms of gallic acid equivalents *per* milligram of extract (µg GAE/mg E).[9]

Total flavonoid content (TFC)

TFC was quantified using the aluminum trichloride method.[10] An aliquot of 50 µL of the PEE was mixed with 130 µL methanol, 10 µL of aluminum nitrate, and 10 µL potassium acetate. After 40 min of incubation, the absorbance was measured at 415 nm. The results are expressed in micrograms of quercetin equivalents *per* milligram of extract (µg QE/mg E).

High-performance liquid chromatography (HPLC)

Separation and detection of propolis compounds were performed using a Shimadzu high-performance liquid chromatography (Shimadzu Cooperation, Japan) system. The detection system was a Shimadzu model SPD-M20A diode array, and the delivery system comprised a Shimadzu model LC-20AT. Separation was attained using an internal ODS-3 column (4 µm, 4.0 mm x 150 mm) and an Inertsil ODS-3 guard column. The elution program was as follows: the mobile phase included 0.1% aqueous acetic acid and methanol.

After being diluted in 1 mL of methanol (8 $mg.mL^{-1}$), it was passed through a polytetrafluoroethylene filter with a 0.45 µm pore size. 20 µL was the injection volume. The HPLC-diode array detector (HPLC-DAD) system was used for quantitative and qualitative analysis using 42 standards: fumaric acid, gallic acid, *p*-benzoquinone, protocatechuic acid, theobromine, theophylline, catechin, 4-hydroxybenzoic acid, 6,7-dihydroxycoumarin, methyl-1,4 benzoquinone, vanillic acid, caffeic acid, vanillin, chlorogenic acid, *p*-coumaric acid, ferulic acid, cynarin, coumarin, propyl gallate, rutin, *trans*-cinnamic acid, ellagic acid, myricetin, fisetin, quercetin, *trans*-cinnamic acid, luteolin, rosmarinic acid, kaempferol, apigenin, chrysin, 4-hydroxy resorcinol, 14-dichlorobenzene, pyrocatechol, 4-hydroxybenzaldehyde, epicatechin, 24-dihydroxybenzaldehyde, hesperidin, oleuropein, naringenin, hesperetin, genistein, and curcumin.

Detection was performed using a DAD, and a wavelength of 254 nm was used to identify molecules. Results are expressed as micrograms *per* gram of dry weight.

DPPH-free radical scavenging activity

Essentially, 160 µL of DPPH solution (60 µM) was mixed with 40 µL of PEE at different concentrations. After 30 min of incubation in darkness, the prepared mixture was tested for absorbance at 517 nm. The results of DPPH scavenging effect were represented as 50% inhibition concentration (IC_{50}) and contrasted with standards butylated hydroxyanisole (BHA) and butylated hydroxytoluene (BHT).[11]

Cupric ion-reducing antioxidant capacity (CUPRAC)

The CUPRAC assay was conducted using the approach described by Apak et al.[12] Briefly, a mixture of 50 µL of copper (II) chloride (10 mM), 50 µL of neocuprine (7.5 mM), and 60 µL of ammonium acetate buffer solution (1M, pH: 7.0) was used. Subsequently, PEE was added to the initial mixture at a volume of 40 µL. After 60 min of incubation, the absorbance was measured at 450 nm, and the findings are represented as $A_{0.5}$ (µg/mL).

Reducing power assay

A volume of 10 µL of solution was mixed with 50 µL of phosphate buffer (pH 6.6) and 50 µL of potassium ferricyanide (1%). The

mixture was then incubated for 20 min at 50 ˚C. Following this, the initial mixture was combined with 50 µL of trichloroacetic acid (10%), 40 µL of distilled water, and 10 µL of ferric chloride solution (0.1%). At 700 nm, the absorbance was measured.[13]

ABTS cation radical decolorization

The $ABTS^{\bullet+}$ scavenging activity was determined using the method of Re et al.[14] In short, $ABTS^{\bullet+}$ solution was prepared by the reaction between ABTS (7 mm) in water and potassium persulfate (2.45 mm) and stored for 12 hours in the dark. Prior to use, the absorbance of the ABTS solution was adjusted to 0.70 ± 0.02 (734 nm). Afterward, 40 µL of the solution was mixed with 160 µL of the dilute $ABTS^{\bullet+}$ solution. After 10 min of incubation, absorbance was measured at 734 nm. The results were established as a 50% IC_{50} (IC_{50}= µg/mL).

Galvinoxyl radical (GOR) scavenging

40 µL of different concentrations of the extracts were mixed with 160 µL of a 0.1 mmol/L galvinoxyl solution. The obtained mixtures were incubated for 2 hours. The absorbance was read at 428 nm.[15]

Phenanthroline assay

The copper-phenanthroline assay was performed using the Szydłowska-Czerniak et al.[16] method. A volume of 30 µL of 0.5% 1,10-phenanthroline solution (0.5%) was mixed with 50% $FeCl_3$ (0.2%) and 10 µL of solution. Using methanol, the volume was made up to 200 µL. The incubation was performed in the dark for 20 min.

Antimicrobial activity determination

Selected microorganisms

Antibacterial activity was evaluated against MDR clinical bacteria isolated from human urine samples. The strains were collected from the laboratory of bacteriology at the Public Medical Hospital in the province of Oum El Bouaghi, Algeria. Gram-negative bacteria (three MDR clinical isolates of *Escherichia coli* and *Pseudomonas aeruginosa*, one MDR clinical isolate of *Klebsiella pneumoniae*, and one MDR clinical isolate of *Serratia odorifera*), whereas only four MDR clinical isolates of *S. aureus* were employed in this study. The bacterial resistance profiles of each strain to antibiotics are depicted in Table 1.

Disc diffusion assay

The disk diffusion assay was performed in accordance with the National Committee of Clinical Laboratory Standards. Culture suspensions (0.5 McFarland) were inoculated on fresh Mueller-Hinton agar plates. Afterward, 20 µL of PEE (20 mg/mL) was impregnated in sterile filter discs (Whatman paper no. 4) and deposited on the surfaces of the pre-inoculated plates. The Petri plates were incubated at 37 ˚C for 24 hours. Antibacterial standards included ampicillin (AMP, 10 µg/disc), kanamycin (K, 10 µg/disc), and streptomycin (S, 10 µg/disc).

Determination of minimum inhibitory (MIC) and, minimum bactericidal (MBC)

MIC and MBC were evaluated using the microdilution assay. PEE dilutions were prepared using dimethylsulfoxide (DMSO 15%), and the concentration ranged from 20 to 0.625. An aliquot of 10 µL of each bacterial strain was inoculated into the wells of a 96-well microliter plate containing 170 µL of Mueller-Hinton Broth (MHB). Then, 20 µL of different final concentrations of PEE were transferred to each well. MBC was determined by overlying 10 µL of the test dilutions from each clear well on fresh Luria-Bertani (LB) agar plates. After that, the plates were incubated for 24 hours at 37 ˚C. The lowest concentration with no bacterial growth was defined as MBC. Inocula and medium were used as positive controls.[17]

Table 1. MDR profiles of different strains used in this study

Strains	Resistance profiles
S. aureus MDR1	TE, AK, AML, OX, P, FOX, TI, CL, E, TCC, OF, AMP, C
S. aureus MDR2	FOX, TI, AMP, K, TE, AK, AML, P, CTX, S, CL, E, OF, CIP
S. aureus MDR3	AMP, K, TE, AK, AML, OX, CTX, FOX, TI, CL, TOB, E, C, GEN, OF, CIP, TCC
S. aureus MDR4	OX, FOX, K, P, TI, S, CL, TCC
P. aeruginosa MDR1	AMP, FOS, AML, OX, FTN, CTX, SXT, TI, S, CL, GEN, CAZ, OF, CIP
P. aeruginosa MDR2	AMP, K, C, TE, COT, FOS, AML, OX, CTX, FOX, TI, CL, TOB, CAZ, OF, CIP
P. aeruginosa MDR3	CTX, FOX, SXT, CL, CAZ, AMP, TE, COT, AML, OX, FTN
E. coli MDR1	CTX, SXT, TI, AMP, VA, C, COT, AML, P, S, CL, CAZ, TCC
E. coli MDR2	AMP, VA, K, TE, COT, AML, P, CTX, SXT, TI, E, CAZ, OF, CIP
E. coli MDR3	AMP, VA, TE, COT, AML, FTN, SXT, TI, CL, GEN, TCC
S. odorefera MDR	RIF, P, TI, E
K. pneumoniae MDR	TOB, E, GEN, CAZ, CIP, AMP, VA, TE, COT, AML, P, CTX, SXT, TI

MDR: Multidrug-resistant, RIF: Rifampicin (5 µg), AMP: Ampicillin (10 µg), VA: Vancomycin (30 µg), K: Kanamycin (30 µg), C: Chloramphenicol (30 µg), TE: Tetracyclin (30 µg), COT: Co-trimoxazole (25 µg), FOS: Fosfomycin (50 µg), AK: Amikacine (30 µg), AML: Amoxicillin (30 µg), OX: Oxacillin (1 µg), P: Penicillin (10 µg), FTN: Nitrofurantoine (300 µg), CTX: Cefotaxim (30 µg), FOX: Cefoxitin (30 µg), SXT: Trimethoprim sulfamethoxazole (25 µg), TI: Ticarcillin (75 µg), S: Streptomycin (10 µg), CL: Colistin (10 µ g), TOB: Tobramycin (10 µg), E: Erythromycin (15 µg), GEN: Gentamicin (10 µg), CAZ: Ceftazidime (30 µg), OF: Ofloxacin (5 µg), CIP: Ciprofloxacin (5 µg), TCC: Ticarcilin-clavulanic acid (75/10 µg)

Influence of propolis extract on biofilm formation

An antibiofilm assay was employed to examine the antiadhesion activity. Only 5 strains were selected for this test namely: *E. coli* MDR1, *P. aeruginosa* MDR1, *S. aureus* MDR1, *K. pneumoniae* MDR, and *S. odorifera* MDR. The test was performed using the crystal violet assay.[18] A volume of 20 µL of overnight isolate cultures was dispensed into the wells of 96 well microliter plates previously containing 170 µL of MHB, and then 10 µL of dissolved DMSO was added to each well at concentrations ranging from 20 to 0.625 mg/mL. Wells with bacteria and MHB served as controls. The following equation was used to estimate the percentage of biofilm inhibition:

Biofilm inhibition (%) = [optical density (OD) Control-OD Sample/OD Control x 100]

Violacein Inhibition (VI) assay

C. violaceum 12472 (CV12472) was used to test the effect of PEE on violacein production. A volume of 10 µL of an overnight broth culture of *C. violaceum 12472* was dispensed into 96 well plates previously filled with 170 µL of LB broth (LBB) and incubated at 30 °C for 24 hours in the presence of various concentrations of PEE. Wells with LBB and inoculum were regarded as a positive control.[19] Inhibition of violacein production was measured using a microplate reader (OD= 585 nm). Violacein repression percentage was calculated using the following formula:

Violacein inhibition (%) = [(OD Control-OD Sample)/(OD Control)] x 100

Bioassay for quorum sensing inhibition using CV026

To achieve this test, the method specified by Koh and Tham.[20] was applied. The process was completed by mixing 5 mL of molten soft agar with 100 µL of *C. violaceum* 026 (CV026) bacterial suspension, further supplementing 20 µl of C6HSL and 10 µL of kanamycin. The latter suspension was spread across the surface of solidified LB agar (LBA) plates. Then, 6 mm wells were created through the LBA, and 50 µL different concentartions of PEE (20-2.5 mg/mL) were added to each well. The plates were incubated at 30 °C for 3 days. The presence of white or cream-colored halo around the wells signals quorum sensing (QS) inhibition, the results was measured in mm.

Statistical analysis

Graph Pad Prism 9.3.1 (Graph Pad Software, USA) was used for data analysis. One-way ANOVA followed by Tukey's multiple comparison test was employed for statistical analyses. Results were considered statistically significant at $p < 0.05$.

RESULTS AND DISCUSSION

TPC and TFC

The TPC and TFC were determined as a measure of the number of propolis bioactive components. The results are displayed in Table 2. The propolis from the Guelma (PEEG) sample shows the highest TPC, followed by the Propolis Ethanolic Extract from Ain-Fakroun (PEEF) sample. Interestingly, our results present a higher TPC than previous studies conducted in different local regions in Algeria.[21,22] Moreover, a more considerable variability in TPC was shown in propolis collected from several parts of the world.[23] Conversely, these findings contradict the results of Bouaroura et al.[24] who studied propolis from the same region (Guelma) and reported a complete lack of TPC, which emphasizes the intense variability in propolis contents. Regarding TFC, the results also displayed that the PEEG sample exhibited the highest content, greater than that reported by Boulechfar et al.[25] Although the study samples were harvested in the same season and extracted using the same method, the two extracts were significantly different. This difference is mainly attributed to plant origin of the propolis and, more specifically, to the vegetation where bees gather propolis.[26]

Table 2. Total phenolic and flavonoid content of PEE

Propolis extracts	TPC (µg GAE/mg E)	TFC (µg QE/mg E)
PEEG	188.50 ± 0.33[a]	144.23 ± 1.03[a]
PEEF	136.35 ± 3.56[b]	126.38 ± 1.62[b]

All values are expressed as mean ± standard deviation (n=3). Small letters ([a,b]) highlight the significant difference ($p < 0.05$) for TPC and TFC, respectively, among both extract. TPC is expressed as µg Gallic acid equivalent/mg of extract, and TFC is expressed as µg Quercetin equivalent/mg of extract. PEE: Propolis ethanolic extracts, TPC: Total phenolic content, TFC: Total flavonoid content, PEEF: Propolis Ethanolic Extract from Ain-Fakroun, PEEG: Propolis from the Guelma

Table 3. Chemical composition of PEE using HPLC-DAD analyses

Compound	RT	PEEG (mg/g)	PEEF (mg/g)
Protocatechic acid	22.39	0.03	0.04
Vanillic acid	34.68	TR	TR
Caffeic acid	35.19	1.14	TR
Chlorogenic acid	38.88	ND	ND
p-Coumaric acid	40.81	TR	TR
Ferulic acid	42.92	ND	TR
Cynarin	43.85	6.12	5.96
Prophylgallate	46.98	ND	ND
Rutin	47.52	ND	0.74
Ellagic acid	50.00	ND	ND
Fisetin	51.24	ND	ND
Quercetin	55.42	0.38	0.34
Luteolin	57.87	ND	ND
Kaempferol	62.48	0.93	0.03
Apigenin	64.07	0.04	TR
Chrysin	72.77	ND	0.59
Hesperidin	47.38	0.58	ND
Oleuropein	49.54	ND	ND
Naringenin	55.51	1.04	ND
Hesperetin	57.47	0.68	3.70

PEE: Propolis ethanolic extracts, HPLC-DAD: High-performance liquid chromatography, RT: Retention time, PEEF: Propolis Ethanolic Extract from Ain-Fakroun, PEEG: Propolis from the Guelma, ND: Not detected, TR: < 0.01 mg/g

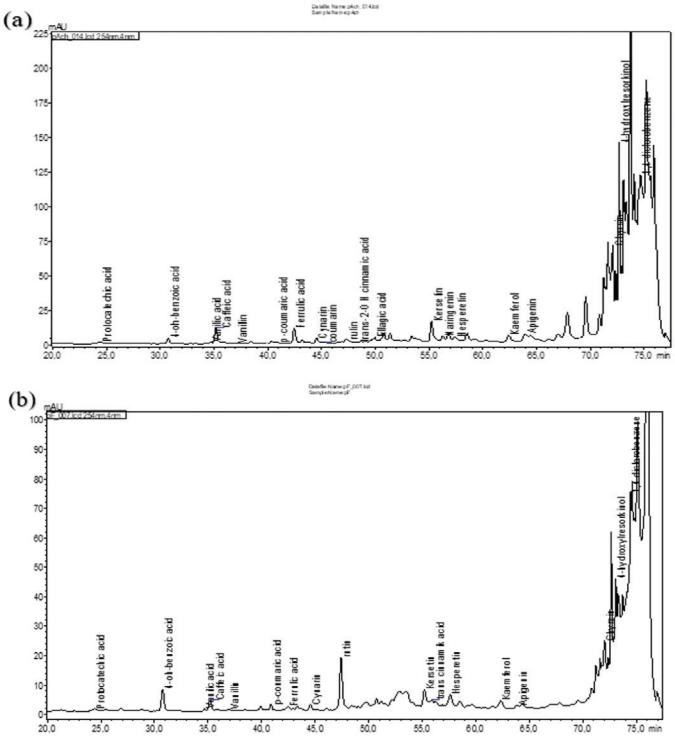

Figure 1. HPLC-DAD chromatogram of PEE. (a) PEEG, (b) PEEF

HPLC-DAD: High-performance liquid chromatography, PEE: Propolis ethanolic extracts, PEEF: Propolis Ethanolic Extract from Ain-Fakroun, PEEG: Propolis from the Guelma

Phenolic composition

HPLC-DAD analyses were performed, and the results are illustrated in Figure 1 and Table 3. From the 42 standard compounds quantified, only 9 compounds were detected in the PEEG sample, while 7 compounds were detected in the PEEF sample. The PEEG and PEEF samples exhibited almost similar compositions but with different amounts. The most abundant flavonoid detected in the PEEG and PEEF samples was cynarin, with an amount of 6.12 and 5.96 mg/g, respectively. Interestingly, caffeic acid, apigenin, naringenin, and hesperidin were detected only in the PEEG sample, whereas rutin and chrysin were detected only in the PEEF sample. Overall, the main components identified in our propolis samples are similar to those previously described in different local regions in Algeria.[27-29] Likewise, the phenolic compounds were approximately identical to those identified in propolis from different parts of the world.[30,31] The abundance of flavonoids in both propolis samples correlates with many previous studies confirming poplar as a botanical source of propolis.[24] Moreover, the botanical origin of cynarin identified in both PEEs was unknown, but it was inferred from a chemotaxonomic point of view that this compound would be collected by bees from exudates of plants belonging to the Asteraceae family, specifically *Cynara cardunculus* L.[32] This species is in the surrounding areas of the apiaries not only in the two sites of the collection state but also in many northeast Algerian localities.[33] It is worth mentioning that this report is the first on the occurrence of cynarin in Algerian propolis content.

Antioxidant activities of PEE

As previously mentioned, excess production of free radicals leads to many disorders and may cause many chronic diseases. Therefore, antioxidant capacity of the propolis was determined, and the results are presented in Table 4. According to our DPPH results, the PEEG sample had the strongest antioxidant activity with an IC_{50} of 74.24 ± 1.91 µg/mL, but lower than the BHT and BHA standards. In contrast, PEEF showed no capacity to scavenge the radical DPPH. Regarding the results of the ABTS assay, the PEEG sample had a more potent scavenging capacity than the DPPH results, with an IC_{50} value of 10.46 ± 1.40 µg/mL, which seems important compared to BHT and BHA standards. Similarly, both extracts demonstrated high antioxidant potential in the remaining assays, except for the reducing power assay. Recently, many studies have been conducted on propolis because of its natural antioxidant potential. This potent activity is mainly related to its chemical components, which are capable of reducing radicals. This implies the beneficial efficacy of propolis for treating pathological damage caused by free radicals. Considering the employed assays, *e.g.*, GOR and Phen, the antioxidant activity of the two tested samples was almost close to each other. This close similarity may be due to the phenolic profiles since the two extracts share some components such as cynarin, quercetin, kaemferol, hesperetin, and protocatechuic acid. The capacity of scavenging DPPH by the PEEG sample may be correlated to caffeic acid, which was absent in the remaining sample. Interestingly, this compound is well known for its high antiradical activity.[34] According to Jun et al.,[35] both propolis samples fall into the category of active antioxidants (IC_{50}: 50-100 ppm).

Antibacterial activity of PEE

The antibacterial effects of PEE are presented in Tables 5 and 6. As can be seen, the PEEG sample showed a remarkable antibacterial effect against the tested *S. aureus* MDR strains. In contrast, the PEEF sample was only active against two strains of *S. aureus*. In contrast, PEEG demonstrated minimal efficacy against Gram-negative bacteria, whereas the PEEF sample did not show any inhibitory effects on Gram-negative strains. The microdilution approach revealed that the PEEG sample exhibited the highest bacteriostatic activity against *S. aureus* MDR strains with a MIC value ranging from 2.5 to 20 mg/mL. In contrast, less activity was recorded against Gram-negative bacteria. The highest bactericidal effect was observed for PEEG (MBC= 5 mg/mL) against *S. aureus* MDR1.

PEEF showed no bactericidal activity against all tested strains. Plants are a valuable source of bioactive compounds with various pharmacological effects. Many studies have reported the potential efficiency of plants in causing several disorders related to bacterial infections, especially those related to MDR bacteria.[36] Considering that propolis is a plant-derived product and thus the abundance of several plant-bioactive compounds within its chemical content is widespread. Many researchers have focused on the possible use of propolis as an alternative antimicrobial agent for the treatment of infections caused by MDR pathogenic bacteria.

Table 4. Antioxidant activity of propolis extracts by different assays

Extracts	Antioxidant activity					
	DPPH assay IC_{50} (µg/mL)	ABTS assay IC_{50} (µg/mL)	Reducing power assay $A_{0.5}$ µg/mL	CUPRAC assay $A_{0.5}$ µg/mL	GOR IC_{50} (µg/mL)	Phen $A_{0.5}$ µg/mL
PEEG	73.55 ± 6.35^{c}	10.46 ± 1.40^{b}	NA	20.61 ± 2.93^{c}	41.68 ± 5.61^{b}	22.26 ± 0.13^{b}
PEEF	NA	24.29 ± 2.05^{c}	NA	68.87 ± 1.10^{d}	46.30 ± 2.79^{b}	20.91 ± 1.39^{b}
BHT	22.32 ± 1.19^{b}	1.29 ± 0.30^{a}	8.41 ± 0.67^{a}	9.62 ± 0.87^{b}	3.32 ± 0.18^{a}	2.24 ± 0.17^{a}
BHA	5.73 ± 0.41^{a}	1.81 ± 0.10^{a}	9.01 ± 1.46^{a}	3.64 ± 0.19^{a}	5.38 ± 0.06^{a}	0.93 ± 0.07^{a}

Linear regression analysis was used to compute the IC_{50} and $A_{0.5}$, which were reported as Mean ± SD (n = 3). The values in the same columns with different superscripts (^{a}, ^{b}, ^{c}, or ^{d}) are significantly different ($p < 0.05$). IC_{50} is defined as the concentration of 50% inhibition percentages while $A_{0.5}$ is defined as concentration at 0.50 absorbance, CUPRAC: Cupric ion-reducing antioxidant capacity, GOR: Galvinoxyl radical, BHA: Butylatedhydroxyanisole, BHT: Butylatedhydroxytoluene, NA: No absorbance, IC: Inhibition concentration, PEEF: Propolis Ethanolic Extract from Ain-Fakroun, PEEG: Propolis from the Guelma

Table 5. Antimicrobial activity of the PEEG sample against MDR bacteria

Strains	PEEG			Amp (10 µg/disc; 50 mg/mL)	K (10 µg/disc; 50 mg/mL)	S (10 µg/disc; 50 mg/mL)
	Mean ± SD* (mm)	MIC	MBC			
Gram-positive bacteria						
S. aureus MDR1	18.67 ± 1.53^{aA}	2.5	5	11^{B}	15^{B}	9^{B}
S. aureus MDR2	13.33 ± 0.58^{bcA}	5	10	17^{B}	13^{A}	-
S. aureus MDR3	11.00 ± 2.00^{bA}	20	+20	13^{A}	10^{A}	10^{A}
S. aureus MDR4	15.00 ± 0.00^{cA}	5	20	29^{B}	17^{A}	10^{B}
Gram-negative bacteria						
P. aeruginosa MDR1	9.33 ± 0.58^{aA}	10	20	-	10^{A}	12^{B}
P. aeruginosa MDR2	-	+20	NT	-	12	13
P. aeruginosa MDR3	10.00 ± 0.00^{aA}	20	+20	-	-	11^{A}
E. coli MDR1	9.67 ± 2.08^{aA}	20	+20	-	16^{B}	12^{A}
E. coli MDR2	-	+20	NT	-	15	R
E. coli MDR3	-	+20	NT	-	-	11
Serratia odorifera MDR	-	10	20	-	21	14
Klebsiella pneumoniae MDR	14.00 ± 1.73^{bA}	20	NT	-	12^{A}	-

The PEEG inhibition zone (20 µL/disk; 200 µg/disc) are presented as an average of three repetitions (mm ± standard deviation). The letters $^{a\text{-}c,A,B}$: Indicate a significant difference according to Tukey test ($p < 0.05$). PEEG means of different strains are compared using lowercase while uppercases are used to compare means between PEEG and each antibiotic for the same strain, SD: Standard deviation, MDR: Multidrug-resistant, MIC: Minimal inhibitory concentration (mg/mL), MBC: Minimal bactericidal concentration (mg/mL), (-): No activity, NT: Not tested, PEEG: Propolis from the Guelma

From the results mentioned above, propolis possesses significant antibacterial activity against MDR bacteria. Similarly, a study demonstrated that Palestinian propolis is active against MDR clinical isolates.[37] These findings agree with previous research indicating that Gram-positive bacteria are more susceptible to propolis than Gram-negative bacteria. This sensitivity is probably related to differences in the membrane structure of bacteria. Furthermore, in some cases, the diameter zone recorded for the PEEG sample against *S. aureus* MDR strains was even more significant than those produced by different antimicrobial agents, which indicates the efficacy of propolis against MDR bacteria compared with the commonly used antibacterial treatment. Overall, this activity correlates with propolis bioactive contents such as flavonoids, which are known for their remarkable ability of bacterial inhibition.[38] Cynarin was the major compound identified and many studies reported the antimicrobial properties of this compound[39]. In addition, other polyphenols, such as caffeic acid, possess highly potent antibacterial activity. However, many related reports have associated this activity with the synergistic interaction between different propolis active components.[40]

Antibiofilm activity of PEE

The results of the antibiofilm activity of PEE are shown in Figure 2. PEEG sample significantly inhibited biofilm formation at MIC concentration in each strain and the highest inhibition was recorded against *S. aureus* MDR1 (Figure 3). Lower activity was registered against the remaining strains. The PEEF sample showed eradication only against *S. aureus* MDR1 strain at MIC and MIC/2. Bacterial biofilms are one of the major factors

Table 6. Antimicrobial activity of the PEEF sample against MDR bacteria

Strains	PEEF			Amp (10 µg/disc; 50 mg/mL)	K (10 µg/disc; 50 mg/mL)	S (10 µg/disc; 50 mg/mL)
	Mean ± SD (mm)	MIC	MBC			
Gram-positive bacteria						
S. aureus MDR1	10.34 ± 2.52^{aA}	20	+20	11^{A}	15^{B}	9^{A}
S. aureus MDR2	-	+20	NT	17	13	-
S. aureus MDR3	-	20	+20	13	10	10
S. aureus MDR4	13.00 ± 1.00^{aA}	10	+20	29^{B}	17^{B}	10^{A}
Gram-negative bacteria						
P. aeruginosa MDR1	-	+20	NT	-	10	12
P. aeruginosa MDR2	-	+20	NT	-	12	13
P. aeruginosa MDR3	-	+20	NT	-	-	11
E. coli MDR1	-	+20	NT	-	16	12
E. coli MDR2	-	+20	NT	-	15	R
E. coli MDR3	-	+20	NT	-	-	11
S. odorifera MDR	-	+20	NT	-	21	14
K. pneumoniae MDR	-	+20	NT	-	12	-

The PEEF inhibition zone (20 µL/disk; 200 µg/disc) are presented as an average of three repetitions (mm ± SD). The letters "^{a}" indicate no significate difference, ^{A,B}: Indicate a significant difference according to Tukey test ($p < 0.05$). PEEF means of different strains are compared using lowercase while uppercases are used to compare means between PEEF and each antibiotic for the same strain, SD: Standard deviation, MIC: Minimal inhibitory concentration (mg/mL), MBC: Minimal bactericidal concentration (mg/mL), (-): No activity, NT: Not tested, MDR: Multidrug-resistant, PEEF: Propolis Ethanolic Extract from Ain-Fakroun

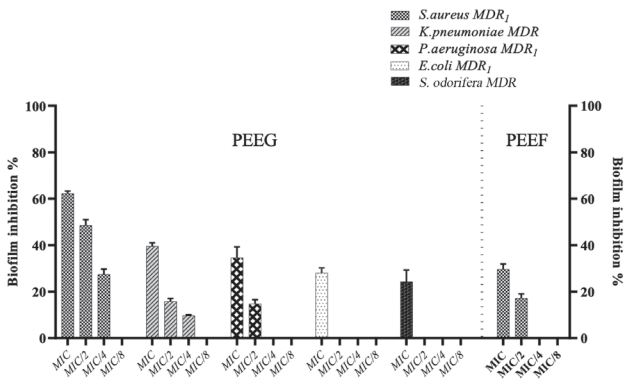

Figure 2. The effect of varied concentrations (MIC, MIC/2, MIC/4, and MIC/8) of PEEG and PEEF samples on biofilm formation of five MDR strains including, *S. aureus* MDR1, *K. pneumoniae* MDR, *P. aeruginosa* MDR1, *E. coli* MDR1, and *S. odorifera* MDR. The data represent the mean of three independent assessments. The error bars reflect standard deviations

MIC: Minimal inhibitory concentration, MDR: Multidrug-resistant,

that contribute to the progression and persistence of chronic infections, as the destructive effect of antibiotics is becoming more difficult.[41]

These findings agree with those of a study by Daikh et al.[29] at a concentration of 300 µg/mL, Algerian propolis extract significantly inhibited the biofilm formation of virulent *S. aureus*. In line with these results, Brazilian green propolis has shown antibiofilm activity against the MDR strains of *K. pneumoniae* and *P. aeruginosa*.[42] Many studies have highlighted the inhibitory effects of flavonoids and polyphenols on bacterial

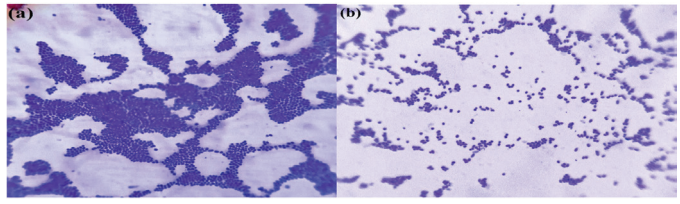

Figure 3. A representative image revealing the significant inhibition in biofilm formation by *S. aureus* MDR1 using light microscopic observation (magnification x 40): (a) before treatment with PEEG and (b) after treatment with PEEG at MIC concentration by crystal violet staining assay

MIC: Minimum inhibitory concentration

Table 7. VI and anti-quorum sensing activities of PEEG and PEEF samples

	PEEF		PEEG	
	VI (%)	QS (mm)	VI (%)	QS (mm)
MIC*	44.86 ± 2.49^{a}	-	62.39 ± 1.19^{a}	-
MIC/2	41.15 ± 0.77^{a}	-	38.36 ± 0.00^{b}	-
MIC/4	34.87 ± 1.46^{b}	-	36.45 ± 0.00^{b}	-
MIC/8	18.45 ± 1.60^{c}	-	31.22 ± 0.42^{c}	-
MIC/16	-	-	26.66 ± 0.98^{d}	-
MIC/32	-	-	24.20 ± 1.20^{e}	-

The letters (a-d) indicate a significant difference according to Tukey test ($p < 0.05$), *: MIC values were 20 mg/mL for *C. violaceum CV12472* and *C. violaceum CV026*, (-): No inhibition, QS: Quorum sensing, PEEF: Propolis Ethanolic Extract from Ain-Fakroun, PEEG: Propolis from the Guelma, VI: Violacein inhibition (%)

biofilms. The variability of flavonoids observed in both propolis extracts could account for their different *in vitro* effects. For example, the stronger activity of the PEEG extract in reducing biofilm production could be due to it is content of caffeic acid and quercetin compared with PEEF. Moreover, quercetin, kaempferol, apigenin, and naringenin were identified as biofilm inhibitors.[43]

VI and QSI of propolis extracts

The MIC values of the PEEG and PEEF samples against both strains were determined and shown in Table 7. It is clear from the results that both PEEs inhibited violacein production by *C. violaceum 12472* in a dose-dependent manner. The PEEG sample was more potent in VI than the PEEF sample. Moreover, at lower doses of MIC/8, the PEEF sample showed no suppression of violacein synthesis. Unexpectedly, there was no inhibition of QS of *C. violaceum 026*, on LB Petri dish agar was observed.

CV12472 can produce violacein pigment under a cell-to-cell communication mechanism called QS. Therefore, disruption of this phenomenon is necessary to overcome persistent infections.[44] The obtained results prove that propolis inhibits the QS process. These findings correlate with the study by Sorucu and Ceylan[45], which demonstrated that propolis has a high efficiency in disturbing the QS mechanism. Several types of phytochemicals, such as polyphenols and flavonoids, can affect the QS process in some bacteria by reducing the expression of several QS-controlled genes. Furthermore, recent findings have demonstrated the potent efficiency of different flavonoids, such as naringenin, kaempferol, quercetin, and apigenin, in inhibiting chemical signaling process.[45-48]

CONCLUSION

Recently, the widespread presence of MDR pathogens and the scarcity of novel antimicrobial agents have been considered an alarming threat to global health. To mitigate these issues, many researchers have focused on plant-derived products such as propolis. Herein, the antibacterial activity against several MDR pathogens has been reported. It was found that PEEG possessed the highest antimicrobial activity against several MDR strains. Furthermore, the antibiofilm and anti-quorum sensing activities of both extracts make them of considerable interest because they can disrupt microbial virulence factors and thus demonstrate efficacy against microbial resistance. According to the antioxidant activity results, both samples exhibited appreciable antioxidant activity, proving that propolis can eliminate the harmful effects of free radicals. Overall, these findings indicate that propolis could be used as an alternative remedy for severe pathology related to microbial resistance and oxidative stress. However, further analyses are needed to elucidate the main active compounds and mechanisms responsible for the different biological activities of propolis.

Acknowledgments

We would like to express our deepest gratitude to Prof. Mehmet Öztürk and Prof. Özgür Ceylan from the University of Muğla Sıtkı Koçman University, Türkiye, for the material support provided and for offering a collaborative and conductive platform for the current research. A further acknowledgment and recognition goes to the staff members of the biotechnology research center, Constantine, especially Dr. Chawki Bensouici, for his generous support and unconditional assistance to the study.

Ethics

Ethics Committee Approval: Not applicable, there are no researches conducted on animals or humans.

Informed Consent: Not required.

Authorship Contributions

Concept: W.H., A.Z., Design: W.H., A.Z., Data Collection or Processing: W.H., A.Z., M.M., C.B., Analysis or Interpretation: M.Ö., Ö.C., W.H., Literature Search: A.Z., Writing: N.G., W.H., A.Z.

Conflict of Interest: No conflict of interest was declared by the authors.

Financial Disclosure: This research was funded by the Ministry of Higher Education and Scientific Research, Algeria, through Doctoral Mobility Short Program 2019.

REFERENCES

1. Atanasov AG, Zotchev SB, Dirsch VM. International natural product sciences taskforce; supuran CT. Natural products in drug discovery: advances and opportunities. Nat Rev Drug Discov. 2021;20:200-216.
2. Wieczorek PP, Hudz N, Yezerska O, Horčinová-Sedláčková V, Shanaida M, Korytniuk O, Jasicka-Misiak I. Chemical variability and pharmacological potential of propolis as a source for the development of new pharmaceutical products. Molecules. 2022;27:1600.
3. Zulhendri F, Chandrasekaran K, Kowacz M, Ravalia M, Kripal K, Fearnley J, Perera CO. Antiviral, antibacterial, antifungal, and antiparasitic properties of propolis: a review. Foods. 2021;10:1360.
4. Minarini LADR, de Andrade LN, de Gregorio E, Grosso F, Naas T, Zarrilli R, Camargo ILBC. Editorial: antimicrobial resistance as a global public health problem: how can we address it? Front Public Health. 2020;8:612844.
5. Jiang H, Luan Z, Fan Z, Wu X, Xu Z, Zhou T, Wang H. Antibacterial, antibiofilm, and antioxidant activity of polysaccharides obtained from fresh sarcotesta of *Ginkgo biloba*: bioactive polysaccharide that can be exploited as a novel biocontrol agent. Evid Based Complement Alternat Med. 2021;2021:5518403.
6. Iskandar K, Murugaiyan J, Hammoudi Halat D, Hage SE, Chibabhai V, Adukkadukkam S, Roques C, Molinier L, Salameh P, van Dongen M. Antibiotic discovery and resistance: the chase and the race. Antibiotics (Basel). 2022;11:182.
7. Sharifi-Rad M, Anil Kumar NV, Zucca P, Varoni EM, Dini L, Panzarini E, Rajkovic J, Tsouh Fokou PV, Azzini E, Peluso I, Prakash Mishra A, Nigam M, El Rayess Y, Beyrouthy ME, Polito L, Iriti M, Martins N, Martorell M, Docea AO, Setzer WN, Calina D, Cho WC, Sharifi-Rad J. Lifestyle, oxidative stress, and antioxidants: back and forth in the pathophysiology of chronic diseases. Front Physiol. 2020;11:694.
8. Mahmoud AM, Wilkinson FL, Sandhu MA, Lightfoot AP. The interplay of oxidative stressand inflammation: mechanistic insights and therapeutic potential of antioxidants. Oxid Med Cell Longev. 2021;2021:9851914.

9. Singleton VL, Rossi JA. Colorimetry of total phenolics with phosphomolybdic-phosphotungstic acid reagents. Am J Enol Vitic. 1965;16:144-158.
10. Topçu G, Ay M, Bilici A, Sarıkürkçü C, Öztürk M, Ulubelen A. A new flavone from antioxidant extracts of *Pistacia terebinthus*. Food Chem. 2007;103:816-822.
11. Blois MS.Antioxidant determinations by the use of a stable free radical. Nature. 1958;181:1199-1200.
12. Apak R, Güçlü K, Ozyürek M, Karademir SE. Novel total antioxidant capacity index for dietary polyphenols and vitamins C and E, using their cupric ion reducing capability in the presence of neocuproine: CUPRAC method. J Agric Food Chem. 2004;52:7970-7981.
13. Oyaizu M. Studies on products of browning reaction antioxidative activities of products of browning reaction prepared from glucosamine. Jap J Nutr Diet. 1986;44:307-315.
14. Re R, Pellegrini N, Proteggente A, Pannala A, Yang M, Rice-Evans C. Antioxidant activity applying an improved ABTS radical cation decolorization assay. Free Radic Biol Med. 1999;26:1231-1237.
15. Shi H, Noguchi N, Niki E. Galvinoxyl method for standardizing electron and proton donation activity. Methods Enzymol. 2001;335:157-166.
16. Szydłowska-Czerniak A, Dianoczki C, Recseg K, Karlovits G, Szłyk E. Determination of antioxidant capacities of vegetable oils by ferric-ion spectrophotometric methods. Talanta. 2008;76:899-905.
17. Magina MD, Dalmarco EM, Wisniewski A Jr, Simionatto EL, Dalmarco JB, Pizzolatti MG, Brighente IM. Chemical composition and antibacterial activity of essential oils of *Eugenia* species. J Nat Med. 2009;63:345-350.
18. O'Toole GA. Microtiter dish biofilm formation assay. J Vis Exp. 2011;2437.
19. Choo JH, Rukayadi Y, Hwang JK. Inhibition of bacterial quorum sensing by vanilla extract. Lett Appl Microbiol. 2006;42:637-641.
20. Koh KH, Tham FY. Screening of traditional Chinese medicinal plants for quorum-sensing inhibitors activity. J Microbiol Immunol Infect. 2011;44:144-148.
21. Belfar ML, Lanez T, Rebiai A, Ghiaba Z. Evaluation of antioxidant capacity of propolis collected in various areas of Algeria using electrochemical techniques. Int J Electrochem Sci. 2015;10:9641-9651.
22. Nedji N, Loucif-Ayad W. Antimicrobial activity of Algerian propolis in foodborne pathogens and its quantitative chemical composition. Asian Pacific J Trop Dis. 2014;4:433-437.
23. Shehata MG, Ahmad FT, Badr AN, Masry SH, El-Sohaimy SA. Chemical analysis, antioxidant, cytotoxic and antimicrobial properties of propolis from different geographic regions. Ann Agric Sci. 2020;65:209-217.
24. Bouaroura A, Segueni N, Diaz JG, Bensouici C, Akkal S, Rhouati S. Preliminary analysis of the chemical composition, antioxidant and anticholinesterase activities of Algerian propolis. Nat Prod Res. 2020;34:3257-3261.
25. Boulechfar S, Zellagui A, Bensouici C, Asan-Ozusaglam M, Tacer S, Hanene D. Anticholinesterase, anti-α-glucosidase, antioxidant and antimicrobial effects of four Algerian propolis. J Food Meas Charact. 2022;16:793-803.
26. Ecem Bayram N, Gerçek YC, Bayram S, Toğar B. Effects of processing methods and extraction solvents on the chemical content and bioactive properties of propolis. J Food Meas Charact. 2020;14:905-916.
27. Piccinelli AL, Mencherini T, Celano R, Mouhoubi Z, Tamendjari A, Aquino RP, Rastrelli L. Chemical composition and antioxidant activity of Algerian propolis. J Agric Food Chem. 2013;61:5080-5088.
28. Narimane S, Demircan E, Salah A, Ozcelik BÖ, Salah R. Correlation between antioxidant activity and phenolic acids profile and content of Algerian propolis: influence of solvent. Pak J Pharm Sci. 2017;30(4 Suppl):1417-1423.
29. Daikh A, Segueni N, Dogan NM, Arslan S, Mutlu D, Kivrak I, Akkal S, and Rhouati S. Comparative study of antibiofilm, cytotoxic activity and chemical composition of Algerian propolis. J Apic Res. 2019;59:1-10.
30. Alday-Provencio S, Diaz G, Rascon L, Quintero J, Alday E, Robles-Zepeda R, Garibay-Escobar A, Astiazaran H, Hernandez J, Velazquez C. Sonoran propolis and some of its chemical constituents inhibit *in vitro* growth of *Giardia lamblia* trophozoites. Planta Med.2015;81:742-747.
31. Kubina R, Kabała-Dzik A, Dziedzic A, Bielec B, Wojtyczka RD, Bułdak RJ, Wyszyńska M, Stawiarska-Pięta B, Szaflarska-Stojko E. The ethanol extract of polish propolis exhibits anti-proliferative and/or pro-apoptotic effect on HCT 116 colon cancer and Me45 malignant melanoma cells *in vitro* conditions. Adv Clin Exp Med. 2015;24:203-212.
32. Mandim F, Dias MI, Pinela J, Barracosa P, Ivanov M, Stojković D, Soković M, Santos-Buelga C, Barros L, Ferreira ICFR. Chemical composition and *in vitro* biological activities of cardoon (*Cynara cardunculus* L. var. *altilis* DC.) seeds as influenced by viability. Food Chem. 2020;323:126838.
33. Issasfa B, Benmansour T, Valle V, Boukhatem M, Bouakba M. Contribution à l'étude ducomportement mécanique des matériaux bio-sourcés de type composite (*Cynara cardunculus*/polyester). 2015.
34. Hachem K, Bokov D, Mahdavian L. Antioxidant capacity of caffeic acid phenethyl ester in scavenging free radicals by a computational insight. Polycycl Aromat Compd. 2022;43:1-18.
35. Jun M, Fu HY, Hong J, Wan X, Yang CS, Ho CT. Comparison of antioxidant activities of isoflavonesfrom kudzu root (*Pueraria lobata* Ohwi). J Food Sci. 2003;68:2117-2122.
36. Aydın B, Yuca H, Karakaya S, Bona GE, Göger G, Tekman E, Şahin AA, Sytar O, Civas A, Canlı D, Pınar NM, Guvenalp Z. The anatomical, morphological features, and biological activity of *Scilla siberica* subsp. *armena* (Grossh.) Mordak (Asparagaceae). Protoplasma. 2023;260:371-389.
37. Daragmeh J, Imtara H. *In vitro* evaluation of Palestinian propolis as a natural product with antioxidant properties and antimicrobial activity against multidrug-resistant clinical isolates. J Food Qual. 2020;2020:1-10.
38. Nichitoi MM, Josceanu AM, Isopescu RD, Isopencu GO, Geana EI, Ciucure CT, Lavric V. Polyphenolics profile effects upon the antioxidant and antimicrobial activity of propolis extracts. Sci Rep. 2021;11:20113.
39. Zhu X, Zhang H, Lo R. Phenolic compounds from the leaf extract of artichoke (*Cynara scolymus* L.) and their antimicrobial activities. J Agric Food Chem. 2004;52:7272-7278.
40. Ristivojević P, Trifković J, Andrić F, Milojković-Opsenica D. Poplar-type propolis: chemical composition, botanical origin and biological activity. Nat Prod Commun. 2015;10:1869-1876.
41. Kart D, Kuştimur AS. Investigation of gelatinase gene expression and growth of *Enterococcus faecalis* clinical isolates in biofilm models. Turk J Pharm Sci. 2019;16:356-361.

42. Santos PBDRED, Ávila DDS, Ramos LP, Yu AR, Santos CEDR, Berretta AA, Camargo SEA, Oliveira JR, Oliveira LD. Effects of Brazilian green propolis extract on planktonic cells and biofilms of multidrug-resistant strains of *Klebsiella pneumoniae* and *Pseudomonas aeruginosa*. Biofouling. 2020;36:834-845.

43. Slobodníková L, Fialová S, Rendeková K, Kováč J, Mučaji P. Antibiofilm activity of plant polyphenols. Molecules. 2016;21:1717.

44. Tamfu AN, Kucukaydin S, Ceylan O, Sarac N, Duru ME. Phenolic composition, enzyme inhibitory and anti-quorum sensing activities of cinnamon (*Cinnamomum zeylanicum* Blume) and basil (*Ocimum basilicum* Linn). Chem Africa. 2021;4:759-767.

45. Sorucu A, Ceylan Ö. Determination of antimicrobial and anti-quorum sensing activities ofwater and ethanol extracts of propolis. Ankara Univ Vet Fak Derg. 2021;68:373-381.

46. Nazzaro F, Fratianni F, Coppola R. Quorum sensing and phytochemicals. Int J Mol Sci. 2013;14:12607-12619.

47. Savka MA, Dailey L, Popova M, Mihaylova R, Merritt B, Masek M, Le P, Nor SR, Ahmad M, Hudson AO, Bankova V. Chemical composition and disruption of quorum sensing signaling in geographically diverse United States propolis. Evid Based Complement Alternat Med. 2015;2015:472593.

48. Asfour HZ. Anti-quorum sensing natural compounds. J Microsc Ultrastruct. 2018;6:1-10.

Turk J Pharm Sci 2024;21(1):81-86
DOI: 10.4274/tjps.galenos.2023.87450

ORIGINAL ARTICLE

Investigation of the Expression of CYP3A4 in Diabetic Rats in Xenobiotic Metabolism

Naile Merve GÜVEN[1,2], İrem KARAÖMERLİOĞLU[3], Ebru ARIOĞLU İNAN[4], Benay CAN EKE[1]*

[1]Ankara University, Faculty of Pharmacy, Department of Pharmaceutical Toxicology, Ankara, Türkiye
[2]Ankara University, Graduate School of Health Sciences, Ankara, Türkiye
[3]Turkish Medicines and Medical Devices Agency, Ankara, Türkiye
[4]Ankara University, Faculty of Pharmacy, Department of Pharmacology, Ankara, Türkiye

ABSTRACT

Objectives: This study investigated the impact of a high-fat diet streptozotocin (STZ)-induced diabetes and dapagliflozin treatment on hepatic protein expression of CYP3A4.

Materials and Methods: In our study, 34 male Sprague-Dawley rats were randomly divided into four groups: Control, high-fat diet and STZ-induced diabetes, dapagliflozin-treated control, and dapagliflozin-treated diabetes. In the microsomes obtained from the livers of these rats, the protein expression levels of CYP3A4 were determined by Western blotting.

Results: Hepatic CYP3A4 protein expression levels in the control group treated with dapagliflozin were significantly decreased compared with those in the control group. In addition, hepatic CYP3A4 protein expression levels were decreased in dapagliflozin-treated diabetic Sprague-Dawley rats compared with those in both control and diabetic group rats, but the difference between the groups was not statistically significant.

Conclusion: According to these two results, the use of dapagliflozin inhibited hepatic CYP3A4 protein expression.

Keywords: CYP3A4, dapagliflozin, diabetes mellitus, microsome, protein expression

INTRODUCTION

Cytochrome P450 monooxygenases (CYP450), a superfamily of heme-containing proteins, are responsible for the biotransformation of a vast majority of both endobiotics and xenobiotics by converting these lipophilic compounds into their hidrophilic forms.[1,2] More than 95% of available pharmaceuticals used clinically are metabolized by CYP1A2, CYP2C9, CYP2C19, CYP2D6, CYP2E1, and CYP3A4. Different CYP450s, which have varying degrees of abundance in the smooth endoplasmic reticulum of the human hepatocyte, have been determined to be 13% CYP1A2, 4% CYP2A6, 1% CYP2B6, 20% CYP2C, 2% CYP2D6, 7% CYP2E1, and 30% CYP3A4.[3] CYP3A4 is a major CYP450 enzyme that particularly mediates biotransformation of approximately 50% of marketed drugs, including benzodiazepines (alprazolam, diazepam, and midazolam), calcium channel blockers (amlodipine, diltiazem, and verapamil), immunosuppressives (cyclosporine, tacrolimus, and sirolimus), macrolide antibiotics (clarithromycin, erythromycin), and statins (atorvastatin, simvastatin). Along with many medications, CYP3A4 also catalyzes the metabolism of several endogenous molecules such as steroids (estradiol, progesterone, testosterone) and vitamin D.[4,5] CYP3A4 is also responsible for inactivating aflatoxin B1, which is an environmental carcinogen.[6] A high level of CYP3A4 gene expression is found in the liver of humans. In addition, extrahepatic tissues expressing CYP3A4 include the prostate, breast, intestine, colon, small intestine, and brain.[7]

Diabetes mellitus (DM) is a heterogeneous group of diseases characterized by hyperglycemia due to an absolute or relative deficiency of insulin secretion and/or action. Hyperglycemia associated with DM, which is a chronic disease, damages the heart, blood vessels, eyes, kidneys, and nerves.[8] There are two

*Correspondence: eke@pharmacy.ankara.edu.tr, Phone: +90 312 203 31 15, ORCID-ID: orcid.org/0000-0001-9817-9034
Received: 22.02.2023, Accepted: 30.04.2023

main types of DM: type 1 and type 2. Type 1 DM (T1DM), an autoimmune disease, results from a lack of insulin production caused by damage to pancreatic beta cells. Type 2 DM (T2DM) has three characteristic features: insulin resistance, beta cell secretory dysfunction, and increased production of hepatic glucose.[9,10] The consequences of DM, which is a treatable disease, can be prevented or delayed by diet, physical activity, medications, regular screening, and treatment for complications.[11] Dapagliflozin, chosen as an antidiabetic agent in our study, is a medicine used in the management of T2DM by selectively inhibiting sodium-glucose co-transporter 2 (SGLT2), thus preventing the reabsorption of glucose from the urine. In January 2014, the United States Food and Drug Administration approved its use in combination with diet and exercise to treat adult T2DM patients by providing glycemic control. According to the results of some *in vitro* studies examining the relationship between dapagliflozin metabolism and CYP450 enzymes, dapagliflozin metabolism can be catalyzed by CYP1A1, CYP1A2, CYP2A6, CYP2C9, CYP2D6, and CYP3A4.[12,13] Sprague-Dawley rats with T2DM induced by a combination of a high-fat diet and STZ were used in our study. High-fat diet leads to insulin resistance in rats. In addition, treatment with STZ contributes to beta cell dysfunction. Namely, co-administration of a high-fat diet and STZ creates the metabolic profile observed in humans who suffer from T2DM.[14]

Various components influence the expression of each CYP450, including genetic polymorphisms, xenobiotics, cytokines, hormones, disease states, sex, age, and others.[15] Factors that induce CYP3A4 include a wide variety of medicines such as antiandrogens, antibiotics, antiemetics, antiepileptics, antineoplastic agents, antipyretic analgesics antiretroviral barbiturates, cystic fibrosis medications, glucocorticoid, retinoid receptor modulators, steroidogenesis inhibitors, kinase inhibitors, and different types of herbal compounds such as ginkgolide A and B, hyperforin, and quercetin. Moreover, dichlorodiphenyltrichloroethane and endrin, which are organochlorine pesticides, as well as ethanol have been associated with CYP3A4 induction.[16] The induction of CYP3A4 by different exogenous substances, which upregulate gene transcription by binding to the pregnan X receptor or constitutive androstane receptor, is an important factor regulating its expression.[17] The activity and expression level of the CYP3A4 enzyme has also been associated with environmental factors such as diet and xenobiotic exposure. Because CYP3A4 is widely distributed throughout the intestinal mucosa, CYP3A4 enzyme levels are affected by fasting symptoms and are increased during starvation. There is a gender-specific difference in CYP3A4 induction in humans. Studies have shown that women are more likely to have a higher CYP3A4 metabolism rate.[18]

Among the factors mentioned above, DM can modulate CYP450 enzyme levels, drug metabolism, and drug response. Moreover, patients with DM often require pharmaceutical therapy more frequently than healthy individuals. For these two reasons, it is important to understand how DM affects the biotransformation of endogenous and exogenous compounds.[19,20] The effects of both types of diabetes on CYP450 enzyme expression and activity have been shown in different human samples, experimental animal models, and cell lines. A number of xenobiotic-metabolizing enzymes are affected by DM, including CYP1A1, CYP1B1, CYP2B1, CYP2B4, CYP2C6, CYP2C11, CYP2C23, CYP2E1, CYP3A1, CYP3A4, CYP3A11, CYP3A5, CYP7A1.[21-28] However, the number of studies examining the effects of DM on CYP3A4 protein expression is limited. Researchers found that the levels of CYP3A4 proteins and catalytic activity were significantly reduced by DM.[28] T2DM is acknowledged as a chronic condition characterized by low inflammation. In patients with T2DM, certain cytokines are associated with changes in CYP450 enzyme expression levels and/or activity. There is a correlation between T2DM and increased levels of inflammatory markers, especially interleukin-6 and tumor necrosis factor-alpha. Many drug-metabolizing enzymes, particularly CYP450 enzymes in the CYP3A subfamily, are downregulated in response to higher levels of interleukin-6 and tumor necrosis factor-alpha.[29] In contrast to these findings, another study showed that both T1DM and T2DM significantly increased hepatic CYP3A expression.[30] CYP3A4 enzyme inhibition and/or induction increases the risk of undesirable drug-drug interactions and subsequent drug toxicity. Because CYP3A4 is the main and most important enzyme involved in the metabolism of more than half of the drugs prescribed and administered, it is thought that this may be the principal cause for clinical failures and withdrawal of marketed drugs.[31]

Our study aimed to understand the alteration of CYP3A4 expression under diabetic conditions. For this purpose, CYP3A4 hepatic expression was investigated in liver microsomes obtained from control, high-fat diet, STZ-induced diabetes, dapagliflozin-treated control, and dapagliflozin-treated diabetes Sprague-Dawley rats using Western blot.

MATERIALS AND METHODS

Animals and study design

Four to five-week-old male Sprague-Dawley rats (100-150 g) were obtained from Bilkent University, Genetics and Biotechnology Research Center (Ankara, Türkiye). The rats were housed with 2 or 3 rats in each cage and maintained on a 12 hours light/dark cycle at constant room temperature (22 ± 1 °C) with tap water and standard rat chow (Purina) *ad libitum*. One week after quarantine, rats were given either standard chow or a high-fat diet (35% fat; Arden Research & Experiment) during the rest of the experiment. Rats in the control group received only citrate buffer (pH: 4.5) intraperitoneally. After another 4-5 weeks, diabetes was induced, followed by a single-dose injection of STZ (25 mg/kg; *i.p.*) dissolved in citrate buffer (0.1 N; pH 4.5) in rats fed a high-fat diet. After 72 hours of STZ injection, blood glucose levels were evaluated for each rat from the tail. A second or third STZ injection was administered to animals whose blood glucose levels were <200 and <140 mg/dL. Rats were accepted as diabetic when their blood glucose level was higher than 140 mg/dL. After diabetes had been established, half of the control and diabetic group rats

were orally administered 1 mg/kg/day of dapagliflozin for 12 weeks. Dapagliflozin suspension was prepared by pulverizing Forziga® tablets (10 mg as 12.3 mg dapagliflozin propanediol monohydrate) and then dissolving them in distilled water. Among the pharmaceutically inactive ingredients in the tablets were microcrystalline cellulose, anhydrous lactose, crospovidone, silicon dioxide, and magnesium stearate. They are coated with polyvinyl alcohol, titanium dioxide, polyethylene glycol, talc, and yellow iron oxide. Thus, the animals were divided into four groups: Control (n= 10), diabetic rats (n= 6), control rats treated with dapagliflozin (n= 10), and diabetic rats treated with dapagliflozin (n= 8). All animal procedures were performed in accordance with the guidelines of the Ankara University Animal Care and Use Committee (14.03.2018/2018-6-45).

Preparation of microsomes

Twelve weeks after treatment, rats were sacrificed under anesthesia. Liver tissue was rapidly excised, weighed, and preserved at -80 ˚C until use. Liver tissues (approximately 1.5 g) were homogenized in a Potter Elvehjem homogenizer using 1.15% potassium chloride (*w/v*) (Sigma-Aldrich) at 3000 rpm in an ice-cold bath. The homogenate was then centrifuged at 11,000 g for 25 min. The supernatant fractions were centrifuged again at 108,000 g for 60 min. After ultracentrifugation, microsomal pellets were resuspended in 20% glycerol (Sigma-Aldrich), and microsomal fractions were stored at -80 ˚C.

Western blotting

Protein levels of CYP3A4 were assessed by western blotting. First, the total protein content was measured using the BCA Protein Assay Kit (Pierce). Samples were heated with sample buffer (Sigma-Aldrich) at 70 ˚C for 5 minutes to denature the protein. 30 µg of samples were loaded onto a 10% SDS-PAGE gel. Proteins were separated using electrophoresis conducted at 100 V for approximately 2 hours. In the following gel electrophoresis, separated proteins were transferred onto nitrocellulose membranes (Biorad) *via* the wet transfer method at 100 V for 2 hours. After transfer, the membranes were blocked with 5% BSA (Sigma-Aldrich) in Tris-buffered saline containing Tween 20 (Sigma-Aldrich) at room temperature for 1 hour. The membranes were then incubated with primary antibody (Abcam; 1:5000 dilution) at 4 ˚C overnight. Horseradish peroxidase-conjugated goat anti-rabbit immunoglobulin G (Advansta; 1:5000 dilution) was used as the secondary antibody. Detection of specific bands was performed by chemiluminescence using an ECL reagent (Advansta). Imaging was conducted using the Li-Cor Odyssey imaging system. Beta-actin (Biolegend; 1/2000 dilution) was used as a loading control to normalize the density of each band.

Statistical analysis

All statistical analyses were performed using the Statistical Package for the Social Sciences (SPSS, version 25). The Shapiro-Wilk test was used to check the normal distribution of all variables. Statistically significant differences between groups were analyzed using a one-way analysis of variance, followed by a *post*-hoc least significant difference test. The data are expressed as mean, standard error, and standard deviation. A $p < 0.05$ was considered statistically significant.

RESULTS

Blood glucose levels and body weight of the animals

Diabetic rats exhibited statistically significantly higher blood glucose levels, as compared with rats of control and treatment groups ($p < 0.05$). The body weight of the dapagliflozin-treated control group was found to be statistically significantly lower than that of the control group ($p < 0.05$). Body weights of the dapagliflozin-treated control group were lower than those of the diabetes and dapagliflozin-treated diabetes groups. However, no statistically significant difference in body weight was found between the dapagliflozin-treated control group and each of the diabetes and dapagliflozin-treated diabetes groups ($p > 0.05$). Data on blood glucose levels and body weights at the time of death are indicated in Table 1.

CYP3A4 protein levels in the livers of animals

The protein expression level of CYP3A4 in dapagliflozin-treated rats was statistically significantly decreased compared with the control rats ($p < 0.05$). In addition, the hepatic CYP3A4 protein expression level in the high-fat diet and STZ-induced diabetes group was lower than that in the control group. Still, the difference between these two groups was not statistically significant ($p > 0.05$). It was also reported that CYP3A4 protein expression levels of rats placed in dapagliflozin-treated diabetes were lower than those of the control and diabetes groups, but higher than those of the dapagliflozin-treated control group. Still, the difference between groups was not statistically significant ($p > 0.05$). Protein expression bar graphs and representative protein bands for each group are given in Figures 1 and 2.

DISCUSSION

DM is a metabolic disease characterized by insufficient benefit of organisms from carbohydrates, lipids, and proteins and hyperglycemia caused by defects in insulin secretion, insulin effect, or both. DM has been demonstrated to regulate protein expression of the CYP450 enzyme. Alterations in the expression of CYP450 enzymes are associated with changes in metabolism caused by diabetes (increased ketone bodies,

Table 1. Blood glucose levels and body weights at the time of death for each group of animals

	Control	Diabetes	Dapagliflozin-treated control	Dapagliflozin treated diabetes
Body weight (g)	430.2 ± 7.374	410.67 ± 18.204	303.3 ± 55.059*	418.75 ± 7.343
Blood glucose levels (mg/dL)	100.2 ± 2.149	233.67 ± 54.769$^{\Delta}$	98.7 ± 2.135	129 ± 12.186

Significant changes are expressed as *($p < 0.05$; One-Way ANOVA, *post*-hoc-LSD) compared with the control group, $^{\Delta}$($p < 0.05$; One-Way ANOVA, *post*-hoc-LSD) compared with the control and treatment groups, LSD: Least significant difference test

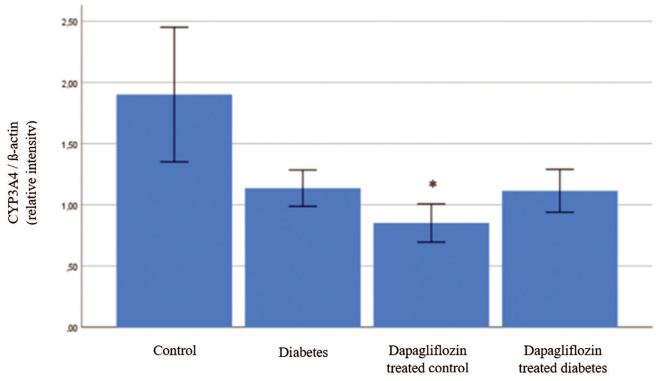

Figure 1. Hepatic CYP3A4 protein expression levels for each animal group. Significant changes are expressed as *($p < 0.05$; One-Way ANOVA, post-hoc-LSD) compared with the control group, LSD: Least significant difference test

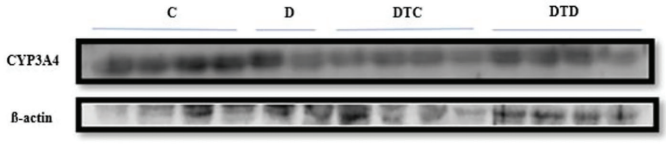

Figure 2. Western blot images of protein/loading control for each group
C: Control; D: Diabetes, DTC: Dapagliflozin-treated control, DTD: Dapagliflozin-treated diabetes

lipids, and carbohydrates) and regulation of some hormones such as insulin, and glucagon. Research has reported that the protein expression of CYP3A4, which is one of the most important enzymes in the processes of biotransformation, is affected by DM. Considering this information, our study has several implications. First, it shows that diabetes downregulates CYP3A4 protein expression in the rat liver microsome. This result was consistent with a previous study, which revealed that the CYP3A4 hepatic expression level was significantly lower in diabetic human liver microsomes. The same study also showed that there was no significant difference in CYP3A5 protein levels between diabetic and non-diabetic individuals.[28] However, little is known about how CYP3A5 protein expression is affected in rat liver microsomes under diabetic conditions. Changes caused by DM in metabolic processes, such as elevations in ketone bodies, lipids, and carbohydrates, as well as hormonal regulation, such as insulin, glucagon, leptin, and growth hormone, may influence hepatic CYP450 expression.[32] Different opinions have been suggested regarding the mechanism of decreased CYP3A4 hepatic expression in individuals with DM. These mechanisms include the effects of pro-inflammatory cytokines, non-cytokinin components, oxidative stress, and obesity. It has been reported that elevated levels of cytokines (interleukin-1ß, interleukin-6, and tumor necrosis factor alpha) contribute to a decrease in CYP3A4 enzyme expression in individuals with DM.[28] In addition, another study suggested that the protein level and activity of CYP3A4 were reduced in liver microsomes of DM and non-alcoholic fatty liver disease patients. Contrary to these results, it was demonstrated that the induction activity and upregulated protein level of CYP3A4 were found in HepG2 cells incubated with serum from rats developing diabetes with STZ. Based on the results of the study, AMP-activated protein kinase, protein kinase C (PKC), and nuclear factor kappa B pathways were most likely involved in oleic acid-induced CYP3A4 activity, whereas PKC might be involved in palmitic acid-induced activity.[33] Similar to the results of the previous study, markedly increased hepatic CYP3A protein levels were determined in both STZ-induced T1DM and db/db T2DM mice. Although there are differences in their pathophysiology, these two diseases seem to have the same modulating effect on CYP3A expression.[30] When all these results are considered together, it seems that CYP3A4 protein expression and activity are modulated differently by DM in human samples, diabetic animal models, and cell cultures. A disruption of CYP3A4 protein expression and activity associated with DM may alter the xenobiotic elimination half-life and bioavailability, efficacy, and safety of CYP3A4 substrates. A second important implication of our study is that the hepatic CYP3A4 protein expression level of dapagliflozin-treated control rats was found to be significantly lower than that of the control group. Based on this result, the use of dapagliflozin is most likely to inhibit hepatic CYP3A4 protein expression. Therefore, drugs that are CYP3A4 substrates, such as acetaminophen, lovastatin, diltiazem, and vardenafil, should be used with caution in patients with DM using dapagliflozin.[34] According to rat, dog, monkey, and human liver microsomal studies, dapagliflozin undergoes oxidative metabolism. Various human CYP450 enzymes metabolized dapagliflozin *in vitro*, and the highest metabolism was attributed to the enzymes CYP2D6, CYP1A2, CYP3A4, CYP2C9, CYP1A2, CYP3A5, and CYP2E1 in the order of highest to lowest.[35] According to this information and the results obtained from our study, inhibition of the hepatic expression of CYP3A4, which is involved in the metabolism of dapagliflozin, by dapagliflozin may also cause a decrease in the biotransformation of the aforementioned drug. In a study in which STZ-induced T1DM rats, it was found that combining dapagliflozin with a low dose of insulin stabilizes CYP1A, CYP2D, CYP2E, and CYP3A activities.[36] In addition, blood glucose levels and body weights at the time of death were measured for each group of animals. Blood glucose levels in diabetic rats were significantly higher than those in control and dapagliflozin-treated control rats. Accordingly, it was demonstrated that the STZ-induced DM model was confirmed. Body weights were found to be statistically significantly lower in the dapagliflozin-treated control group than in the control group. The mechanism of action of dapagliflozin is glucose excretion, suggesting that it may have decreased body weight in the treated groups.

Our study reported the effect of DM on CYP3A4 expression in rat liver, but the impact of DM on CYP3A4 enzymatic activity and/or mRNA level is still needed to be studied. In addition, the mechanism behind this decrease in CYP3A4 expression has yet to be clarified in our study. Further research is required to shed light on these issues. To the best of our knowledge, this study is the first to investigate the effect of dapagliflozin on CYP3A4 expression. Therefore, it is essential to support our study by designing studies in which the number of animals

is increased and the relationship between dapagliflozin and CYP3A4 expression in different species of experimental animals is evaluated. Our study was performed exclusively on male rats. However, the impact of the gender factor should also be assessed in other studies involving female rats. Moreover, the effect of STZ administration on CYP3A4 expression in early and late applications can be evaluated. When the studies are examined, it is seen that the antidiabetic agent whose effect on CYP450 expression and activity is investigated is generally insulin. Therefore, it is important to design studies that examine the effect of antidiabetic agents other than insulin on CYP450 enzyme expression. Research on the expression of other CYP450 enzymes involved in dapagliflozin metabolism in addition to CYP3A4 in diabetic conditions will also be complementary to our study.

CONCLUSION

The findings of our study showed that hepatic CYP3A4 protein expression levels in the control group treated with dapagliflozin were significantly decreased compared with those in the control group. Besides, we reported that hepatic CYP3A4 protein expression levels were decreased in dapagliflozin-treated diabetic Sprague-Dawley rats compared with those in both control and diabetic group rats. But, the difference between groups was not statistically significant. According to these two results, the use of dapagliflozin inhibited hepatic CYP3A4 protein expression. This result was consistent with the data of two previous studies. Another important conclusion of our study was regarding the physical and biochemical characteristics of rats. Blood glucose levels of both control and dapagliflozin-treated control groups were lower than those of the diabetes and dapagliglozin-treated diabetes groups, but this difference was not statistically significant. On the other hand, blood glucose levels of diabetic rats were found to be significantly higher than those of the control and administration groups. Accordingly, the control of the DM model induced by STZ and a high-fat diet was provided. Body weights of the dapagliflozin-treated control group at the time of death were lower than those of the diabetes and dapagliglozin-treated diabetes groups, but this difference was not statistically significant. Moreover, body weights at the time of death were found to be statistically significantly lower in rats of the dapagliflozin-treated control group than in rats of the control group. According to these data, a significant decrease in body weight of dapagliflozin-treated control rats was associated with the mechanism of action of dapagliflozin, leading to the excretion of urinary glucose. Finally, we showed for the first time the impact of dapagliflozin treatment on hepatic CYP3A4 protein expression levels. CYP3A4 metabolically processes many clinically used drugs, including dapagliflozin and endogenous substances. Diabetic conditions, complications related to diabetes, and antidiabetic agents are among the factors that play a role in regulating CYP3A4 protein expression. Therefore, it is necessary to design studies that examine the relationship between these factors and CYP3A4 protein expression.

Ethics

Ethics Committee Approval: All procedures used in this study were approved by the Ankara University Local Ethics Committee for Animal Experiments (2018-6-45).

Informed Consent: Not required.

Authorship Contributions

Surgical and Medical Practices: E.A.I., I.K., Concept: N.M.G., B.C.E., Design: N.M.G., B.C.E., Data Collection or Processing: N.M.G., B.C.E., Analysis or Interpretation: N.M.G., B.C.E., Literature Search: N.M.G., B.C.E., Writing: N.M.G., B.C.E.

Conflict of Interest: No conflict of interest was declared by the authors.

Financial Disclosure: This study was financially supported by Scientific Research Projects (BAP) of Ankara University (18L0237010).

REFERENCES

1. Kiani YS, Jabeen I. Lipophilic Metabolic efficiency (LipMetE) and drug efficiency indices to explore the metabolic properties of the substrates of selected cytochrome P450 isoforms. ACS Omega. 2019;5:179-188.
2. Rourke JL, Sinal CJ. Biotransformation/metabolism. In: Wexler P, ed. Encyclopedia of Toxicology (3rd ed). Cambridge; Academic Press; 2014:490-502.
3. Jin SE, Ha H, Seo CS, Shin HK, Jeong SJ. Expression of cytochrome P450s in the liver of rats administered with socheongryong-tang, a traditional herbal formula. Pharmacogn Mag. 2016;12:211-218.
4. Bauters T. Clinically relevant drug interactions in HSCT. In: Carreras E, Dufour C, Mohty M, Kröger N, eds. The EBMT Handbook: Hematopoietic Stem Cell Transplantation and Cellular Therapies. (7th ed). Cham (CH); Springer; 2019: Chapter 31.
5. Thummel KE. Gut instincts: CYP3A4 and intestinal drug metabolism. J Clin Invest. 2007;117:3173-3176.
6. Martínez-Jiménez CP, Jover R, Donato MT, Castell JV, Gómez-Lechón MJ. Transcriptional regulation and expression of CYP3A4 in hepatocytes. Curr Drug Metab. 2007;8:185-194.
7. Wei Z, Jiang S, Zhang Y, Wang X, Peng X, Meng C, Liu Y, Wang H, Guo L, Qin S, He L, Shao F, Zhang L, Xing Q. The effect of microRNAs in the regulation of human CYP3A4: a systematic study using a mathematical model. Sci Rep. 2014;4:4283.
8. Alam U, Asghar O, Azmi S, Malik RA. General aspects of diabetes mellitus. Handb Clin Neurol. 2014;126:211-222.
9. Steck AK, Rewers MJ. Genetics of type 1 diabetes. Clin Chem. 2011;57:176-185.
10. Shi Z, He Z, Wang DW. CYP450 epoxygenase metabolites, epoxyeicosatrienoic acids, as novel anti-inflammatory mediators. Molecules. 2022;27:3873.
11. World Health Organization (2019). Available from: https://www.who.int/news-room/fact-sheets/detail/diabetes
12. Balakumar P, Sundram K, Dhanaraj SA. Dapagliflozin: glucuretic action and beyond. Pharmacol Res. 2014;82:34-39.
13. Kasichayanula S, Liu X, Lacreta F, Griffen SC, Boulton DW. Clinical pharmacokinetics and pharmacodynamics of dapagliflozin, a selective

inhibitor of sodium-glucose co-transporter type 2. Clin Pharmacokinet. 2014;53:17-27.

14. Gheibi S, Kashfi K, Ghasemi A. A practical guide for induction of type-2 diabetes in rat: Incorporating a high-fat diet and streptozotocin. Biomed Pharmacother. 2017;95:605-613.
15. Zanger UM, Schwab M. Cytochrome P450 enzymes in drug metabolism: regulation of gene expression, enzyme activities, and impact of genetic variation. Pharmacol Ther. 2013;138:103-141.
16. Hakkola J, Hukkanen J, Turpeinen M, Pelkonen O. Inhibition and induction of CYP enzymes in humans: an update. Arch Toxicol. 2020;94:3671-3722.
17. Wolbold R, Klein K, Burk O, Nüssler AK, Neuhaus P, Eichelbaum M, Schwab M, Zanger UM. Sex is a major determinant of CYP3A4 expression in human liver. Hepatology. 2003;38:978-988.
18. Crago J, Klaper RD. Influence of gender, feeding regimen, and exposure duration on gene expression associated with xenobiotic metabolism in fathead minnows (Pimephales promelas). Comp Biochem Physiol C Toxicol Pharmacol. 2011;154:208-212.
19. Yoshinari K, Takagi S, Sugatani J, Miwa M. Changes in the expression of cytochromes P450 and nuclear receptors in the liver of genetically diabetic db/db mice. Biol Pharm Bull. 2006;29:1634-1638.
20. Gravel S, Chiasson JL, Dallaire S, Turgeon J, Michaud V. Evaluating the impact of type 2 diabetes mellitus on CYP450 metabolic activities: protocol for a case-control pharmacokinetic study. BMJ Open. 2018;8:e020922.
21. Oh SJ, Choi JM, Yun KU, Oh JM, Kwak HC, Oh JG, Lee KS, Kim BH, Heo TH, Kim SK. Hepatic expression of cytochrome P450 in type 2 diabetic Goto-Kakizaki rats. Chem Biol Interact. 2012;195:173-179.
22. Arinç E, Arslan S, Bozcaarmutlu A, Adali O. Effects of diabetes on rabbit kidney and lung CYP2E1 and CYP2B4 expression and drug metabolism and potentiation of carcinogenic activity of N-nitrosodimethylamine in kidney and lung. Food Chem Toxicol. 2007;45:107-118.
23. Takatori A, Akahori M, Kawamura S, Itagaki S, Yoshikawa Y. The effects of diabetes with hyperlipidemia on P450 expression in APA hamster livers. J Biochem Mol Toxicol. 2002;16:174-181.
24. Dey A, Williams RS, Pollock DM, Stepp DW, Newman JW, Hammock BD, Imig JD. Altered kidney CYP2C and cyclooxygenase-2 levels are associated with obesity-related albuminuria. Obes Res. 2004;12:1278-1289.
25. Cheng Q, Aleksunes LM, Manautou JE, Cherrington NJ, Scheffer GL, Yamasaki H, Slitt AL. Drug-metabolizing enzyme and transporter expression in a mouse model of diabetes and obesity. Mol Pharm. 2008;5:77-91.
26. Bao LD, Li CQ, Peng R, Ren XH, Ma RL, Wang Y, Lv HJ. Correlation between the decrease of cholesterol efflux from macrophages in patients with type II diabetes mellitus and down-regulated CYP7A1 expression. Genet Mol Res. 2015;14:8716-8724.
27. Raza H, Prabu SK, Robin MA, Avadhani NG. Elevated mitochondrial cytochrome P450 2E1 and glutathione S-transferase A4-4 in streptozotocin-induced diabetic rats: tissue-specific variations and roles in oxidative stress. Diabetes. 2004;53:185-194.
28. Dostalek M, Court MH, Yan B, Akhlaghi F. Significantly reduced cytochrome P450 3A4 expression and activity in liver from humans with diabetes mellitus. Br J Pharmacol. 2011;163:937-947.
29. Darakjian L, Deodhar M, Turgeon J, Michaud V. Chronic inflammatory status observed in patients with type 2 diabetes induces modulation of cytochrome p450 expression and activity. Int J Mol Sci. 2021;22:4967.
30. Patoine D, Petit M, Pilote S, Picard F, Drolet B, Simard C. Modulation of CYP3a expression and activity in mice models of type 1 and type 2 diabetes. Pharmacol Res Perspect. 2014;2:e00082.
31. Sevrioukova IF, Poulos TL. Current approaches for investigating and predicting cytochrome p450 3a4-ligand interactions. Adv Exp Med Biol. 2015;851:83-105.
32. Park SY, Kim CH, Lee JY, Jeon JS, Kim MJ, Chae SH, Kim HC, Oh SJ, Kim SK. Hepatic expression of cytochrome P450 in Zucker diabetic fatty rats. Food Chem Toxicol. 2016;96:244-253.
33. Hu N, Hu M, Duan R, Liu C, Guo H, Zhang M, Yu Y, Wang X, Liu L, Liu X. Increased levels of fatty acids contributed to induction of hepatic CYP3A4 activity induced by diabetes-in vitro evidence from HepG2 cell and Fa2N-4 cell lines. J Pharmacol Sci. 2014;124:433-444.
34. DRUGBANK, Cytochrome P-450 CYP3A4 Substrates. Available from: https://go.drugbank.com/categories/DBCAT002646
35. Available from: https://www.accessdata.fda.gov/drugsatfda_docs/nda/2014/202293Orig1s000PharmR.pdf
36. Sayed N, Murata I, Abdalla O, Kilany O, Dessouki A, Sasaki K. Effects of dapagliflozin in combination with insulin on cytochrome P450 activities in a diabetes type 1 rat model. J Vet Med Sci. 2021;83:1597-1603.

Turk J Pharm Sci 2024;21(1):87
DOI: 10.4274/tjps.galenos.2024.e001

ERRATUM

DOI: 10.4274/tjps.galenos.2023.50880

ÜNAL G, SEZGİN SD, SANCAR M. Evaluation of SARS-CoV-2 antibody levels in pharmacists and pharmacy staff following coronavac vaccination. Turk J Pharm Sci 2023;20:347-351.

Institutions have been updated at the request of the author. The corrected section is shown below:

Güneş ÜNAL[1], Simla Dilara SEZGİN[1], Mesut SANCAR[2]*

[1]Istanbul Chamber of Pharmacists, Istanbul, Türkiye
[2]Marmara University, Faculty of Pharmacy, Department of Clinical Pharmacy, Istanbul, Türkiye

On the first page, the institutions of the authors have been corrected as follows:

Güneş ÜNAL[1,2], Simla Dilara SEZGİN[1], Mesut SANCAR[3]*

[1]İstanbul Chamber of Pharmacists, İstanbul, Türkiye
[2]İstanbul Medipol University, Institute of Health Sciences, İstanbul, Türkiye
[3]Marmara University, Faculty of Pharmacy, Department of Clinical Pharmacy, İstanbul, Türkiye